

Aus der Berufsgenossenschaftlichen Unfallklinik
Klinik für Unfall- und Wiederherstellungschirurgie an der
Universität Tübingen

**Progress and limitations in the development of improved
hepatocyte cultures**

**Inaugural-Dissertation
zur Erlangung des Doktorgrades
der Humanwissenschaften**

**der Medizinischen Fakultät
der Eberhard Karls Universität
zu Tübingen**

vorgelegt von

Ruoß, Marc Simon

2021

Dekan:	Professor Dr. B. Pichler
1. Berichterstatter:	Professor Dr. A. Nüssler
2. Berichterstatter:	Professor Dr. Dr. P. Ruth
Tag der Disputation:	20.04.2021

Table of Contents

List of abbreviations	I
List of figures	III
List of tables	IV
Chapter 1: Introduction	1
1.1 Isolation, purification, and shipment of PHH	2
1.2 Challenges and limitations during the cultivation of PHH	4
1.3 Usage and optimization of various cell types as alternative to PHH for the use in drug metabolism and toxicity testing	4
1.3.1 Use of stem cells as a model for drug metabolism and toxicity testing	5
1.3.2 Use of different hepatoma cell lines as a model for drug metabolism and toxicity testing	6
1.4 Optimization of the culture conditions for the cultivation of PHH and HCC lines by mimicking the <i>in vivo</i> situation	9
1.4.1 Influence of the culture medium and media supplements on the functionality of the cells	10
1.4.2 Influence of extracellular matrix (ECM) proteins for the culture of PHH .	13
1.4.3 Influence of matrix stiffness on the metabolic function of PHH	14
1.4.4 Approaches for the cultivation of hepatic cells on a 3D matrix	15
1.4.5 Scaffold-free 3D culture of hepatic cells	20
1.4.6 Mimicking the <i>in vivo</i> environment by using co-culture models	22
Chapter 2: Aim of the study	24
2.1 The objectives for this thesis are:	26
Chapter 3: Publication I	27

3.1 Synopsis:	27
Chapter 4: Publication II	48
4.1 Synopsis:	48
Chapter 5: Publication III	67
5.1 Synopsis:	67
Chapter 6: Publication IV	88
6.1 Synopsis:	88
Chapter 7: Discussion	109
7.1 Availability of hepatic cells for <i>in vitro</i> models for pre-clinical drug testing .	110
7.2 Establishment of cultivation techniques for long-term culture of primary hepatocytes.....	115
7.3 Development of <i>in vitro</i> models capable of mimicking the physiological environment of the human liver, but also disease-specific changes that lead to altered drug metabolism.....	117
7.4 Development of quantification methods to normalize the results even with complex cultivation approaches	122
7.5 Conclusion and possible future research directions	124
Chapter 8: Abstract	129
Chapter 9: Zusammenfassung	131
References	133
Declaration	161
Author Contributions.....	162
Acknowledgements	166

List of abbreviations

2D	Two-dimensional
3D	Three-dimensional
5-AZA	5-Azacytidine
5-AZA-dC	5-Aza-2'-deoxycytidine
AFM	Atomic force microscopy
APS	Ammonium persulfate
AUC	Area under the curve
BAA	Bisacrylamide
BCS	Bovine calf serum
cDNA	Complementary DNA
CK18	Cytokeratin 18
Ct	Cycle threshold
CYP	Cytochrome P450
cDNA	Complementary DNA
DMEM	Dulbecco's Modified Eagle's Medium
DMSO	Dimethyl sulfoxide
DNMT	DNA methyltransferases
DNMTi	DNA methyltransferase inhibitors
ECM	Extracellular matrix
EDC	1-ethyl-3-(3-dimethylaminopropyl)carbodiimide hydrochloride
EMT	Epithelial–Mesenchymal Transition
ESCs	Embryonic stem cells
FCS	Fetal calf serum
GFP	Green fluorescent protein
GST	Glutathione S-transferase
HCC	Hepatocellular carcinoma
HDAC	Histone deacetylase

HDACi	Histone deacetylase inhibitor
HLCs	Hepatocyte-like cells
HNF4 α	Hepatocyte nuclear factor 4 α
HPV	Human papillomavirus
iPSCs	induced pluripotent stem cells
JCRB	Japanese Collection of Research Bioresources Cell Bank
KDM4C	Lysine Demethylase 4C
KDM6B	Lysine Demethylase 6B
LOD	Limits of Detection
LOQ	Limits of Quantitation
LPS	Lipopolysaccharide
mRNA	messenger RNA
MSCs	Mesenchymal stem cells
NHS	N-hydroxysuccinimide
NIH	National Institutes of Health
OSM	Oncostatin M
P/S	Penicillin-streptomycin
PBS	Phosphate-buffered saline
PEG	Polyethylene glycol
pHEMA	Poly(2-hydroxyethyl methacrylate)
PLGA	Poly-(lactic co glycolic acid)
PHH	Primary human hepatocytes
qPCR	quantitative Polymerase Chain Reaction
RGD	Proteins that contain Arg-Gly-Asp (RGD)
SEM	Scanning electron microscope
SNAIL	Snail1
SRB	Sulforhodamine B
TEMED	Tetramethylethylenediamine
TSA	Trichostatin A
UGT	Uridine diphosphate-glucuronyltransferase

List of figures

Figure 1 Characteristics of freshly isolated human hepatocyte.	2
Figure 2 Optimization of culture conditions for freshly isolated human hepatocytes (PHH) and hepatocellular carcinoma cell lines	10
Figure 3 Development of a 3D scaffold Co-Culture model, which represents some parameters of the healthy and the fibrotic altered liver.	120
Figure 4 Schematic illustration of the application of a scaffold-based 3D co-culture model	121
Figure 5 Techniques and approaches for improved culture of freshly isolated human hepatocytes (PHH) and liver cell lines by adapting the culture conditions and mimicking the <i>in vitro</i> situation.....	126

List of tables

Table 1 Tested approaches to modify and improve the culture media of PHH and hepatic cell lines	12
Table 2 Examples of 3D cultivation approaches.....	19

Chapter 1: Introduction

The approval processes for a new drug take, on average, 12 years and cost up to US\$1 billion (Van Norman, 2016). This development process takes place in several stages. In the first step, substances that interact with the desired target are selected using a high-throughput approach from a substance library. This is followed by extensive *in vitro* and *in vivo* experiments in which the selected substances are tested inter alia for their pharmacological efficacy and possible toxic side effects (Ware and Khetani, 2017). Despite these extensive pre-clinical test approaches, one third of the substances fail due to organ toxicity in the clinical phase. Moreover, only about 10% of the substances which enter the clinical phase reach approval (Kola and Landis, 2004). Hepatotoxicity is the most common reason for such a failure of a substance in clinical as well as pre-clinical drug development, and also for withdrawal when a drug reaches the market (Fung et al., 2016, O'Brien et al., 2006). Given that the liver plays a central role in the metabolism of drugs, it is not surprising that it is also particularly susceptible to drug-related side effects. In addition, such hepatotoxic side effects can be predicted only insufficiently in animal studies due to interspecies differences. This phenomenon makes it difficult to exclude hepatotoxic substances at an early stage of drug development (Olson et al., 2000). Predictive *in vitro* models are therefore required to predict such adverse drug reactions. Freshly isolated human hepatocytes (PHH) would be the model of choice for such an *in vitro* model, as they have a metabolism comparable to the *in vivo* situation (Bachmann et al., 2015, Godoy et al., 2013). However, for a variety of reasons, PHH can only be used to a limited extent in the testing of new drugs (Ruoss et al., 2020b, Godoy et al., 2013, Vinken and Hengstler, 2018). The main reason is that PHH de-differentiate *in vitro* after only a short time; this de-differentiation is associated with a significant loss of metabolic activity (Godoy et al., 2013, Godoy et al., 2016, Bachmann et al., 2015). In addition to this factor, the availability of suitable cells is limited (Ruoss et al., 2020b). PHH are isolated from liver capsules, which are often taken as residual tissue in large tumor operations (Knobeloch et al., 2012, Pfeiffer et al., 2015). These surgeries can only be performed in specialized clinics, and this process often

requires transport of the cells to the lab where they are used (Ruoss et al., 2018). Both the number of suitable donors and the number of cells per donor is limited (Lee et al., 2014b). In addition to this factor, the donors of the tissues that are used for the PHH isolation are often elderly patients with pre-existing diseases; a pre-treatment with drugs, including chemotherapeutic agents, is common (Bhogal et al., 2011, Ruoss et al., 2020b). This results in damage to the PHH and an altered metabolism (Morgan, 2009, Merrell and Cherrington, 2011).

In the past 40 years, various attempts have been made to address the limitations described above and develop a suitable *in vitro* model for drug toxicity testing. These include optimization of the isolation process and transport of the PHH as well as improvement of the cell culture conditions during PHH cultivation (Ruoss et al., 2020b). Furthermore, various approaches have been tested using other cell types, such as various cancer cell lines, as a replacement for PHH (Lin et al., 2012). The different approaches and their opportunities—as well as their limitations—are described below.

1.1 Isolation, purification, and shipment of PHH

Liver tissue that is used for PHH isolation is usually obtained during large tumor surgeries (Knobeloch et al., 2012). The tissue donors are generally 50-80 years old and often suffer from primary and secondary liver tumors (Figure 1).

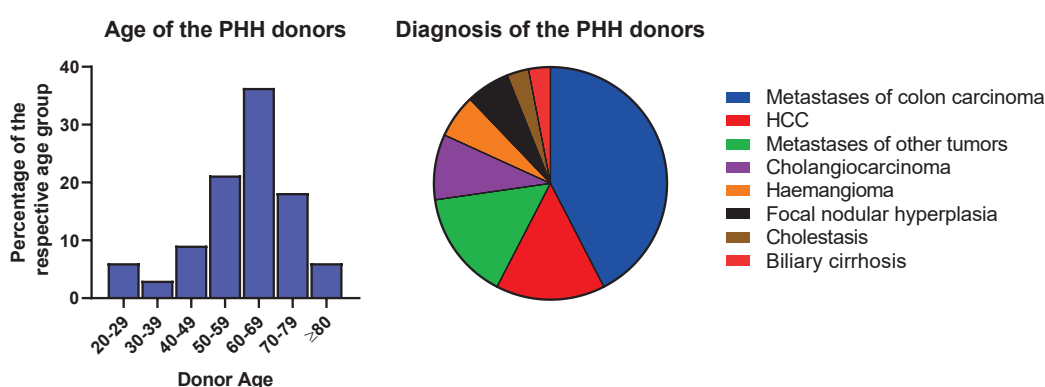


Figure 1 Characteristics of freshly isolated human hepatocyte (PHH) donors; image adapted from (Ruoss et al., 2020b).

PHH isolation from liver tissue can involve mechanical, chemical, and enzymatic methods (Lee and Lee, 2014). Since mechanical and chemical isolation are associated with significant loss of cell viability, PHH are usually isolated from the tissue via a two-step collagenase digestion (Kegel et al., 2016, Knobloch et al., 2012, Lee and Lee, 2014). The quality of isolated PHH depends on several factors. In addition to donor-dependent factors, which influence the initial quality of the cells, time is crucial. Cell isolation should be started within the first hour after hepatectomy, since the viability of the cells decreases to 50%, in comparison to the value of immediate isolation, 3-5 hours after resection (Bhogal et al., 2011). The proportion of dead PHH can be decreased after isolation by Percoll density centrifugation; however, this process is also partially associated with a significant loss of viable cells (Pfeiffer et al., 2015, Ruoss et al., 2018).

After successful isolation, PHH can be directly plated or used as a suspension culture (Godoy et al., 2013). Furthermore, it is possible to cryopreserve PHH or send them overnight in suspension on ice. Both approaches allow the transport of the cells to another place as well as the usage at a later time point. However, in the case of cryopreservation as well as when shipped in suspension, there can be a decrease in viability and a reduction in the metabolic activity (Richert et al., 2006, Hengstler et al., 2000, Duret et al., 2015).

Overall, the complete isolation and purification process, as well as the first few hours in culture, significantly affect the PHH metabolic activity. The isolation process itself results in irreversible metabolic changes (Cassim et al., 2017, Vildhede et al., 2015, Lauschke et al., 2016). As shown by a proteome analysis, more than 450 proteins in PHH are significantly deregulated 24 hours after isolation (Bell et al., 2016). Furthermore, by 4-6 hours after isolation, the messenger RNA (mRNA) expression of *CYP3A4*, which is one of the most important phase I enzymes in drug metabolism, is reduced by 70-80%. This finding illustrates how quickly PHH de-differentiation occurs (Martinez-Jimenez et al., 2007).

1.2 Challenges and limitations during the cultivation of PHH

PHH cultivated in two-dimensional (2D) monoculture provide over a 24-72-hour period the major functions of the liver, such as drug metabolism, urea detoxification, and the synthesis of plasma proteins (Godoy et al., 2013, Gomez-Lechon et al., 2014). Therefore, they are considered to be the gold standard for *in vitro* drug metabolism and toxicity testing (Ruoss et al., 2020b, Bachmann et al., 2015). However, these cells rapidly lose their morphology and liver-specific functions in culture, a phenomena which often make it impossible to detect metabolism-mediated hepatotoxicity of drugs (Schyschka et al., 2013). In addition to the rapid de-differentiation, the limited availability of PHH is another drawback that prevents the use of these cells as a standard model for drug *in vitro* testing (Ruoss et al., 2020b, Zeilinger et al., 2016). In contrast to the *in vivo* situation in which a massive proliferation of PHH occurs after an injury, there is no appreciable proliferation *in vitro* (Garnier et al., 2018, Fausto and Campbell, 2003). This reason underlies why in recent years the suitability of other cell types including cancer cell lines or different kinds of stem cells as an alternative to PHH for *in vitro* toxicity evaluation has been tested (Gomez-Lechon et al., 2014, Zeilinger et al., 2016). The sections below describe some attempts that have been developed to increase the metabolic properties of these cells (Snykers et al., 2009, Steenbergen et al., 2018, Seeliger et al., 2013, Lin et al., 2012).

1.3 Usage and optimization of various cell types as alternative to PHH for the use in drug metabolism and toxicity testing

In contrast to PHH, stem cells and hepatic cancer cell lines have the great advantage of unlimited availability (Godoy et al., 2015, Guo et al., 2011, Lin et al., 2012). Cell lines in particular have the further advantage of a high degree of standardization because there are no donor-related differences (Lin et al., 2012). Various cell types have been evaluated as a model for drug metabolism and toxicity testing; their advantages but also their limitations are described below.

1.3.1 Use of stem cells as a model for drug metabolism and toxicity testing

Different kinds of stem cells, including embryonic stem cells, induced pluripotent stem cells (iPSCs), or mesenchymal stem cells (MSCs), can be differentiated into hepatocyte-like cells (HLCs) (Wei et al., 2018, Hu and Li, 2015).

Embryonic stem cells (ESCs) have the best pre-conditions for a successful differentiation into HLCs because there is no expected disturbance of the differentiation, due to an incomplete trans-differentiation or a further existing expression of the transfected pluripotency genes (Esrefoglu, 2013, Cieslar-Pobuda et al., 2017, Palakkan et al., 2017). However, for ethical reasons, the use of embryonic stem cells is controversial. In various countries, including Germany, experiments with this cell type are prohibited or severely restricted, a factor which makes the use of alternatives, including the above-mentioned cell types, necessary (Brewer, 2006, Lo and Parham, 2009).

iPSCs have nearly the same genetic and functional properties as ESCs (Liang and Zhang, 2013). They are derived from somatic cells, and thus the ethical issue of the destruction of an embryo is not required (Zacharias et al., 2011). However, the transfection of somatic cells with pluripotency genes results in extensive cell alterations, including subtle changes in gene regulation (Liang and Zhang, 2013, Palakkan et al., 2017). In addition, viral transduction results in a non-specific insertion pattern that may be associated with uncontrolled proliferation as well as abnormal development and differentiation of the cells (Cieslar-Pobuda et al., 2017).

The usage of MSCs as a source for differentiation into HLCs has several advantages. They can be isolated without ethical concerns, e.g., from adipose tissue, which can be easily removed during routine surgeries (Kim and Park, 2017). Furthermore, MSCs can proliferate *in vitro*, a factor that allows an increase in the number of cells that are available for experiments. Moreover, these cells show high plasticity, a factor that allows them to differentiate not only in cells of the mesenchymal lineage but also to cells of the other germ layers, including HLCs (Puglisi et al., 2011). Caused by already existing epigenetic marks this trans-

differentiation is only possible to a limited extent (Kim et al., 2011, Godoy et al., 2015). However, it is possible to partially remove these marks by using epigenetic modifiers such as 5-azacytidine (5-AZA) and trichostatin A (TSA) to facilitate differentiation toward HLCs (Snykers et al., 2009, Seeliger et al., 2013).

Regardless of the origin of the utilized stem cells, differentiation of the cells in the direction of mature hepatocytes is required. For this purpose, several differentiation protocols have been developed (Godoy et al., 2015, Godoy et al., 2013). Differentiation occurs through the addition of cytokines and growth factors, most of which are known to play a crucial role in embryonic development of the liver (Seeliger et al., 2013, Vosough et al., 2013). Although many different approaches for the differentiation of stem cells into HLCs have been developed in recent years, complete differentiation to PHH has not yet been achieved (Godoy et al., 2015, Godoy et al., 2016). Rather, different studies have shown that there are still significant differences between HLCs and PHH (Godoy et al., 2018, Hurrell et al., 2018, Kratochwil et al., 2017).

1.3.2 Use of different hepatoma cell lines as a model for drug metabolism and toxicity testing

Different liver tumor cell lines are already being used during *in vitro* screening of new drugs, although their drug-metabolizing activity is significantly reduced compared to PHH (Lin et al., 2012, Sison-Young et al., 2015, Guo et al., 2011). The major advantages of hepatic cell lines are the unlimited availability of the cells and the extensive standardization of the culture conditions (Sison-Young et al., 2017, Castell et al., 2006). This unlimited availability results from their replicative immortality, which is an important characteristic of tumor cells (Zeilinger et al., 2016). Along with these changes in cellular energetics, genomic stability and epigenetics are also altered in these cells, phenomena that partially explain the above mentioned low metabolic activity (Hanahan and Weinberg, 2011).

The frequently used hepatoma cell lines are inter alia HepG2, Huh7, and HepaRG (Guo et al., 2011, Sison-Young et al., 2015). While HepaRG cells express many

drug-metabolizing enzymes similar to hepatocytes, the metabolic activity of HepG2 and Huh7 cells is significantly lower (Guo et al., 2011, Poloznikov et al., 2018, Kratochwil et al., 2017). However, the metabolic activity of HepG2 is still at a comparable level to what could be achieved with commercially available iPSC-derived hepatocytes (Kratochwil et al., 2017). In addition, HepG2 cells are, despite their low metabolic activity, a more sensitive model for predicting drug-induced liver injury compared to HepaRG. This feature may represent one explanation for why they are currently the most widely used as a model for toxicity studies (Sison-Young et al., 2017). Another explanation for the frequent use of HepG2 as well as Huh7 cells may be the fact that a costly and time-consuming differentiation phase is not required, in contrast to HepaRG cells and particularly stem cells (Guillouzo et al., 2007, Godoy et al., 2015, Sison-Young et al., 2017).

In recent years, many approaches have been tested to improve the metabolic activity of hepatoma cell lines (Zeilinger et al., 2016). Some of these approaches try to partially reverse the tumorigenic alterations of these cells in order to reactivate their metabolic activity (Gailhouste et al., 2018). The so-called epithelial-mesenchymal transition (EMT) is one example of such a modification that occurs in the course of tumor progression (Sajadian et al., 2016, Hanahan and Weinberg, 2011). During this process, epithelial cells convert into a mesenchymal phenotype, a phenomenon that is accompanied by a de-differentiation of the cells associated with the loss of their metabolic activity (Roche, 2018). A key player during this process is the transcription factor Snail, which is a transcriptional repressor of the epithelial marker gene E-cadherin (Wang et al., 2013b). The downregulation of E-cadherin is associated with invasive growth and metastasis in hepatocellular carcinoma (HCC) (Sajadian and Nussler, 2015). In addition, Snail affects the expression of the hepatic key regulator HNF4 α , which is related to a loss of metabolic function of the cells (Cicchini et al., 2006, Kamiyama et al., 2007).

Epigenetic alternations that occur during tumor progression also affect the expression of the epithelial marker and hepatic function genes, including E-cadherin and HNF4 α (Stadler and Allis, 2012, Ruoß et al., 2019). Such epigenetic alternations

occur at three different stages: on the positioning of the nucleosome, by modification of the histones, or by methylation of the DNA (Sajadian and Nussler, 2015). In all these stages, the accessibility to the DNA and thus the expression of the corresponding genes is regulated. Epigenetic changes in HCC include, for example, increased acetylation of histones as well as global hypermethylation of the DNA (Wahid et al., 2017, Egger et al., 2004). These modifications lead to silencing of tumor suppressor genes as well as to inhibition of genes involved in hepatic function (Esteller, 2006, Peng and Zhong, 2015, Ingelman-Sundberg et al., 2013).

Several studies have investigated whether these epigenetic changes can be reversed through the use of epigenetic modifiers (Snykers et al., 2009, Sajadian and Nussler, 2015). Among others, the histone deacetylase inhibitor TSA and the DNA methylation inhibitor 5-AZA have been used for this purpose (Snykers et al., 2009, Ruoß et al., 2019). The use of these substances leads to the desired epigenetic changes, which are associated with a reduction in proliferation and an increased expression of hepatic functional genes (Sajadian et al., 2015, Freese et al., 2019, Snykers et al., 2009). Another study also showed that the use of 5-AZA in combination with vitamin C leads to epigenetic changes in the cells and positively influences their EMT status (Ruoß et al., 2019, Sajadian et al., 2016). This result demonstrates the close correlation between EMT status and epigenetics in cancer cells.

Overall, the epigenetic reactivation of tumor cells is an interesting approach for improving their metabolic activity. However, until now it remains unclear to what extent such a reactivation is possible in comparison to PHH. Moreover, the mode of action of the utilized epigenetic modifiers is relatively non-specific, a factor that could also adversely affect the differentiation-state and the functionality of the cells (Dannenberg and Edenberg, 2006).

In addition to the above-described approaches to increase metabolic activity by partially reversing tumorigenic alterations, various other approaches have been tested in recent years for this purpose. Many of them aim to improve the culture

conditions of the cells (Steenbergen et al., 2013, Camp and Capitano, 2007, Damania et al., 2018, Nishikawa et al., 2017). These techniques are not limited to cell lines: They are also used to maintain the function of PHH over a longer period of time. This approach is described in the next section.

1.4 Optimization of the culture conditions for the cultivation of PHH and HCC lines by mimicking the *in vivo* situation

Over the last 40 years, many attempts have been made to cultivate hepatocytes over a longer period of time while preserving their functionality. Despite the development of many different—sometimes very complex—approaches and the publication of more than 14,000 manuscripts on this topic since 1980 (found in PubMed using the keywords “hepatocyte culture”), this goal has not yet been sufficiently achieved (Ruoss et al., 2020b). Still, by the usage of various approaches that often aim to mimic the *in vivo* situation, it is possible to slow down the de-differentiation of PHH and thus maintain their functionality over a limited period (Bachmann et al., 2015, Burkhardt et al., 2014, Soldatow et al., 2013). Some of the most promising approaches, which often also aim to improve the function of hepatic cell lines, are described below and summarized in Figure 2

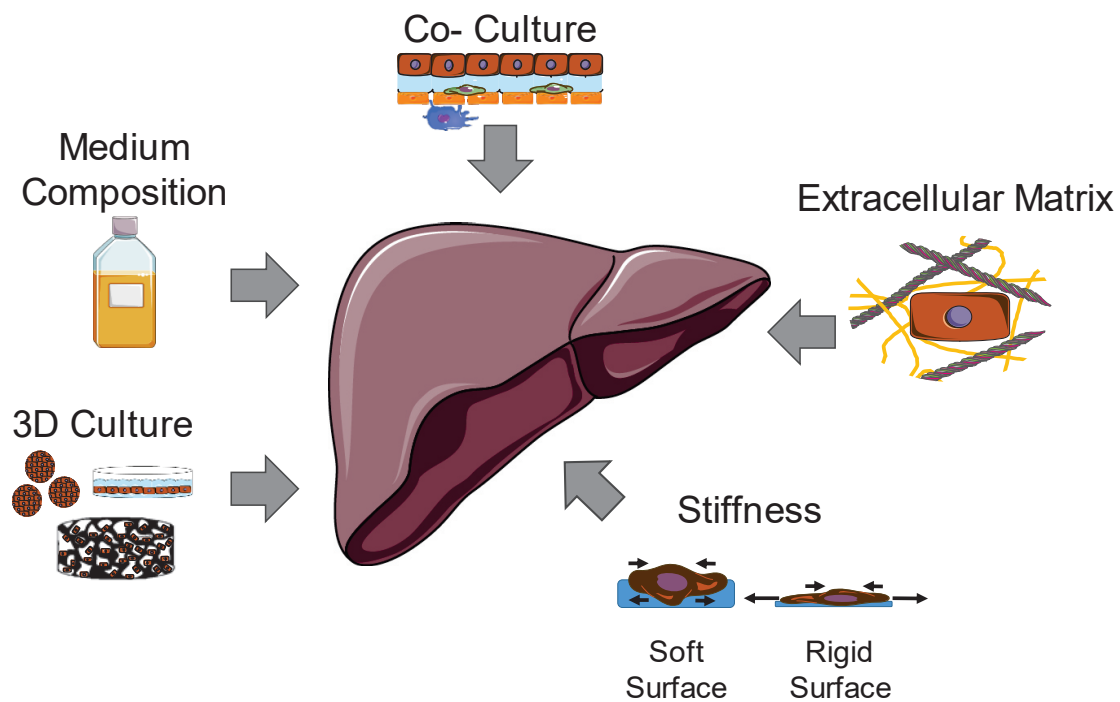


Figure 2 Optimization of culture conditions for freshly isolated human hepatocytes (PHH) and hepatocellular carcinoma cell lines, adapted from (Ruoss et al., 2020b). This figure was produced using Servier Medical Art (<http://smart.servier.com/>).

1.4.1 Influence of the culture medium and media supplements on the functionality of the cells

In order to ensure optimal functionality of the cells, they are incubated in a medium that contains all necessary nutrients, cytokines, and growth factors. For the cultivation of hepatocytes, a specially developed medium, the so-called Williams medium, is often used, to which fetal calf serum (FCS), HEPES, sodium pyruvate, non-essential amino acids, glutamine, hydrocortisone, and insulin are added (Kegel et al., 2016). Insulin helps to maintain the morphology of the cells in culture while hydrocortisone is necessary to maintain the functionality of the hepatocytes (Kinoshita and Miyajima, 2002, Michalopoulos and Pitot, 1975). In contrast, Dulbecco's modified Eagle's medium (DMEM) is often used for the cultivation of cell lines; it contains only FCS (Lin et al., 2012). Different studies have shown that the metabolic activity of cell lines is increased by modifying the culture medium or by adding other factors. In the case of hepatocytes, functionality is maintained over a period of time by modifying the culture medium (Ahn et al., 2019, Burley and Roth,

2007, Choi et al., 2009, Steenbergen et al., 2018). Further, some studies have shown that the addition of various factors also increases the viability and metabolic function of hepatocytes in culture (Sun et al., 2019, Donato et al., 1991, Katsura et al., 2002). Table 1 summarizes approaches that have been tested to improve the culture conditions of hepatocytes or hepatic cell lines by modification of the culture media. To improve the reproducibility of *in vitro* studies and for animal welfare reasons, alternatives to the commonly used FCS, e.g., platelet rich plasma or human serum, have been tested in various studies with hepatocytes and cell lines (Johansson et al., 2003, Katsura et al., 2002, Pramfalk et al., 2016, Steenbergen et al., 2018). One reason for this is that FCS contains a complex mixture of proteins and growth factors, of which not all ingredients are known. Another reason is that the origin of FCS makes its standardized production impossible, a factor that severely hinders the reproducibility of results (van der Valk and Gstraunthaler, 2017). As various studies have shown, other factors, such as glucose concentration within the media, also influence the metabolic activity of hepatocytes and hepatic cell lines (Davidson et al., 2016, Ferretti et al., 2019).

Table 1 Tested approaches to modify and improve the culture media of PHH and hepatic cell lines

	Aim	Used additive/ modified media ingredient	Results	Ref.
Hepatocytes	Different glucose concentrations and their effect on the metabolic activity of PHH	PHH were cultivated over 18 days using different glucose concentrations. In addition to the physiological glucose concentration, hypo- and hyperglycemia were mimicked.	Under hypoglycemic conditions, the expression of the hepatic key regulator gene HNF4 α and the activity of CYP3A4 increased compared to the physiological glucose concentration at all measured time points. On day 18, there was increased gene expression of albumin. In contrast, CYP1A2 activity was increased under hyperglycemic conditions; there was no positive effect under the hypoglycemic condition.	(Davidson et al., 2016)
	Comparison of five different media compositions	Nicotinamide, branched-chain amino acids (such as isoleucine), various other amino acids, galactose, and pyruvate were added to the culture medium in different concentrations; their effect on CYP activity of cultured hepatocytes was studied.	The addition of nicotinamide to a serum-free medium (Ham's F12, hormone supplemented) increased CYP activity. An increase in the concentration of branched-chain amino acids led to a slight additional increase in CYP activity. By increasing the concentration of various amino acids, galactose, and pyruvate, there was a further increase in CYP activity.	(Donato et al., 2008b)
	Maintenance of PHH functions in long-term culture	PHH were cultivated within a medium supplemented with keratinocyte-stimulating factor and human serum.	Keratinocyte-stimulating factor supplementation maintained albumin synthesis over \geq 28 days. The additional replacement of FCS with human serum maintained albumin production until day 56.	(Katsura et al., 2002)
		PHH were treated with a small molecule cocktail to prevent mechanical-tension-induced hepatocyte dedifferentiation by targeting actin/actomyosin dynamics.	The treatment of hepatocytes with the small molecule cocktail maintained the activity of various CYP enzymes such as CYP3A4 over a period of 3 weeks. Hepatocytes pretreated for 3 weeks were able to repopulate <i>Fah</i> ^{-/-} mouse livers and allow the survival of these animals in a manner comparable to the use of freshly isolated hepatocytes.	(Sun et al., 2019)
Cell lines	Enhancement of the metabolic activity of HepaRG cells	HepaRG cells were treated with CHIR99021, which is an inducer of the Wnt/ β -catenin signaling.	There was a concentration-dependent increase in gene expression and CYP1A2, CYP3A4, and CYP2E1 activity, accompanied by a higher sensitivity to acetaminophen.	(Ahn et al., 2019)
	Enhancement of the metabolic activity of HepG2 cells	HepG2 cells were cultured over 7 days using various concentrations of retinoic acid.	Treatment with retinoic acid slowed down the proliferation of the HepG2 cells. This effect was combined with a higher gene expression of hepatic transcription factors such as HNF1 α and HNF4 α . In addition, there were higher albumin and urea secretion rates in retinoic-acid-treated cells.	(Burley and Roth, 2007)
	Enhancement of the metabolic activity of Huh7 cells	Confluent Huh7 cells were treated over 20 days with 1% DMSO.	The DMSO-treated Huh7 cells showed higher expression of several phase I/II enzymes. The expression of some hepatic transcription factors like HNF4 α could be increased to a level which is comparable to human hepatocytes. In addition, there was an increased metabolic activity of the some CYP enzymes—CYP3A4 and CYP2C9—and some phase II enzymes—UGT2B7.	(Choi et al., 2009)
		FCS was replaced by human serum.	Huh7 cells cultured in human-serum-containing-media result in a growth arrest after one week in culture. By further culturing the cells in human-serum-containing media over 27 days, there was increased expression and activity of several CYP enzymes. The metabolic profile of the cells and their morphology also changed in the direction of hepatocytes.	(Steenbergen et al., 2018)

CYP, cytochrome P450; DMSO, dimethyl sulfoxide; FCS, fetal calf serum; PHH, freshly isolated human hepatocytes; UGT, Uridine diphosphate-glucuronyltransferase

1.4.2 Influence of extracellular matrix (ECM) proteins for the culture of PHH

PHH are usually cultivated in cell culture plates coated with type I collagen (Knobeloch et al., 2012). Although this coating allows PHH to adhere, it only reflects the *in vivo* situation in a very rudimentary way. The extracellular matrix of the human liver mainly comprises fibronectin in addition to the already mentioned collagen type I. It also contains lower amounts of collagen types III, IV, V, and VI as well as other ECM proteins such as elastin (Martinez-Hernandez and Amenta, 1993, Kanta, 2016, Klaas et al., 2016). These proteins form the subtle and very complex ECM network of the liver (Ruoss et al., 2020b). Together with the numerous fenestrations and gaps in the sinusoidal endothelial cells, this structure enables polarization of the PHHs as well as the rapid bidirectional exchange of macromolecules between PHHs and plasma (Gissen and Arias, 2015, Treyer and Musch, 2013).

Various studies have attempted to better mimic the natural ECM. For example, it has been shown that fibronectin coating is superior to collagen in promoting cell adherence in PHH as well as the expression of certain liver-specific genes and the synthesis of albumin in Huh7 cells (Wang et al., 2016, Ruoss et al., 2020b). Furthermore, a combination of fibronectin and collagen—which corresponds more to the natural ECM composition—has been successfully used for the cultivation of PHH (Donato et al., 2008b). In addition to the usage of specific ECM proteins, a complex mixture of various ECM proteins shows positive effects during the cultivation of hepatocytes. These include the commercially available Matrigel—which is obtained from Engelbreth-Holm-Swarm mouse sarcoma and contains growth factors in addition to various ECM proteins (Kleinman et al., 1982). Moreover, as shown by another study, differentiated pre-adipocytes can be used to produce a complex mixture of ECM proteins and growth factors that can be used for the cultivation of hepatocytes. Primary rat hepatocytes cultured on this so-called adipogel maintain their metabolic functions (urea production and albumin synthesis) at a higher level compared to cells plated on Matrigel (Sharma et al., 2010). Another promising approach is the use of natural liver ECM as a coating material (Ruoss et al., 2020b, Mazza et al., 2017). In order to obtain these ECM proteins, the liver tissue

must first be decellularized; the remaining matrix can then be pulverized into a powder and enzymatically cleaved with pepsin. The resulting ECM solution can then be used to coat culture plates as well as hydrogel or a scaffold ingredient in a three-dimensional (3D) culture approach (Lee et al., 2014a, Damania et al., 2018). Due to its origin, this ECM mixture best represents the *in vivo* situation. As has been shown in various studies, such a coating positively affects the functionality of PHH and improves differentiation of stem cells (Lee et al., 2014a). Another interesting approach is the use of synthetic ECM proteins. The usage of different compositions of these proteins allows one to mimic disease-specific ECM changes *in vitro* (Huettnner et al., 2018). Synthetic ECM proteins are much more suitable for such a model than their natural counterparts because each parameter can be standardized. Overall, the use of synthetic polymers is not limited to the use as a coating material for the 2D culture. These ECM proteins can also be used in 3D hydrogel or scaffolds, for example, as components of the ink in a 3D printing approach (Huettnner et al., 2018, Heydari et al., 2020).

1.4.3 Influence of matrix stiffness on the metabolic function of PHH

The substrate's stiffness influences various cellular processes, such as cell proliferation and differentiation status as well as the metabolic activity of the cells (Wells, 2008a, Perez Gonzalez et al., 2018). One study showed that stem cells can be differentiated in distinct directions by only modulating matrix stiffness, which indicates the importance of stiffness for cell behavior (Engler et al., 2006). In primary hepatocytes, there are stiffness-dependent changes in cell morphology as well as the expression and activity of hepatocyte-specific enzymes. Overall, a softer surface that corresponds to a healthy liver is advantageous compared to a stiffer surface or cell culture plastic (Natarajan et al., 2015). Depending on the measurement method employed, there are different values given in the literature for the stiffness of the healthy liver. These values range from 150 Pa, measured with atomic force microscopy (AFM), to 6 kPa, measured by Fibroscan (Wong et al., 2010, Mueller and Sandrin, 2010, Desai et al., 2016). It is difficult to judge which measurement method better reflects the actual stiffness of the liver because both approaches have

their limitations. In the case of the Fibroscan measurement, the stiffness of the liver is measured from the outside, which means that the stiffness of the liver capsule, which is stiffer than the tissue itself, is also taken into account (Mueller and Sandrin, 2010). On the other hand, AFM-based measurement requires freezing the liver tissue during sample preparation, a process that results in damage to the tissue and thus affects the determination of the stiffness (Desai et al., 2016).

However, stiffness is not only an important parameter *in vitro*: There is an association between metabolic activity and liver stiffness in the clinic. One study evaluated the metabolic capacity of chronic alcoholics with different liver stiffness. Patients with liver stiffness below 8 kPa showed induction of cytochrome P450s (CYPs) and drug transporters, while the group with stiffness above 8 kPa showed inhibition of CYP enzymes (Theile et al., 2013). Such stiffness-dependent differences in drug metabolism are interesting not only for the individual patient, where inhibition of certain CYP enzymes can lead to a toxic overdose of a drug, but also for risk assessment before the approval of a new drug (Ruoss et al., 2020a).

1.4.4 Approaches for the cultivation of hepatic cells on a 3D matrix

PHH are arranged in the liver lobules to form a polarized epithelium (Gissen and Arias, 2015). This organization, as well as the interaction with the ECM and the other cell types found in the liver, are essential for the functionality of PHH (Vinken et al., 2006, Godoy et al., 2013). Such a complex structure cannot be mimicked in conventional 2D monoculture; thus, some attempts have been made to develop cell culture models that better represent the *in vivo* situation (Bachmann et al., 2015).

The cultivation of cells in a 3D matrix is one such approach. In contrast to the usual 2D culture, the cells can be cultivated embedded in a 3D matrix, which is more similar to the *in vivo* situation. Depending on the choice of matrix, factors such as stiffness and ECM proteins can also be adapted to the *in vivo* situation (Ruoss et al., 2020b, Jain et al., 2014).

In recent years, several matrix-based 3D models made from a variety of natural and synthetic materials have been developed. These include, in addition to hydrogels,

various types of scaffolds. Some of the most promising approaches are described in more detail below and are summarized in Table 2.

1.4.4.1 Hydrogels

Hydrogels consist of natural or synthetic polymers, which have a high swelling capacity and together with liquid form a 3D matrix (Bachmann et al., 2015). Depending on the hydrogel used, the cells can either be applied directly on top of it or resuspended in it. A sandwich culture, in which the cells are cultivated between two hydrogel layers, is also a commonly used (Ruoss et al., 2020b).

Frequently used natural polymers include the above-described Matrigel as well as collagen, which can be isolated from rat tails, among other sources (Knobeloch et al., 2012). PHH cultivation in a collagen sandwich culture results in a phenotype that resembles the *in vivo* situation (De Bruyn et al., 2013). This is associated with the re-establishment of cell-cell contacts and longer maintenance of liver-specific functions (CYP activities, activity of transport proteins, and urea and albumin synthesis). These factors lead to a greater sensitivity to drugs such as paracetamol (Bachmann et al., 2015, Schyschka et al., 2013).

In contrast to rat tail collagen, which contains almost exclusively type I collagen, Matrigel comprises a mixture of various ECM proteins, mainly laminin, collagen IV, nidogen, as well as several growth factors (Hughes et al., 2010). This complex mixture seems to be more beneficial for the culture of PHH compared to collagen because a comparison of both Matrigel and collagen sandwich cultures showed that rat hepatocytes cultured on Matrigel maintain their metabolic function better than those cultured in collagen (Borlak et al., 2015). However, Matrigel's complex composition also has its drawbacks: The exact composition is still unknown and significant differences occur among batches, a phenomenon which makes standardization difficult (Hughes et al., 2010). In addition, Matrigel cannot represent the natural ECM of the liver, since several ECM proteins found in the liver are not contained in it (Ruoss et al., 2020b).

Another approach is the usage of ECM from decellularized tissue for the production of hydrogels. Such hydrogels made from decellularized liver contain an ECM that is similar to the *in vivo* situation. Rat hepatocytes cultured on such a hydrogel show from day 7 onward higher CYP1A1 activity compared to cells cultured in collagen type I (Nakamura and Ijima, 2013). However, standardization is also difficult with this condition. Besides, the availability of human material, which would be the best choice, is limited.

Various synthetic materials such as polyethylene glycol (PEG) are suitable for the production of hydrogels. In contrast to natural hydrogels, these materials per se do not have the optimal properties to facilitate cellular attachment and cultivation. Instead, they can form a well-defined basic structure (Zhu and Marchant, 2011, Jain et al., 2014). This structure can be modified in various ways that enable cell attachment and allow a broad range of possible applications (Ye et al., 2019). For example, crosslinking with poly-(N-isopropyl acrylamide) allows detaching the cells from the hydrogel after cultivation only by a change in temperature (Nagase et al., 2018).

1.4.4.2 Scaffold culture

In contrast to the cultivation of cells on hydrogels, cells cultured on a scaffold are not entirely enclosed by or embedded in the matrix. Instead, a scaffold provides a porous structure that allows the adherence of the cells in a 3D matrix. To provide the cells with an ideal environment, the porous structure of the scaffold should allow a good supply of nutrients to the cells and sufficient removal of waste products (O'Brien, 2011). This requires a good permeability of the scaffold matrix and specific size of the pores (Heydari et al., 2020). As different studies have shown, a pore size of 80-100 μm seems to be ideal for the cultivation of hepatocytes (Ruoss et al., 2020b). This pore size allows the adherence of several of the 20-30 μm large hepatocytes (Kegel et al., 2016) within one pore, and thus the cells can form cell-cell as well as cell-matrix contacts. In general, various natural and synthetic materials are used for the fabrication of the scaffold matrix (Heydari et al., 2020, Bachmann et al., 2015). The methods used to create scaffolds are also diverse. Some examples are

described in Table 2. Besides the use of decellularized tissue, scaffolds made with a 3D printer or electrospinning are often used for hepatocyte cultivation (Ruoss et al., 2020b). In addition, so-called cryogels are suitable for the cultivation of hepatocytes. To produce these cryogels, the individual scaffold components, which are present as monomers/polymers within an aqueous solution, are frozen. While the water forms ice crystals in the frozen state, the remaining scaffold components polymerize and form the scaffold matrix. After thawing, interconnected pores remain at the places where the ice crystals were before; these pores are responsible for the porous structure of the cryogel (Hixon et al., 2017, Ruoss et al., 2020a). In contrast to scaffolds that are produced using, for example, a 3D printer, the possible variation of cryogels concerning their pore size—and in particular to their geometric shape—is limited. However, this type of scaffold production has the great advantage that, compared to the other methods mentioned, no expensive equipment is required for scaffold manufacturing (Heydari et al., 2020).

Table 2 Examples of 3D cultivation approaches

	Manufacturing technique	Matrix composition/ scaffold manufacturing	Results	Ref.
Hydrogel	Collagen sandwich	Collagen isolated from rat tails (mainly consists of type I collagen)	There was better maintenance of the gene expression of some hepatic genes including the CYP enzymes; enhanced sensitivity to acetaminophen in sandwich cultured hepatocytes.	(Godoy et al., 2016, Knobloch et al., 2012, Schyschka et al., 2013)
	Matrigel	A complex mixture of ECM proteins, mainly laminin, collagen IV, and enactin, extracted from mouse Engelbreth-Holm-Swarm sarcoma	Rat hepatocytes cultured in Matrigel showed a higher expression of the hepatic key regulator HNF4 α compared to cells cultured in a collagen sandwich. In addition, the activity and protein expression of several CYP enzymes were higher. Matrix-related effects but not cell-cell interactions preserved cell functions of Matrigel-cultured cells.	(Hughes et al., 2010, Borlak et al., 2015, Moghe et al., 1997)
	Decellularized extracellular liver matrix	The solubilized extracellular matrix of decellularized rat livers was used.	The culture of rat hepatocytes on a liver-ECM-based hydrogel increased cellular function compared to cells cultured on a collagen gel. This positive effect on albumin secretion, urea synthesis, and CYP1A1 activity was further increased by enrichment of ECM proteins, especially collagen within the hydrogel.	(Nakamura and Ijima, 2013, Bual and Ijima, 2019)
Scaffold	Cryogel	PEG-6000, sodium alginate, and gelatin were cross-linked to the cryogel using glutaraldehyde and CaCl ₂ .	Albumin synthesis, urea production, and CYP1A1 activity of HepG2 and Huh7 were measured. These metabolic functions were increased in the 3D compared to the 2D culture. This positive effect could be further increased by using PNIPAAm for hepatosphere formation.	(Kumari et al., 2016)
	Salt leaching method	Salt particles were dissolved in an aqueous silk fibroin solution. Due to the saturation of the solution, most of the salt was retained as solid particles. Around these salt particles, the silk fibroin formed a stable porous matrix.	Rat hepatocytes that were mixed with Matrigel prior to seeding on the silk scaffold showed an increased hepatic function (CYP, urea, and albumin) as well as a higher expression of hepatic function genes, e.g., HNF4 α , especially when the hepatocytes were co-cultured with stellate cells.	(Kim et al., 2005, Wei et al., 2018)
	Electrospinning	The application of a strong electric field to a PLGA polymer solution creates fibers that are then spun to the 3D PLGA scaffold. ECM proteins (collagen type I or fibronectin) were chemically linked in different concentrations to the scaffold to provide the cells with a more <i>in vivo</i> -like environment.	Human hepatocytes cultured on the PLGA electrospun scaffold, which contains collagen, exhibited higher albumin, CYP3A4, and CYP2C9 gene expression compared to sandwich cultured cells. Also, the production of urea and the synthesis of albumin were increased. The activity of the measured CYP enzymes was comparable to the sandwich culture.	(Bhardwaj and Kundu, 2010, Brown et al., 2018)
	3D printing	3D-printed scaffolds were fabricated using a heated gelatin solution; this solution was printed onto pre-cooled glass slides. Scaffolds were printed 6-layers high using a strut spacing of 700 μ m and a strut diameter of 200 μ m. Two different angles (60 or 90°) between neighboring layers were tested. To stabilize the scaffolds, the gelatin was cross-linked using EDC and NHS.	Huh7 cells cultured on the 3D printed scaffolds showed higher CYP3A4 and CYP2C9 activity compared to 2D cultured cells. Also, the number of formed bile canaliculi was increased in comparison to the 2D culture. Overall, the cells cultured on scaffolds with a strut angle of 60° between neighboring layers a higher metabolic function than the cells which were plated onto the scaffolds which a strut angle of 90°.	(Lewis et al., 2018)
	Decellularized liver	Human liver tissue was perfused with PBS and frozen. Subsequently, the tissue was cut into small cubes. These cubes were decellularized using a multi-step decellularization protocol. Prior seeding of the human liver scaffolds they were sterilized followed by the seeding of the cells on top of the scaffolds.	HepG2 cells plated on the human liver scaffolds showed increased expression of albumin and UGT1A1 in comparison to cells plated in 2D prior to a cultivation time of 14 days. The scaffolds were also tested in a dynamic perfusion culture system: The albumin production increased over a period of 7 days.	(Mazza et al., 2017)

2D, two dimensional; 3D, three dimensional; CYP, cytochrome P450; ECM, extracellular matrix; EDC, 1-ethyl-3-(3-dimethylaminopropyl) carbodiimide hydrochloride; PBS, phosphate-buffered saline; PLGA, poly-(lactic-co-glycolic acid); NHS, N-hydroxysuccinimide; UGT, Uridine diphosphate-glucuronyltransferase

1.4.5 Scaffold-free 3D culture of hepatic cells

The cultivation of liver cells in a 3D environment is also possible without the use of foreign materials. This may be achieved by the self-organization of the cells and their formation of small cell aggregates. Depending on the cell type and utilized culture method, these scaffold-free 3D micro tissues can be divided into spheroids and organoids, which are separately described below.

1.4.5.1 Spheroid culture

The natural tendency of many cells to aggregate has been exploited for the generation of spheroids (Pampaloni et al., 2007). In contrast to the generation of organoids, mature cells such as cancer cells or primary hepatocytes are used for the generation of the spheroids (Godoy et al., 2013). For spheroid generation, it is necessary that the cells cannot adhere to the culture plate. To achieve this goal, different methods have been developed, including the use of non-adherent cell culture plates, culturing cells on materials such as agarose, which do not allow cell adherence, and the so-called hanging drop technique where the spheroids are generated in a drop of the medium that hangs on the underside of culture plate lids (Tung et al., 2011, Nath and Devi, 2016). There are many other techniques available for generating spheroids. For example, spheroids can also be generated using magnetic levitation. Therefore, it is necessary that magnetic nanoparticles are incorporated into the cells before the spheroids are generated by exposing the cells to a magnetic field (Kim et al., 2013, Nath and Devi, 2016). The cultivation of hepatocytes in spheroid culture results in prolonged maintenance of the metabolic function compared to conventional 2D culture. For example, PHH cultured as spheroids retain stable activity of several CYP enzymes between day 8 and day 35. Also, there is stable production of albumin during this period (Bell et al., 2016). Another study, which compared spheroid cultures of hepatocytes to sandwich cultured cells, showed a higher level of ADME proteins in the case of spheroid cultures. There was also higher activity of several CYP enzymes. Furthermore, there was higher sensitivity to known hepatotoxins like diclofenac and troglitazone in the spheroid cultured hepatocytes within this study (Bell et al., 2018).

1.4.5.2 Organoid culture

In contrast to spheroid cultures, stem cells instead of mature cells are used to generate organoids (Ruoss et al., 2020b). In addition to embryonic stem cells, the usage of iPSCs and organ-restricted adult stem cells are possible (Prior et al., 2019, Clevers, 2016). The addition of cytokines and growth factors, as well as the self-organization of the cells within the 3D environment, allow recapitulation of cellular processes that take place in the organism during embryonic development or tissue repair (Clevers, 2016, Lancaster and Knoblich, 2014). These differentiation processes lead to the generation of an organ-like mini tissue that can be further used for *in vitro* studies.

The generation of liver organoids involves mimicking mechanisms that are responsible for liver regeneration after injury (Clevers, 2016, Lancaster and Knoblich, 2014). Depending on the type of liver injury, two fundamentally different mechanisms for liver regeneration are known. Chronic liver damage leads to the proliferation and differentiation of liver precursor cells (oval cells), which are located near the bile duct tree. By contrast, acute damage of the liver—for example, during partial liver resection—leads to a massive proliferation of the remaining hepatocytes. Both cellular mechanisms can be used for the generation of liver organoids. Regardless of the employed mechanism, organoid generation requires an expansion of the cells in a 3D environment (Hu et al., 2018, Huch et al., 2013, Huch et al., 2015). Through the addition of cytokines and growth factors as well as self-organization, the cells grow and differentiate into mature organoids with, to a certain extent, the functions of human hepatocytes (Prior et al., 2019). One study demonstrated that the differentiated liver organoids produce albumin and store glycogen. The differentiation also increases CYP3A4 activity (Hu et al., 2018). Additionally, alpha-fetoprotein is highly expressed. Since this protein is the fetal precursor of albumin, it is assumed that the organoids are more likely to be a fetal precursor of hepatocytes, not to mature hepatocytes. Therefore, it is necessary to improve the differentiation protocols in the future to be able to differentiate the organoids completely into the mature state.

1.4.6 Mimicking the *in vivo* environment by using co-culture models

The liver is composed of individual liver lobules, which consist of hepatocytes and non-parenchymal cells. Hepatocytes make up 80% of the liver volume and are responsible for most of the liver functions. Non-parenchymal cells, such as sinusoidal endothelial cells, Kupffer cells, hepatic stellate cells, and Ito cells, make up only about 6.5% of the liver volume but are still crucial for the maintenance of hepatocyte function. In addition, these cells play a decisive role in pathological processes as well as in substance-induced damage to the liver (Kmiec, 2001, Arias et al., 2020). Notably, hepatic stellate cells are mainly responsible for the excessive production of extracellular matrix proteins, a phenomenon that occurs in the development of liver fibrosis (Wells, 2008a). Besides, Kupffer cells, as well as other immune cells, play a significant role in the development of an immune-mediated liver injury (Adams et al., 2010). Therefore, it is not surprising that such processes cannot be mimicked *in vitro* using a hepatocyte monoculture. For this reason, a wide variety of co-culture models have been established in recent years; they either aim to better mimic immune-mediated drug-induced hepatotoxicity *in vitro* or maintain the function of cultured hepatocytes for a more extended time (Bhatia et al., 1999, Rose et al., 2016, Khetani and Bhatia, 2008). Also, when using hepatic cell lines, there is a beneficial effect on the metabolic function and/or a better prediction of immune-mediated hepatotoxicity when using co-culture models (Granitzny et al., 2017, Wewering et al., 2017, Cui et al., 2018). Examples for co-culture approaches using hepatocytes or hepatic cell lines are described in more detail below.

1.4.6.1 Using co-cultures to improve the metabolic functions of hepatic cells

One study revealed that 3T3-J2 cells but not primary human liver sinusoidal endothelial cells or umbilical vein endothelial cells can maintain metabolic activity (urea and albumin production and CYP 3A4 activity) of primary human hepatocytes cultured within a micro-patterned approach over a period of 21 days. Culturing primary human hepatocytes in a triple co-culture model, along with 3T3-J2 cells and human liver sinusoidal endothelial cells, further improves the metabolic function of the hepatocytes. In addition, there is stable expression of several endothelial genes over this time period (Ware et al., 2018). In the case of HepG2, a number of

researchers have reported a positive effect on metabolic activity using a co-culture together with 3T3-J2 cells. This type of co-culture leads to increased urea production and improved albumin synthesis (Cui et al., 2018, Cui et al., 2019, Shao et al., 2019). In one of those studies, there was increased CYP3A4 activity. Within this study, they also tested a triple co-culture (HepG2, 3T3-J2, and human umbilical vein endothelial cells). HepG2 cell metabolic activity was further increased by the additional use of human umbilical vein endothelial cells (Shao et al., 2019). There was a positive effect on the gene expression of several CYP enzymes and the activity of CYP 3A4 by co-culture of HepG2 cells with bovine pulmonary artery endothelial cells in another study (Ohno et al., 2008).

1.4.6.2 Using co-culture models for the prediction of immune-mediated hepatotoxicity

The influence of immune mediated factors on the hepatotoxicity of drugs has been described in several studies. For this reason, recent attention has focused on providing co-culture models that can reproduce such interactions between immune cells and hepatic cells *in vitro*. One study established a co-culture model with rat hepatocytes and Kupffer cells. Endotoxin stimulation in co-culture, but not in hepatocyte monoculture, led to a higher sensitivity toward substances associated with immune-mediated hepatotoxicity such as trovafloxacin. In addition, there were lipopolysaccharide (LPS)- and co-culture-dependent changes in cytokine profiles and Cyp3A activity that reflect the mode of action of the tested substances *in vitro* (Rose et al., 2016). In another study, a co-culture of HepG2 and THP1 cells used to predict immune mediated hepatotoxicity of drugs. In that study, the co-culture showed an increased cytotoxicity to troglitazone and a hormetic response to diclofenac and ketoconazole; both effects are known for idiosyncratic drug-induced liver injury-positive substances (Granitzny et al., 2017).

Chapter 2: Aim of the study

Innovative approaches for the further development of *in vitro* studies are necessary in order to increase their predictive power while significantly reducing the number of animal experiments during the pre-clinical testing of new drugs. Such *in vitro* models must be permanently available on a sufficient scale to allow reliable screening of new substances. PHH are actually the most suitable cell-type for such a model because they have a comparable metabolism to the *in vivo* situation (Dambach et al., 2005). So far, the use of these cells in routine testing has been restricted due to their limited availability and metabolic stability (Godoy et al., 2013). The insufficient availability is partly due to the fact that the cells can only be isolated in special clinics that perform major liver surgeries. Furthermore, the indications for such operations where sufficient residual tissue is available for the isolation of PHH are limited and it is not plannable if and when cells can be isolated (Ruoss et al., 2020b). In addition, the transport of the isolated cells to the user, e.g., as a cell suspension on ice, is associated with a massive loss of living cells as well as a reduction in the metabolic activity of the remaining cells. (Ruoss et al., 2018). A further limitation in the use of PHH is the fact that these cells lose their metabolic activity after only a few days in culture, a phenomenon that significantly limits their use in long-term experiments (Bachmann et al., 2015). By optimizing the cultivation conditions, for example, by using a more *in vivo* -like 3D environment, it is possible to slow down the de-differentiation process and thus increase the time for possible experiments. (Soldatow et al., 2013, Bachmann et al., 2015). However, cultivation of functionally active PHHs over several weeks is currently not possible.

For the abovementioned reasons, hepatic cell lines are currently also used for the pre-clinical testing of new drugs (Donato et al., 2008a, Lin et al., 2012, Sison-Young et al., 2017). The advantage of these cells is their availability in sufficient quantities at any time. In addition, the use of cell lines allows a high degree of standardization of the results. A decisive disadvantage of these cells is their limited metabolic activity, which is in some cases many times lower than that found in PHH (Kratochwil et al., 2017, Rodriguez-Antona et al., 2002). Various studies have attempted to

overcome this drawback and increase the metabolic activity of hepatic cell lines. Promising approaches include epigenetic reactivation of the tumor cells or the cultivation of the cells in a 3D culture (Snykers et al., 2009, Kumari et al., 2016, Luckert et al., 2017).

The adverse effects of drugs are often based on complex interactions of the cells with their environment; hence, it is necessary to be able to simulate such interactions *in vitro*. This includes interactions with other cells within the liver, which can be mimicked by using a co-culture model (Bale et al., 2016, Rose et al., 2016). In addition, the interaction with the extracellular matrix can be mimicked by using a 3D culture approach (Bachmann et al., 2015, Ruoss et al., 2020b). An ideal cultivation system in this context would be a model that can represent the physiological situation of the human liver as well as mimic disease-specific changes (Huettnner et al., 2018, Ruoss et al., 2020a). This approach is important, because such differences as increased liver stiffness in the clinical entity of liver fibrosis, also influence the metabolism of drugs *in vivo* (Theile et al., 2013). However, the successful establishment and application of such models, as well as the development of even more complex disease specific 3D co-culture models, requires that the results can be meaningfully evaluated and normalized. Common methods, which are successfully used in two dimensional (2D) culture, are only minimally applicable because they can neither analyze the different cells separately in a co-culture nor be reliably used in a 3D culture (Ruoss et al., 2020).

2.1 The objectives for this thesis are:

- Establish a carrier that allows the transport of human hepatocytes without a significant loss in cell viability and their metabolic function;
- Extend the cultivation time of functionally competent primary human hepatocytes by cultivating them on a 3D scaffold;
- Test different approaches to increase the metabolic activity of the hepatic cell line HepG2:
 - by epigenetic reactivation and
 - by cultivation in a 3D culture;
- Establish a scaffold-based 3D model that represents the stiffness of the healthy liver and the fibrotic liver;
- Establish a quantification method that allows the cell-type-specific quantification of scaffold based 3D co-cultures

Chapter 3: Publication I

Ruoß, M.; Häussling, V.; Schügner, F.; Olde Damink, L.H.H.; Lee, S.M.L.; Ge, L.; Ehnert, S.; Nussler, A.K. **A Standardized Collagen-Based Scaffold Improves Human Hepatocyte Shipment and Allows Metabolic Studies over 10 Days.** Bioengineering 2018, 5, 86.

3.1 Synopsis:

Animal experiments are considered to be the gold standard for testing new drugs. In contrast to cell culture experiments, the effects of a substance on the whole organism can be investigated (Ferreira et al., 2019). However, human metabolism differs considerably from that of commonly used experimental animals. Hence, the toxic effects of new drugs that occur in humans often cannot be predicted in animal models (Dambach et al., 2005). To exclude such effects at the early stage of drug development, it is necessary to provide predictive *in vitro* models. Given that freshly isolated primary human hepatocytes have a metabolism comparable to the *in vivo* situation, they are considered to be the gold standard for such a predictive *in vitro* toxicity model for testing new drugs (Bachmann et al., 2015). Due to various factors, their use in this field is limited. The main reasons are the limited availability of the cells and the fact that they lose their metabolic activity after only a few days in culture. It is in principle possible to freeze hepatocytes to allow the transport of the cells and their constant availability; however, the cryopreservation of the cells results in a massive loss of viability and reduced metabolic activity, factors that limit the usefulness of cryopreserved hepatocytes (Godoy et al., 2013). Alternatively, it is possible to send the cells in suspension on ice, which reduces cell damage compared to cryopreservation, but also leads to a significant loss of living cells. In order to minimize the loss of cells and their metabolic activity during the transport, this study aimed to develop a carrier that allows the shipment of cells from point A to point B as gently as possible. We tested whether the Optimaix-3D Scaffold from Matricel is suitable for this purpose. We also investigated whether it is possible to maintain the metabolic activity of hepatocytes over 10 days by cultivating them on the Optimaix-3D scaffold; cells cultured in 2D were used as a control.

The scaffold characterization results showed that the Optimaix-3D Scaffold is ideally suited for the cultivation of hepatocytes. It has a pore size of $88.9 \pm 21 \mu\text{m}$ and a high porosity and permeability, factors that ensure a good supply of nutrients to the cells. Besides, the scaffold has a stiffness comparable to that of the human liver. Furthermore, the Optimaix-3D Scaffold consists of collagen, which is also an essential component of the ECM in the human liver.

Our data showed that the loss of hepatocyte viability caused by shipment can be significantly reduced by direct plating before shipment compared to shipment as a cell suspension. This outcome was the same for hepatocytes plated in 2D or on the Optimaix-3D Scaffold. However, the Optimaix-3D Scaffold's porous structure and the resulting increased surface area allows the transport of a higher cell number in the same area.

We also showed that the cultivation of hepatocytes on the Optimaix-3D Scaffold has a positive effect on their metabolic activity. Compared to the conventional 2D culture, there is significantly higher albumin production and urea detoxification capacity. In addition, CYP enzymatic activity is more stable over 10 days.

In summary, we demonstrated that the Optimaix-3D Scaffold is suitable for the transport of hepatocytes from point A to point B as well as their cultivation over a 10-day period. In addition, the scaffold fits into the hole of a 96-well plate, a factor which also makes it interesting for high-throughput applications. However, the use of the Optimaix-3D Scaffold is also subject to limitations. For example, we could not get the cells off the scaffold without significant loss of viability. This factor makes it impossible for the user to plate the hepatocytes again. On the other hand, there is a low viability loss during transport. In addition, there is good potential standardization for this model, and thus it is interesting for numerous applications.

Article

A Standardized Collagen-Based Scaffold Improves Human Hepatocyte Shipment and Allows Metabolic Studies over 10 Days

Marc Ruoff ¹, Victor Häussling ¹, Frank Schügner ², Leon H. H. Olde Damink ², Serene M. L. Lee ^{3,4}, Liming Ge ³, Sabrina Ehnert ^{1,†} and Andreas K. Nussler ^{1,*,†}

¹ Department of Traumatology, Siegfried Weller Institute, Eberhard Karls University, 72076 Tübingen, Germany; m.ruoss@hotmail.de (M.R.); victor.haessling@hotmail.de (V.H.); sabrina.ehnert@gmail.com (S.E.)

² Matricel GmbH, 52134 Herzogenrath, Germany; schuegner@matricel.de (F.S.); olde_damink@matricel.de (L.H.H.O.D.)

³ Hepacult GmbH, 82152 Martinsried/Planegg, Germany; Serene.Lee@med.uni-muenchen.de (S.M.L.L.); liming.ge@hepacult.de (L.G.)

⁴ Biobank of the Department of General, Visceral and Transplantation Surgery, Hospital of the LMU, 81377 Munich, Germany

* Correspondence: andreas.nuessler@gmail.com; Tel.: +49-7071-606-1065

† These authors contributed equally to this work.

Received: 24 August 2018; Accepted: 14 October 2018; Published: 16 October 2018



Abstract: Due to pronounced species differences, hepatotoxicity of new drugs often cannot be detected in animal studies. Alternatively, human hepatocytes could be used, but there are some limitations. The cells are not always available on demand or in sufficient amounts, so far there has been only limited success to allow the transport of freshly isolated hepatocytes without massive loss of function or their cultivation for a long time. Since it is well accepted that the cultivation of hepatocytes in 3D is related to an improved function, we here tested the Optimaix-3D Scaffold from Matricel for the transport and cultivation of hepatocytes. After characterization of the scaffold, we shipped cells on the scaffold and/or cultivated them over 10 days. With the evaluation of hepatocyte functions such as urea production, albumin synthesis, and CYP activity, we showed that the metabolic activity of the cells on the scaffold remained nearly constant over the culture time whereas a significant decrease in metabolic activity occurred in 2D cultures. In addition, we demonstrated that significantly fewer cells were lost during transport. In summary, the collagen-based scaffold allows the transport and cultivation of hepatocytes without loss of function over 10 days.

Keywords: drug-induced hepatotoxicity; pre-clinical drug testing; cells shipment; natural collagen scaffolds

1. Introduction

Drug-induced hepatotoxicity is the leading cause of acute liver failure and post-marketing withdrawal of drugs. Thus, a major challenge when developing new drugs is their assessment of undesired side effects in humans [1]. In order to ensure the highest degree of safety and efficacy of a potential drug, many time-consuming and expensive pre-clinical tests must be performed. Consequently, to limit developmental costs there is an enormous demand for predictive in vitro test systems in order to discriminate, as early as possible, between promising and inadequate drug candidates. Pre-clinical drug testing is typically done using animal models; however, animal models used by the pharmaceutical industry are, so far, not very representative for the human situation [2–4]. Because of the poor predictive power of current preclinical models, 90% of the drugs approved for

29

the clinical phase do not enter the market or must be taken off the market on the basis of long-term experience in humans [5]. The development of an in vitro test system that allows the early detection of hepatotoxicity would not only reduce time and costs for drug testing but also increase human safety and reduce animal tests.

It is widely accepted that reliable predictions could only be made with a human in vitro models to exclude or further develop new drugs [6]. However, all of these models show several limitations. So far, many different cell types including (fresh, cryopreserved, and immortalized) primary hepatocytes [7–9], hepatic cell lines [10], and stem cell-derived hepatocyte-like cells [11] have been tested. However, only freshly isolated primary human hepatocytes (PHHs) show a metabolic profile that is comparable to the in vivo situation [12], making them the currently used ‘gold standard’. However, usage of PHHs has also its disadvantages.

Firstly, the origin of these cells is mostly from already medicated tumor patients. Therefore, the cells could have an altered metabolism, which does not represent the situation in the disease the drug is designed for. Furthermore, the dependence on human donors implies that the cells are not available in sufficient quantities anytime and anywhere [13].

Secondly, cryopreservation of the cells is also a limited alternative, because it is frequently associated with an enormous loss in number and function of the PHHs [14]. Therefore, PHHs are mostly shipped as a cooled suspension on ice [15]. However, this kind of transport also damages the cells by hypothermia. Thus, the viability of the PHHs decreases during transport and the remaining cells show impaired cell attachment and reduced function [16]. In general, transportation of PHHs at 37 °C, where cells remain largely intact, is possible but this form of transport is logistically unwieldy: (i) before cells can be shipped it is mandatory to wait until cells attach onto the culture plastic; (ii) plates have to be sealed tightly and packages have to be handled carefully not to spill the medium, as loss of medium (dry wells) stresses the cells and increases the risk for contaminations; and (iii) additionally, plated cells require much more space compared to the transport in suspension.

Last but not least, hepatocytes lose their metabolic activity in the conventional 2D culture after a few days [15,17]. Therefore, in recent years, an increasing number of approaches have been focused on the cultivation of hepatocytes in 3D culture systems, as a 3D environment is supposed to improve the metabolic function of the cells. In these systems, different matrices, either derived from natural or synthetic compounds, were used to mimic a 3D environment. From these studies it is known, that an ideal scaffold should have an interconnected pore structure and a high porosity to ensure penetration of the cells, as well as adequate diffusion of nutrients to cells and of waste products away from the cells within the scaffold [18].

Cells interact with scaffolds mainly via chemical groups (ligands) on the material surface. Scaffolds synthesized from natural extracellular materials (e.g., collagen) naturally have these ligands in the form of Arg-Gly-Asp (RGD) binding sequences. The ligand density is determined by the specific surface area (within a pore) to which cells may adhere. Thus, the mean pore size of a scaffold represents another key component defining cell attachment, survival, and function [19,20]. In addition to the pore size, porosity and the water-uptake capacity of the scaffold are also important parameters in cell-scaffold interaction. They determine the interconnectivity of the pores, how deep the cells can penetrate into the scaffolds and whether the cells inside the scaffold can be supplied with nutrients [21]. Besides, the stiffness of the surface also has a huge influence on the functionality of the cells [22]. Especially in liver the stiffness is often associated with different disease states. While a healthy liver has a stiffness of approximately 6 kPa, a fibrotic and cirrhotic liver is much stiffer (>12.5 kPa to 75 kPa) [23].

Besides using 3D matrices, fluid-flow systems were also established to preserve the metabolic function of PHHs over a long time period [15]. Although these attempts were able to maintain the metabolic activity of the cells a bit longer than in 2D cultures, up until now all of these recent 3D scaffolds had limitations [18]. The increasing complexity of a model in combination with the high variance of human material makes standardization almost impossible. Additionally, these scaffolds are often not suitable for 96-well plates. Thus, these systems can barely be used for high-throughput

methods. In addition, these systems have been explored so far mainly with rat hepatocytes instead of human ones [24–26], which makes the translation extremely difficult for testing of new drugs.

Thus, the aim of this study was to test the well standardized Optimaix-3D Scaffold, which can be used for several standard plate formats, including 96-well plates, for its suitability for PHHs transport and long-term functional culture. The physical characterization of the novel collagen-based scaffold includes the determination of its pore size, porosity, permeability, water-uptake capacity, and stiffness. It was further tested whether the 3D cultivation allows the cells to be sent more gently and to be cultivated over 10 days without loss of viability. In addition, the influence of the scaffold cultivation on the main metabolic functions (CYP activities, urea, and albumin synthesis) of PHHs was measured for up to 10 days and compared to conventional 2D cultures.

2. Materials and Methods

2.1. Scaffold Manufacturing

The collagen scaffolds (Optimaix-3D) used in these studies were produced by the company Matricel. The scaffold manufacturing process is based on a so-called directional solidification method [27]. In brief, the developed method for scaffold manufacturing starts with the preparation of a homogeneous aqueous dispersion of collagen. In the subsequent controlled freezing process, finger-shaped ice crystals that grow through the dispersion are generated, so that the collagen fibers are not trapped within the ice crystals but concentrate in the interstitial space. During the subsequent freeze-drying, the ice sublimates and the open porous collagen structure remains. This basic collagen scaffold structure is further cross-linked with 1-ethyl-3-(3-dimethylaminopropyl) carbodiimide hydrochloride (EDC) in order to adapt the stability against degradation by cells that are cultivated within the scaffold.

2.2. Physical Characterization of Scaffolds

2.2.1. Pore Size

To analyze the pore size, the organic matrix components of the scaffold were stained with sulforhodamine B (0.08% SRB in 1% acetic acid), which binds to protonated amino acids under acidic conditions. Unbound SRB was removed by washing the scaffolds three times with 1% acetic acid solution. With the red fluorescent signal of the bound SRB, the porous structure of the cryogels could be visualized with a fluorescence microscope (EVOS FL AF 4301, life technologies, Darmstadt, Germany). Using the ImageJ software, version 1.5 (National Institutes of Health, Bethesda, MD, USA), the shape and size of the pores were determined [21].

2.2.2. Porosity

The porosity of the scaffold was calculated using a method published by Shimizu et al. [28]. The porosity in percent was determined using the equation:

$$\text{Porosity (\%)} = \left(1 - \frac{(\text{scaffold wet weight (g)} - \text{scaffold dry weight (g)})}{(\text{scaffold volume (mm}^3\text{) / density of water (g/mm}^3\text{)})} \right) \times 100\%$$

The volume of the scaffolds was calculated based on its diameter (5 mm) and height (1.5 mm) to be 29.5 mm³. The dry weight of the scaffolds in grams was determined with an analytical balance. Scaffolds were then submerged in sterile water for 1 h and were weighed to obtain the wet weight of the scaffolds in grams.

2.2.3. Permeability

The permeability of the scaffold was calculated by a method published recently [29]. Briefly, a stable hydrostatic pressure was applied to the top surface of the porous scaffold. The quantity

of water permeated through the scaffold per minute was weighed and then used to calculate the permeability according to Darcy's law.

$$\text{Porosity } (\mu\text{m}^2) = \frac{\text{viscosity water (Pa} \times \text{s)} \times \frac{\text{water passed through the scaffold mm}^3}{\text{min}}}{\frac{\text{cross sectional area of the scaffold (mm}^2) \times \text{constant pressure (Pa)}}{\text{length of the scaffold (mm)}}},$$

To determine the volume of water that passed through the scaffold per minute, the water was collected and weighed (g) using an analytical balance. Multiplication with the specific density of water (0.997 g/cm³) gave the required volume in mm³.

To determine the constant pressure applied, the height of the water column (90.1 mm) was multiplied by the cross-sectional area of the scaffold (78.5 mm²). The weight of the resulting water volume (in average 2.5 g/s) was calculated to be 150 cm³/min by multiplying the water volume with the specific density of water (0.997 g/cm³). By dividing with the gravitational force (~9.8 m/s²) the constant pressure applied was determined to be 881 Pa.

2.2.4. Water-Uptake and Swelling Ratio

The water-uptake and swelling ratio were obtained according to a previously described method [30]. The water-uptake as well as the swelling ratio was calculated according to the following equations:

$$\text{Swelling ratio (\%)} = \frac{(\text{scaffold wet weight (g)} - \text{scaffold dry weight (g)})}{\text{scaffold dry weight (g)} \times 100},$$

$$\text{Water uptake (\%)} = \frac{(\text{scaffold wet weight (g)} - \text{scaffold dry weight (g)})}{\text{scaffold wet weight (g)} \times 100},$$

The dry and wet weights (in grams) of the scaffolds were determined with an analytical balance as described above.

2.2.5. Matrix Stiffness

The scaffold stiffness is defined by the Young's modulus, which describes the ratio of stress σ and strain ε independent of the size or the shape of samples. Briefly, Optimaix-3D scaffolds (3 mm height \times 10 mm diameter) are compressed four times uniaxial, by a cyclic compression of 10% height, with a velocity of 5 mm/min, using a ZwickiLine Z 2.5TN (Zwick GmbH & Co. KG, Ulm, Germany). The required load is measured real-time by a Xforce HP 5N sensor (Zwick GmbH & Co. KG (Ulm, Germany) The resulting load-deformation curve is converted into a stress-strain curve, using the area and initial sample height. In the region of linear elastic deformation, the Young's modulus [31] is then calculated, using the following formula:

$$\text{Young's modulus (MPa)} = \frac{\text{applied force (N)} \times \text{initial scaffold height (mm)}}{\text{area of the scaffold (mm}^2) \times \text{change in height (mm)}},$$

2.3. Hepatocyte Isolation, Shipment, and Culture

PHHs were isolated from liver resections by a two-step EDTA/collagenase perfusion technique as described previously [32,33]. Double-coded liver pieces used for PHHs isolation were provided by the Biobank of the Department of General, Visceral and Transplantation Surgery in Ludwig-Maximilians University (LMU). This Biobank operates under the administration of the Human Tissue and Cell Research (HTCR) Foundation. The framework of HTCR Foundation [34], which includes obtaining of written informed consent from all donors, has been approved by the ethics committee of the Faculty of Medicine at the LMU (approval number 025-12) as well as the Bavarian State Medical Association (approval number 11142) in Germany.

PHHs were shipped overnight as a cell suspension with up to a maximum of 5×10^7 viable cells per mL Cold Storage Solution (Hepacult GmbH, Martinsried/Planegg, Germany), in cryo-vials on ice [32].

Upon arrival, cells were washed once with PBS. The cell number and viability was determined by Trypan blue exclusion method, using a Neubauer counting chamber. To improve the viability, a Percoll density gradient centrifugation was performed for 20 min at 1300 g (Percoll solution was diluted with PBS to obtain a total density of 1.0675 g/L). The PHHs were washed once with PBS and resuspended in Williams Medium E supplemented with 10% fetal bovine serum, 100 U/mL penicillin, 0.1 mg/mL streptomycin, 15 mM HEPES (pH 7.0–7.6), 1 mM Glutamine, 1 mM sodium pyruvate, 1 mM human insulin, 0.8 µg/mL hydrocortisone and 1% nonessential amino acids. Cells were counted again and seeded onto culture dishes or the Optimaix-3D scaffolds from Matricel.

Both in 2D and 3D 0.3×10^6 million cells were plated. For better cell adherence 24-well culture dishes that were used for 2D culture were coated with rat tail collagen as described [9]. For cell seeding on the scaffold, the so called ‘Drop-on’ seeding method, recommended by the manufacturer, was used [35]. Therefore, cells were re-suspended in the medium at a concentration of 10 million PHHs/mL. 30 µL of this cell suspension was pipetted onto the scaffold to achieve nearly complete rehydration. After an attachment period of 2 h, additional medium was added (500 µL/well, 24-well-plate) to the scaffolds. The scaffolds fit also into a single well of a 96-well plate; however, in order to increase the comparability between 2D and 3D (same amount of medium), 24-well plates were also used for metabolic activity measurements of the 3D culture. To test whether the scaffold was also suitable for the shipping of the PHHs, cells were plated after isolation as described above in 2D and onto Optimaix-3D scaffolds. The exact procedure is schematically shown in Figure 1. Both cultures as well as cells in suspension were sent at 37 °C overnight. At the next day cells were purified as described before and plated out in 2D or onto Optimaix-3D scaffolds at the same concentration as described before. For comparison of the viability of each condition a measurement of resazurin conversion was carried out as described in Section 2.4.4.

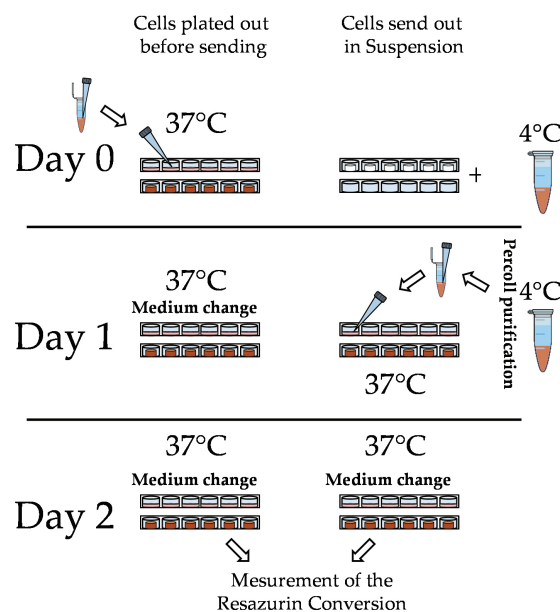


Figure 1. Schematic illustration of the transport schemes: on day 1, the primary human hepatocytes (PHHs) were purified and sent either in suspension or directly plated onto 2D culture plates and Optimaix-3D scaffold. Then, cells were sent at 37 °C (plated cells) or at 4 °C (cells in suspension) overnight. On day 1, the medium was changed in the plated cultures, while the cells in suspension were purified and plated out (2D, Optimaix-3D scaffold). Two days after isolation, a viability determination of all conditions was carried out by measuring resazurin conversion.

2.4. Functional Testing

Main metabolic functions, like urea and albumin production and activities of CYP enzymes were measured on days 3 and 10 of culture. For normalization, Resazurin conversion was determined.

2.4.1. Urea Measurement

The cells were washed once with PBS. Subsequently, the urea quantification was carried out, using a protocol described by Seeliger et al. [11]. Briefly, cells were incubated for 24 h with medium without additives, in the presence or absence of 5 mM NH₄Cl or 5 mM NH₄Cl and 0.1 M ornithine. 80 µL of the supernatant was mixed with 60 µL of *O*-phthalaldehyde solution (1.5 mM *O*-phthalaldehyde, 4 mM Brij-35, 0.75 M H₂SO₄) and 60 µL of NED reagent (2.3 mM *N*-(1 Naphthyl) ethylenediamine dihydrochloride, 0.08 M boric acid, 4 mM Brij-35, 2.25 M H₂SO₄) and incubated for 1 h at 37 °C. The absorbance was measured at 460 nm and compared to a urea standard curve (0–100 µg/mL) on the same plate.

2.4.2. Albumin ELISA

The produced albumin was quantified with the human albumin ELISA kit (E80-129 from Bethyl Laboratories, Montgomery, USA) according to the manufacturer's instructions. Briefly, 96-well-plates were coated with the primary antibody for 1 h at room temperature (RT). After washing five times with washing buffer (50 mM Tris, 140 mM NaCl, 0.05% Tween 20), unspecific binding sites were blocked with blocking solution (50 mM Tris, 140 mM NaCl, 1% BSA) for 1 h at RT. After another 5 washes, albumin standard and sample (diluted 1:50 in sample conjugate buffer) were applied to the plate and incubated for one hour at RT. After another 5 washes, the secondary antibody was added to each well and incubated for 1 h at RT. After the last 5 washes, the luminescence solution (100 mM Tris, 125 nM Luminol, 200 nM p-Coumaric acid, 0.08% 30% H₂O₂ solution) was pipetted into the wells and the luminescence was measured in the Omega plate reader BMG LABTECH, Ortenberg, Germany. The albumin quantity was calculated using a standard curve.

2.4.3. CYP Activity Measurement

CYP enzyme activities of CYP2B6, CYP2D6, CYP2C9 and CYP3A4, being responsible for the metabolism of most drugs [36], were measured as recently described [37]. Briefly, the chosen substrates, the selected concentrations, the incubation times and the measured metabolites are summarized in Table 1. Methanol, which was the initial solvent of the CYP substrates, was removed before use by evaporation, and the substrates were dissolved in culture medium. The cells were incubated with 500 µL of the respective reaction solution. After the described incubation times, the supernatants were removed and frozen at –80 °C until measurement. The enzymatic activity was measured by the company Pharmacelsus (Saarbrücken, Germany) using a LC-HPLC/MS-based methodology [37].

Table 1. Substrates, concentrations, conditions, and measured reactions of the CYP activity measurement.

Substrate	Isoenzyme	Incubation Time in h	Concentration	Reaction
Bupropion	CYP 2B6	1	100 µM	Bupropion-hydroxylation
Diclofenac	CYP 2C9	1	9 µM	Diclofenac-4'-hydroxylation
Testosterone	CYP 3A4	1	50 µM	testosterone-6β-hydroxylation
Bufuralol	CYP 2D6	2	9 µM	Bufuralol-1-hydroxylation

2.4.4. Resazurin Conversion

After each functional test, the wells/scaffolds were washed once with PBS and then incubated with a 0.0025% resazurin solution (in medium) for 1 h at 37 °C. The fluorescence of the produced resorufin was measured at 544 nm/590–10 nm using the Omega Plate Reader [38].

2.4.5. Statistic

Statistical significance of differences between two groups was evaluated by non-parametric Mann-Whitney-U-test. For comparison of the differences between more than two groups, non-parametric Kruskal-Wallis H-test followed by Dunn's multiple comparison test was performed (GraphPad Prism 5.00 Software, San Diego, CA, USA). Data are represented as means \pm SEM of at least three independent experiments ($N \geq 3$). All statistical comparisons were performed two-sided in the sense of an exploratory data analysis using $p < 0.05$ (*), $p < 0.01$ (**), and $p < 0.001$ (***) as level of significance.

3. Results

3.1. Characterization of the Optimaix-3D Collagen Scaffold

Optimaix-3D scaffolds were prepared by a so-called directional solidification method, which includes subsequent freeze-drying cycles [27]. Scaffold properties are summarized in Table 2.

Table 2. Characteristics of Optimaix-3D scaffold.

Optimaix-3D Scaffold	Pore Size (Mean Diameter/ μm)	Porosity (%)	Permeability (μm^2)	Water-Uptake (%)	Swelling-Ratio (%)
Average	88.9	96.3	54.5	97.1	3386.6
Standard Deviation	21.1	0.3	4.0	0.1	127.2

The pore size (mean diameter) of the scaffold, which was measured from four independent scaffolds with the ImageJ software (five pores/scaffold were analyzed), ranged from 55–140 μm , with the most pores being between 80 μm and 100 μm (Figure 2a,c). The porosity of the scaffold that were measured four times independently was approximately 96%. Together with the high permeability of 54 μm^2 , which was measured from three independent scaffolds (three times each scaffold), this is an indicator for a high interconnectivity of the pores [39]. This high porosity even allows visual analysis (light microscopy) of the plated PHHs. Normally, in a scaffold culture, it is not possible to take light micrographs, but the high porosity of the Optimaix-3D scaffolds (height = 1.5 mm) allows enough light to penetrate the scaffold for light microscopy (Figure 2d). The water-uptake of the Optimaix-3D scaffold was >97%. Together with the swelling ratio of 3387%, this represents the strong hydrophilic nature of the scaffold. The dry Optimaix-3D scaffold has a high stiffness of 148 kPa, which allows easy handling of the scaffolds. When soaked with medium, the wet Optimaix-3D scaffold showed a stiffness of nearly 7.5 kPa (Figure 2b) which is comparable to the stiffness of the healthy human liver [23].

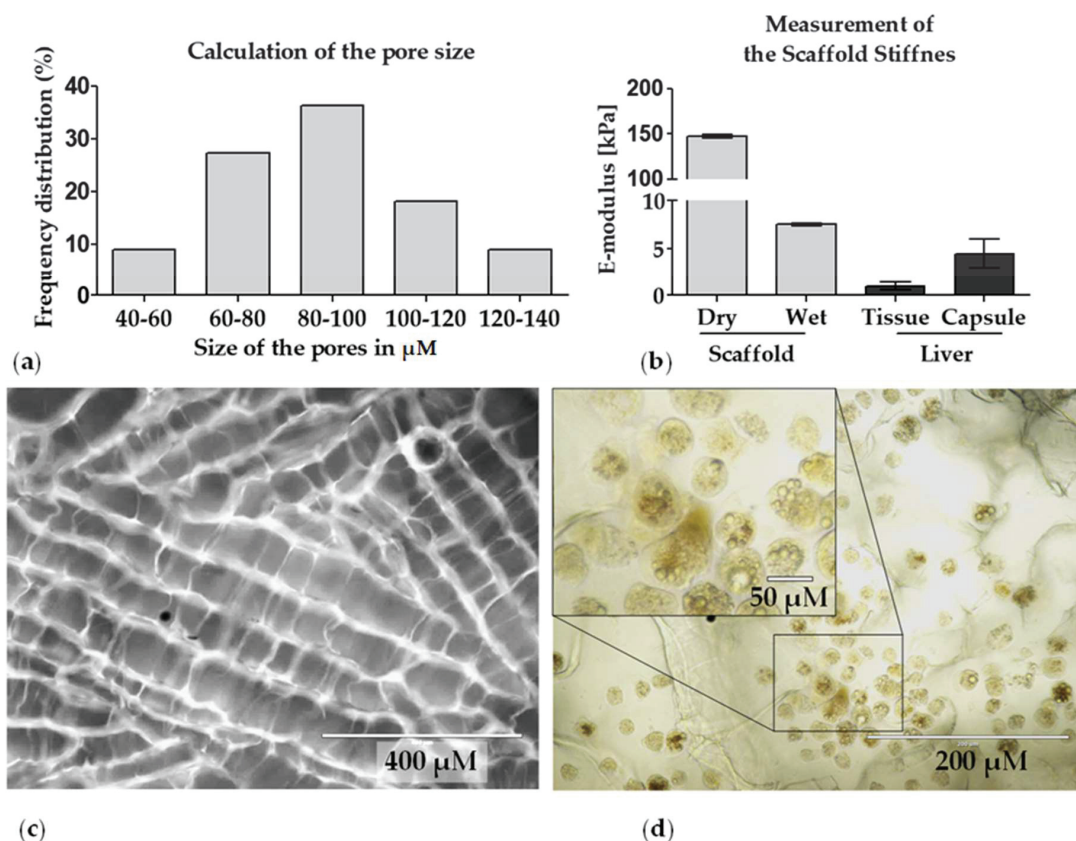


Figure 2. Physical characteristics of the Optimaix-3D scaffold: (a) pore size distribution was determined with the ImageJ software. ($N = 4, n = 5$). (b) The stiffness of the scaffold was measured with the help of a Zwick material testing machine ($N = 4, n = 3$). (c) Representative fluorescent microscopic picture of the pore structure in the Optimaix-3D scaffold. For visualization Optimaix-3D scaffolds were stained with SRB. (d) Microscopic image of the scaffold colonized with PHHs.

3.2. Loss of PHHs During Transport Is Significantly Reduced When Shipped on Optimaix-3D Scaffold

So far, it has not been possible to send PHHs on ice or cryopreserved without a massive loss of function and viability [40,41]. Therefore, we investigated if it is possible to ship PHHs plated onto Optimaix-3D scaffolds (Matricel) compared to conventional 2D culture plates overnight. Nowadays nearly half of the PHHs shipped in suspension in cold storage solution get lost during transport [41], as can be seen in Figure 3a, which include data of nine shipments. An actual comparison that includes data of the 2D/3D shipment experiments can be found in Table 3. This was partly due to the decreased viability of the cells upon arrival (Figure 3b), which raised the need for additional purification step, as the proteases released from the dead PHHs may damage the healthy cells and adversely affect their adherence. Thus, for purification, a Percoll density centrifugation was typically performed, which resulted in increased viability of the cells (Figure 3b) but decreased significantly the number of viable cells (Figure 3a).

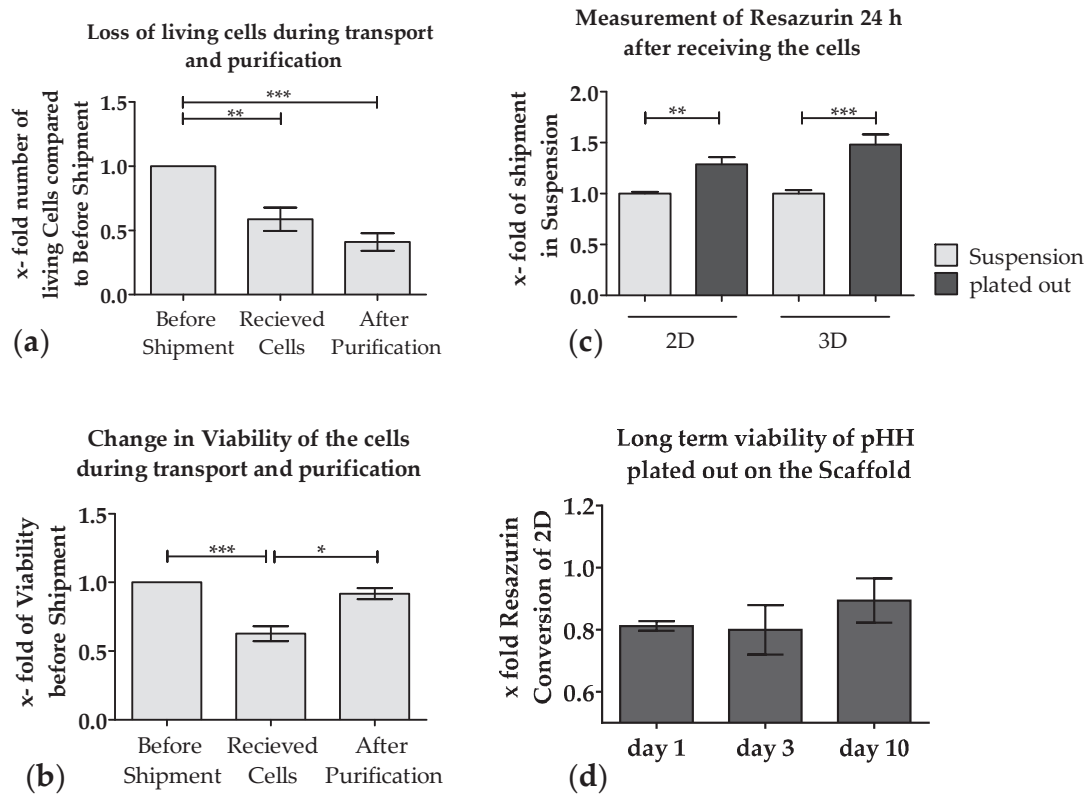


Figure 3. Effect of shipment on the viability and adherence of PHHs. Freshly isolated PHHs were shipped overnight in cold storage solution. Total cell numbers and the viability of the cells were measured before shipping, before and after Percoll purification. **(a)** Amount of living PHHs decreased during transport and purification. **(b)** Viability of PHHs can be increased by using Percoll density purification. **(c)** Viability (Resazurin conversion) of PHHs shipped overnight either adherent or in suspension (with purification and plating upon arrival). Data shown represent an average of $N = 9$ (PHH were shipped and purified nine times independently **(a,b)**). **(c)** ($N = 3, n = 20$) cells were shipped three times independently, cultured both directly on scaffold and onto plates (2D) or in parallel in suspension and then plated after shipment. **(d)** shows long time viability of PHH plated out on scaffold over 10 days that were quantified by measurement of the resazurin conversion (values of 3D were normalized to the values of 2D on the same day $N = 3, n = 3$ (mean \pm SEM). * $p \leq 0.05$; ** $p \leq 0.01$; *** $p \leq 0.01$).

Although the loss in viability resulting from shipment was compensated by the Percoll density purification, the cells that were sent in suspension and subsequently plated showed significantly lower adherence compared to cells directly cultured onto Optimaix-3D scaffolds or on collagen-coated plates (2D) (Figure 3c). When comparing PHHs sent in 2D with those on the Optimaix-3D scaffolds, it is remarkable that the cells on the Optimaix-3D scaffolds survive the shipping better than the cells in 2D-culture (Figure 3c). As shown in Figure 3d, approximately 80% of the cells adhere on the scaffold surface compared to 2D, which can be explained by the fact that some cells are rinsed off after 2 h when medium is added. However, the relative viability on the scaffold is close to the cells cultured in 2D.

Table 3. Loss of living hepatocytes by shipping and subsequent purification.

	Amount of Living Cells before Shipment (in mio)	Viability before Shipment	Amount of Living Cells after Percoll Purification (in mio)	Viability after Percoll
Donor 1	119	80%	54	76%
Donor 2	111	85%	43	74%
Donor 3	78	83%	25	80%
Average	103	82%	40	77%

3.3. Metabolic Function of PHHs on the Optimaix-3D Collagen Scaffold

The next step of the present study was to monitor the hepatic function of the PHHs cultured on this new scaffold in comparison to the conventional 2D culture. It is well recognized that cultured PHHs rapidly lose their metabolic function *in vitro* [12]. Therefore, to investigate if PHHs cultured on Optimaix-3D scaffolds maintain their metabolic function longer than in 2D cultures, we analyzed the main hepatic functions like CYP activity, urea, and albumin synthesis on days 3 and 10 of culture.

3.3.1. 3D Environment by the Optimaix-3D Scaffolds Supports Urea Production in PHHs

The basal urea production of PHHs cultured on Optimaix-3D scaffolds was approximately 50% higher compared to PHHs in 2D cultures. Furthermore, basic urea production of PHHs in 2D cultures rapidly declined within 10 days. In contrast, the basic urea production in 3D cultures remained constant over 10 days (Figure 4a). Upon addition of ammonia, cells in a 3D culture produced significantly more urea on day 3 and day 10 than in 2D cultures, clearly demonstrating an improved detoxification capacity in 3D cultures (Figure 4b). In 2D cultures, however, this could only be obtained on day 3, when cultures were supplemented with the co-factor ornithine (Figure 4c).

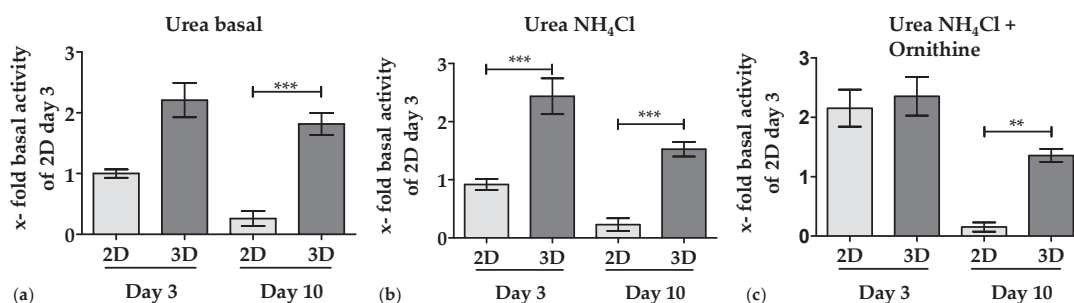


Figure 4. Urea production and ammonia detoxification. (a) Basic urea production by PHHs over 24 h in 2D (bright bars) and 3D (dark bars) cultures. (b) Urea production by PHHs after 24 h following the incubation with NH_4Cl in 2D (bright bars) and 3D (dark bars) cultures. (c) Urea production by PHHs after 24 h incubation with NH_4Cl plus ornithine in 2D (bright bars) and 3D (dark bars) cultures. Data were normalized to the resazurin conversion (viable cells). Data represent an average of $N = 3$ independent experiments ($n = 3$). Bars represent mean \pm SEM ** $p \leq 0.01$; *** $p \leq 0.001$ as indicated.

3.3.2. 3D Environment of the Optimaix-3D Scaffolds Favors Albumin Synthesis in PHHs

Another important function of the liver is the synthesis of albumin [42]. As depicted in Figure 5, after 3 days of culture, twice as much albumin production by PHHs was measured in Optimaix-3D cultures compared to the same PHHs cultured in 2D. On day 10, albumin production drops in 2D cultures by approximately 38% compared to day 3. On the contrary, in Optimaix-3D cultures, albumin synthesis even increased with increasing culture time, resulting in a 16-fold higher albumin production in Optimaix-3D cultures compared to 2D cultures.

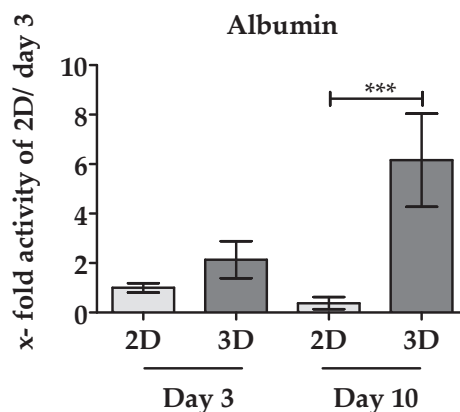


Figure 5. Synthesis of albumin by PHHs in 2D and 3D culture. Supernatants after 24 h incubation time were collected on day 3 and 10 of culture. Albumin production was measured by human Albumin ELISA. Results of 2D cultures are given as bright bars, results of Optimaix-3D cultures are given in dark bars. Data were normalized to the resazurin conversion (viable cells). Data represent an average of N = 4 independent experiments (n = 3). Bars represent mean ± SEM. *** p ≤ 0.001 as indicated.

3.3.3. The Activity of CYP Enzymes was Constant in 3D over 10 Days

Basal activities of CYP3A4 and CYP2D6 in PHHs were relatively low when cultured in 2D, thus no significant drop in activity was detected over 10 days. In contrast, both enzyme activities were more than doubled when PHHs were cultured on Optimaix-3D scaffolds. CYP3A4 activity remained more or less constant over the culture period of 10 days (Figure 6a). On the contrary CYP2D6 activity showed a time-dependent decrease over 10 days in 3D culture but remained higher than in 2D when PHHs were cultured on Optimaix-3D scaffolds (Figure 6d). At day 3 in culture CYP2C9 and CYP2B6 activities were comparable between PHHs in 2D and in 3D (Optimaix-3D scaffolds). While their activity strongly declined in 2D cultures, they remained stable in 3D (Optimaix-3D scaffolds) cultures over 10 days (Figure 6b,c).

For all measured CYP activities, a high donor variance was detected, which is in agreement with the literature [43]. For a better overview, activities of each donor are also presented in a heat map in Figure 6e.

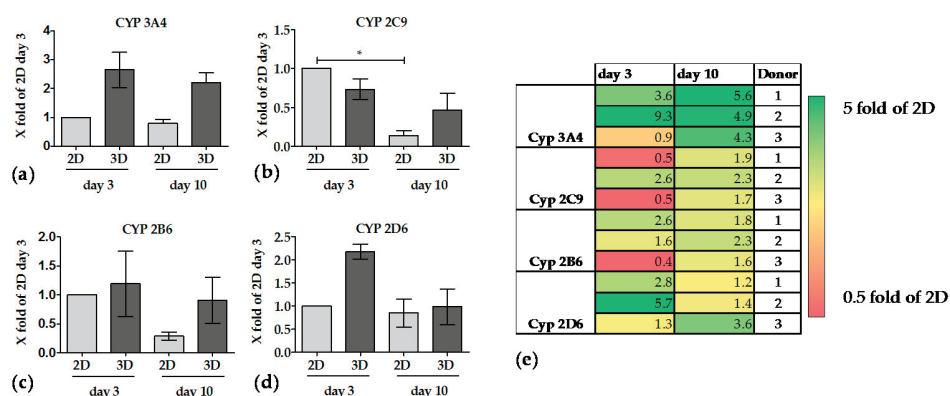


Figure 6. Activity of CYP enzymes, which are involved in drug metabolism. Supernatants were collected after incubation with specific substrates as indicated in Materials and Methods at days 3 and 10 of culture. (a–d) shows the CYP activities of CYP 3A4, 2C9, 2B6 and CYP 2D6. Values of 2D cultures are summarized in bright bars. Values of 3D cultures are summarized in dark bars. Bars represent mean ± SEM of three independent experiments (N = 3, n = 3) * p ≤ 0.05 as indicated. (e) Overview of the individual donor differences is represented in a heat map showing the CYP activities in 3D cultures compared to 2D cultures.

4. Discussion

For many years, it has been known that due to large inter-species differences in metabolism, animal models are not able to predict hepatotoxicity in humans reliably [4]. Although great efforts have been made to overcome this deficit in the past 20 years, so far no reproducible system exists to predict *in vitro* metabolism in humans. It is widely accepted that neither hepatic cell lines nor stem cell-derived hepatocyte-like cells are able to mimic the metabolism of drugs *in vitro* [15]. The only exception is the so-called 'gold standard' of PHHs, which show a metabolic profile comparable to the *in vivo* situation for a limited time. However, the use of PHHs as a routine test system for the pharmaceutical industry is limited because of several reasons.

First, the cells are not always or at any time available in sufficient (large) quantities. Additionally, they can only be isolated in specialized centers from liver capsules, which are obtained during large tumor operations. Besides, the fact that the cells' metabolism might be affected due to the medication of the patients, the isolated cells need to be distributed to academic, regulatory affairs or industrial research institutions. Thus, PHHs need to be shipped from point A to point B. Nowadays, there are three standard methods for this procedure: (i) either the cells are cryopreserved; (ii) sent in suspension at 4 °C; or (iii) directly plated onto culture plates [15]. Each of these procedures has advantages and disadvantages. While experiments using cryopreserved PHHs can be planned ahead, the cells show a massive loss of viability associated with a reduced metabolic activity after thawing [40,41]. As also demonstrated in the present manuscript, transport of PHHs at 4 °C in suspension causes a massive loss of cell viability. Although the viability could be significantly improved by Percoll density gradient centrifugation, the overall cell numbers were strongly reduced. Furthermore, their adherence and consequently metabolic activity was affected, which is in line with our laboratory observations and other published reports [40,41]. In order to prevent this, many attempts have been made to improve cryopreservation and thawing of PHHs [15], or to optimize the solution, in which the cells are transported in cell suspension [16]. Despite all efforts that have been made in recent years, the shipping results remain unsatisfactory, with a frequently high loss of cell viability, cell attachment and function [14,44].

Another limitation is the conventional monolayer culture technique for PHHs, which is far from its natural environment and results in a reduced and limited metabolic capacity [12,45]. According to PubMed in the past 10 years over 600 papers on hepatocytes and 3D culture were published. This research led to substantial improvement in the field of bioengineering with the aim to culture PHHs in an environment that resembles the liver [18]. Nevertheless, direct comparison among the different scaffolds and systems is barely possible due to the various technologies used. Custom-made scaffolds frequently lack reproducibility. Thus, we have chosen here a scaffold, named Optimaix-3D, which is reproducibly manufactured (by Matricel) in a controlled freezing process from a defined collagen dispersion. This procedure results in an even pore structure (mean pore diameter of 88.9 μm) [46]. Studies have shown that PHHs require the interaction with Extracellular matrix (ECM) components, such as collagen, to maintain their specific functions [47]. The ECM protein collagen plays an important role in the maintenance of organs and tissues [48]. It is therefore often used as a biomaterial in medical application and in bioengineering [49]. It is biodegradable and in contrast to albumin or gelatin only weakly antigenic [48]. Collagen is also one of the important ECM proteins of the healthy liver [50]. As such, the Optimaix-3D scaffold, which is made of collagen, could potentially be an ideal carrier for PHHs for transport purposes and/or metabolic studies.

In our hands, the hydrated Optimaix-3D scaffold showed a stiffness of approximately 7.5 kPa. This stiffness is in the range of a healthy liver, which has a stiffness between 2.9 kPa and 6 kPa, depending on individual differences and the method used for measurement [23,51,52]. Compared to plastic, which has a stiffness in the gigapascal range [22], the scaffold is in terms of the stiffness within the physiological range of a healthy human liver [23,53]. The stiffness of the scaffold seems to be important not only for *in vitro* studies [22] but also *in vivo*, as studies have clearly shown that liver stiffness negatively influences the drug metabolism in patients [53].

There are not many studies regarding the ideal pore size of scaffolds for the cultivation of PHHs. However, Ranucci et al. described that cell adherence as well as albumin production is particularly high at pore sizes of 10 μm and 80 μm , but not at a pore size of 18 μm . The authors explain their findings with the fact that the cell morphology seems to be best preserved in cultures with a pore size of 10 μm , while cell-cell contacts might be best formed in 80 μm pores [20]. Optimal cell-cell-interaction might be responsible for the improved functionality of the Optimaix-3D scaffold which has a pore size of 88 μm . As the authors of this study further explained, the effects of 80 μm pores is particularly high in terms of functionality, when the cell concentration is relatively high to form cell-cell contacts [20]. This is also the case in the Optimaix scaffold, on which 300,000 cells are cultured at a scaffold volume of 30 mm^3 . From physical scaffold characterization as well as microscopic analyses of cryogels, it is well known that interconnected pores allow better cell migration and deliver an optimal nutrient supply [21]. Compared with other cryogels described in the literature for the cultivation of various cell types, including liver cells e.g., Damania et al. 2018, Amirikia et al. 2017, and Galperin et al. 2010 [54–56], Optimaix-3D scaffolds have a very ordered and directed pore structure, which is most likely the reason for the very high permeability and high flow rates measured. Since hepatic cord structures are also composed of microscale alignments of linear unit structures [57], the Optimaix-3D scaffolds might imitate this natural environment as seen in Figure 2c.

We first tested if Optimaix-3D scaffolds could serve as an alternative approach for commonly used cryopreservation PHHs or shipping in cell suspension at 4 $^{\circ}\text{C}$. We and others have clearly shown [15,44] that the shipment of PHHs in suspension results frequently in a significant loss in quantity and viability of cells. Although the percentage of viable cells can be largely restored by Percoll density gradient centrifugation, the damage caused by the cooling cannot be compensated, resulting in a lower cell attachment and reduced function [58,59]. It is noteworthy that PHHs shipped on scaffold survived the transport much better than PHHs plated directly onto conventional culture plates in the monolayer technology (Figure 3c) and have a better metabolic function. A comparison of different shipment methods which also include cryopreservation of the cell could be found in Table 4. On an Optimaix-3D scaffold, with a height of 3 mm, 500,000 PHHs can be seeded. This scaffold easily fits into a cavity of a 96-well-plate. In contrast, to plate the same amount of cells in 2D requires 20–25 cavities of a 96-well-plate. The seeding efficiency on the scaffold is approximately 80% compared to 2D, which is comparable to that of other scaffolds described in the literature [60].

Table 4. Comparison of various shipment methods.

Shipment Method	Survival of the Cells after Shipment	Adherence Time before Shipment	Advantages	Disadvantages	Ref.
Suspension	Low	No	Cells can be plated out by the recipient on demand	Cell loss during shipment, Reduced cell attachment metabolic capacity in culture	[14,44,59]
Cryopreserved hepatocytes	Low	No	Cells can be used anytime, anywhere	Massive cell loss during freezing/thawing, Low metabolic activity	[14,40]
2D culture	High	4 h	Cells can be plated in the different well-plate formats	Cell shipment requires a large volume. Risk of contamination	[15,17]
Optimaix-3D Collagen Scaffold	High	2 h	Seeding large cell numbers in a low volume Cells maintain metabolic functions over 10 days	Cell detachment difficult	This work

Furthermore, it is possible that the cell amount, which can be loaded on the scaffold, can be further improved by applying a fluid flow. A study carried out by Thevenot et al., which compared various seeding methods, showed that the dynamic seeding methods allowed a higher loading capacity [61].

So far, it is extremely difficult to detach cells quantitatively from scaffolds without a substantial cell loss [62]. Therefore, the methods for cell de-attachment from scaffolds should be improved in the future.

Our data of cultured PHHs on Optimaix-3D scaffolds showed significantly improved cell viability and an increased metabolic activity of cells over a culture period of 10 days.

With regard to the urea production in 2D cultures, we observed that urea production remains largely constant between day 3 and day 10. It is noteworthy that PHHs cultured onto the Optimaix-3D showed a continuous higher basal urea formation than 2D cultures over ten days. In 2D cultures, the addition of ammonium chloride plus ornithine results in an increased urea production, on day 3 but not on day 10. However, the addition of ammonia alone is not metabolized by primary human hepatocytes. It is well known that cellular ATP is necessary for ammonia uptake into the urea cycle to form urea [63]. Therefore it is conceivable, that a high cellular loss of ATP during liver cell transportation in suspension [14] is responsible for the lack and/or delayed urea formation. In the same line of evidence Liu et al. clearly showed that cold storage of cells reduces the metabolic testing capacity, including the ammonia detoxification capacity [64]. Based on these data, it seemed that hepatocytes recover faster in 3D than in 2D cultures, suggesting a lack of additional cofactors necessary to fully transform ammonia into urea.

In the case of albumin synthesis, there is even an increase in albumin production between day 3 and day 10, when PHHs are cultured on Optimaix-3D scaffolds, while in 2D a drop in albumin production was observed. This finding supports ours and others hypotheses that the 3D environment in general and the Optimaix-3D scaffold in particular maintains the metabolic function of PHHs [18]. An explanation for this high basal urea and albumin synthesis observed in our Optimaix-3D cultures could be the naturally occurring zonation of the liver. Cells that receive high levels of nutrients and oxygen (periportal cells) are more involved in urea detoxification and albumin production, while perivenous cells (low oxygen) are involved in drug metabolism [65]. The open pore structure of Optimaix-3D scaffolds may result in better oxygen and nutrient supply for liver cells. This effect may be dominant at the beginning of the experiment, while the cells in 2D are still in a differentiated state. In the course of the experiment, the cultivation of cells on a scaffold leads to a slowdown of de-differentiation, which would be another key advantage over 2D cell cultivation [15].

Thus, it is not surprising that the effect of the 3D cultivation on CYP activity was not as pronounced early in the culture period, when CYP activities in 3D were only slightly higher than in 2D cultures. However, over a 10-day culture period, the CYP activities remained fairly constant in the PHHs cultured on the Optimaix-3D scaffolds, while CYP activities in 2D rapidly declined. This is in line with another report, showing that a 3D environment has a positive effect on the CYP activities [18]. When we compare our results to already published data, the CYP enzyme activities in 2D confirm or previous findings. As shown by Lin et al. the RNA expression of CYP2B6 and CYP2C9 has been declined after a period of five days. In case of CYP3A4 there is almost no RNA and Protein expression after 7 days [10]. In recent years, much has happened to improve the cultivation of hepatocytes, especially the cultivation of hepatocytes in spheroids or on scaffolds show positive results. For example, the culture of rat hepatocytes on a silk scaffold showed an increase in albumin production over 10 days, however, only in co-culture with hepatic stellate cells. The urea production at later time points is also higher both in 3D and in the 2D co-culture. The metabolic activity of the CYP enzymes (CYP3A, CYP1A2) was only measured after 5 days. However, at this time point the cells in co-culture seemed to improve the metabolic function more than in the 3D system. However, the authors have not normalized these data, therefore, it cannot be ruled out that the positive effects seen in the 2D co-culture is only due to an improved survival of the hepatocytes [24]. Damania et al. have published a cryogel coated with extracellular liver matrix which should mimic the natural ECM of the liver. These authors observed an improved functionality of human hepatocytes plated on coated scaffolds, including albumin and urea production, especially on day 3. Unfortunately, a comparison with the corresponding 2D culture was not performed [54]. In the same line of evidence,

Bell et al. showed a significantly improved maintenance of hepatocyte function by cultivating liver cells in a spheroid culture. Depending on the investigated CYP enzymes, maintenance of the activity was possible over 10–14 days. In this publication, liver cells in spheroids were compared with cells cultured in a Matrigel sandwich. Interestingly, Bell et al. performed their experiments in a 96-well format using ultra-low attachment plates with very low cell numbers (1500 viable cells per well), which allows the use of high-throughput methods to a certain extent. Since the formation of spheroids takes approximately 7–10 days, a direct comparison with 2D and the same primary hepatocytes is impossible, because of declining enzyme activity in 2D. Therefore, the authors have normalized their results to the amount of seeded cells [66] which does not really represent the cell number on the day of the measurement. Siltans et al. used another method to form hepatocyte spheroids: microcapsules with a liquid core and poly-(ethylene glycol) gel shell that allowed to form spheroids with only 150 cells per capsule. However, several capsules were plated per well, to obtain measurable results [5]. While the encapsulated hepatocytes showed an increased albumin production between day 4 and day 6, the corresponding 2D culture showed a decrease in albumin production. These authors claim that urea production on day 8 is highest in the encapsulated hepatocytes compared to the controls, but no comparison to other time points has been performed. In addition, the authors have executed co-cultures with murine fibroblasts, which slightly improved the metabolic function of the hepatocyte spheroid culture. The albumin production of the co-culture setup showed a continuous increase over 12 days. A direct comparison among different papers of other metabolic functions is again difficult since these authors have chosen only one particular time point [67].

In summary, many other 3D cultivation methods have been published with partly very complex compositions, which makes a controlled standardization and comparison to other models almost impossible. However, the scaffold described in this manuscript is characterized by a high degree of reproducibility. In addition, Optimaix can be applied to routine 96-well-plates that allows a high-throughput process. Other recent work with spheroid/organoid 3D cultures seems to be similar to standardize to 96-well formats; however, the normalization of results to the applied cell number and a direct comparison with 2D is difficult [68,69]. The reason is that the spheroid formation takes time, which does not allow a direct comparison with the basal PHH metabolic activities [70]. Finally, there is also evidence showing no metabolic improvement of hepatocytes cultured onto 3D spheroids compared to conventional 2D culture [71].

5. Conclusions

Our results clearly show that the viability of the cells can be maintained significantly better by transport on the Optimaix-3D Scaffold from Matricel compared to the conventional shipment as a cooled suspension. Additionally, it is possible to utilize this scaffold to maintain the main hepatic functions, such as drug metabolism, urea production, and albumin synthesis over a period of 10 days. Furthermore, the scaffold has nearly the same stiffness as a healthy liver. With its high porosity and permeability, it is not only ideal for supplying the cells with nutrients, but also for use within a bioreactor. Due to the good biocompatibility of the collagen used for the scaffold, it might be also possible to use a scaffold seeded with PHHs in regenerative medicine.

Author Contributions: A.K.N. and M.R. conceived and designed the experiments; M.R. performed the experiments; M.R. and V.H. analyzed the data; F.S. and L.H.H.O.D. developed the scaffolds and provided them for the experiments, S.M.L.L. and L.G. were responsible for human hepatocyte isolation and shipment, M.R., S.E., and A.K.N. wrote the paper.

Funding: This project was funded by the Federal Ministry for Economic Affairs and Energy within the framework of the ZIM program (AZ: ZF4301401CS6, ZF4301001CS6, ZF4301101CS6).

Conflicts of Interest: The authors declare no conflict of interest.

Abbreviations

PHH	Primary human hepatocytes
NIH	National Institutes of Health
RGD	Arginylglycylaspartic acid
CYP	CYP450 monooxygenase
ECM	Extracellular matrix
EDC	1-ethyl-3-(3-dimethylaminopropyl)carbodiimide hydrochloride

References

1. Kaplowitz, N. Idiosyncratic drug hepatotoxicity. *Nat. Rev. Drug Discov.* **2005**, *4*, 489–499. [[CrossRef](#)] [[PubMed](#)]
2. Olson, H.; Betton, G.; Robinson, D.; Thomas, K.; Monro, A.; Kolaja, G.; Lilly, P.; Sanders, J.; Sipes, G.; Bracken, W.; et al. Concordance of the toxicity of pharmaceuticals in humans and in animals. *Regul. Toxicol. Pharmacol.* **2000**, *32*, 56–67. [[CrossRef](#)] [[PubMed](#)]
3. Ballet, F. Hepatotoxicity in drug development: Detection, significance and solutions. *J. Hepatol.* **1997**, *26* (Suppl. 2), 26–36. [[CrossRef](#)]
4. Lewis, D.F.; Ioannides, C.; Parke, D.V. Cytochromes P450 and species differences in xenobiotic metabolism and activation of carcinogen. *Environ. Health Perspect.* **1998**, *106*, 633–641. [[CrossRef](#)] [[PubMed](#)]
5. Paul, S.M.; Mytelka, D.S.; Dunwiddie, C.T.; Persinger, C.C.; Munos, B.H.; Lindborg, S.R.; Schacht, A.L. How to improve R&D productivity: The pharmaceutical industry's grand challenge. *Nat. Rev. Drug Discov.* **2010**, *9*, 203–214. [[PubMed](#)]
6. Soldatow, V.Y.; LeCluyse, E.L.; Griffith, L.G.; Rusyn, I. In vitro models for liver toxicity testing. *Toxicol. Res.* **2013**, *2*, 23–39. [[CrossRef](#)] [[PubMed](#)]
7. Ramachandran, S.D.; Vivarès, A.; Klieber, S.; Hewitt, N.J.; Muenst, B.; Heinz, S.; Walles, H.; Braspenning, J. Applicability of second-generation upcyte@human hepatocytes for use in CYP inhibition and induction studies. *Pharmacol. Res. Perspect.* **2015**, *3*, e00161. [[CrossRef](#)] [[PubMed](#)]
8. Kafert-Kasting, S.; Alexandrova, K.; Barthold, M.; Laube, B.; Friedrich, G.; Arseniev, L.; Hengstler, J.G. Enzyme induction in cryopreserved human hepatocyte cultures. *Toxicology* **2006**, *220*, 117–125. [[CrossRef](#)] [[PubMed](#)]
9. Knobeloch, D.; Ehnert, S.; Schyschka, L.; Büchler, P.; Schoenberg, M.; Kleeff, J.; Thasler, W.E.; Nussler, N.C.; Godoy, P.; Hengstler, J.; et al. Human hepatocytes: Isolation, culture, and quality procedures. In *Human Cell Culture Protocols*; Mitry, R.R., Hughes, R.D., Eds.; Humana Press: Totowa, NJ, USA, 2012; pp. 99–120.
10. Lin, J.; Schyschka, L.; Mühl-Benninghaus, R.; Neumann, J.; Hao, L.; Nussler, N.; Dooley, S.; Liu, L.; Stöckle, U.; Nussler, A.K.; et al. Comparative analysis of phase I and II enzyme activities in 5 hepatic cell lines identifies Huh-7 and HCC-T cells with the highest potential to study drug metabolism. *Arch. Toxicol.* **2012**, *86*, 87–95. [[CrossRef](#)] [[PubMed](#)]
11. Seeliger, C.; Culmes, M.; Schyschka, L.; Yan, X.; Damm, G.; Wang, Z.; Kleeff, J.; Thasler, W.E.; Hengstler, J.; Stöckle, U. Decrease of global methylation improves significantly hepatic differentiation of Ad-MSCs: Possible future application for urea detoxification. *Cell Transplant.* **2013**, *22*, 119–131. [[CrossRef](#)] [[PubMed](#)]
12. Godoy, P.; Schmidt-Heck, W.; Natarajan, K.; Lucendo-Villarin, B.; Szkolnicka, D.; Asplund, A.; Bjorquist, P.; Widera, A.; Stoeber, R.; Campos, G.; et al. Gene networks and transcription factor motifs defining the differentiation of stem cells into hepatocyte-like cells. *J. Hepatol.* **2015**, *63*, 934–942. [[CrossRef](#)] [[PubMed](#)]
13. Zeilinger, K.; Freyer, N.; Damm, G.; Seehofer, D.; Knöspel, F. Cell sources for in vitro human liver cell culture models. *Exp. Biol. Med.* **2016**, *241*, 1684–1698. [[CrossRef](#)] [[PubMed](#)]
14. Stéphenne, X.; Najimi, M.; Sokal, E.M. Hepatocyte cryopreservation: Is it time to change the strategy? *World J. Gastroenterol.* **2010**, *16*, 1–14. [[PubMed](#)]
15. Godoy, P.; Hewitt, N.; Albrecht, U.; Andersen, M.; Ansari, N.; Bhattacharya, S.; Bode, J.; Bolleyn, J.; Borner, C.; Böttger, J.; et al. Recent advances in 2D and 3D in vitro systems using primary hepatocytes, alternative hepatocyte sources and non-parenchymal liver cells and their use in investigating mechanisms of hepatotoxicity, cell signaling and ADME. *Arch. Toxicol.* **2013**, *87*, 1315–1530. [[CrossRef](#)] [[PubMed](#)]

16. Ostrowska, A.; Gu, K.; Bode, D.C.; Van Buskirk, R.G. Hypothermic storage of isolated human hepatocytes: A comparison between university of wisconsin solution and a hypothermosol platform. *Arch. Toxicol.* **2009**, *83*, 493–502. [[CrossRef](#)] [[PubMed](#)]
17. Godoy, P.; Hengstler, J.G.; Ilkavets, I.; Meyer, C.; Bachmann, A.; Muller, A.; Tuschl, G.; Mueller, S.O.; Dooley, S. Extracellular matrix modulates sensitivity of hepatocytes to fibroblastoid dedifferentiation and transforming growth factor beta-induced apoptosis. *Hepatology* **2009**, *49*, 2031–2043. [[CrossRef](#)] [[PubMed](#)]
18. Bachmann, A.; Moll, M.; Gottwald, E.; Nies, C.; Zantl, R.; Wagner, H.; Burkhardt, B.; Sanchez, J.J.; Ladurner, R.; Thasler, W.; et al. 3D cultivation techniques for primary human hepatocytes. *Microarrays* **2015**, *4*, 64–83. [[CrossRef](#)] [[PubMed](#)]
19. O'Brien, F.J. Biomaterials & scaffolds for tissue engineering. *Mater. Today* **2011**, *14*, 88–95.
20. Ranucci, C.S.; Kumar, A.; Batra, S.P.; Moghe, P.V. Control of hepatocyte function on collagen foams: Sizing matrix pores toward selective induction of 2-D and 3-D cellular morphogenesis. *Biomaterials* **2000**, *21*, 783–793. [[CrossRef](#)]
21. Kumari, J.; Karande, A.A.; Kumar, A. Combined effect of cryogel matrix and temperature-reversible soluble–insoluble polymer for the development of in vitro human liver tissue. *ACS Appl. Mater. Interfaces* **2016**, *8*, 264–277. [[CrossRef](#)] [[PubMed](#)]
22. Wells, R.G. The role of matrix stiffness in regulating cell behavior. *Hepatology* **2008**, *47*, 1394–1400. [[CrossRef](#)] [[PubMed](#)]
23. Mueller, S.; Sandrin, L. Liver stiffness: A novel parameter for the diagnosis of liver disease. *Hepat. Med. Evid. Res.* **2010**, *2*, 49–67. [[CrossRef](#)]
24. Wei, G.; Wang, J.; Lv, Q.; Liu, M.; Xu, H.; Zhang, H.; Jin, L.; Yu, J.; Wang, X. Three-dimensional coculture of primary hepatocytes and stellate cells in silk scaffold improves hepatic morphology and functionality in vitro. *J. Biomed. Mater. Res. Part A* **2018**, *106*, 2171–2180. [[CrossRef](#)] [[PubMed](#)]
25. Yan, S.; Wei, J.; Liu, Y.; Zhang, H.; Chen, J.; Li, X. Hepatocyte spheroid culture on fibrous scaffolds with grafted functional ligands as an in vitro model for predicting drug metabolism and hepatotoxicity. *Acta Biomater.* **2015**, *28*, 138–148. [[CrossRef](#)] [[PubMed](#)]
26. Rajendran, D.; Hussain, A.; Yip, D.; Parekh, A.; Shirrao, A.; Cho, C.H. Long-term liver-specific functions of hepatocytes in electrospun chitosan nanofiber scaffolds coated with fibronectin. *J. Biomed. Mater. Res. Part A* **2017**, *105*, 2119–2128. [[CrossRef](#)] [[PubMed](#)]
27. Heschel, I.; Rau, G. Method for Producing Porous Structures. U.S. Patent No. 6,447,701 B1, 10 September 2002.
28. Shimizu, K.; Ito, A.; Honda, H. Enhanced cell-seeding into 3D porous scaffolds by use of magnetite nanoparticles. *J. Biomed. Mater. Res. Part B Appl. Biomater.* **2005**, *77*, 265–272. [[CrossRef](#)] [[PubMed](#)]
29. Fan, J.; Jia, X.; Huang, Y.; Fu, B.M.; Fan, Y. Greater scaffold permeability promotes growth of osteoblastic cells in a perfused bioreactor. *J. Tissue Eng. Regen. Med.* **2015**, *9*, E210–E218. [[CrossRef](#)] [[PubMed](#)]
30. Chung, E.J.; Ju, H.W.; Park, H.J.; Park, C.H. Three-layered scaffolds for artificial esophagus using poly(ϵ -caprolactone) nanofibers and silk fibroin: An experimental study in a rat model. *J. Biomed. Mater. Res. Part A* **2015**, *103*, 2057–2065. [[CrossRef](#)] [[PubMed](#)]
31. Tamjid, E.; Simchi, A.; Dunlop, J.W.C.; Fratzl, P.; Bagheri, R.; Vossoughi, M. Tissue growth into three-dimensional composite scaffolds with controlled micro-features and nanotopographical surfaces. *J. Biomed. Mater. Res. Part A* **2013**, *101*, 2796–2807. [[CrossRef](#)] [[PubMed](#)]
32. Lee, S.M.L.; Schelcher, C.; Demmel, M.; Hauner, M.; Thasler, W.E. Isolation of human hepatocytes by a two-step collagenase perfusion procedure. *J. Vis. Exp.* **2013**, *79*, 50615. [[CrossRef](#)] [[PubMed](#)]
33. Pfeiffer, E.; Kegel, V.; Zeilinger, K.; Hengstler, J.G.; Nussler, A.K.; Seehofer, D.; Damm, G. Featured article: Isolation, characterization, and cultivation of human hepatocytes and non-parenchymal liver cells. *Exp. Biol. Med.* **2015**, *240*, 645–656. [[CrossRef](#)] [[PubMed](#)]
34. Thasler, W.E.; Weiss, T.S.; Schillhorn, K.; Stoll, P.-T.; Irrgang, B.; Jauch, K.-W. Charitable state-controlled foundation human tissue and cell research: Ethic and legal aspects in the supply of surgically removed human tissue for research in the academic and commercial sector in Germany. *Cell Tissue Bank.* **2003**, *4*, 49–56. [[CrossRef](#)] [[PubMed](#)]
35. Jurgens, W.J.; Kroeze, R.J.; Bank, R.A.; Ritt, M.J.; Helder, M.N. Rapid attachment of adipose stromal cells on resorbable polymeric scaffolds facilitates the one-step surgical procedure for cartilage and bone tissue engineering purposes. *J. Orthop. Res.* **2011**, *29*, 853–860. [[CrossRef](#)] [[PubMed](#)]

36. Zanger, U.M.; Schwab, M. Cytochrome p450 enzymes in drug metabolism: Regulation of gene expression, enzyme activities, and impact of genetic variation. *Pharmacol. Ther.* **2013**, *138*, 103–141. [[CrossRef](#)] [[PubMed](#)]
37. Hoffmann, S.A.; Müller-Vieira, U.; Biemel, K.; Knobloch, D.; Heydel, S.; Lübberstedt, M.; Nüssler, A.K.; Andersson Tommy, B.; Gerlach, J.C.; Zeilinger, K. Analysis of drug metabolism activities in a miniaturized liver cell bioreactor for use in pharmacological studies. *Biotechnol. Bioeng.* **2012**, *109*, 3172–3181. [[CrossRef](#)] [[PubMed](#)]
38. Ehnert, S.; Falldorf, K.; Fentz, A.-K.; Ziegler, P.; Schröter, S.; Freude, T.; Ochs, B.G.; Stacke, C.; Ronniger, M.; Sachtleben, J.; et al. Primary human osteoblasts with reduced alkaline phosphatase and matrix mineralization baseline capacity are responsive to extremely low frequency pulsed electromagnetic field exposure—Clinical implication possible. *Bone Rep.* **2015**, *3*, 48–56. [[CrossRef](#)] [[PubMed](#)]
39. Loh, Q.L.; Choong, C. Three-dimensional scaffolds for tissue engineering applications: Role of porosity and pore size. *Tissue Eng. Part B Rev.* **2013**, *19*, 485–502. [[CrossRef](#)] [[PubMed](#)]
40. Hengstler, J.G.; Utesch, D.; Steinberg, P.; Platt, K.L.; Diener, B.; Ringel, M.; Swales, N.; Fischer, T.; Biefang, K.; Gerl, M. Cryopreserved primary hepatocytes as a constantly available in vitro model for the evaluation of human and animal drug metabolism and enzyme induction. *Drug Metab. Rev.* **2000**, *32*, 81–118. [[CrossRef](#)] [[PubMed](#)]
41. Duret, C.; Moreno, D.; Balasiddaiah, A.; Roux, S.; Briolotti, P.; Raulet, E.; Herrero, A.; Ramet, H.; Biron-Andreani, C.; Gerbal-Chaloin, S.; et al. Cold preservation of human adult hepatocytes for liver cell therapy. *Cell Transplant.* **2015**, *24*, 2541–2555. [[CrossRef](#)] [[PubMed](#)]
42. Arias, I.M.; Wolkoff, A.W.; Boyer, J.L.; Shafritz, D.A.; Fausto, N.; Alter, H.J.; Cohen, D.E. *The Liver: Biology and Pathobiology*; John Wiley & Sons: Hoboken, NJ, USA, 2011.
43. Zhang, H.; Gao, N.; Tian, X.; Liu, T.; Fang, Y.; Zhou, J.; Wen, Q.; Xu, B.; Qi, B.; Gao, J.; et al. Content and activity of human liver microsomal protein and prediction of individual hepatic clearance in vivo. *Sci. Rep.* **2015**, *5*, 17671. [[CrossRef](#)] [[PubMed](#)]
44. Pless-Petig, G.; Singer, B.B.; Rauen, U. Cold storage of rat hepatocyte suspensions for one week in a customized cold storage solution—Preservation of cell attachment and metabolism. *PLoS ONE* **2012**, *7*, e40444. [[CrossRef](#)] [[PubMed](#)]
45. Schyschka, L.; Sanchez, J.J.; Wang, Z.; Burkhardt, B.; Muller-Vieira, U.; Zeilinger, K.; Bachmann, A.; Nadalin, S.; Damm, G.; Nussler, A.K. Hepatic 3D cultures but not 2D cultures preserve specific transporter activity for acetaminophen-induced hepatotoxicity. *Arch. Toxicol.* **2013**, *87*, 1581–1593. [[CrossRef](#)] [[PubMed](#)]
46. Schoof, H.; Apel, J.; Heschel, I.; Rau, G. Control of pore structure and size in freeze-dried collagen sponges. *J. Biomed. Mater. Res.* **2001**, *58*, 352–357. [[CrossRef](#)] [[PubMed](#)]
47. Baiocchi, A.; Montaldo, C.; Conigliaro, A.; Grimaldi, A.; Correani, V.; Mura, F.; Ciccocanti, F.; Rotiroti, N.; Brenna, A.; Montalbano, M.; et al. Extracellular matrix molecular remodeling in human liver fibrosis evolution. *PLoS ONE* **2016**, *11*, e0151736. [[CrossRef](#)] [[PubMed](#)]
48. Lee, C.H.; Singla, A.; Lee, Y. Biomedical applications of collagen. *Int. J. Pharm.* **2001**, *221*, 1–22. [[CrossRef](#)]
49. Khan, R.; Khan, M.H. Use of collagen as a biomaterial: An update. *J. Indian Soc. Periodontol.* **2013**, *17*, 539–542. [[CrossRef](#)] [[PubMed](#)]
50. Martinez-Hernandez, A.; Amenta, P.S. The hepatic extracellular matrix. *Virchows Arch. A Pathol. Anat. Histopathol.* **1993**, *423*, 77–84. [[CrossRef](#)] [[PubMed](#)]
51. Yin, M.; Talwalkar, J.A.; Glaser, K.J.; Manduca, A.; Grimm, R.C.; Rossman, P.J.; Fidler, J.L.; Ehman, R.L. A preliminary assessment of hepatic fibrosis with magnetic resonance elastography. *Clin. Gastroenterol. Hepatol.* **2007**, *5*, 1207–1213.e2. [[CrossRef](#)] [[PubMed](#)]
52. Fung, J.; Lee, C.-K.; Chan, M.; Seto, W.-K.; Wong, D.K.-H.; Lai, C.-L.; Yuen, M.-F. Defining normal liver stiffness range in a normal healthy chinese population without liver disease. *PLoS ONE* **2013**, *8*, e85067. [[CrossRef](#)] [[PubMed](#)]
53. Theile, D.; Haefeli, W.E.; Seitz, H.K.; Millonig, G.; Weiss, J.; Mueller, S. Association of liver stiffness with hepatic expression of pharmacokinetically important genes in alcoholic liver disease. *Alcohol. Clin. Exp. Res.* **2013**, *37* (Suppl. 1), E17–E22. [[CrossRef](#)] [[PubMed](#)]
54. Damania, A.; Kumar, A.; Teotia, A.K.; Kimura, H.; Kamihira, M.; Ijima, H.; Sarin, S.K.; Kumar, A. Decellularized liver matrix-modified cryogel scaffolds as potential hepatocyte carriers in bioartificial liver support systems and implantable liver constructs. *ACS Appl. Mater. Interfaces* **2018**, *10*, 114–126. [[CrossRef](#)] [[PubMed](#)]

55. Amirikia, M.; Shariatzadeh, S.M.A.; Jorsaraei, S.G.A.; Soleimani-Mehranjani, M. Impact of pre-incubation time of silk fibroin scaffolds in culture medium on cell proliferation and attachment. *Tissue Cell* **2017**, *49*, 657–663. [[CrossRef](#)] [[PubMed](#)]
56. Galperin, A.; Long, T.J.; Ratner, B.D. Degradable, thermo-sensitive poly(*N*-isopropyl acrylamide)-based scaffolds with controlled porosity for tissue engineering applications. *Biomacromolecules* **2010**, *11*, 2583–2592. [[CrossRef](#)] [[PubMed](#)]
57. Yamada, M.; Sugaya, S.; Naganuma, Y.; Seki, M. Microfluidic synthesis of chemically and physically anisotropic hydrogel microfibers for guided cell growth and networking. *Soft Matter* **2012**, *8*, 3122–3130. [[CrossRef](#)]
58. Berendsen, T.A.; Izamis, M.L.; Xu, H.; Liu, Q.; Hertl, M.; Berthiaume, F.; Yarmush, M.L.; Uygun, K. Hepatocyte viability and atp content decrease linearly over time during conventional cold storage of rat liver grafts. *Transplant. Proc.* **2011**, *43*, 1484–1488. [[CrossRef](#)] [[PubMed](#)]
59. Rauen, U.; Polzar, B.; Stephan, H.; Mannherz, H.G.; Groot, H.D. Cold-induced apoptosis in cultured hepatocytes and liver endothelial cells: Mediation by reactive oxygen species. *FASEB J.* **1999**, *13*, 155–168. [[CrossRef](#)] [[PubMed](#)]
60. Kim, Y.B.; Kim, G. Rapid-prototyped collagen scaffolds reinforced with PCL/ β -TCP nanofibres to obtain high cell seeding efficiency and enhanced mechanical properties for bone tissue regeneration. *J. Mater. Chem.* **2012**, *22*, 16880–16889. [[CrossRef](#)]
61. Thevenot, P.; Nair, A.; Dey, J.; Yang, J.; Tang, L. Method to analyze three-dimensional cell distribution and infiltration in degradable scaffolds. *Tissue Eng. Part C Methods* **2008**, *14*, 319–331. [[CrossRef](#)] [[PubMed](#)]
62. Kurashina, Y.; Takemura, K.; Miyata, S.; Komotori, J.; Koyama, T. Effective cell collection method using collagenase and ultrasonic vibration. *Biomicrofluidics* **2014**, *8*, 054118. [[CrossRef](#)] [[PubMed](#)]
63. Watford, M. The urea cycle: Teaching intermediary metabolism in a physiological setting. *Biochem. Mol. Biol. Educ.* **2006**, *31*, 289–297. [[CrossRef](#)]
64. Liu, H.; Yu, Y.; Glorioso, J.; Mao, S.; Rodysil, B.; Amiot, B.P.; Rinaldo, P.; Nyberg, S.L. Cold storage of rat hepatocyte spheroids. *Cell Transplant.* **2014**, *23*, 819–830. [[CrossRef](#)] [[PubMed](#)]
65. Schleicher, J.; Tokarski, C.; Marbach, E.; Matz-Soja, M.; Zellmer, S.; Gebhardt, R.; Schuster, S. Zonation of hepatic fatty acid metabolism—The diversity of its regulation and the benefit of modeling. *Biochim. Biophys. Acta* **2015**, *1851*, 641–656. [[CrossRef](#)] [[PubMed](#)]
66. Bell, C.C.; Dankers, A.C.A.; Lauschke, V.M.; Sison-Young, R.; Jenkins, R.; Rowe, C.; Goldring, C.E.; Park, K.; Regan, S.L.; Walker, T.; et al. Comparison of hepatic 2D sandwich cultures and 3D spheroids for long-term toxicity applications: A multicenter study. *Toxicol. Sci.* **2018**, *162*, 655–666. [[CrossRef](#)] [[PubMed](#)]
67. Siltanen, C.; Diakatou, M.; Lowen, J.; Haque, A.; Rahimian, A.; Stybayeva, G.; Revzin, A. One step fabrication of hydrogel microcapsules with hollow core for assembly and cultivation of hepatocyte spheroids. *Acta Biomater.* **2017**, *50*, 428–436. [[CrossRef](#)] [[PubMed](#)]
68. Rothschild, D.E.; Srinivasan, T.; Aponte-Santiago, L.A.; Shen, X.; Allen, I.C. The ex vivo culture and pattern recognition receptor stimulation of mouse intestinal organoids. *J. Vis. Exp.* **2016**, *111*, 54033. [[CrossRef](#)] [[PubMed](#)]
69. Fey, S.J.; Wrzesinski, K. Determination of drug toxicity using 3D spheroids constructed from an immortal human hepatocyte cell line. *Toxicol. Sci.* **2012**, *127*, 403–411. [[CrossRef](#)] [[PubMed](#)]
70. Bell, C.C.; Hendriks, D.F.G.; Moro, S.M.L.; Ellis, E.; Walsh, J.; Renblom, A.; Fredriksson Puigvert, L.; Dankers, A.C.A.; Jacobs, F.; Snoeys, J.; et al. Characterization of primary human hepatocyte spheroids as a model system for drug-induced liver injury, liver function and disease. *Sci. Rep.* **2016**, *6*, 25187. [[CrossRef](#)] [[PubMed](#)]
71. Ullah, I.; Kim, Y.; Lim, M.; Oh, K.B.; Hwang, S.; Shin, Y.; Kim, Y.; Im, G.-S.; Hur, T.-Y.; Ock, S.A. In vitro 3-D culture demonstrates incompetence in improving maintenance ability of primary hepatocytes. *Anim. Cells Syst.* **2017**, *21*, 332–340. [[CrossRef](#)]



Chapter 4: Publication II

Ruoß, M.; Damm, G.; Vosough, M.; Ehret, L.; Grom-Baumgarten, C.; Petkov, M.; Nadalin, S.; Ladurner, R.; Seehofer, D.; Nussler, A.; Sajadian, S. **Epigenetic Modifications of the Liver Tumor Cell Line HepG2 Increase Their Drug Metabolic Capacity.** Int. J. Mol. Sci. 2019, 20, 347.

4.1 Synopsis:

In addition to PHH, different hepatic tumor cell lines are used as *in vitro* model within the first stages of drug development. (Lin et al., 2012). In contrast to PHH, these cells have the advantage that they are available in sufficient quantities at any time and in any place (Donato et al., 2015, Sison-Young et al., 2017). The fact that all cells of a cell line have the same genetic background allows a high degree of standardization of the results. The major disadvantage of using hepatic cell lines is their low metabolic activity compared to PHH. This factor results inter alia from de-differentiation processes that occur during tumor development, including epigenetic changes as well as processes such as the so-called EMT, which can also be observed during tumor progression in a wide variety of tumors (Hanahan and Weinberg, 2011, Ingelman-Sundberg et al., 2013, Sciacovelli and Frezza, 2017). However, as various studies have shown, it is possible to partially reverse these existing epigenetic changes (Snykers et al., 2009, Seeliger et al., 2013). Furthermore, halting proliferation as well as a shift of the EMT status toward a more epithelial phenotype, can be achieved. This phenomenon is possible by treating the cells with the epigenetically active agents such as the chemotherapeutic agent 5-AZA and vitamin C (Sajadian et al., 2016). Trans-differentiation of mesenchymal stem cells to hepatocyte-like cells can also be improved by the use of 5-AZA (Seeliger et al., 2013).

This study aimed to investigate whether it is possible to epigenetically reactivate hepatic tumor cells by using 5-AZA in combination with vitamin C to increase their metabolic activity. At the same time, we tested whether the addition of insulin and hydrocortisone to the culture medium is suitable to further increase the cells' metabolic activity. Insulin and hydrocortisone are usually added to the culture

medium during the cultivation of hepatocytes, but not for the cultivation of hepatic cell lines. (Michalopoulos and Pitot, 1975, Kinoshita and Miyajima, 2002).

In this study, we first investigated how the expression of different chromatin-modifying enzymes differs between human hepatocytes and different hepatic cell lines (HepG2, Huh7, HLE, and AKN1). At the same time, we tested the influence of the treatment of the cells with 5-AZA and vitamin C on the expression of different chromatin-modifying enzymes of the individual cell lines. All tested cell lines differ significantly from PHH in the expression of various chromatin-modifying enzymes. A comparison of the different cell lines revealed that the expression profile of the hepatoma cell line HepG2 is most similar to the PHH and differs significantly from the expression profile of the other tested cell lines. In contrast to these cell lines, the expression of the different chromatin-modifying enzymes in HepG2 cells is generally downregulated compared to PHH, whereas the opposite occurs in the other cell lines. Due to the fact that HepG2 cells are most similar in their expression profile to the PHH, we used these cells for additional experiments.

We demonstrated that the expression profile of genes known to play an essential role in the metabolism of human hepatocytes can be influenced positively by treatment with vitamin C alone, but especially in combination with 5-AZA. We obtained these results using an Epigenetic Chromatin Modification Enzyme PCR Array and confirmed them mainly by quantitative polymerase chain reaction (qPCR). The use of different housekeeping factors can explain some deviations between the array and the qPCR. The qPCR-based gene analysis also showed that insulin and hydrocortisone do not influence the expression of chromatin-modifying enzymes.

In subsequent experiments, we showed that treatment with 5-AZA and vitamin C positively influences the expression of different epithelial genes (E-cadherin, CK18, and HNF4 α) and leads to a downregulation of the EMT marker gene Snail. Additional treatment with insulin and hydrocortisone exerted a positive influence on the expression of the epithelial marker genes E-cadherin and CK18.

Furthermore, the expression and activity of various CYP enzymes involved in the metabolism of drugs tended to be increased by treatment with 5-AZA and vitamin C, especially when we treated the cells with insulin and hydrocortisone. However, it became clear that the measured gene expression, as well as the measured CYP activity of HepG2, differed several fold from PHH. A possible cause for the significant differences in the expression and activity of CYP enzymes may be the massive deregulation of various genes, such as SUV39H1, SMYD3, SETDB2, ESCO2, and AURK A and B, all of which we identified using the Epigenetic Chromatin Modification Enzyme PCR Array. We did not identify an influence of these genes on the metabolic activity of PHH, but is very likely that their expression is de-regulated in comparison to fresh isolated PHH in all tested cell lines and, to a lesser extent, in de-differentiated PHH on day 7 in culture. Besides, we found that regardless of the tested cell line, treatment with 5-AZA and vitamin C shows no or only a slight positive effect on these genes.

In summary, this study showed that treatment with 5-AZA and vitamin C positively influences the expression of certain chromatin-modifying enzymes as well as the EMT status of the HepG2 cells. However, this alteration did not significantly improve the expression and activity of the CYP enzymes. We consider the massive deregulation of various other chromatin-modifying enzymes as a possible cause for this discrepancy. For the first time, we also identified a possible association between these enzymes and the metabolic activity of hepatocytes.



Article

Epigenetic Modifications of the Liver Tumor Cell Line HepG2 Increase Their Drug Metabolic Capacity

Marc Ruoff^{1,†}, Georg Damm^{2,†}, Massoud Vosough³, Lisa Ehret¹, Carl Grom-Baumgarten¹, Martin Petkov¹, Silvio Naddalin⁴, Ruth Ladurner⁴, Daniel Seehofer², Andreas Nussler^{1,*} and Sahar Sajadian¹

¹ Siegfried Weller Institute, BG Trauma Clinic, Eberhard Karls University Tübingen, 72076 Tübingen, Germany; m.ruoss@hotmail.de (M.R.); lisa.ehret@gmx.de (L.E.); carlgrom-baumgarten@web.de (C.G.-B.); petkov.martin12@gmail.com (M.P.); sahar.sajadian@gmail.com (S.S.)

² Department of Hepatobiliary Surgery and Visceral Transplantation, University of Leipzig, 04103 Leipzig, Germany; georg.damm@medizin.uni-leipzig.de (G.D.); daniel.seehofer@medizin.uni-leipzig.de (D.S.)

³ Royan Institute for Stem Cell Biology and Technology, Department of Stem Cells and Developmental Biology, Tehran 16635-148, Iran; masvos@yahoo.com

⁴ Department of General, Visceral and Transplant Surgery, University Hospital Tübingen, 72076 Tübingen, Germany; silvio.nadalin@med.uni-tuebingen.de (S.N.); ruth.ladurner@med.uni-tuebingen.de (R.L.)

* Correspondence: andreas.nuessler@gmail.com; Tel.: +49-7071-606-1065

† These authors contributed equally to this work.

Received: 20 December 2018; Accepted: 14 January 2019; Published: 16 January 2019



Abstract: Although human liver tumor cells have reduced metabolic functions as compared to primary human hepatocytes (PHH) they are widely used for pre-screening tests of drug metabolism and toxicity. The aim of the present study was to modify liver cancer cell lines in order to improve their drug-metabolizing activities towards PHH. It is well-known that epigenetics is strongly modified in tumor cells and that epigenetic regulators influence the expression and function of Cytochrome P450 (CYP) enzymes through altering crucial transcription factors responsible for drug-metabolizing enzymes. Therefore, we screened the epigenetic status of four different liver cancer cell lines (Huh7, HLE, HepG2 and AKN-1) which were reported to have metabolizing drug activities. Our results showed that HepG2 cells demonstrated the highest similarity compared to PHH. Thus, we modified the epigenetic status of HepG2 cells towards 'normal' liver cells by 5-Azacytidine (5-AZA) and Vitamin C exposure. Then, mRNA expression of Epithelial-mesenchymal transition (EMT) marker SNAIL and CYP enzymes were measured by PCR and determinate specific drug metabolites, associated with CYP enzymes by LC/MS. Our results demonstrated an epigenetic shift in HepG2 cells towards PHH after exposure to 5-AZA and Vitamin C which resulted in a higher expression and activity of specific drug metabolizing CYP enzymes. Finally, we observed that 5-AZA and Vitamin C led to an increased expression of Hepatocyte nuclear factor 4 α (HNF4 α) and E-Cadherin and a significant down regulation of Snail1 (SNAIL), the key transcriptional repressor of E-Cadherin. Our study shows, that certain phase I genes and their enzyme activities are increased by epigenetic modification in HepG2 cells with a concomitant reduction of EMT marker gene SNAIL. The enhancing of liver specific functions in hepatoma cells using epigenetic modifiers opens new opportunities for the usage of cell lines as a potential liver in vitro model for drug testing and development.

Keywords: tumor cells; epigenetic reprogramming; drug metabolism; hepatoma cell lines; primary human hepatocytes

1. Introduction

Drug metabolism is understood to mean the biochemical process which describes the modification of drugs, which has the purpose to inactivate a substance and excrete it from the body. Changes in the gene expression of enzymes specialized in drug metabolism may result in altered metabolism of the respective substance [1]. In recent years, it has been shown in many studies that the epigenetic regulation of drug-metabolizing enzymes is an important mechanism here. Epigenetic regulation occurs in three stages: 1. nucleosome positioning 2. histone modification 3. DNA methylation [2]. Recent studies have revealed that epigenetic factors regulate the expression of drug-metabolizing enzymes and the drug transporter [1,3]. Over recent years, modifying the epigenetic status of genes responsible for increasing Cytochrome P450 (CYP) enzyme activities attracted more attention [4]. Epigenetic modifications are closely linked to the so-called Epithelial-mesenchymal transition (EMT) [5]. The EMT process not only has a pronounced influence on cell metabolism but also plays an important role in the degree of differentiation of the cells, embryogenesis, liver fibrosis and metastasis of cancer cells [6,7]. EMT additionally enables an increased immunosuppression and drug resistance, which correlates with the epigenetic status of the tumor cell [8]. EMT in hepatocytes is associated with an overexpression of Snail1 (SNAIL), which downregulates the key epithelial marker gene E-Cadherin and other hepatic differentiation key factors such as HNF4 α [8,9]. It was shown that the most important hepatic genes like Hepatocyte nuclear factor 4 α (HNF4 α) are influenced by epigenetic regulators such as HDACi (Histone deacetylase inhibitors) and DNMTi (DNA methyltransferase inhibitors) [10]. Epigenetic modification promotes growth arrest and up-regulates the expression of the hepatic key regulator gene *HNF4 α* in various hepatoma cells which induces increased CYP expression and Albumin production [11]. Therefore, modifying and triggering the epigenetic state of hepatoma cell lines may change the expression of genes responsible for CYP activities. Recently, we have demonstrated that the cytidine analogue 5-Azacytidine (5-AZA) and Vitamin C reduce the gene and protein expression of SNAIL in the Hepatocellular carcinoma (HCC) cell lines Huh7 and HLE [12]. Various studies focused on the effect of DNMTi such as 5-AZA and 5-Aza -2'-deoxycytidine (5-AZA-dC) on the expression of crucial phase I and II biotransformation genes and some of them suggested improvement of the CYP3A4, CYP3A7, CYP1B, UDP-Glucuronosyltransferase-2B15 and Glutathione S-transferase P1 gene expression [10]. Additionally, it is known that insulin contributes to the preservation of hepatocytes morphology and the glucocorticoids support the maintenance of differentiation which is crucial for the function of CYPs [13,14].

Therefore, the overall aim of this study was to improve the metabolic function of liver tumor cell lines towards primary human hepatocytes (PHH) by modifying their epigenetic status. First, we have examined the expression level of epigenetic modifying enzymes in four hepatoma cell lines (HepG2, Huh7, HLE and AKN1) that have been reported having less liver metabolic functions [15,16] than freshly isolated PHH. The cell line HepG2 shows the highest similarity in its epigenetic profile compared to PHH was used for further testing. Here we have shown how the expression levels of metabolic related genes and enzyme activities change after treatment with Vitamin C in combination with 5-AZA. Moreover, we investigated the influence of these changes on the EMT and the hepatic key regulator genes. Finally, we tested the effect of classical media supplements from hepatocyte culture media, such as insulin and hydrocortisone on CYP activity in hepatoma cell lines, that are usually not included in the maintenance medium of these hepatoma cell lines [15] may further improve the hepatic metabolic function of liver tumor cells.

2. Results

2.1. The Regulation of the Epigenetic Enzymes in HepG2 is Most Closely Comparable to the Expression of Primary Human Hepatocytes

For epigenetic characterization of the investigated liver cell lines, we investigated the expression of chromatin remodeling enzymes and compared to the results to PHH. For the characterization, we used

the Human Epigenetic Chromatin Modification Enzymes PCR Array from QIAGEN. The analysis of the real-time PCR results revealed that each individual tumor cell line showed an individual profile of chromatin-modifying genes compared to human hepatocytes (Figure 1, Supplementary Figure S1). The largest differences in the pattern of chromatin modifying proteins were seen in the Huh7 cells compared to PHH, whereas HepG2 cells showed the highest similarity to PHH among all tested liver tumor cell lines. Therefore, in the further course of the study we have focused on the usage of the cell line HepG2. Then, we tested the possibility whether or not 5-AZA and/or Vitamin C incubation reduces existing epigenetic differences compared to PHH and whether these epigenetic modifications result in an increase of the metabolic function of the HepG2 cell line.

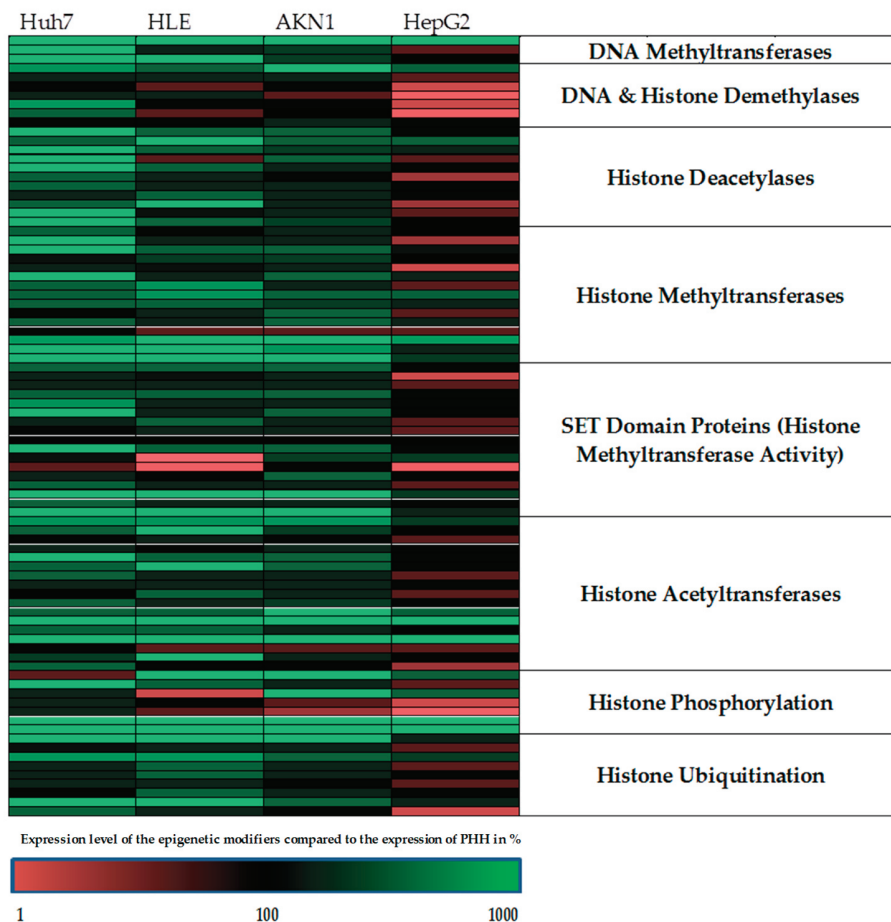


Figure 1. Summary of Human Epigenetic Chromatin Modification Enzymes PCR Array. The expression of 84 chromatin modification genes of four different hepatic cell lines in comparison with fresh isolated primary human hepatocytes (PHH) was shown as a heat map. The green color shows an upregulation of epigenetic modifier genes compared to PHH whereas the red color shows a downregulation of the corresponding genes compared to PHH.

2.2. Treatment of HepG2 with Epigenetic Modifying Compounds Revealed a Positive Impact on the Expression of Genes From Xenobiotic Metabolism

Since the HepG2 cell line showed epigenetically the highest similarity to PHH, this cell line was chosen for further investigations. Exposure of HepG2 cells to 5-AZA and Vitamin C resulted in dramatic changes in the expression of chromatin-modifying enzymes (Figure 2) that are known for their significant role in the maintenance of metabolic properties of hepatocytes. The stimulation with Vitamin C alone also leads to changes, but to a lesser extent, and therefore the combination of 5-AZA plus Vitamin C was used for the further experiments. The expression of all 84 measured genes can be

found in the Supplementary Materials section (Supplementary Figure S2). As shown in Figure 2 the treatment of the cells with 5-AZA plus Vitamin C has an effect on the expression level of most of the investigated genes.

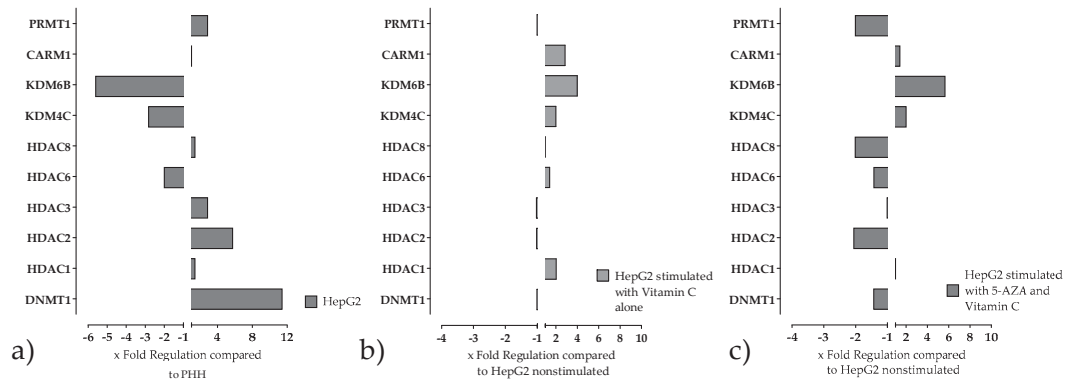


Figure 2. Expression of chromatin modifying genes in HepG2 cells before and after stimulation with Vitamin C alone or in combination with 5-Azacytidine (5-AZA) was measured by using the Chromatin Modification Array. Genes responsible for the maintenance of metabolic properties of primary human hepatocytes (PHH) are selected. (a) Expression of chromatin modification genes in HepG2 compared to PHH (b) Changes in the expression of chromatin modification genes in HepG2 caused by treatment with Vitamin C compared to non-stimulated HepG2 cells. (c) Changes in the expression of chromatin modification genes in HepG2 caused by 5-AZA in combination with Vitamin C compared to non-stimulated HepG2 cells.

2.3. Stimulation of HepG2 Cells with Epigenetic Modifying Compounds Result in Changes in Gene Expression of Epigenetic Modifying Enzymes

The results of the Chromatin Modification Array have been validated by qPCR. Additionally, it was tested, whether insulin and hydrocortisone show a positive effect on the expression of the measured genes. These two substances were chosen because it is well known that they play an important role in hepatic differentiation and maintenance of the function of PHH in vitro.

As shown in Figure 3 The treatment of cells with 5-AZA and Vitamin C with/without insulin and hydrocortisone changed the expression of all measured genes compared to non-treated one. The treatment decreased the level of the mRNA expression of histone deacetylase (*HDAC*) 1 and 2, which reached the level of PHH.

In contrast, lysine demethylase 6B (*KDM6B*) gene expression increased significantly by 5-AZA and Vitamin C, although the expression level didn't reach the level of PHH. The addition of insulin and hydrocortisone to the treatment showed a further improvement for lysine demethylase 4C (*KDM4C*) compared to treatment with only 5-AZA and Vitamin C stimulated cells. All other investigated genes are not affected by additional treatment.

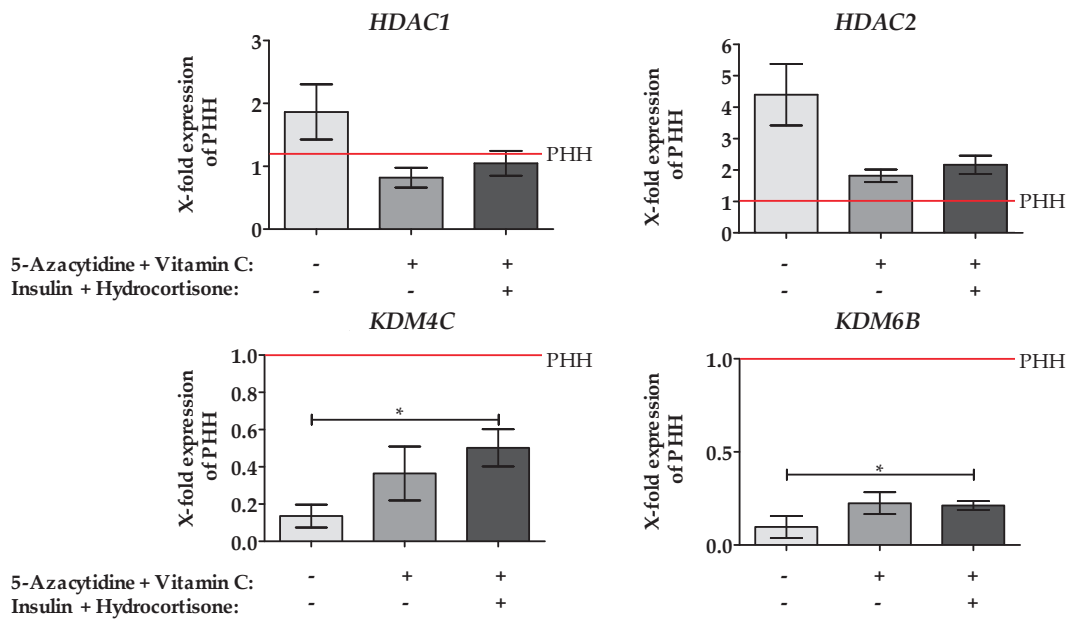


Figure 3. Effect of epigenetic modifying compounds on the expression of Chromatin Modifying enzymes. The expression levels of different chromatin modifying enzymes were measured by qRT-PCR. Unstimulated HepG2 cells (grey bars), as well as HepG2 cells after 48 h stimulation with 10 μ M 5-AZA plus 0.5 mM Vitamin C with (dark bars)/without (black bars) Insulin and hydrocortisone, were used. As a control, freshly isolated hepatocytes were used, (red line). Values were normalized to *GAPDH* and represent the mean of $N = 3$, $n = 3$. For the positive control a pooled sample of five different primary human hepatocyte (PHH) donors was used. Bars represent mean \pm SEM * $p \leq 0.05$ as indicated.

2.4. Stimulation of HepG2 Cells with 5-AZA Plus Vitamin C Led to the Downregulation of the EMT Marker Gene *SNAIL*, an Increase of Epithelial Marker Genes and the Hepatic Key Regulator *HNF4 α*

In our previous study, we have shown, treating hepatoma cell lines with 5-AZA and Vitamin C decreased *SNAIL* expression which is associated with an increased expression of the epithelial marker gene *E-Cadherin* [12]. As shown in Figure 4, we found similar results in the hepatoblastoma cell line HepG2. Interestingly, adding insulin and hydrocortisone to the medium enhance the expression *E-Cadherin* more than threefold compared to PHH. The expression of the epithelial gene *Cytokeratin 18 (CK18)* was increased by the treatment with 5-AZA plus Vitamin C and almost reached the level of PHH by further addition of insulin and hydrocortisone. Furthermore, we observed a slight change in *HNF4 α* gene expression after incubation of HepG2 cells with 5-AZA plus Vitamin C, which was not further increased after insulin and hydrocortisone supplementation. Although the treatment with 5-AZA and Vitamin C significantly increased *HNF4 α* expression, it was still less than 10% of *HNF4 α* expression observed in PHH.

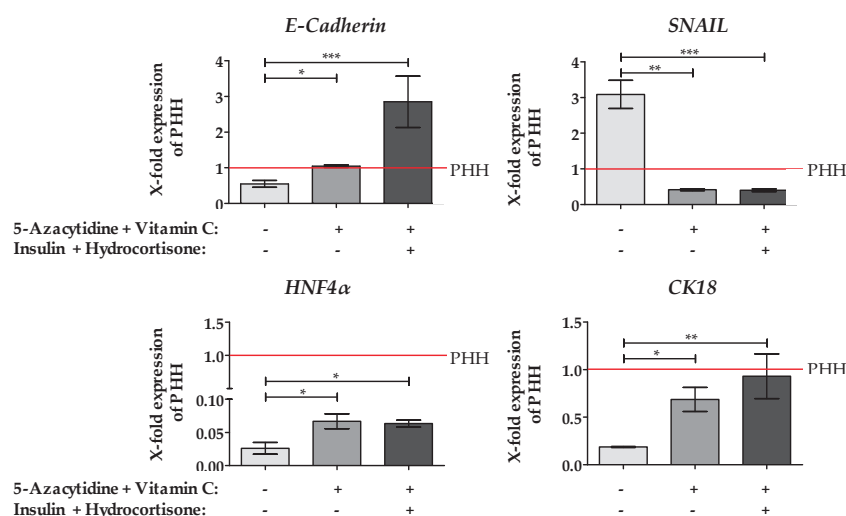


Figure 4. Effect of epigenetic modifying compounds on the expression of epithelial and EMT marker genes. Treatment of the cells with 10 μM 5-Azacytidine (5-AZA) plus 0.5 mM Vitamin C (dark bars) and in the presence of insulin plus hydrocortisone (black bars) resulted in significant changes of epithelial and EMT marker genes. The expression level of the EMT marker Snail1 (*SNAIL*), the epithelial marker genes *E-Cadherin* and Cytokeratin 18 (*CK18*) and the hepatic key regulator gene Hepatocyte nuclear factor 4α (*HNF4α*) were measured by qRT-PCR. Unstimulated HepG2 cells (grey bars) as well as PHH (red line) served as control and reference culture. Values were normalized to *GAPDH* and represent the mean of $N = 3$, $n = 3$. As positive reference served a pool of five different primary human hepatocyte (PHH) donors. Bars represent Mean ± SEM, * $p \leq 0.05$, ** $p \leq 0.01$, *** $p \leq 0.001$ as indicated.

2.5. Treatment of HepG2 Cells with 5-AZA Plus Vitamin C in Combination with Insulin and Hydrocortisone Resulted in an Increased CYP450 Gene Expression and Enzyme Activity

The next aim was to verify if the above described molecular changes after AZA plus Vitamin C incubation had any positive impact on CYP450 gene expression and enzyme activity. Additionally, we wanted to test if the supplementation with insulin and hydrocortisone leads to a further increase of gene expression and activity of the CYP450 enzymes. Therefore, we investigated the gene expression of the following CYPs: *CYP1A2*, *CYP3A4* and *CYP2C9*. As depicted from Figure 5 we observed an upregulation of all three CYP genes after incubation of HepG2 cells with 5-AZA, Vitamin C, insulin and hydrocortisone. It is noteworthy that incubation of HepG2 with 5-AZA plus Vitamin C alone did not result in any *CYP3A4* upregulation, but supplementation of insulin and hydrocortisone did. Nevertheless, although we observed an increased CYP gene expression following 5-AZA, Vitamin C, insulin plus hydrocortisone in HepG2 cells, the gene expression of the cell line is still much lower than in freshly isolated human hepatocytes.

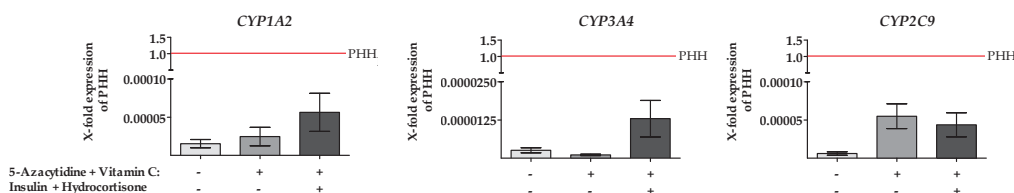


Figure 5. Incubation of HepG2 cells with 10 μM 5-Azacytidine plus 0.5 mM Vitamin C (dark bars) and in the presence of insulin plus hydrocortisone (black bars) increased basal Cytochrome P450 (CYP) gene expression. The gene expression of *CYP1A2*, *3A4* and *CYP2C9* were measured by qRT-PCR after 48 h of incubation. Unstimulated controls (grey bars) as well as primary human hepatocytes (PHH) (red line) were also cultured for 48 h. The values were normalized to *GAPDH*. Data represent the mean of $N = 3$, $n = 3$. As positive reference served a pool of five different PHH donors.

Next, we measured the CYP450 enzyme activity after incubation with epigenetic modifiers. Using LC/MS technology the metabolism of specific drugs was carried out [17]. The results of the activity measurements (Figure 6) showed only a modest increase of CYP3A4, CYP2D6 and CYP2C9 enzyme activities in HepG2 cells stimulated with 5-AZA and Vitamin C. Additional supplementation of insulin and hydrocortisone to the medium resulted in a further modest increase. However, the shown increases are not significant and are still far from the activities of PHH. For CYP1A2 no activity could be measured in HepG2.

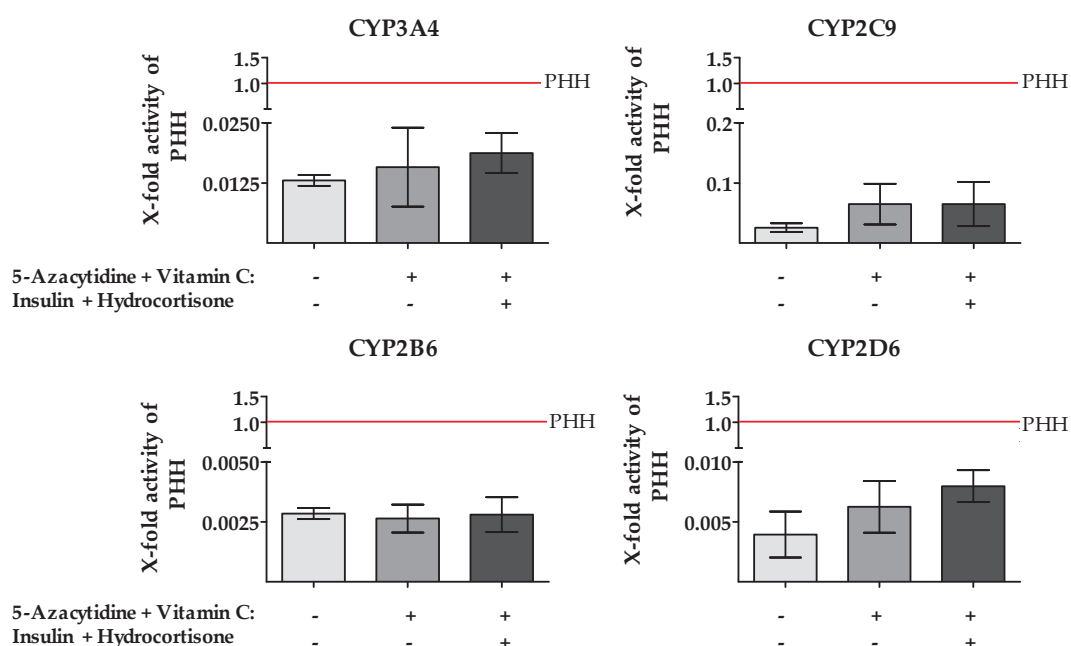


Figure 6. Activities of Cytochrome P450 (CYP) enzymes involved in drug metabolism are slightly increased after treatment with 5-Azacytidine (5-AZA) and Vitamin C. Supernatants were collected after incubation with specific substrates as indicated in materials and methods (4.4.6). Unstimulated HepG2 cells (grey bars) as well as HepG2 cells after 48 h stimulation with 10 μ M 5-AZA plus 0.5 mM Vitamin C with (dark bars)/without (black bars) insulin and hydrocortisone were used. For control, freshly isolated primary human hepatocytes (PHH) from three donors were used, shown as red line. Bars represent mean \pm SEM of three independent experiments; supernatants of at least three wells were pooled.

The result of our study indicated that 5-AZA and Vitamin C change the expression of some epigenetic markers that affect some crucial genes in terms of hepatic functions. These alterations are associated with an increase in the expression of epithelial marker genes such as *HNF4 α* and *E-Cadherin* as well as a decrease of the EMT marker gene *SNAIL*. However, there is no significant increase in the expression or activity of drug metabolizing enzymes. So as to identify chromatin-modifying genes that may be associated with low gene expression and activity of the CYP enzymes we looked again at the chromatin array data to see if there are any genes that are de-regulated in hepatoma cell lines but have not yet been linked to the metabolic activity of PHH. As shown in Figure 7, these criteria apply to the genes *SUV39H1*, *SMYD3*, *SETDB2*, *ESCO2*, *AURK A* and *AURK B*. As the results show, these genes are massively de-regulated in all tested cell lines. However, the gene expression profile of the cell line HepG2 is still the closest to PHH, compared to the other tested cell lines. A change in the expression of these genes can also be found, to a lesser extent, in de-differentiated PHH at day 7 after plating. Stimulation with 5-AZA and Vitamin C has no significant effect on the expression of these genes in HepG2. The expression of all 84 measured genes after treatment with Vitamin C alone or with 5-AZA plus Vitamin C can be found in the Supplementary Materials section (Figure S2).

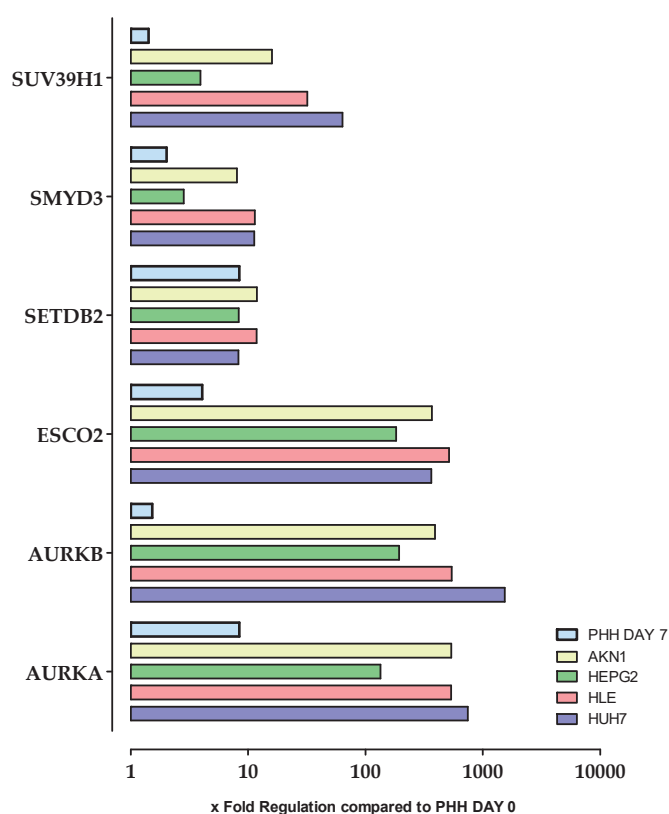


Figure 7. Chromatin modifying enzymes which are dramatically de-regulated in all tested cell lines and also de-regulated during primary human hepatocyte (PHH) de-differentiation in culture. Genes which are significantly de-regulated were selected. Expression of Chromatin Modification genes in hepatoma cell lines and PHH (day 7 after plating) were measured by using the Chromatin Modification Array.

3. Discussion

The culture of PHH, as well as hepatoma cell lines, are two of the most common in vitro liver models to evaluate drug metabolism and hepatotoxicity. Unfortunately, cultured primary hepatocytes lose their drug metabolic capacity rapidly in culture and they have large batch-to-batch variations. In contrast, hepatoma cell lines have an unlimited life span and they consist of a more stable phenotype than primary hepatocytes. Additionally, hepatoma cell lines are constantly available, but they show low CYP activities [18]. One of the main causes of the reduced metabolic activity of tumor cell lines are epigenetic changes, which might be associated with a so-called EMT. Recently we could clearly show that the treatment with a combination of 5-AZA and Vitamin C not only leads to a stop of proliferation but also results in a positive effect on EMT in HCC cell lines [12]. Moreover, we have shown that epigenetic changes of Ad-MSCs increased the metabolic capacity of differentiated hepatocyte-like cells. An increased gene expression and activity of CYP 450 (CYP1A2, CYP2E1, CYP3A4/7, CYP2D6, CYP2B6) enzymes were achieved by treatment with the epigenetic modifiers 5-AZA plus Vitamin C [19]. The aim of this study was to investigate whether epigenetic modifications in human hepatoma cell lines used to study drug metabolism would increase their metabolic capacity.

Our results clearly show that all of the tested liver tumor cell lines that are commonly used for drug metabolism show large differences in their epigenetic profile compared to PHH. Among the tested cell lines, it is striking that the hepatoblastoma cell line HepG2 differ significantly in the expression of epigenetic modifying enzymes from other tested HCC cell lines. In addition, our results showed that HepG2 cell line is most comparable in their epigenetic profile to PHH, which was the reason for continuing our research for this manuscript with this cell line. Despite the highest similarity of epigenetic profile between HepG2 and PHH, there are still significant differences. For example,

the expression of *HDAC2* is up-regulated in HepG2 compared to PHH, this upregulation was also found in HCC tissue [20]. The overexpression of this HDAC correlates with the dedifferentiation state and increased proliferative activity of tumor cells [20]. Our results also demonstrated that *PRMT1* is upregulated in HepG2 cells. This correlates with the findings of Gou et al. who found an upregulation of *PRMT1* in several liver cancer cells as well as in HCC tissue. Furthermore, the authors have shown that knockdown of *PRMT1* reverses EMT in HCC cell lines underlining the important role between *PRMT1* and EMT and proliferation [21]. The downregulation of *KDM4C* which we have found in untreated HepG2 cells is also an important finding since it has diverse targets in oncogenic or tumor suppressor functions [22]. The reduction of *KDM4C* gene expression in HepG2 most likely causes the methylation of *E-Cadherin* promoter [23]. Additionally, we found a low basal *KDM6B* gene expression in HepG2 cells compared to PHH that is in line with findings in various cancers, including liver carcinoma [24]. *KDM6B* is of particular importance because its function as a histone demethylase that specifically demethylates Lys-27 of histone H3 tri- and dimethyl (me_{3/2}) [25] and therefore explains the low basal *HNF4α* levels observed in HepG2 cells. The hepatic key regulator *HNF4α* showed only minimal levels of H3K27me₃ enrichment at these promoters in primary hepatocytes. In other cells, removal of H3K27me₃ from the *HNF4α* promoter resulted in transcriptional activation and expression of liver enrichment transcription factors [26]. A degradation of this methylation in HepG2 could be associated with an increased expression of *HNF4α* which can be attributed to the activity of *KDM6B* [25]. The literature data for the expression of *HDAC1* and *8* as well as *CARM1* indicating that these genes also have influence on tumorigenesis, EMT and the hepatic function [4,10,27,28] but they are not de-regulated in HepG2 however, we have found a de-regulation in the other tested HCC cell lines, which was another reason for using the cell line HepG2 for the further experiments.

In the second part of our study, we investigated whether the epigenetic modifications in HepG2 could be altered by treatment with 5-AZA plus Vitamin C towards PHH. Our results clearly show that HepG2 treatment with 5-AZA plus Vitamin C led to a significant reduction of the EMT marker gene *SNAIL* and a significant increase of *E-Cadherin* gene expression, which is in line with other human cancer cell lines [29]. Interestingly, additional stimulation of cells with insulin plus hydrocortisone further enhances *E-Cadherin* expression which confirms observations by Zhaeentan et al. showing that glucocorticoids increased *E-cadherin* gene expression [30]. The increased expression of *HNF4α* which results from the treatment with 5-AZA plus Vitamin C could be explained by the downregulation of *SNAIL* [9]. Moreover, *HNF4α* is essential in liver development and differentiation, lipid homeostasis, bile acid synthesis, as well as the expression of phase I, II, and III drug metabolizing genes. Aberrations in *HNF4α* functionality are known from the development of severe cirrhotic livers, alcoholic liver disease, tumor necrosis factor- α -induced hepatotoxicity, and hepatocellular carcinoma where *HNF4α* has an anti-proliferative effect and serves as a tumor suppressor [31]. We have also found a strong increase of *CK18* gene expression following the incubation with 5-AZA, Vitamin C, insulin and hydrocortisone. *CK18* is one of the crucial epithelial markers and was expressed after treatment comparable to PHH [32]. Since treatment with 5-AZA plus Vitamin C results in a positive change of the expression of epigenetic modifiers and in downregulation of the EMT marker gene *SNAIL* along with an increase of epithelial gene expression markers, we hypothesized an increased metabolic activity of CYP enzymes. However, our results only show a slight, but not significant, increase in CYP gene expression and activity compared to PHH. This is in line with data of Dannenberg et al. showing especially for *CYP3A4* a 1.8-fold increase after the treatment with 5-aza-dC in HepG2 cells. Moreover, this study also demonstrated that additional treatment with the HDAC inhibitor TSA did not contribute to an improvement in metabolic activity [33]. However, based on our earlier results, the question arises why a positive change on the expression and activity of CYP enzymes can be achieved in Ad-MSCs, which were differentiated under treatment with 5-AZA [19], but not in hepatoma cells. One possible explanation could be given by the results of Weng et al. showing that the profile of epigenetically modifying enzymes from embryonic stem cells was much closer to the profile of PHH [34]. Most striking was the de-regulation of the DNA methyltransferase 3B (*DNMT3B*) gene

and the depletion of DNMT3B from soluble fraction after 5-aza-dC treatment, resulted in an enhanced differentiation of Ad-MSCs [35]. Although HepG2 cells have the closest epigenetic profile to PHH from all investigated liver cell lines, which was even further improved after 5-AZA and Vitamin C treatment, the overall improvement of metabolic activity in HepG2 cells remained bleak. Therefore, for a substantial improvement of the metabolic profile in hepatoma cell lines, further studies are needed to identify additional key regulators. Nevertheless, our results are important because they clearly show that also other as the known epigenetic modifying enzymes such as HDACs or DNMT [10] influence the metabolic profile of hepatoma cell lines. The function of these genes with respect to drug metabolism was until now unknown. In summary, our findings support earlier results suggesting that drug induced epigenetic alteration of HCCs might be useful, for example, with combination therapy with 5-AZA and Vitamin C, as it increases expression of epithelial genes and as described by Sajadian et al. to stop or at least reduce tumor proliferation and reverse EMT [12]. However, as shown in our data presented here, additional inhibition of genes such as *Aurora kinases A and B* or *ESCO2*, which are still strongly de-regulated, might be useful to increase the expression of known hepatic functional genes such as *HNF4α* to the level of hepatocytes [9]. It may also be possible to increase other genes such as *KDM4C* or *KDM6B* which, as already described, also have an influence on the expression of hepatic genes on the expression level of hepatocytes [22,25]. Overall, this could also be accompanied by an increase in the expression of the CYP enzymes, which would then make the epigenetic modified cells to an interesting in vitro test system for the development of new drugs.

4. Materials and Methods

4.1. Tissue Samples

Liver cells were isolated from macroscopically tumor free tissue that remained from resected human liver of patients with primary or secondary liver tumors or benign local liver tissue. The liver capsules, were collected at the clinic of General, Visceral and Transplant Surgery (Tübingen) and the clinic of Hepatobiliary Surgery and Visceral Transplantation (Leipzig). Informed consent of the patients for the use of tissue for research purposes was obtained according to the ethical guidelines of the Ethic commission of the medical faculty of the University of Tübingen, Tübingen, Germany project number: 368/2012BO2 (02 August 2012) and the Ethic commission of the medical faculty of the University of Leipzig, Leipzig, Germany project number: 177/16-IK (12 July 2016).

4.2. Isolation of Primary Human Hepatocytes

PHH were isolated using a two-step EDTA/collagenase perfusion technique as described elsewhere [36,37]. The cells were shipped overnight in ChillProtect Plus solution (Biochrom, Berlin Germany). Upon arrival, the cell number and viability were determined in a Neubauer counting chamber using Trypan blue. If the viability of the isolated cells as determined by Trypan blue staining was below 70%, density gradient centrifugation was performed to remove non-viable cells. In brief, the cell pellet containing the PHH fraction was subjected on a 25% Percoll solution (total density: 1.0675 g/L) and centrifuged at $1250 \times g$, 20 min, 4 °C without brake. The resulting PHH fraction was washed with PBS (w/o Mg^{2+} , Ca^{2+}) and re-suspended in PHH culture medium (Williams Medium E supplemented with 10% Fetal bovine serum, 100 U/mL Penicillin, 0.1 mg/mL Streptomycin, 15 mM HEPES, 1 mM Glutamine, 1 mM Sodium pyruvate, 1 mM human Insulin, 0.8 µg/mL Hydrocortisone and 1% Nonessential amino acids).

4.3. Culture of Primary Cells and Cell Lines

4.3.1. Primary Cells

For adherence, culture dishes were coated with rat tail collagen as described elsewhere [9]. Cells were seeded in a density of 1.5×10^5 cells/cm² and cultured in PHH culture media.

4.3.2. Cell Lines

The common liver cancer cell lines HepG2, Huh7 and HLE as well as the cell line AKN1 were used in this study. HepG2 and HLE cell line were purchased from ATCC, Huh7 from JCRB (Japanese Collection of Research Bioresources Cell Bank, Osaka, Japan). The cell line AKN1 was isolated and developed as described elsewhere [16]. The cell lines were cultured as described [38]. An overview of the cell lines used can be found in Table 1.

Table 1. Description of the used cell lines.

Cell Line	Origin/Disease	Donor	Reference
HepG2	hepatoblastoma	15 year old Caucasian male	[39]
Huh7	HCC	57 year old Japanese male	[40]
HLE	HCC	68-year-old patient	[41]
AKN1	Healthy	10 year old male	[16]

The absence of mycoplasma contamination was regularly confirmed using a commercially available test kit (Mycroalert Detection Kit Cat. No: LT07, Lonza, Basel, Switzerland). The HCC cell lines were plated on day 0 in a density of 8×10^3 cells/cm². On day 1, the medium was removed and the cells were washed once with PBS. Subsequently, the cells were incubated for 48 h in a stimulation medium. The stimulation medium contained 5-AZA and Vitamin C (see Condition 1). Additional incubation with hydrocortisone and insulin was achieved by adding these compounds to the medium containing 5-AZA, and Vitamin C (see Condition 2) at day 2. The schedule of the stimulation is shown below in Table 2.

Table 2. Compounds of stimulation medium, and timeline of stimulation.

Supplement	Concentration	Day	Unstimulated	Condition 1	Condition 2
FCS	10%	0–3	+	+	+
P/S	1%	0–3	+	+	+
5-Azacytidin	10 μ M	1–3	-	+	+
Vitamin C	0.5 mM	1–3	-	+	+
Human Insulin	1 mM	2–3	-	-	+
Hydrocortisone	0.8 μ g/mL	2–3	-	-	+

4.4. Epigenetic Modification Array

To investigate the variation of chromatin modification among HCC cell lines and PHH, a Chromatin Modification array was used. Huh7, HepG2, HLE, AKN1 were investigated and compared to PHH. RNA of 5 different passage numbers of HCC cell lines and 5 different donors of PHH were isolated. RNA of different passage numbers/different PHH donors were pooled. The pooled RNA was purified with Rneasy Lipid Tissue Mini Kit according to manufacturer's instruction (QIAGEN, Germantown, MD, USA).

RT² First strand synthesis kit was used in order to eliminate genomic DNA contamination and reverse transcription was performed according to manufacturer's protocol (QIAGEN). RT² SYBR Green mastermix (QIAGEN) was used for performing real-time PCR for RT² PCR array according to manufacturer's protocol, in brief: denaturation for 10 min at 95 °C, amplification with 40 cycles and 15 s at 95 °C, 1 min at 60 °C and 15 s at 72 °C (Step One Plus™ Real-Time PCR System, (Life Technologies, Carlsbad, CA, USA). The Human Epigenetic Chromatin Modification Enzymes RT² Profiler™ PCR Array (Cat. No: 33231 PAHS-085ZA, QIAGEN). The array measures the expression of 84 genes which encode for epigenetic key enzymes responsible for modifying histones as well as the packing of DNA strands into chromosomes and are consequently linked to the regulation of gene expression.

The array includes genes acting as DNA methyltransferases, enzymes that catalyze histone acetylation, methylation, phosphorylation, ubiquitination and histone deacetylases and demethylases.

4.5. cDNA Synthesis and RT-PCR

Real-time RT-PCR for detection of mRNA expression was performed as described previously [38]. In brief, for the mRNA expression studies, total RNA was extracted using TriFast reagent (Peqlab, Erlangen, Germany). Complementary DNA (cDNA) was synthesized by First Strand cDNA Synthesis Kit (Thermo Scientific, Waltham, MA, USA). For quantitative real-time PCR (qRT-PCR), 40 ng of template cDNA was used for the expression level of each target gene (Gene sequences of the primers which were used can be found in Table 3 using SYBR Green qPCR (Thermo Scientific) and the Step One Plus® Real-Time PCR System Kit (Life Technologies). All genes examined were normalized to a housekeeping gene encoding *GAPDH*. Relative expression values were calculated from Ct values using the $\Delta\Delta_{CT}$ method with freshly isolated hepatocytes as a control. Fold induction was calculated according to the formula $2^{(Rt-Et)}/2^{(Rn-En)}$ [42]. PCRs were performed as follows: denaturation for 10 min at 95 °C, amplification with 40 cycles and 15 s at 95 °C, 40 s at a primer specific annealing temperature (as shown in Table 3), and 15 s at 72 °C. Each sample was set up in triplicates, and the experiment was repeated at least twice. Statistical significance of difference in target genes expression level between different treatments was assessed by One-way ANOVA.

Table 3. Primers which were used for qRT-PCR.

Gen	Forward/Reverse Sequences	Annealing Tm	Product Length (bp)	GenBank Accession
<i>hHNF4A</i>	CAGGCTCAAGAAATGCTTCC GGCTGCTGCTCATAGCTT	59	101	NM_001287184.1
<i>hCK18</i>	GAGTATGAGGCCCTGCTGAACAT GCGGGTGGTGGTCTTTTGAT	65	150	NM_199187.1
<i>hHDAC1</i>	AACTGCTAAAGTATCACCAGAGGGT CCGGTCCGTGGTGTAGAAGG	62	92	NM_004964.2
<i>hHDAC2</i>	TGAAGGAGAAGGAGGTCGAA GGATTATCTTCTTCTTAACGTCTG	59	124	NM_001527.3
<i>hCYP1A2</i>	GCTTCGGACAGCACTTCCT AGAAGTCCAGGGGTTCCCG	63	105	NM_000761.4
<i>hCYP3A4</i>	AGCCAGCAAAGAGCAACAC TCCATATAGATAGAGGACCAGG	60	147	NM_017460.5
<i>hCYP2C9</i>	GACATGAACAACCCTCAGGACTTT TGCTTGTCGTCTCTGTCCCA	62	145	NM_000771.3
<i>hKDM4C</i>	TGGATCCCAGATAGCAATGA TGTCTTCAAATCGCATGTCA	59	110	NM_001304340.1
<i>hKDM6B</i>	GGAGGCCACACGCTGCTAC GCCAGTATGAAAGTCCAGAGCTG	63	112	NM_001348716.1
<i>hSNAIL</i>	ACCACTATGCCGCGCTCTT GGTCGTAGGGCTGCTGGAA	60	115	NM_005985.3
<i>hGAPDH</i>	TGCACCACCAACTGCTTAGC GGCATGGACTGTGGTCATGAG	59	87	NM_002046.3

4.6. CYP Activity Measurement

CYP enzyme activities of CYP2B6, CYP2D6, CYP2C9, and CYP3A4, were measured, as described. Briefly, the chosen substrates, the selected concentrations, the incubation times, and the measured metabolites are summarized in Table 4 Methanol, which was the initial solvent of the CYP substrates, was removed before use by evaporation, and the substrates were dissolved in culture medium. The cells were incubated with 100 μ L of the respective reaction solution. After the described incubation times, the supernatants were removed and frozen at -80 °C until measurement. The enzymatic activity was measured by the company Pharmacelsus, Saarbrücken, Germany using a LC/MS based methodology [17,43].

Table 4. Substrates, concentrations, conditions and measured reactions of the CYP activity measurement.

Substrate	Isoenzyme	Incubation Time in Hours	Concentration	Reaction
Bupropion	CYP2B6	1	100 μ M	Bupropion-hydroxylation
Diclofenac	CYP2C9	1	9 μ M	Diclofenac-4'-hydroxylation
Testosterone	CYP3A4	1	50 μ M	Testosterone-6 β -hydroxylation
Bufuralol	CYP2D6	2	9 μ M	Bufuralol-1-hydroxylation

4.7. SRB Staining for Normalisation of the Results

For normalization of the result from the CYP activity measurement, a Sulforhodamine B (SRB) staining was performed as described by Skehan et al. [44]. Therefore, cells were fixed to culture plastic with ice cold fixation buffer (95% Ethanol, 100 μ L/well). The cells were incubated for at least 1 h at -20 °C. Then fixation buffer was removed, and cells were washed with H₂O. Fixed cells were stained for 30 min (dark, RT) with 0.4% SRB dissolved in 1% acetic acid (100 μ L/well). Then, SRB solution was removed and cells were washed three times with 1% acetic acid in order to wash out unbound dye. Plates were air dried and bound SRB was solubilized with 10 mM un-buffered TRIS (pH = 10.5; 100 μ L/well) for 10–15 min on a shaker (RT, in the dark). The OD at 565 nm (SRB) and 690 nm (impurities) were measured with OMEGA plate reader (BMG Labtech, Ortenberg, Germany).

4.8. Statistic Analysis

Statistical significance of differences between two groups was evaluated by non-parametric Mann–Whitney U-test. For comparison of the differences between more than two groups non-parametric Kruskal-Wallis H-test followed by Dunn's multiple comparison test was performed using GraphPad Prism 5.00 Software, San Diego, CA, USA. Data are represented as means \pm SEM of at least three independent experiments ($N \geq 3$). All statistical comparisons were performed two-sided in the sense of an exploratory data analysis using $p < 0.05$ (*), $p < 0.01$ (**), and $p < 0.001$ (***) as level of significance.

5. Conclusions

Our results show that the epigenetic status of the hepatoblastoma cell line HepG2 shows the highest similarity with PHH compared to the other tested liver cancer cell lines (Huh7, HLE and AKN1). Also a shift of the epigenetic status of HepG2 cells, by stimulation with the epigenetic modifiers 5-AZA plus Vitamin C towards a profile characteristic for PHH could be achieved. Although these modifications lead to a reduction in the expression of the EMT marker gene *SNAIL* and induction in the expression of epithelial genes, but not to a significant increase in the expression and activity of CYP enzymes. As a possible reason, existing epigenetic modifications could be identified, which are deregulated in all four tested hepatoma cell lines as well as in long-term cultured hepatocytes. These genes are not linked yet to the metabolic activity of liver cells. Our results suggest that further epigenetic key players, which were identified in this study, are responsible for the hepatic differentiation as well as for the activity of the CYP enzymes. Changing the expression of these genes may not only be an approach to improving the metabolic activity of the cells, but may be additionally potential targets for tumor therapy.

Supplementary Materials: Supplementary materials can be found at <http://www.mdpi.com/1422-0067/20/2/347/s1>.

Author Contributions: M.R., S.S. and A.N. conceived and designed the experiments; M.R. S.S. and L.E. performed the experiments; M.R. and S.S. analyzed the data; G.D., S.N., R.L. and D.S. contributed materials; M.V. contributed to data interpretation; M.R., G.D., A.N., and S.S. wrote the manuscript C.G.-B. and M.P. provide technical support and editing the manuscript.

Funding: This study was partially funded by the Ministerium für Ländlichen Raum und Verbraucherschutz/Baden-Württemberg (BW 05110214). Additionally, we acknowledge support by Deutsche Forschungsgemeinschaft and Open Access Publishing Fund of University of Tübingen.

Acknowledgments: We would like to thank Silvia Wagner for coordination of the liver tissue collection of the donor material which was isolated in Tübingen.

Conflicts of Interest: The authors declare no conflict of interest.

Abbreviations

CYP	Cytochrome P450
cDNA	Complementary DNA
EMT	Epithelial–Mesenchymal Transition
PHH	primary human hepatocytes
SRB	Sulforhodamine B
5-AZA	5-aza-2'-deoxycytidine
CK18	Cytokeratin 18
HNF4 α	Hepatocyte nuclear factor 4 α
SNAIL	Snail1
KDM6B	Lysine Demethylase 6B
KDM4C	Lysine Demethylase 4C
JCRB	Japanese Collection of Research Bioresources Cell Bank
5-AZA-dC	5-Aza-2'-deoxycytidine
HCC	hepatocellular carcinoma
HDAC	Histone deacetylase
HDACi	Histone deacetylase inhibitor
DNMT	DNA methyltransferases
DNMTi	DNA methyltransferase inhibitors

References

- Peng, L.; Zhong, X. Epigenetic regulation of drug metabolism and transport. *Acta Pharm. Sin. B* **2015**, *5*, 106–112. [[CrossRef](#)] [[PubMed](#)]
- Egger, G.; Liang, G.; Aparicio, A.; Jones, P.A. Epigenetics in human disease and prospects for epigenetic therapy. *Nature* **2004**, *429*, 457–463. [[CrossRef](#)] [[PubMed](#)]
- Ingelman-Sundberg, M.; Zhong, X.B.; Hankinson, O.; Beedanagari, S.; Yu, A.M.; Peng, L.; Osawa, Y. Potential role of epigenetic mechanisms in the regulation of drug metabolism and transport. *Drug. Metab. Dispos.* **2013**, *41*, 1725–1731. [[CrossRef](#)] [[PubMed](#)]
- Park, H.J.; Choi, Y.J.; Kim, J.W.; Chun, H.S.; Im, I.; Yoon, S.; Han, Y.M.; Song, C.W.; Kim, H. Differences in the epigenetic regulation of cytochrome p450 genes between human embryonic stem cell-derived hepatocytes and primary hepatocytes. *PLoS ONE* **2015**, *10*, e0132992. [[CrossRef](#)]
- Stadler, S.C.; Allis, C.D. Linking epithelial-to-mesenchymal-transition and epigenetic modifications. *Semin. Cancer Biol.* **2012**, *22*, 404–410. [[CrossRef](#)] [[PubMed](#)]
- Thiery, J.P.; Acloque, H.; Huang, R.Y.; Nieto, M.A. Epithelial-mesenchymal transitions in development and disease. *Cell* **2009**, *139*, 871–890. [[CrossRef](#)]
- Sciacovelli, M.; Frezza, C. Metabolic reprogramming and epithelial-to-mesenchymal transition in cancer. *FEBS J.* **2017**, *284*, 3132–3144. [[CrossRef](#)]
- Serrano-Gomez, S.J.; Maziveyi, M.; Alahari, S.K. Regulation of epithelial-mesenchymal transition through epigenetic and post-translational modifications. *Mol. Cancer* **2016**, *15*, 18. [[CrossRef](#)]
- Cicchini, C.; Filippini, D.; Coen, S.; Marchetti, A.; Cavallari, C.; Laudadio, I.; Spagnoli, F.M.; Alonzi, T.; Tripodi, M. Snail controls differentiation of hepatocytes by repressing hnf4alpha expression. *J. Cell Physiol.* **2006**, *209*, 230–238. [[CrossRef](#)]
- Snykers, S.; Henkens, T.; De Rop, E.; Vinken, M.; Fraczek, J.; De Kock, J.; De Prins, E.; Geerts, A.; Rogiers, V.; Vanhaecke, T. Role of epigenetics in liver-specific gene transcription, hepatocyte differentiation and stem cell reprogramming. *J. Hepatol.* **2009**, *51*, 187–211. [[CrossRef](#)]
- Yamashita, Y.; Shimada, M.; Harimoto, N.; Rikimaru, T.; Shirabe, K.; Tanaka, S.; Sugimachi, K. Histone deacetylase inhibitor trichostatin a induces cell-cycle arrest/apoptosis and hepatocyte differentiation in human hepatoma cells. *Int. J. Cancer* **2003**, *103*, 572–576. [[CrossRef](#)]

12. Sajadian, S.O.; Tripura, C.; Samani, F.S.; Ruoss, M.; Dooley, S.; Baharvand, H.; Nussler, A.K. Vitamin c enhances epigenetic modifications induced by 5-azacytidine and cell cycle arrest in the hepatocellular carcinoma cell lines hle and huh7. *Clin. Epigenetics*. **2016**, *8*, 46. [[CrossRef](#)]
13. Michalopoulos, G.; Pitot, H.C. Primary culture of parenchymal liver cells on collagen membranes. Morphological and biochemical observations. *Exp. Cell Res.* **1975**, *94*, 70–78. [[CrossRef](#)]
14. Kinoshita, T.; Miyajima, A. Cytokine regulation of liver development. *Biochim. Biophys. Acta* **2002**, *1592*, 303–312. [[CrossRef](#)]
15. Lin, J.; Schyschka, L.; Muhl-Benninghaus, R.; Neumann, J.; Hao, L.; Nussler, N.; Dooley, S.; Liu, L.; Stockle, U.; Nussler, A.K.; et al. Comparative analysis of phase i and ii enzyme activities in 5 hepatic cell lines identifies huh-7 and hcc-t cells with the highest potential to study drug metabolism. *Arch. Toxicol.* **2012**, *86*, 87–95. [[CrossRef](#)]
16. Nussler, A.K.; Vergani, G.; Gollin, S.M.; Dorko, K.; Morris, S.M., Jr.; Demetris, A.J.; Nomoto, M.; Beger, H.G.; Strom, S.C. Isolation and characterization of a human hepatic epithelial-like cell line (akn-1) from a normal liver. *In Vitro Cell Dev. Biol. Anim.* **1999**, *35*, 190–197. [[CrossRef](#)]
17. Ruoff, M.; Häussling, V.; Schügner, F.; Olde Damink, L.; Lee, S.; Ge, L.; Ehnert, S.; Nussler, A. A standardized collagen-based scaffold improves human hepatocyte shipment and allows metabolic studies over 10 days. *Bioengineering* **2018**, *5*, 86. [[CrossRef](#)]
18. Rodriguez-Antona, C.; Donato, M.T.; Boobis, A.; Edwards, R.J.; Watts, P.S.; Castell, J.V.; Gomez-Lechon, M.J. Cytochrome p450 expression in human hepatocytes and hepatoma cell lines: Molecular mechanisms that determine lower expression in cultured cells. *Xenobiotica* **2002**, *32*, 505–520. [[CrossRef](#)]
19. Seeliger, C.; Culmes, M.; Schyschka, L.; Yan, X.; Damm, G.; Wang, Z.; Kleeff, J.; Thasler, W.E.; Hengstler, J.; Stockle, U.; et al. Decrease of global methylation improves significantly hepatic differentiation of ad-mscs: Possible future application for urea detoxification. *Cell Transplant.* **2013**, *22*, 119–131. [[CrossRef](#)]
20. Quint, K.; Agaimy, A.; Di Fazio, P.; Montalbano, R.; Steindorf, C.; Jung, R.; Hellerbrand, C.; Hartmann, A.; Sitter, H.; Neureiter, D.; et al. Clinical significance of histone deacetylases 1, 2, 3, and 7: Hdac2 is an independent predictor of survival in hcc. *Virchows Arch.* **2011**, *459*, 129–139. [[CrossRef](#)]
21. Gou, Q.; He, S.; Zhou, Z. Protein arginine n-methyltransferase 1 promotes the proliferation and metastasis of hepatocellular carcinoma cells. *Tumour Biol.* **2017**, *39*, 1010428317691419. [[CrossRef](#)]
22. Filipp, F.V. Crosstalk between epigenetics and metabolism-yin and yang of histone demethylases and methyltransferases in cancer. *Brief Funct. Genomics* **2017**, *16*, 320–325. [[CrossRef](#)]
23. Dong, C.; Wu, Y.; Yao, J.; Wang, Y.; Yu, Y.; Rychahou, P.G.; Evers, B.M.; Zhou, B.P. G9a interacts with snail and is critical for snail-mediated e-cadherin repression in human breast cancer. *J. Clin. Invest.* **2012**, *122*, 1469–1486. [[CrossRef](#)]
24. Agger, K.; Cloos, P.A.; Rudkjaer, L.; Williams, K.; Andersen, G.; Christensen, J.; Helin, K. The h3k27me3 demethylase jmj3d contributes to the activation of the ink4a-arf locus in response to oncogene- and stress-induced senescence. *Genes Dev.* **2009**, *23*, 1171–1176. [[CrossRef](#)]
25. Zhang, P.P.; Wang, X.L.; Zhao, W.; Qi, B.; Yang, Q.; Wan, H.Y.; Shuang, Z.Y.; Liu, M.; Li, X.; Li, S.; et al. DNA methylation-mediated repression of mir-941 enhances lysine (k)-specific demethylase 6b expression in hepatoma cells. *J. Biol. Chem.* **2014**, *289*, 24724–24735. [[CrossRef](#)]
26. Kochat, V.; Equbal, Z.; Baligar, P.; Kumar, V.; Srivastava, M.; Mukhopadhyay, A. Jmj3d aids in reprogramming of bone marrow progenitor cells to hepatic phenotype through epigenetic activation of hepatic transcription factors. *PLoS ONE* **2017**, *12*, e0173977. [[CrossRef](#)]
27. Wu, J.; Du, C.; Lv, Z.; Ding, C.; Cheng, J.; Xie, H.; Zhou, L.; Zheng, S. The up-regulation of histone deacetylase 8 promotes proliferation and inhibits apoptosis in hepatocellular carcinoma. *Dig. Dis. Sci.* **2013**, *58*, 3545–3553. [[CrossRef](#)]
28. Zhong, X.Y.; Yuan, X.M.; Xu, Y.Y.; Yin, M.; Yan, W.W.; Zou, S.W.; Wei, L.M.; Lu, H.J.; Wang, Y.P.; Lei, Q.Y. Carn1 methylates gapdh to regulate glucose metabolism and is suppressed in liver cancer. *Cell Rep.* **2018**, *24*, 3207–3223. [[CrossRef](#)]
29. Sugimachi, K.; Tanaka, S.; Kameyama, T.; Taguchi, K.; Aishima, S.; Shimada, M.; Sugimachi, K.; Tsuneyoshi, M. Transcriptional repressor snail and progression of human hepatocellular carcinoma. *Clin. Cancer Res.* **2003**, *9*, 2657–2664.

30. Zhaeentan, S.; Amjadi, F.S.; Zandie, Z.; Joghataei, M.T.; Bakhtiyari, M.; Aflatoonian, R. The effects of hydrocortisone on tight junction genes in an in vitro model of the human fallopian epithelial cells. *Eur. J. Obstet. Gynecol. Reprod. Biol.* **2018**, *229*, 127–131. [[CrossRef](#)]
31. Zhang, Q.; Lei, X.; Lu, H. Alterations of epigenetic signatures in hepatocyte nuclear factor 4alpha deficient mouse liver determined by improved chip-qpcr and (h)medip-qpcr assays. *PLoS ONE* **2014**, *9*, e84925.
32. Weng, Y.R.; Cui, Y.; Fang, J.Y. Biological functions of cytokeratin 18 in cancer. *Mol. Cancer Res.* **2012**, *10*, 485–493. [[CrossRef](#)]
33. Dannenberg, L.O.; Edenberg, H.J. Epigenetics of gene expression in human hepatoma cells: Expression profiling the response to inhibition of DNA methylation and histone deacetylation. *BMC Genomics* **2006**, *7*, 181. [[CrossRef](#)]
34. Weng, M.K.; Natarajan, K.; Scholz, D.; Ivanova, V.N.; Sachinidis, A.; Hengstler, J.G.; Waldmann, T.; Leist, M. Lineage-specific regulation of epigenetic modifier genes in human liver and brain. *PLoS ONE* **2014**, *9*, e102035. [[CrossRef](#)]
35. Oka, M.; Meacham, A.M.; Hamazaki, T.; Rodic, N.; Chang, L.J.; Terada, N. De novo DNA methyltransferases dnmt3a and dnmt3b primarily mediate the cytotoxic effect of 5-aza-2'-deoxycytidine. *Oncogene* **2005**, *24*, 3091–3099. [[CrossRef](#)]
36. Pfeiffer, E.; Kegel, V.; Zeilinger, K.; Hengstler, J.G.; Nussler, A.K.; Seehofer, D.; Damm, G. Featured article: Isolation, characterization, and cultivation of human hepatocytes and non-parenchymal liver cells. *Exp. Biol. Med.* **2015**, *240*, 645–656. [[CrossRef](#)]
37. Knobloch, D.; Ehnert, S.; Schyschka, L.; Buchler, P.; Schoenberg, M.; Kleeff, J.; Thasler, W.E.; Nussler, N.C.; Godoy, P.; Hengstler, J.; et al. Human hepatocytes: Isolation, culture, and quality procedures. *Methods Mol. Biol.* **2012**, *806*, 99–120.
38. Sajadian, S.O.; Ehnert, S.; Vakilian, H.; Koutsouraki, E.; Damm, G.; Seehofer, D.; Thasler, W.; Dooley, S.; Baharvand, H.; Sipos, B.; et al. Induction of active demethylation and 5hmc formation by 5-azacytidine is tet2 dependent and suggests new treatment strategies against hepatocellular carcinoma. *Clin. Epigenetics.* **2015**, *7*, 98. [[CrossRef](#)]
39. Lopez-Terrada, D.; Cheung, S.W.; Finegold, M.J.; Knowles, B.B. Hep g2 is a hepatoblastoma-derived cell line. *Hum. Pathol.* **2009**, *40*, 1512–1515. [[CrossRef](#)]
40. Nakabayashi, H.; Taketa, K.; Miyano, K.; Yamane, T.; Sato, J. Growth of human hepatoma cells lines with differentiated functions in chemically defined medium. *Cancer Res.* **1982**, *42*, 3858–3863.
41. Doi, I.; Namba, M.; Sato, J. Establishment and some biological characteristics of human hepatoma cell lines. *Gann* **1975**, *66*, 385–392.
42. Saha, S.; Bardelli, A.; Buckhaults, P.; Velculescu, V.E.; Rago, C.; St Croix, B.; Romans, K.E.; Choti, M.A.; Lengauer, C.; Kinzler, K.W.; et al. A phosphatase associated with metastasis of colorectal cancer. *Science* **2001**, *294*, 1343–1346. [[CrossRef](#)]
43. Hoffmann, S.A.; Muller-Vieira, U.; Biemel, K.; Knobloch, D.; Heydel, S.; Lubberstedt, M.; Nussler, A.K.; Andersson, T.B.; Gerlach, J.C.; Zeilinger, K. Analysis of drug metabolism activities in a miniaturized liver cell bioreactor for use in pharmacological studies. *Biotechnol. Bioeng.* **2012**, *109*, 3172–3181. [[CrossRef](#)]
44. Skehan, P.; Storeng, R.; Scudiero, D.; Monks, A.; McMahon, J.; Vistica, D.; Warren, J.T.; Bokesch, H.; Kenney, S.; Boyd, M.R. New colorimetric cytotoxicity assay for anticancer-drug screening. *J. Natl. Cancer Inst.* **1990**, *82*, 1107–1112. [[CrossRef](#)]



© 2019 by the authors. Licensee MDPI, Basel, Switzerland. This article is an open access article distributed under the terms and conditions of the Creative Commons Attribution (CC BY) license (<http://creativecommons.org/licenses/by/4.0/>).

Chapter 5: Publication III

Ruoß, M.; Rebholz, S.; Weimer, M.; Grom-Baumgarten, C.; Athanasopulu, K.; Kemkemer, R.; Käß, H.; Ehnert, S.; Nussler, A.K. **Development of Scaffolds with Adjusted Stiffness for Mimicking Disease-Related Alterations of Liver Rigidity.** J. Funct. Biomater. 2020, 11, 17.

5.1 Synopsis:

Drug-induced hepatotoxic side effects are the most common reason why drugs fail in clinical trials or have to be withdrawn from the market after approval (Kaplowitz, 2005). One reason for this failure is the lack of predictive *in vivo* models, which is mainly due to species differences in the metabolism of drugs between humans and laboratory animals (Olson et al., 2000). There are also significant intraspecific differences in drug metabolism. In addition to age, gender, or genetic background, disease-specific changes in the liver also play an essential role (Bachtiar and Lee, 2013, Soldin and Mattison, 2009, Mangoni and Jackson, 2004, Cheng and Morgan, 2001). For example, one study showed that changes in liver stiffness, which can be found in patients who suffer from liver fibrosis or cirrhosis, lead to altered expression of drug-metabolizing enzymes (Theile et al., 2013). Such changes require individualized therapies as well as the use of models that can represent these individual differences during pre-clinical drug development. In animal studies, such changes can be mimicked by using disease models, but this is not yet possible *in vitro* (Liu et al., 2013). The aim of this study was, therefore, to develop such an *in vitro* model that can mimic the *in vivo* environment of the healthy as well as an altered fibrotic liver. For this purpose, we developed pHEMA/BAA-based cryogels, which can represent the physiological as well as the pathological liver rigidities that occur in healthy subjects and patients who suffer from liver cirrhosis, respectively.

To provide the cells with an ideal environment, we tested whether the pre-incubation of the scaffolds with RGD-rich substances is useful. We demonstrated that pre-incubation with FCS-containing medium has a positive effect on cell adherence. This effect was particularly pronounced in the scaffold representing the healthy liver. At this scaffold, the length of pre-incubation influences the number of cells adhered to

the scaffold. As demonstrated by SEM images, the pre-incubation of the scaffold results in the deposition of particles on the scaffold surface. These depositions alter the scaffold surface and may possibly explain the positive effects of the pre-incubation concerning cell adherence.

In subsequent experiments, we investigated whether the different stiffness of the scaffolds affects the metabolic activity of the cells. Cells plated onto the scaffold—with a stiffness that corresponds to the human liver—generally exhibit higher metabolic activity of the measured phase I/II enzymes compared to cells plated onto the stiffer fibrotic liver scaffold.

When evaluating these promising results, one must consider that we used HepG2 in this study. These cells have some of the functions of human hepatocytes and are therefore often used as an alternative for them (Lin et al., 2012), but they differ significantly from them, especially in their metabolic activity (Rodriguez-Antona et al., 2002).

In addition, it might also be useful to develop further develop the here established *in vitro* model system in such a direction that it can mimic also other aspects of the pathology of liver fibrosis besides liver stiffness. Mimicking changes in the ECM composition or the imitation of inflammation—which are both also associated with liver fibrosis—are possible examples. In addition to hepatocytes, other liver cells such as stellate cells or Kupffer cells play a significant role in the pathogenesis of liver fibrosis; hence, the development of a 3D co-culture model including also this cell types would also be useful.



Article

Development of Scaffolds with Adjusted Stiffness for Mimicking Disease-Related Alterations of Liver Rigidity

Marc Ruoff ^{1,*} , Silas Rebholz ¹, Marina Weimer ^{1,2}, Carl Grom-Baumgarten ¹, Kiriaki Athanasopulu ², Ralf Kemkemer ², Hanno Käß ³, Sabrina Ehnert ¹ and Andreas K. Nussler ¹

¹ Department of Traumatology, Siegfried Weller Institute, Eberhard Karls University, 72076 Tübingen, Germany; silasrebholz@gmail.com (S.R.); marina-weimer@live.de (M.W.); carlgrom-baumgarten@web.de (C.G.-B.); sabrina.ehnert@gmail.com (S.E.); andreas.nuessler@gmail.com (A.K.N.)

² Faculty of Applied Chemistry, Reutlingen University, 72762 Reutlingen, Germany; kiriaki.athanasopulu@reutlingen-university.de (K.A.); ralf.kemkemer@gmail.com (R.K.)

³ Faculty of Basic Science, University of Applied Sciences Esslingen, 73728 Esslingen am Neckar, Germany; hanno.kaess@hs-esslingen.de

* Correspondence: m.ruoss@hotmail.de; Tel.: +49-7071-606-1065

Received: 20 February 2020; Accepted: 11 March 2020; Published: 14 March 2020



Abstract: Drug-induced liver toxicity is one of the most common reasons for the failure of drugs in clinical trials and frequent withdrawal from the market. Reasons for such failures include the low predictive power of in vivo studies, that is mainly caused by metabolic differences between humans and animals, and intraspecific variances. In addition to factors such as age and genetic background, changes in drug metabolism can also be caused by disease-related changes in the liver. Such metabolic changes have also been observed in clinical settings, for example, in association with a change in liver stiffness, a major characteristic of an altered fibrotic liver. For mimicking these changes in an in vitro model, this study aimed to develop scaffolds that represent the rigidity of healthy and fibrotic liver tissue. We observed that liver cells plated on scaffolds representing the stiffness of healthy livers showed a higher metabolic activity compared to cells plated on stiffer scaffolds. Additionally, we detected a positive effect of a scaffold pre-coated with fetal calf serum (FCS)-containing media. This pre-incubation resulted in increased cell adherence during cell seeding onto the scaffolds. In summary, we developed a scaffold-based 3D model that mimics liver stiffness-dependent changes in drug metabolism that may more easily predict drug interaction in diseased livers.

Keywords: scaffold culture; stiffness; in vitro model; pre-coating; Arg-Gly-Asp (RGD)-peptides; cell attachment

1. Introduction

Today the testing of new drugs is mainly performed in animals due to a lack of predictive in vitro models [1]. However, animal experiments have several limitations in predicting liver toxicity of new substances, due to differences between the drug-metabolizing enzymes in humans and animals [2]. Therefore, new models that are able to foresee the in vivo situation more accurately are needed. Freshly isolated human hepatocytes are the gold standard for such models since their metabolic profile is comparable to the in vivo environment [3,4]. However, the use of human liver cells for the testing of new substances is limited since human hepatocytes are scarcely available and suffer frequently from the loss of metabolic function during long-term cultivation [5,6]. In recent years continuously

available liver cell lines were established as an alternative to human hepatocytes to overcome these limitations [7].

Furthermore, numerous attempts have been made to improve cultivation conditions to extend the hepatocytes metabolic activity and to improve the metabolic activity of these cell lines [4,8–10]. Various studies showed that mimicking the *in vivo* environment improves the metabolic capacity of primary liver cells and liver cell lines [4,8,11,12]. In addition to the interaction with other cells that can be provided in a co-culture setup [13], it is also important that the hepatocytes interact with the surrounding matrix [14]. One reason for the rapid loss of the metabolic properties of primary hepatocytes in conventional 2D cultures is the lack of adequate interaction with the surrounding matrix [12]. In recent years, various 3D cultivation methods have been developed, including scaffold culture systems [12,15]. These 3D culture systems can help to maintain the metabolic activity of cells over an extended period of time [4,16]. The metabolic activity is sustained because the cultivation of these cells on scaffolds ensures that cell adherence is not limited to the plane of the cell culture plate but can take place three-dimensionally. Moreover, the porous surface of the scaffold improves the cell nutrients' supply. Although several studies have shown that substrate stiffness greatly influences the functioning of cells, this parameter has been neglected so far in the development of scaffolds for the cultivation of hepatocytes. For instance, one study showed that mesenchymal stem cells could be differentiated into different directions only by using different rigidities [17]. The influence of substrate stiffness on the functioning of hepatocytes is known [18,19]. In line with these publications, it has been shown that rat hepatocytes cultured onto a soft 2D matrix (2 kPa) resulted in a more differentiated and functional hepatocyte phenotype than those cultured directly onto a stiffer surface (55 kPa) or cell culture plastic. Moreover, on day 7, cytochrome P450 (CYP) activity was 2.7 times higher in hepatocytes cultured on the softer matrix than those cultured on normal cell culture plastic [11]. Interestingly, *in vivo*, the metabolic activity of the hepatocytes is also influenced by liver stiffness. Theile et al. observed a significant difference between the activity of drug metabolic enzymes in patients with a liver stiffness lower than 8 kPa compared to patients with a liver stiffness larger than 8 kPa; this result indicates that the hepatic stiffness directly affects the metabolism of drugs *in vivo* [20].

Since such metabolic changes caused by different liver rigidities between healthy subjects and patients with liver fibrosis or cirrhosis may also influence the efficiency and/or toxicity of drugs, these adverse effects should be considered either during drug development or drug prescription to patients with liver diseases. Therefore, the first aim of this study was the development of scaffolds that mimic the stiffness of healthy and fibrotic livers. In addition to stiffness, it is well established that the extracellular matrix (ECM) influences the properties of liver cells [4,21]. In order to provide cells with an optimal environment for attachment and during cultivation on the scaffold, we used different proteinaceous solutions and various incubation intervals to pre-coat scaffolds. We decided to use the cell line HepG2 for establishing and testing our 3D liver scaffolds since cell line is often used as an alternative to primary human hepatocytes in drug metabolism studies [22].

2. Materials and Methods

2.1. Production of the Different pHEMA Based Scaffolds

For a successful culture of hepatic cells, it is necessary to generate a matrix whose properties are as similar as possible to those of the *in vivo* environment. The ideal matrix allows good cell attachment, therefore it must have pores of a sufficiently large diameter, high porosity, and permeability to allow cells to penetrate and adhere [16,23]. Further, a sufficient supply of nutrients must be guaranteed [24]. To achieve this goal, we used poly-(2-hydroxyethyl methacrylate) (pHEMA)/bisacrylamide (BAA)-based cryogels. To increase cell adherence, collagen (self-made rat-tail collagen), concentration 3.5 g/L prepared as described [25] and gelatin solution (30% cold water fish gelatin in ddH₂O) were added to the scaffolds. Several different cryogel compositions were tested. The various concentrations of cryogel components that were tested during the development of the scaffolds are shown in Table S1. The four

that most closely met the above-mentioned criteria regarding the scaffold architecture, which could in addition be reliably reproduced, were selected for further testing. The exact ingredient compositions of the four different scaffold prototypes are listed in Table 1.

Table 1. Quantities of the substances used for cryogel formation.

Substance Concentration	Scaffold 1	Scaffold 2	Scaffold 3	Scaffold 4
ddH ₂ O	5.78 mL	3.78 mL	7.11 mL	5.03 mL
pHEMA 98%	500 µL	500 µL	1 mL	1 mL
BAA 2%	250 µL	250 µL	170 µL	10 µL
Gelatin 30%	2 mL	4 mL	250 µL	2 mL
Collagen 3.5 g/L			1 mL	
TEMED			20 µL	
APS 10%			200 µL	
Glutaraldehyde 25%			250 µL	

poly-(2-hydroxyethyl methacrylate), 2-hydroxyethyl methacrylate; BAA, bisacrylamide; TEMED, tetramethylethylenediamine; APS, aminoperoxodisulfate.

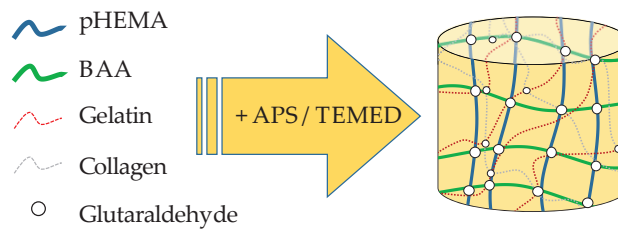
The cryogels were prepared as shown in Figure 1. In brief, the gels were prepared by thoroughly mixing collagen, ddH₂O, and gelatin and then incubating on ice for at least 30 min. Then pHEMA and BAA were added and the solution was thoroughly mixed again. Polymerization was started by adding tetramethylethylenediamine (TEMED), aminoperoxodisulfate (APS), and glutaraldehyde. Then, 10 mL of solution, containing all substances listed in Table 1, were immediately pipetted into several 2 mL syringes, which were placed in a freezer at −18 °C for a minimum of 16 h to allow the polymerization of the scaffold components to form the cryogel. After polymerization, the frozen scaffolds were cut into 3 mm-thick slices. The scaffolds were sterilized in 70% ethanol under agitation for 12 h and then soaked three times in PBS for at least 2 h, to remove the ethanol and non-polymerized scaffold components. Preliminary experiments showed that pre-incubation of the scaffolds for 72 h with medium containing 10% fetal calf serum (FCS) increased cell adherence significantly.

2.2. Scaffold Characterization

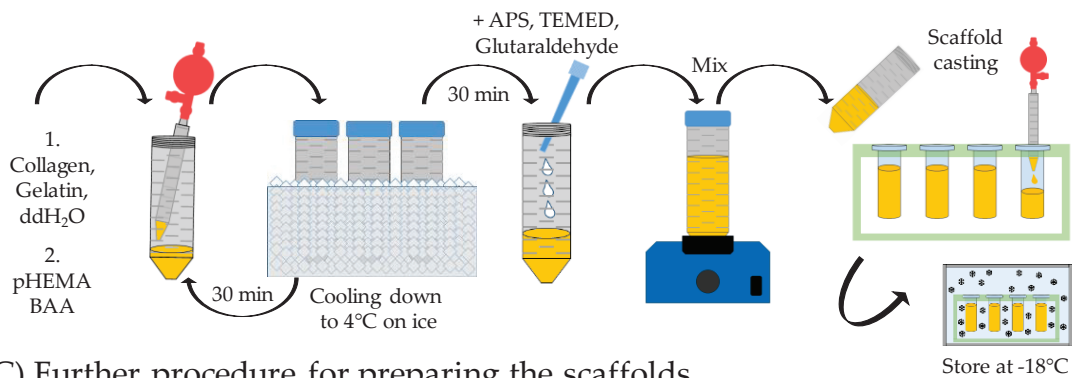
2.2.1. Pore Size

Analyses of pore size and pore structure were performed as previously described [16]. Briefly, the scaffolds were stained using a sulforhodamine B (SRB) solution (0.08% SRB in 1% acetic acid). The scaffolds were washed three times with 1% acetic acid solution to remove unbound SRB. The pore structure of the cryogels was visualized by using red fluorescence to reveal bound SRB. An EVOS fluorescence microscope (Life Technologies, Darmstadt, Germany) was used to obtain fluorescent images. The size and shape of the pores were determined using ImageJ software, version 1.5 (National Institutes of Health, Bethesda, MD, USA).

A) Scheme of cryogel preparation



B) Cryogel manufacturing



C) Further procedure for preparing the scaffolds

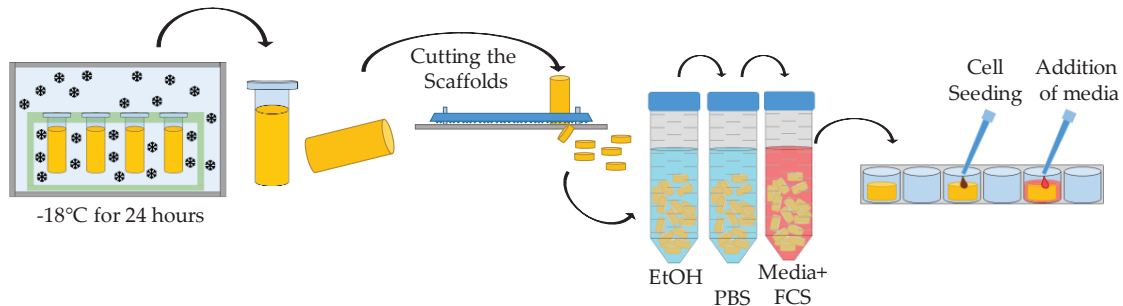


Figure 1. Schematic overview of scaffold production. (A) Formation of a scaffold matrix through the cross-linking of the scaffold components. (B) Mixture of the individual scaffold components and pouring of the scaffolds. (C) Further procedure, cutting the scaffolds, preparation of the scaffolds prior to cell cultivation, and seeding of the cells.

2.2.2. Porosity

The porosity of the various scaffolds was measured using a modified version of the protocol published by Fan et al. [26]. Briefly, scaffolds, with a height of about 3 mm and a diameter of 1 cm that were fully saturated with PBS for at least 30 min were weighed (m_1) and placed in a cell strainer. After centrifugation for 10 min at $4200 \times g$ the scaffolds were weighed again (m_2). The porosity was calculated using the following formula:

$$\text{Porosity (\%)} = \frac{(m_1 - m_2)}{(\rho_w \times V)} \times 100\% \quad V = \text{scaffold volume, } \rho_w = \text{density of PBS.}$$

2.2.3. Scaffold Permeability

The permeability of the scaffolds was determined by measuring the liquid diffusion rate [27]. Briefly, the scaffolds were transferred to a well plate to which enough SRB solution (0.08% in 1% acetic acid) was added to ensure that the scaffolds were surrounded, but not covered. The diffusion

of the red-colored SRB solution into the scaffold was measured over 30 min. Microscopic images were captured every 5 min using a reflected light microscope (Bresser, E122002, Rhede, Germany). The distance from the scaffold border to the dye front was measured and evaluated using ImageJ. At each time-point, the distance was assessed at 20 sites per scaffold. The diffusion rate per minute was calculated. Representative images which illustrate the procedure are shown in Figure S1.

2.2.4. Water Uptake Rate and Swelling Ratio

The water uptake rate and swelling ratio of the scaffold prototypes, with a height of about 3 mm and a diameter of 1 cm, were measured as previously described [28] and calculated using the following equations:

$$\text{Swelling ratio (\%)} = \frac{(\text{scaffold wet weight (g)} - \text{scaffold dry weight (g)})}{\text{scaffold dry weight (g)}} \times 100 \quad (1)$$

$$\text{Water uptake (\%)} = \frac{(\text{scaffold wet weight (g)} - \text{scaffold dry weight (g)})}{\text{scaffold wet weight (g)}} \times 100 \quad (2)$$

The dry and wet weights (in grams) of the scaffolds were measured with an analytical balance as described above.

2.2.5. Matrix Stiffness

A microscale mechanical testing system (Microsquisher, CellScale, Waterloo, Canada) was used to measure the mechanical properties of the various scaffolds [29]. The scaffolds were stored in PBS before measurement to prevent dehydration. PBS soaked scaffolds were used for compression testing. Cylindrical samples with a height of about 3 mm and a diameter of 2 mm were cut out of the different scaffold prototypes. All samples were mechanically compressed with a calibrated tungsten microbeam (diameter 0.558 mm) with a 3 × 3 mm square compression plate at the end. The samples were uniaxially compressed by 10% with force and displacement. Details are given in Table 2

Table 2. Measurement parameters for mechanical properties for pHEMA scaffolds.

Magnitude	Loading Rate	Hold	Recovery	Rest	Repeats
10.0%	10%/100 s	2 s	10 s	0 s	1

These force-displacement data were used to calculate the modulus of elasticity (E) by dividing the nominal stress value (σ) by the maximal nominal strain (ϵ) of the samples.

2.3. Scanning Electron Microscope (SEM) Images

2.3.1. Sample Preparation for the SEM Images

The samples of healthy and cirrhotic livers were used for the SEM images from patients that had undergone tumor resection surgery [6]. The samples were frozen in liquid nitrogen immediately after removal. Informed, written consent was obtained from patients in accordance with the ethical guidelines of the Ethics Commission of the medical faculty of the University of Tübingen, Tübingen, Germany (project number: 298_2012BO1). SEM images of the scaffolds and the liver tissue were obtained after lyophilization.

2.3.2. Preparation of the SEM Images

SEM investigations were performed using a JEOL JSM-7200 FLV setup with a field-emission source (JEOL, Freising, Germany). Prior to imaging, the samples were sputtered with gold. The thickness of the sputter layer was about 20 nm. First, a series of images for each sample was taken to provide an

overview. The illustrations presented in this report are from characteristic areas selected from these images. The size of the structures shown can be determined from the scale bars included in the images.

2.4. Culture of HepG2 Cells and Seeding of the Cells on the Scaffold

The HepG2 cells were cultured as previously described [30]; briefly, the cells were cultivated in a Dulbecco's Modified Eagle's Medium (DMEM) high glucose medium containing 10% FCS, 100 U/mL penicillin, and 100 µg/mL streptomycin. All cell culture reagents were purchased from Sigma Aldrich (St. Louis, MI, USA). The cells were cultured at 37 °C in a humidified atmosphere with 5% CO₂. HepG2 cells from passages two to ten after thawing were used for the experiments as previously described [31]. Before plating, the cells for the experiments were washed with PBS and detached from the cell culture flask using trypsin/EDTA (0.5 g/L trypsin and 0.2 g/L EDTA). Cell detachment was checked with the light microscope, and then trypsin digestion was stopped using FCS-containing culture medium. The cells were centrifuged at 600× *g* for 10 min, then the supernatant was removed, and the cells were resuspended using fresh culture medium. Using a Neubauer chamber, the cells were counted and seeded on the scaffolds in the desired concentration using the "drop-on" seeding method [16,30]. Scaffolds were placed in a 24-well plate, as much of the medium as possible that had been used for the pre-incubation was aspirated and 40 µL of the cell suspension were dispensed onto the central area on the top of the scaffolds. Then, 700 µL of fresh culture medium were added to the cells after 4 h. This amount of media was required to cover the scaffold completely.

2.5. Measurement of Mitochondrial Activity with Resazurin

To measure Resazurin conversion, the scaffolds were washed once with PBS and then incubated with a 0.0025% Resazurin solution (in DMEM medium) for 1 h at 37 °C. The fluorescence of the resorufin thus produced was measured at 544 nm/590–10 nm using the Omega Plate Reader (BMG LABTECH, Ortenberg, Germany) [16].

2.6. Staining of the Cells with Calcein-AM and Hoechst

The cells cultured on the scaffolds were stained with Calcein-AM (final concentration 2 µM) and Hoechst 33342 (final concentration 2 µg/mL) to enable fluorescence microscopy images to be captured. Hoechst dye was used to stain double-stranded DNA; it allows cell nuclei to be detected in the fluorescence microscope channel DAPI (357/447 nm). Calcein-AM was used to stain living cells and was detected in the green fluorescent protein (GFP) channel (470/525 nm). A mixture of both dyes diluted in PBS was added to the cell-seeded scaffolds and incubated for 30 min at 37 °C, protected from light. Then, scaffolds were washed at least three times with PBS. Microscopy of stained cells was performed using the EVOS FL fluorescence microscope (Life Technologies, Darmstadt, Germany).

2.7. Effect of Scaffold Pre-Incubation

2.7.1. Increasing Cell Attachment by Pre-Incubation of Scaffolds

Several solutions were tested to improve the cell adherence by pre-incubation of the scaffolds. We tested Arg-Gly-Asp (RGD)-rich proteinaceous solutions, such as gelatin and human serum, as well as culture media with and without FCS. For this experiment, the scaffolds were pre-incubated for at least 7 days with the RGD-containing solutions. As a control condition scaffolds were incubated in PBS for the same period. The substances used and their concentrations are shown in Table 3. The cells were seeded on the scaffolds in a density of 2×10^5 cells/scaffold as described before, and the conversion of Resazurin was measured after 24 h.

Table 3. Substances used in the pre-incubation experiment.

Substance	Concentration	Note
DMEM	100%	Without additives
DMEM, FCS, P/S	10% FCS, 1% P/S	10,000 units penicillin and 10 mg streptomycin/mL
Collagen	0.14 g/L in PBS	This concentration is usually used for plate coating [25]
Bovine serum albumin	5% in PBS	-
Coldwater fish gelatin	30% in ddH ₂ O	-
Human serum	100%	-
FCS	100%	-
Gelatin, FCS	50% FCS, 15% Gelatin, ddH ₂ O	-

DMEM, Dulbecco's Modified Eagle's Medium; FCS, fetal calf serum; P/S, Penicillin/ Streptomycin.

2.7.2. Length of Pre-incubation of Scaffolds with Culture Medium

For this experiment, scaffolds were prepared as described before. Three scaffolds per experiment were transferred to FCS-containing culture medium at 14, 10, 7, 3, 2, and 1 day(s) before cells were plated on the scaffolds. The remaining scaffolds continued to be incubated in PBS, and 8×10^4 HepG2 cells were plated per scaffold (day 0). A reduction of the cell numbers relative to the previous experiment was required because in this experiment we were not only investigating the cell attachment but also the viability of the cells over 5 days cultured on the scaffold. Resazurin conversion was measured 24 h as well as on day 5 after seeding. Additionally, living cells were stained for microscopy using Calcein-AM on day 5.

2.8. Metabolic Tests of the Cells on the Scaffolds

We measured the activity of different phase I/II enzymes as well as the ability of cells to detoxify ammonia as indicators of hepatic function. Cells were seeded onto scaffolds at a concentration of 2×10^5 cells/scaffold as described above. Since previous studies revealed that the addition of insulin and hydrocortisone to the culture medium increases the activity of CYP enzymes in liver cell lines [32], we supplemented our medium with 1 mM human insulin and 0.8 μ g/mL hydrocortisone 24 h after seeding [32]. Then, cells were incubated on scaffolds for a total time of 72 h since recent studies revealed maximum metabolic changes at this time point [32]. The subsequent metabolic tests were performed as follows.

2.8.1. Urea Measurement

The quantification of urea was carried out using a 3D adaptation [16] of a protocol published by Seeliger et al. [33]. The scaffolds were washed with PBS 72 h after seeding, then the scaffolds were incubated using an additive-free medium for 24 h in the presence of 5 mM ammonium chloride. Then, 80 μ L of the supernatant were mixed with 60 μ L of O-phthalaldehyde solution (1.5 mM O-phthalaldehyde, 4 mM Brij-35, 0.75 M H₂SO₄) and 60 μ L of NED reagent (2.3 mM N-(1 Naphthyl) ethylenediamine dihydrochloride, 80 mM boric acid, and 4 mM Brij-35, 2.25 M H₂SO₄), and incubated for 1 h at 37 °C. The absorbance was measured at 460 nm (Omega Plate Reader) and compared to a urea standard curve (0–100 μ g/mL) on the same plate.

2.8.2. Measurement of Phase I/II Activities

The activity of phase I/II enzymes was measured by fluorescence-based methods, as described by Ehnert et al. [34]. The activity of phase I enzymes CYP 1A2, CYP 3A4, and CYP 2C9, and phase II enzymes, uridine diphosphate glucuronosyltransferase (UGT) and glutathione S-transferase (GST), was measured since these enzymes are essential in the metabolism of several drugs [4,35]. The substrates, the phase II inhibitors, and the products used, as well as the corresponding wavelengths, are summarized

in Table 4. Before measuring, the scaffolds were washed once with PBS and then incubated for 30 min in plain medium-containing substrates and inhibitors as indicated. To exclude the interference of scaffold components with the measurement, scaffolds without cells were used as a background control.

Table 4. Conditions used for phase I/II measurements.

Enzyme	Substrate	c final in μM	Measured Product	Phase II Inhibitors	Measured Wavelength
CYP 1A2	7-Ethoxycoumarin	25	7-Hydroxycoumarin	1.5 mM Salicylamid, 2 mM Probenecid	355/460 nm
CYP 3A4	7-Benzoyloxy-4 (trifluoromethyl) coumarin	5	7-Hydroxy-4 (trifluoromethyl) coumarin	1.5 mM Salicylamid, 2 mM Probenecid	355/520 nm
CYP 2C9	Dibenzylfluorescein	5	Fluorescein	10 μM Dicumarol	485/520 nm
UGT 2B7	4-Methylumbelliferon	6.25	4-Methylumbelliferon	-	355/460 nm
GST	Monochlorobimane	50	Monochlorobimane-glutathione conjugate	-	355/460 nm

2.9. Statistical Analysis

Non-parametric Mann–Whitney U tests were used to assess differences between two groups. Group comparisons involving more than two groups were carried out with the non-parametric Kruskal–Wallis H test, followed by Dunn’s multiple comparison test, implemented in GraphPad Prism 5.00 Software (GraphPad Software, San Diego, CA, USA). Data are represented as means \pm SEM from at least three independent experiments ($N \geq 3$). All statistical comparisons were two-sided as this was an exploratory data analysis and significance is denoted as follows: $p < 0.05$ (*), $p < 0.01$ (**), and $p < 0.001$ (***)

3. Results

3.1. Characterization of the Natural ECM of Healthy and Cirrhotic Liver Tissue

To develop scaffolds corresponding to the healthy and fibrotic liver, it is necessary to characterize the respective in vivo environments and then develop an in vitro model representing these characteristics. Therefore, we captured SEM images of healthy and cirrhotic liver tissue samples (Figure 2A,B). The images show that there are differences between the structure of the ECM of the healthy and cirrhotic liver. The ECM of the healthy liver is, as described before [6], an open-pored, thin-walled structure (Figure 2A), while the cirrhotic tissue has thicker cell walls and slightly larger pores (Figure 2B).

3.2. Testing of Different Scaffolds for the Cultivation of Liver Cells

To mimic the in vivo environment as closely as possible, we carried out preliminary tests on various different pHEMA/BAA-based scaffold prototypes, created by systematically varying single scaffold components. Table 5 and Figure 3 summarize the characteristics of the scaffolds that have a porous structure, allow cell attachment, and match the criteria for pore size and stiffness best. Therefore, they were selected for further investigation. Details of the used scaffolds components and their quantities are given in Table 1. The pore size of the different scaffold prototypes differed significantly between various scaffolds. Scaffold prototype 1 exhibited the largest pores, with a mean pore diameter of $115 \pm 29 \mu\text{m}$, whereas the pores of scaffold prototype 4 had a mean diameter of only $61 \pm 41 \mu\text{m}$. Scaffold prototype 1 also had the highest water uptake capacity and highest swelling ratio, followed by scaffold prototype 3.

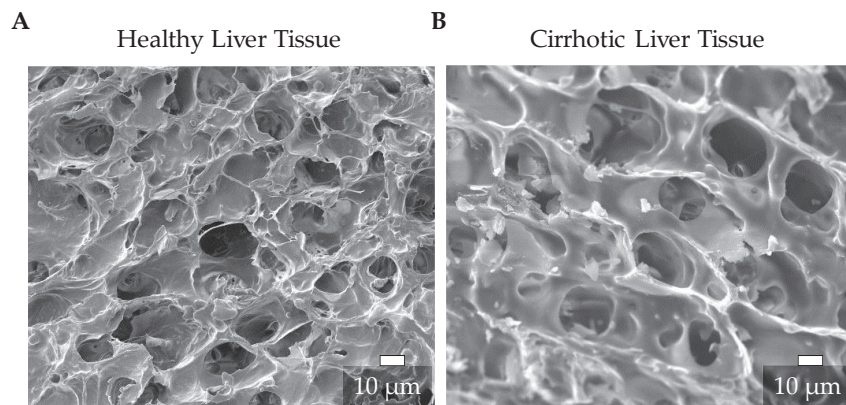


Figure 2. Representative SEM images of the extracellular matrix (ECM) structure of healthy (A) and cirrhotic liver (B) tissue (scale bar 10 µm).

Table 5. Characteristics of the four scaffold prototypes.

Measured Parameter	Scaffold 1	Scaffold 2	Scaffold 3	Scaffold 4
Pore diameter (µm)	115 ± 29	64 ± 13	85 ± 41	61 ± 41
Water uptake (%)	90.4 ± 1.6	83.9 ± 1.9	85.3 ± 4.4	83.4 ± 2.0
Swelling ratio (%)	965 ± 159	528 ± 72	641 ± 207	511 ± 74

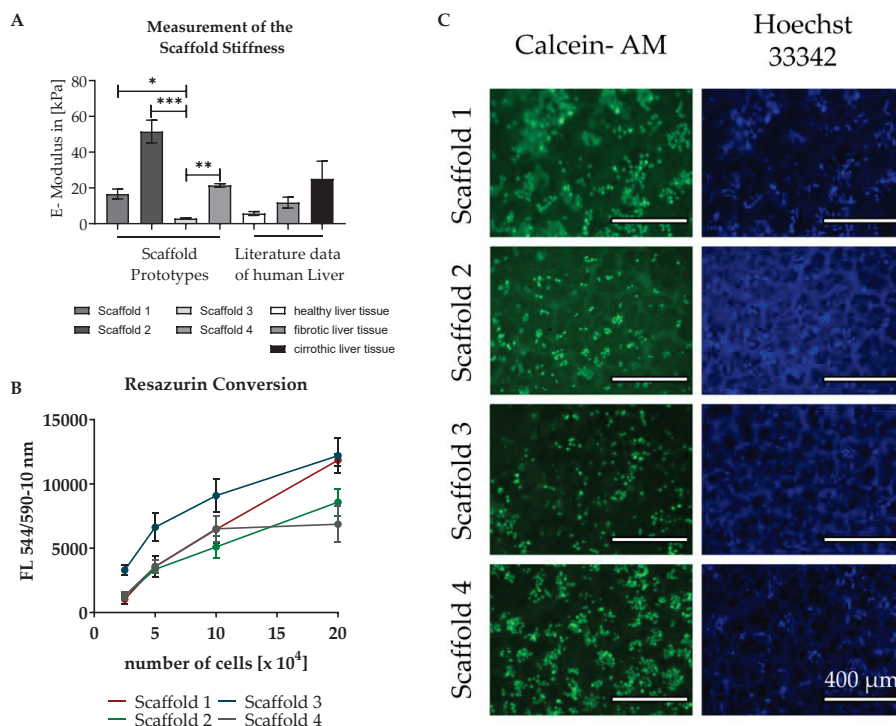


Figure 3. Characterization of the scaffold prototypes. (A) Scaffold stiffness was measured in $N = 3$, $n = 3$, since we were not able to measure the stiffness of liver tissue until now, the values were compared with published data [36] created by Fibroscan measurements. Bars represent mean \pm SEM; $p < 0.05$ (*), $p < 0.01$ (**), $p < 0.001$ (***) as indicated. (B,C) Attachment of cells to the four different scaffold prototypes was tested. HepG2 cells were plated in various concentrations on four different scaffold prototypes and cell attachment was evaluated by measuring Resazurin conversion and Hoechst 33342/Calcein-AM staining 24 h after seeding. The Resazurin conversion data are represented as averages of three independent experiments (each $n = 3$). Lines represent mean \pm SEM. Hoechst 33342 and Calcein-AM staining is shown in representative fluorescence microscopy images of 1×10^5 cells/scaffold.

Scaffold prototype 3, with a stiffness of 2.9 ± 1.3 kPa, showed rigidities similar to a healthy liver [36,37], whereas scaffold prototypes 1 and 4 showed the stiffness characteristics of a fibrotic or cirrhotic liver [36,37] (Figure 3A). As shown in Figure 3B, the adherence of the cells to the different scaffolds was tested by seeding different amounts of HepG2 cells (between 5×10^4 and 2×10^5 cells) on the scaffolds. Attachment of living cells was determined 24 h after seeding by measuring the conversion of Resazurin. Additionally, as shown in Figure 3C, cell attachment to the scaffolds was visualized using Calcein-AM and Hoechst 33342 staining, which causes fluorescence of living cells. Both the microscopic images and the Resazurin measurements showed that cells attached to all the scaffolds tested. Overall cells seeded on scaffold prototype 3 showed the highest conversion of Resazurin. Although all the scaffolds presented here could be used to cultivate HepG2 cells, scaffold prototypes 1 and 3 were deemed the most promising for our purposes due to their pore size, Resazurin turnover, and especially, stiffness. The stiffness of healthy livers can be mimicked with scaffold prototype 3 (healthy liver scaffold), while fibrotic/cirrhotic livers are represented by scaffold prototype 1 (fibrotic liver scaffold).

The selected scaffolds were further characterized in terms of porosity and permeability. The healthy liver scaffold had significantly higher porosity than the fibrotic liver scaffold (Figure 4A), but the two scaffolds had a similar permeability (Figure 4B). In addition, the SEM images revealed that both scaffolds showed a porous structure, with slightly larger pores in the fibrotic liver scaffold. However, both scaffolds had significantly larger pores than the corresponding human liver tissue (Figure 4C).

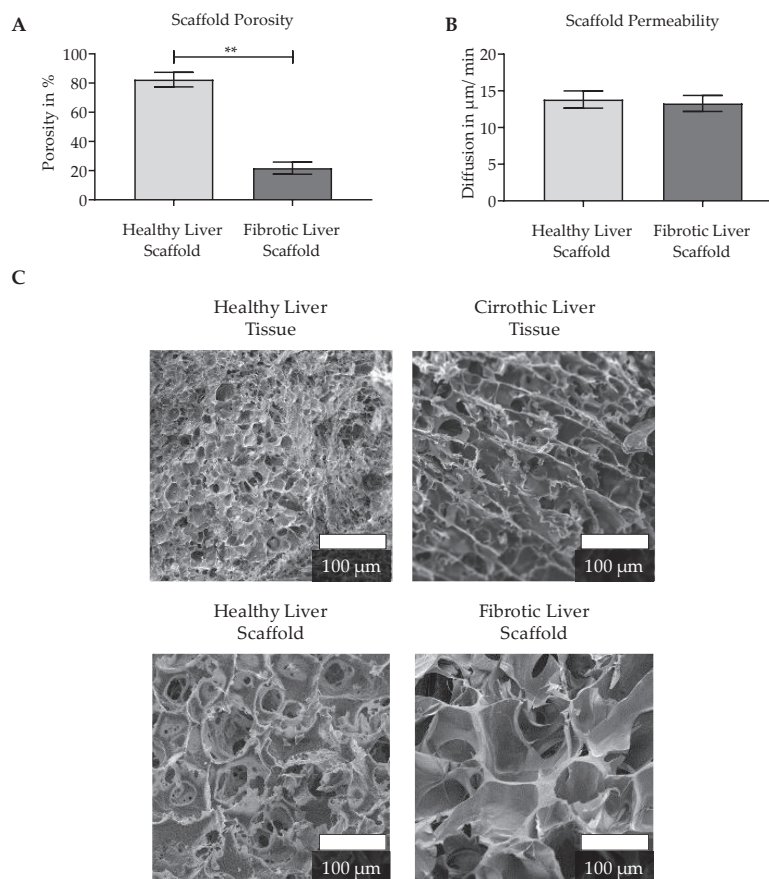


Figure 4. Physical characterization of the pHEMA/BAA-based 3D scaffolds: (A) Determination of the scaffold porosity ($n = 5$), three scaffolds were pooled and measured together. (B) Permeability was measured in a total of 9 scaffolds from three independent scaffold manufacturing days. Bars represent mean \pm SEM; $p < 0.01$ (**) as indicated. (C) SEM images of healthy liver and cirrhotic altered liver tissue and both selected scaffolds (scale bar 100 μm).

3.3. Effect of Scaffold Pre-incubation on Cell Adherence and Their Viability During the Culture

We investigated whether pre-incubation of the scaffolds in culture media containing various RGD-containing substances can increase the adherence of the cells to the scaffolds. As can be seen in Figure 5, pre-incubation had a positive effect on cell adherence in both tested scaffolds. However, the results clearly showed that this effect was much more pronounced in healthy liver scaffolds. There, pre-incubation increased cell attachment by as much as ten times, but in the case of the fibrotic liver scaffold, only a 1.4-fold increase in cell adherence was achieved. The results indicate that due to pre-incubation with FCS-containing medium, the cell adherence to both scaffold types could be increased, which is why this type of pre-incubation was used for both scaffolds later in the study.

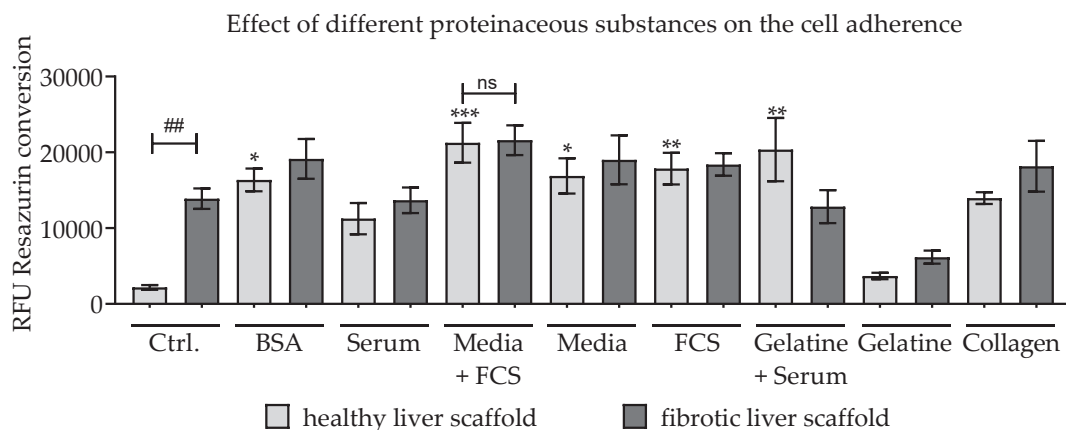


Figure 5. Effect of pre-incubation with various proteinaceous substances. Scaffolds were pre-incubated for at least 7 days with the Arg-Gly-Asp (RGD)-containing solutions. Resazurin conversion was measured 24 h after plating 2×10^5 HepG2 cells/scaffold on pre-coated scaffolds; scaffolds pre-incubated in PBS were used as a control; N = 3, n = 2. Bars represent mean \pm SEM. The significance of differences between pre-incubation with PBS (control) and proteinaceous substances is denoted as follows: * $p < 0.05$, ** $p < 0.01$, *** $p < 0.001$. The difference between the not pre-incubated healthy and fibrotic liver scaffold is indicated as ## $p < 0.01$. The difference between the media and FCS pre-incubated healthy and fibrotic liver scaffolds are indicated as not significant (ns).

In order to provide cells with an ideal environment for attachment on scaffolds and during culture over several days, we investigated the optimal time period for scaffold pre-incubation. Since previous results showed that pre-incubation had a more pronounced effect in ‘healthy’ liver scaffolds, this scaffold type was used to determine the ideal pre-incubation time. To determine the most suitable time period, the scaffolds were pre-incubated over periods of 1, 2, 3, 7, 10, and 14 day(s) using medium containing 10% FCS and 8×10^4 HepG2 cells were seeded on the scaffolds. Resazurin conversion was measured 24 h and five days after seeding. On day five living cells on the scaffold were additionally stained with Calcein-AM. As shown in Figure 6, the length of the pre-incubation had a huge influence on cell attachment properties. In addition, the number of living cells cultured on the scaffolds was significantly influenced after five days by the length of the pre-incubation period. A pre-incubation period of 24–72 h resulted even after a culture period of five days only in a low number of viable cells viable on the scaffold (Figure 6C). In addition, we observed a low level of Resazurin turnover after 24 h (Figure 6A) as well as after five days in culture (Figure 6B). However, using a pre-incubation period of seven days or more, many more living cells attached to the scaffold (Figure 6C). This result was accompanied by a significantly higher Resazurin turnover after 24 h (Figure 6A) as well as after five days (Figure 6B) in culture.

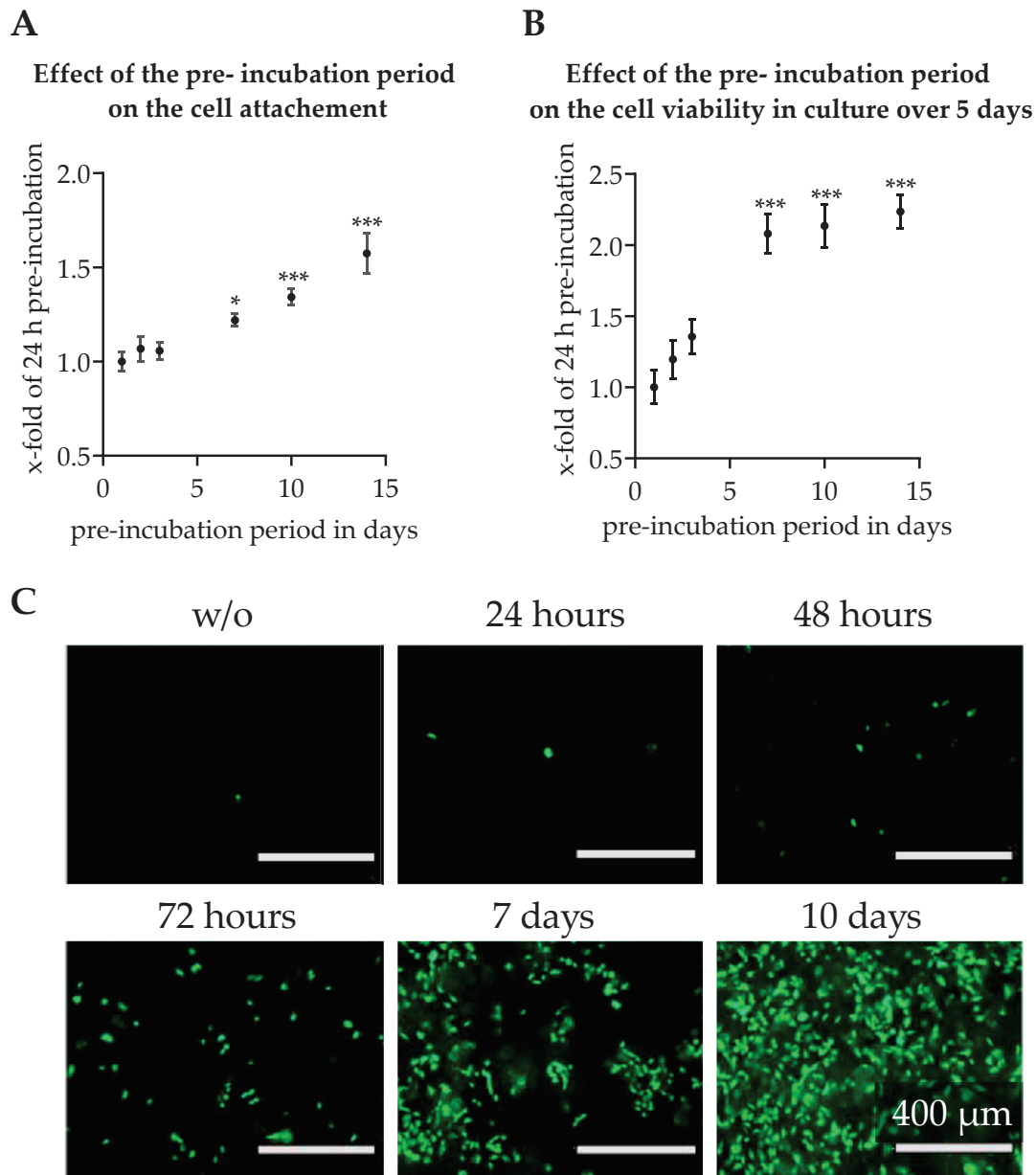


Figure 6. Effect of the length of pre-incubation on the attachment and the maintenance of HepG2 cells plated on the healthy liver scaffold. The scaffolds were pre-incubated with FCS-containing media between 24 h and 14 days. HepG2 cells were seeded on scaffolds. The conversion rate of Resazurin was measured 24 h (A) and five days (B) after seeding. The graphs show mean \pm SEM for $N = 3$, $n = 3$; * $p < 0.05$, *** $p < 0.001$ for comparison with a pre-incubation period of 24 h as indicated. Calcein-AM staining (C) after a culture period of five days; representative images of HepG2 cells plated on scaffolds using different pre-incubation periods.

As described above, the coating of scaffolds, especially the healthy liver scaffold, significantly increased cell adherence. SEM images were captured and analyzed to determine whether this change was accompanied by a modification of the scaffold surface. To do this, both scaffold types were pre-incubated for seven days in FCS-containing medium or PBS (control condition) and then freeze-dried to avoid damaging of the surface structure. As seen in Figure 7, the surface structures of the two types of scaffold differed significantly. The healthy liver scaffold had a rougher surface on which crystal-like constituents were superimposed, whereas the fibrotic liver scaffold appeared rather

smooth, with only small crystals superimposed on the surface. Pre-incubation with the FCS-containing medium did not significantly alter the surface of the fibrotic liver scaffold, but in contrast, resulted in significant changes in the healthy liver scaffold. Large deposits of agglomerates were observed on the surface of healthy liver scaffolds incubated in FCS-containing medium.

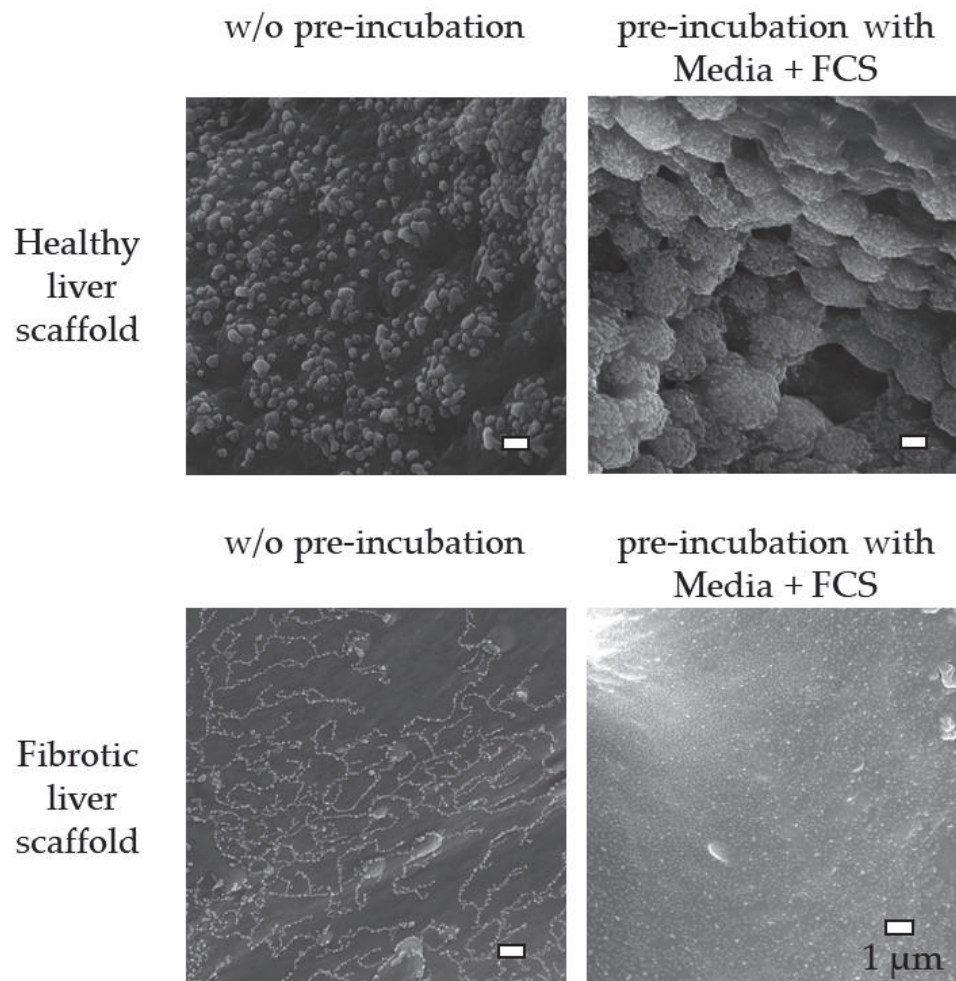


Figure 7. Effect of pre-incubation on the surface of the scaffolds. Representative SEM images of the surface of healthy and fibrotic liver scaffolds with and without (w/o) 7-day pre-incubation in FCS-containing medium (scale bar 1 μ m).

3.4. Evaluation of the Functionality of Hepatic Cells Plated on the Scaffolds

After characterizing the scaffolds, we investigated if stiffness variations had an impact on the metabolic activity of the seeded cells. As depicted from Figure 8, the cultivation of cells on 'healthy' liver scaffolds led to increased metabolic activity of CYP 3A4, CYP 2C9, and UGT compared to cells seeded onto the fibrotic liver scaffold. In contrast, the activity of CYP 1A2, and to a certain extent, GST was higher in cells seeded onto fibrotic liver scaffolds compared to cells cultured onto 'healthy' liver scaffolds. There was no statistically significant difference in urea production between cells cultured either on healthy or fibrotic scaffolds.

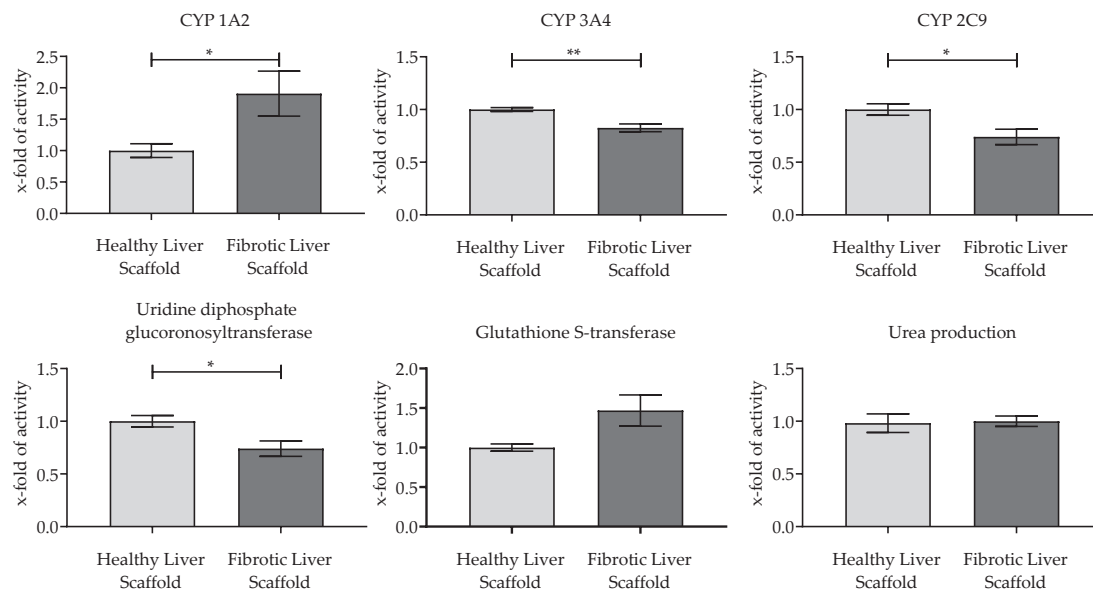


Figure 8. Metabolic activity of HepG2 cells plated on the two scaffolds. The activity of phase I enzymes CYP 1A2, CYP 3A4, and CYP 2C9, and phase II enzymes, UGT and GST, was measured. The detoxification of ammonia was quantified by measuring the urea production. Values are shown as multiples of the activity of cells plated on the healthy liver scaffold, $N = 3$, $n = 3$; bars represent mean \pm SEM; * $p < 0.05$, ** $p < 0.01$ as indicated.

4. Discussion

Disease-specific changes in the liver, that can be found in liver fibrosis and cirrhosis, alter the metabolism of drugs [38]. This not only necessitates individualized therapies but also the use of models that can represent these individual differences during the development and testing of drugs. This can be achieved in animal research through the use of certain disease models [39], but it is not yet possible for in vitro research. Therefore, the aim of this study was the development of such an in vitro model that mimics the in vivo situation of a “healthy” and a fibrotic altered liver. Scaffolds are suitable to imitate the in vivo environment since the cells are cultivated in a three-dimensional environment. It is also possible to imitate the interaction of cells with the ECM. In addition, it is possible to generate scaffolds that correspond in their stiffness to so-called “healthy” livers and a more fibrotic altered liver. This is an important issue since ‘healthy’ livers have a stiffness of approx. 6 kPa, which is much lower compared to the stiffness of cell culture plastics of approx. 100,000 kPa [20,40]. As our results show, it is possible to mimic the rigidity of the human liver and the stiffness of a fibrotic liver using pHEMA/BAA-based scaffolds. The scaffolds we tested were based on the same substances but differed in their gelatin content. By increasing the gelatin concentration, more gelatin molecules were covalently cross-linked by glutaraldehyde to form more stable amide bonds, thus increasing the stiffness of cryogels [41]. This is of particular interest since gelatin is an irreversibly hydrolyzed collagen and therefore has similar binding sites for cells [42,43]. Moreover, an increase in collagen fibers is an important aspect to develop various models of liver fibrosis and cirrhosis [44,45]. Thus, in addition to rigidity, a high ECM deposition can be mimicked by the fibrotic liver scaffolds [46]. It is likely that the higher gelatin concentration of the fibrotic liver scaffold is responsible for the fact that when scaffolds were not subjected to pre-incubation, with medium-containing FCS, cell adherence was significantly higher for the fibrotic scaffold than the healthy liver scaffold [27]. Pre-incubation with FCS-containing medium led to the deposition of agglomerates on the surface of ‘healthy’ liver scaffolds, but not of fibrotic-like liver scaffold surfaces. The accumulation of this agglomerates in the healthy liver scaffold and changes the surface structure of scaffolds; it seems it therefore may be responsible for increased cell attachment [47]. Pre-incubation experiments lined-out that culture medium alone was

able to increase cell adherence. Whether the amino acids content in the medium and/or other medium components was responsible for this positive attachment effect of cells onto the scaffold surface cannot be determined from the SEM images. However, as suggested by Amirikia et al., pre-incubation of scaffolds results in an increase in protein adsorption to the scaffold surface, thus reducing scaffold roughness and water contact angle, and therefore leading to an increased attachment of cells [47]. The same explanation could also account for the positive effect of pre-incubation which we found in our “healthy” liver scaffold.

When comparing the physical characteristics of both scaffold types (healthy and fibrotic-like), it was noticeable that the fibrotic-like liver scaffold had larger pores than the ‘healthy’ liver scaffold. Both scaffolds had significantly larger pores than the corresponding human liver tissues. Having a larger pore size relative to the *in vivo* analog could be desirable because in the *in vitro* model nutrients are not supplied to the cells via the bloodstream. This is in line with previous research that suggested that larger pore size may result in faster cell growth and increased diffusion [16,23,48]. In addition to this, both scaffolds have similar permeability but show different porosities. However, as can be seen from the SEM image, under dry conditions, the fibrotic-like liver scaffold also has an open pore structure. The low porosity value of this scaffold is probably due to water binding to the included gelatin. This could lead to a swelling of the matrix and in turn, reduce the volume of its pores. The lower porosity of the fibrotic liver also seems to be affected by the increased ECM deposition [46], as shown in the SEM images. This scaffold characteristic tends to make the model more similar to the *in vivo* environment. Since the scaffolds have similar permeability, one would not expect the difference in porosity to affect nutrient supply. As described above, the scaffolds were designed to represent liver stiffness of the healthy as well as the fibrotic human liver [20]. Unfortunately, we were not able to determine the stiffness of human liver samples using the same method used for the scaffolds. Therefore, the measured rigidities were compared to literature data determined by other methods [36,37].

Our activity measurements indicate that the cells plated onto softer ‘healthy’ liver scaffolds had higher levels of activity of phase I enzymes CYP 3A4 and CYP 2C9 and phase II enzyme, UGT 2B7; whereas the activity of the phase I enzyme CYP 1A2 and the phase II enzyme GST was higher in cells cultured on fibrotic-like liver scaffolds. The differences between the scaffold types with respect to phase II metabolism is a very interesting finding as it is already known that in liver cirrhosis, respectively steatosis, UGT 2B7 activity is reduced whereas GST activity is induced [49,50]. This result is remarkable since a change in phase II metabolism can lead to the formation of alternative metabolites with different pharmacological and toxicological potentials [51]. When evaluating these results, it must also be taken into account that HepG2 cells were used in this study, which have some of the functions of human hepatocytes, but differ significantly from them, especially in their metabolic activity [31,52]. Further studies are required to rule out that drug and/or substrate compounds might be absorbed to the scaffold surface and therefore deliver false-positive or false-negative results [53]. Although the differences between the two scaffolds concerning stiffness, pore size, and surface structure capture the *in vivo* differences well, the metabolic differences observed in the clinic cannot be attributed solely to the difference in stiffness. It might be useful to develop an *in vitro* model system that represents other aspects of liver fibrosis pathology, such as the change in ECM composition, oxygen tension, or inflammation [6,54,55]. Future 3D liver models should include cells like hepatic stellate and/or Kupffer cells to better mimic liver fibrosis [46].

5. Conclusions

Within this study, we developed scaffolds capturing the stiffness of a healthy and fibrotic-like liver. The coating of healthy liver scaffolds led to a change in the scaffold surface, which was accompanied by a significant increase in cell adherence. In addition, a correlation between the length of the pre-incubation period and the increase in cell adherence was observed. Since there were stiffness-related differences in the metabolic activity of the cells on the two scaffold types, they can be considered as an excellent model for studying how fibrotic-like liver alterations affect the metabolism of drugs.

Supplementary Materials: The following are available online at <http://www.mdpi.com/2079-4983/11/1/17/s1>, Figure S1: The diffusion rate of the red-colored SRB solution into the scaffold was used to determinate the permeability of the scaffolds. The figure shows representative images of the cross-section of the healthy liver scaffold. These images were used for the analysis of the scaffold permeability, Table S1: Concentrations of cryogel components which were tested during the development of the scaffolds.

Author Contributions: Conceptualization, M.R. and A.K.N.; methodology, M.R., M.W., S.R., C.G.-B., H.K., K.A., R.K., and S.E.; validation, A.K.N. and S.E.; formal analysis, M.R., M.W., and S.R.; investigation, M.R., M.W., and S.R.; resources, H.K.; data curation M.R., M.W., and S.R.; writing—original draft preparation, M.R.; writing—review and editing, all authors; visualization, M.R.; supervision, A.K.N. All authors have read and agreed to the published version of the manuscript.

Funding: This research received no external funding.

Acknowledgments: We thank Jürgen Kraut for preparation of the SEM images. We also thank Andrew McCaffrey and Helen Rinderknecht for proofreading the manuscript.

Conflicts of Interest: The authors declare no conflicts of interest.

Abbreviations

APS	Ammonium persulfate
BAA	Bisacrylamide
CYP	Cytochrome P450
DMEM	Dulbecco's Modified Eagle's Medium
ECM	Extracellular matrix
FCS	Fetal calf serum
GFP	Green fluorescent protein
GST	Glutathione S-transferase
PBS	Phosphate-buffered saline
pHEMA	Poly(2-hydroxyethyl methacrylate)
RGD	Proteins that contain Arg-Gly-Asp (RGD)
SEM	Scanning electron microscope
SRB	Sulforhodamine B
TEMED	Tetramethylethylenediamine
UGT	Uridine diphosphate-glucuronyltransferase

References

1. Ware, B.R.; Khetani, S.R. Engineered liver platforms for different phases of drug development. *Trends Biotechnol.* **2017**, *35*, 172–183. [[CrossRef](#)]
2. Martignoni, M.; Groothuis, G.M.; de Kanter, R. Species differences between mouse, rat, dog, monkey and human cyp-mediated drug metabolism, inhibition and induction. *Expert Opin. Drug Metab. Toxicol.* **2006**, *2*, 875–894. [[CrossRef](#)]
3. Soldatow, V.Y.; Lecluyse, E.L.; Griffith, L.G.; Rusyn, I. In vitro models for liver toxicity testing. *Toxicol. Res.* **2013**, *2*, 23–39. [[CrossRef](#)] [[PubMed](#)]
4. Godoy, P.; Hewitt, N.J.; Albrecht, U.; Andersen, M.E.; Ansari, N.; Bhattacharya, S.; Bode, J.G.; Bolleyn, J.; Borner, C.; Bottger, J.; et al. Recent advances in 2D and 3D in vitro systems using primary hepatocytes, alternative hepatocyte sources and non-parenchymal liver cells and their use in investigating mechanisms of hepatotoxicity, cell signaling and adme. *Arch. Toxicol.* **2013**, *87*, 1315–1530. [[CrossRef](#)] [[PubMed](#)]
5. Richert, L.; Liguori, M.J.; Abadie, C.; Heyd, B.; Manton, G.; Halkic, N.; Waring, J.F. Gene expression in human hepatocytes in suspension after isolation is similar to the liver of origin, is not affected by hepatocyte cold storage and cryopreservation, but is strongly changed after hepatocyte plating. *Drug Metab. Dispos. Biol. Fate Chem.* **2006**, *34*, 870–879. [[CrossRef](#)] [[PubMed](#)]
6. Ruoff, M.; Vosough, M.; Königsrainer, A.; Nadalin, S.; Wagner, S.; Sajadian, S.; Huber, D.; Heydari, Z.; Ehnert, S.; Hengstler, J.G.; et al. Towards improved hepatocyte cultures: Progress and limitations. *Food Chem. Toxicol.* **2020**, 111188. [[CrossRef](#)]
7. Donato, M.T.; Tolosa, L.; Gomez-Lechon, M.J. Culture and functional characterization of human hepatoma HepG₂ cells. *Methods Mol. Biol.* **2015**, *1250*, 77–93.

8. Burkhardt, B.; Martinez-Sanchez, J.J.; Bachmann, A.; Ladurner, R.; Nüssler, A.K. Long-term culture of primary hepatocytes: New matrices and microfluidic devices. *Hepatol. Int.* **2014**, *8*, 14–22. [[CrossRef](#)]
9. Ramaiahgari, S.C.; den Braver, M.W.; Herpers, B.; Terpstra, V.; Commandeur, J.N.M.; van de Water, B.; Price, L.S. A 3D in vitro model of differentiated HepG₂ cell spheroids with improved liver-like properties for repeated dose high-throughput toxicity studies. *Arch. Toxicol.* **2014**, *88*, 1083–1095. [[CrossRef](#)]
10. Gailhouse, L.; Liew, L.C.; Yasukawa, K.; Hagiwara, K.; Iwazaki, N.; Yamada, Y.; Hatada, I.; Ochiya, T. Epigenetic reprogramming of human hepatoma cells: A low-cost option for drug metabolism assessment. *Cell. Mol. Gastroenterol. Hepatol.* **2018**, *5*, 454–457.e451. [[CrossRef](#)]
11. Natarajan, V.; Berglund, E.J.; Chen, D.X.; Kidambi, S. Substrate stiffness regulates primary hepatocyte functions. *RSC Adv.* **2015**, *5*, 80956–80966. [[CrossRef](#)]
12. Bachmann, A.; Moll, M.; Gottwald, E.; Nies, C.; Zantl, R.; Wagner, H.; Burkhardt, B.; Sanchez, J.J.; Ladurner, R.; Thasler, W.; et al. 3D cultivation techniques for primary human hepatocytes. *Microarrays* **2015**, *4*, 64–83. [[CrossRef](#)] [[PubMed](#)]
13. Bale, S.S.; Golberg, I.; Jindal, R.; McCarty, W.J.; Luitje, M.; Hegde, M.; Bhushan, A.; Usta, O.B.; Yarmush, M.L. Long-term coculture strategies for primary hepatocytes and liver sinusoidal endothelial cells. *Tissue Eng. Part C Methods* **2015**, *21*, 413–422. [[CrossRef](#)] [[PubMed](#)]
14. Sudhakaran, P.R. Hepatocyte-matrix interaction. *Proc. Indian Acad. Sci. Chem. Sci.* **1999**, *111*, 331.
15. Jain, E.; Damania, A.; Kumar, A. Biomaterials for liver tissue engineering. *Hepatol. Int.* **2014**, *8*, 185–197. [[CrossRef](#)] [[PubMed](#)]
16. Ruoß, M.; Häussling, V.; Schügner, F.; Olde Damink, L.; Lee, S.; Ge, L.; Ehnert, S.; Nussler, A. A standardized collagen-based scaffold improves human hepatocyte shipment and allows metabolic studies over 10 days. *Bioengineering* **2018**, *5*, 86. [[CrossRef](#)]
17. Engler, A.J.; Sen, S.; Sweeney, H.L.; Discher, D.E. Matrix elasticity directs stem cell lineage specification. *Cell* **2006**, *126*, 677–689. [[CrossRef](#)]
18. Cozzolino, A.M.; Noce, V.; Battistelli, C.; Marchetti, A.; Grassi, G.; Cicchini, C.; Tripodi, M.; Amicone, L. Modulating the substrate stiffness to manipulate differentiation of resident liver stem cells and to improve the differentiation state of hepatocytes. *Stem Cells Int.* **2016**, *2016*. [[CrossRef](#)]
19. Desai, S.S.; Tung, J.C.; Zhou, V.X.; Grenert, J.P.; Malato, Y.; Rezvani, M.; Español-Suñer, R.; Willenbring, H.; Weaver, V.M.; Chang, T.T. Physiological ranges of matrix rigidity modulate primary mouse hepatocyte function in part through hepatocyte nuclear factor 4 alpha. *Hepatology* **2016**, *64*, 261–275. [[CrossRef](#)]
20. Theile, D.; Haefeli, W.E.; Seitz, H.K.; Millonig, G.; Weiss, J.; Mueller, S. Association of liver stiffness with hepatic expression of pharmacokinetically important genes in alcoholic liver disease. *Alcohol. Clin. Exp. Res.* **2013**, *37* (Suppl. 1), E17–E22. [[CrossRef](#)]
21. Wang, Y.; Kim, M.H.; Shirahama, H.; Lee, J.H.; Ng, S.S.; Glenn, J.S.; Cho, N.-J. Ecm proteins in a microporous scaffold influence hepatocyte morphology, function, and gene expression. *Sci. Rep.* **2016**, *6*, 37427. [[CrossRef](#)] [[PubMed](#)]
22. Gerets, H.H.J.; Tilmant, K.; Gerin, B.; Chanteux, H.; Depelchin, B.O.; Dhalluin, S.; Atienzar, F.A. Characterization of primary human hepatocytes, HepG₂ cells, and HepaRG cells at the mRNA level and CYP activity in response to inducers and their predictivity for the detection of human hepatotoxins. *Cell Biol. Toxicol.* **2012**, *28*, 69–87. [[CrossRef](#)] [[PubMed](#)]
23. Ye, S.; Boeter, J.W.B.; Penning, L.C.; Spee, B.; Schneeberger, K. Hydrogels for liver tissue engineering. *Bioengineering* **2019**, *6*, 59. [[CrossRef](#)] [[PubMed](#)]
24. Heydari, Z.; Najimi, M.; Mirzaei, H.; Shpichka, A.; Ruoss, M.; Farzaneh, Z.; Montazeri, L.; Piryaei, A.; Timashev, P.; Gramignoli, R. Tissue engineering in liver regenerative medicine: Insights into novel translational technologies. *Cells* **2020**, *9*, 304. [[CrossRef](#)]
25. Knobloch, D.; Ehnert, S.; Schyschka, L.; Büchler, P.; Schoenberg, M.; Kleeff, J.; Thasler, W.E.; Nussler, N.C.; Godoy, P.; Hengstler, J.; et al. Human hepatocytes: Isolation, culture, and quality procedures. In *Human Cell Culture Protocols*; Mitry, R.R., Hughes, R.D., Eds.; Humana Press: Totowa, NJ, USA, 2012; pp. 99–120.
26. Fan, J.; Jia, X.; Huang, Y.; Fu, B.M.; Fan, Y. Greater scaffold permeability promotes growth of osteoblastic cells in a perfused bioreactor. *J. Tissue Eng. Regen. Med.* **2015**, *9*, E210–E218. [[CrossRef](#)]
27. Kumari, J.; Kumar, A. Development of polymer based cryogel matrix for transportation and storage of mammalian cells. *Sci. Rep.* **2017**, *7*, 41551. [[CrossRef](#)]

28. Chung, E.J.; Ju, H.W.; Park, H.J.; Park, C.H. Three-layered scaffolds for artificial esophagus using poly (varepsilon-caprolactone) nanofibers and silk fibroin: An experimental study in a rat model. *J. Biomed. Mater. Res. Part A* **2015**, *103*, 2057–2065. [[CrossRef](#)]
29. Zhang, J.; Muirhead, B.; Dodd, M.; Liu, L.; Xu, F.; Mangiacotte, N.; Hoare, T.; Sheardown, H. An injectable hydrogel prepared using a peg/vitamin e copolymer facilitating aqueous-driven gelation. *Biomacromolecules* **2016**, *17*, 3648–3658. [[CrossRef](#)]
30. Ruoß, M.; Kieber, V.; Rebholz, S.; Linnemann, C.; Rinderknecht, H.; Häussling, V.; Häcker, M.; Olde Damink, L.H.; Ehnert, S.; Nussler, A.K. Cell-type-specific quantification of a scaffold-based 3D liver co-culture. *Methods Protoc.* **2020**, *3*, 1. [[CrossRef](#)]
31. Lin, J.; Schyschka, L.; Muhl-Benninghaus, R.; Neumann, J.; Hao, L.; Nussler, N.; Dooley, S.; Liu, L.; Stockle, U.; Nussler, A.K.; et al. Comparative analysis of phase I and II enzyme activities in 5 hepatic cell lines identifies Huh-7 and HCC-T cells with the highest potential to study drug metabolism. *Arch. Toxicol.* **2012**, *86*, 87–95. [[CrossRef](#)]
32. Ruoß, M.; Damm, G.; Vosough, M.; Ehret, L.; Grom-Baumgarten, C.; Petkov, M.; Naddalin, S.; Ladurner, R.; Seehofer, D.; Nussler, A.; et al. Epigenetic modifications of the liver tumor cell line HepG₂ increase their drug metabolic capacity. *Int. J. Mol. Sci.* **2019**, *20*, 347. [[CrossRef](#)] [[PubMed](#)]
33. Seeliger, C.; Culmes, M.; Schyschka, L.; Yan, X.; Damm, G.; Wang, Z.; Kleeff, J.; Thasler, W.E.; Hengstler, J.; Stöckle, U.; et al. Decrease of global methylation improves significantly hepatic differentiation of ad-mscs: Possible future application for urea detoxification. *Cell Transplant.* **2013**, *22*, 119–131. [[CrossRef](#)] [[PubMed](#)]
34. Ehnert, S.; Knobloch, D.; Blankenstein, A.; Müller, A.; Böcker, U.; Gillen, S.; Friess, H.; Thasler, W.E.; Dooley, S.; Nussler, A.K. Neohepatocytes from alcoholics and controls express hepatocyte markers and display reduced fibrogenic TGF- β /smad3 signaling: Advantage for cell transplantation? *Alcohol. Clin. Exp. Res.* **2010**, *34*, 708–718. [[CrossRef](#)] [[PubMed](#)]
35. Zanger, U.M.; Schwab, M. Cytochrome p450 enzymes in drug metabolism: Regulation of gene expression, enzyme activities, and impact of genetic variation. *Pharmacol. Ther.* **2013**, *138*, 103–141. [[CrossRef](#)]
36. Wong, V.W.; Vergniol, J.; Wong, G.L.; Foucher, J.; Chan, H.L.; Le Bail, B.; Choi, P.C.; Kowo, M.; Chan, A.W.; Merrouche, W.; et al. Diagnosis of fibrosis and cirrhosis using liver stiffness measurement in nonalcoholic fatty liver disease. *Hepatology* **2010**, *51*, 454–462. [[CrossRef](#)]
37. Mueller, S.; Seitz, H.K.; Rausch, V. Non-invasive diagnosis of alcoholic liver disease. *World J. Gastroenterol. WJG* **2014**, *20*, 14626. [[CrossRef](#)]
38. Rodighiero, V. Effects of liver disease on pharmacokinetics. *Clin. Pharmacokinet.* **1999**, *37*, 399–431. [[CrossRef](#)]
39. Liu, Y.; Meyer, C.; Xu, C.; Weng, H.; Hellerbrand, C.; ten Dijke, P.; Dooley, S. Animal models of chronic liver diseases. *Am. J. Physiol. Gastrointest. Liver Physiol.* **2012**, *304*, G449–G468. [[CrossRef](#)]
40. Skardal, A.; Mack, D.; Atala, A.; Soker, S. Substrate elasticity controls cell proliferation, surface marker expression and motile phenotype in amniotic fluid-derived stem cells. *J. Mech. Behav. Biomed. Mater.* **2013**, *17*, 307–316. [[CrossRef](#)]
41. Xing, Q.; Yates, K.; Vogt, C.; Qian, Z.; Frost, M.C.; Zhao, F. Increasing mechanical strength of gelatin hydrogels by divalent metal ion removal. *Sci. Rep.* **2014**, *4*, 4706. [[CrossRef](#)]
42. Zhang, Z.; Li, G.; Shi, B. Physicochemical properties of collagen, gelatin and collagen hydrolysate derived from bovine limed split wastes. *J. Soc. Leather Technol. Chem.* **2006**, *90*, 23.
43. Wissemann, K.W.; Jacobson, B.S. Pure gelatin microcarriers: Synthesis and use in cell attachment and growth of fibroblast and endothelial cells. *In Vitro Cell. Dev. Biol.* **1985**, *21*, 391–401. [[CrossRef](#)] [[PubMed](#)]
44. Masugi, Y.; Abe, T.; Tsujikawa, H.; Effendi, K.; Hashiguchi, A.; Abe, M.; Imai, Y.; Hino, K.; Hige, S.; Kawanaka, M.; et al. Quantitative assessment of liver fibrosis reveals a nonlinear association with fibrosis stage in nonalcoholic fatty liver disease. *Hepatol. Commun.* **2017**, *2*, 58–68. [[CrossRef](#)] [[PubMed](#)]
45. Bataller, R.; Brenner, D.A. Liver fibrosis. *J. Clin. Investig.* **2005**, *115*, 209–218. [[CrossRef](#)]
46. Sacchi, M.; Bansal, R.; Rouwkema, J. Bioengineered 3d models to recapitulate tissue fibrosis. *Trends Biotechnol.* **2020**. [[CrossRef](#)]
47. Amirikia, M.; Shariatzadeh, S.M.A.; Jorsaraei, S.G.A.; Soleimani Mehranjani, M. Impact of pre-incubation time of silk fibroin scaffolds in culture medium on cell proliferation and attachment. *Tissue Cell* **2017**, *49*, 657–663. [[CrossRef](#)]

48. Kumari, J.; Karande, A.A.; Kumar, A. Combined effect of cryogel matrix and temperature-reversible soluble–insoluble polymer for the development of in vitro human liver tissue. *ACS Appl. Mater. Interfaces* **2016**, *8*, 264–277. [[CrossRef](#)]
49. Baltruskeviciene, E.; Kazbariene, B.; Badaras, R.; Bagdonaite, L.; Krikstaponiene, A.; Zdanavicius, L.; Aleknavicius, E.; Didziapetriene, J. Glutathione and glutathione s-transferase levels in patients with liver metastases of colorectal cancer and other hepatic disorders. *Turk. J. Gastroenterol.* **2016**, *27*, 336–341. [[CrossRef](#)]
50. Dietrich, C.G.; Götze, O.; Geier, A. Molecular changes in hepatic metabolism and transport in cirrhosis and their functional importance. *World J. Gastroenterol.* **2016**, *22*, 72. [[CrossRef](#)]
51. Jancova, P.; Anzenbacher, P.; Anzenbacherova, E. Phase ii drug metabolizing enzymes. *Biomed. Pap. Med. Fac. Univ. Palacky Olomouc Czech Repub.* **2010**, *154*, 103–116. [[CrossRef](#)]
52. Kratochwil, N.A.; Meille, C.; Fowler, S.; Klammers, F.; Ekiciler, A.; Molitor, B.; Simon, S.; Walter, I.; McGinnis, C.; Walther, J.; et al. Metabolic profiling of human long-term liver models and hepatic clearance predictions from in vitro data using nonlinear mixed-effects modeling. *AAPS J.* **2017**, *19*, 534–550. [[CrossRef](#)] [[PubMed](#)]
53. Zeilinger, K.; Freyer, N.; Damm, G.; Seehofer, D.; Knöspel, F. Cell sources for in vitro human liver cell culture models. *Exp. Biol. Med.* **2016**, *241*, 1684–1698. [[CrossRef](#)] [[PubMed](#)]
54. Huettner, N.; Dargaville, T.R.; Forget, A. Discovering cell-adhesion peptides in tissue engineering: Beyond rgd. *Trends Biotechnol.* **2018**, *36*, 372–383. [[CrossRef](#)] [[PubMed](#)]
55. Koyama, Y.; Brenner, D.A. Liver inflammation and fibrosis. *J. Clin. Investig.* **2017**, *127*, 55–64. [[CrossRef](#)] [[PubMed](#)]



© 2020 by the authors. Licensee MDPI, Basel, Switzerland. This article is an open access article distributed under the terms and conditions of the Creative Commons Attribution (CC BY) license (<http://creativecommons.org/licenses/by/4.0/>).

Chapter 6: Publication IV

Ruoß, M.; Kieber, V.; Rebholz, S.; Linnemann, C.; Rinderknecht, H.; Häussling, V.; Häcker, M.; Olde Damink, L.H.H.; Ehnert, S.; Nussler, A.K. **Cell-Type-Specific Quantification of a Scaffold-Based 3D Liver Co-Culture.** *Methods Protoc.* 2020, 3, 1.

6.1 Synopsis:

The *in vitro* prediction of hepatotoxic effects of new drugs requires the development of cultivation methods that maintain the metabolic activity of hepatocytes over a longer period of time. For a descriptive prediction of such side effects, it is also necessary to mimic interactions of different cell types that play an essential role in drug-induced hepatotoxicity (Ruoss et al., 2020b). For these reasons, various 3D or co-culture models have been developed in recent years (Soldatow et al., 2013). More sophisticated models that combine 3D and co-culture approaches are also possible (Wei et al., 2018). However, the increasing complexity of these cultivation models also leads to difficulties. For example, one problem is that methods commonly used in conventional 2D monoculture for the quantification of cells and normalization of the results cannot or can only be partially used in more complex cultivation approaches. The reasons for this are, among others, interactions of the test reagents with the scaffold matrix and possible influences of the altered cultivation conditions on the metabolic activity of the cells, which is the endpoint of several quantification techniques (Rai et al., 2018, Ruoß et al., 2020). Until now it has only been possible, to a limited extent, to quantify the different cell types in a co-culture separately. However, since the correct quantification and normalization of the results is essential for their evaluation, it is necessary to develop suitable methods that allow stable and cell-type-specific quantification of the results. Such a method should also work for complex scaffold-based 3D co-cultures.

Therefore, the first aim of this study was to test different available methods for the quantification of 3D cultures. The second aim was to test whether one of these methods is also suitable for the cell type-specific quantification of a co-culture approach. It turned out that DNA-based methods have the decisive advantage over

other methods, such as the measurement of resazurin turnover, because they are working independently of the stress level of the cells and, in contrast to microscopic quantification, do not depend on the visibility of the cells on the scaffold surface. We also found a method that allows the isolation of DNA from cells plated on the scaffold without a significant loss of DNA. This outcome was possible by treating the colonized scaffolds with 98°C hot sodium hydroxide (NaOH).



Comparison of the different DNA-based methods showed that they partially—but significantly—differ in their limit of detection. Furthermore, based on our results, one can assume that the absorption-based measurement of DNA concentration as well as the fluorescence-based measurement using CyQuant are affected by interference (e.g.; from scaffold components). In contrast, both the PCR-based approach and the fluorescence-based measurement of DNA concentration using HOECHST 3342, which were also tested, also allow reliable quantification of the cells in 3D culture. The qPCR-based method we tested allows quantification of the 3D scaffold culture with high sensitivity. In addition, this method has the decisive advantage of allowing a cell type-specific quantification of individual cells in a co-culture by using species-specific primers.

We also showed that this method can be used for the quantification of co-cultures on different scaffold matrices. Also, the usage of conventional PCR delivers reliable results for this purpose. In addition, our results clearly show that a separate quantification of each cell type in a co-culture model is necessary because the adherence or proliferation of cells can differ significantly between the cells plated in monoculture or co-culture.

The only restriction of the developed method is the fact that different cell types must vary in at least on one position in their DNA sequence. Such distinctions between the sequences of different cell types allow the generation of a cell-type-specific primer that target this sequence. The detection of such differences is not only possible in the HepG2 (human), 3T3-J2 (mouse) co-culture model used here. It can also be applied to other differences, such as the use of transfected and non-transfected cells or the use of cell lines from males or females.

Article

Cell-Type-Specific Quantification of a Scaffold-Based 3D Liver Co-Culture

Marc Ruöß ^{1,*} , Vanessa Kieber ¹, Silas Rebholz ¹, Caren Linnemann ¹, Helen Rinderknecht ¹, Victor Häussling ¹, Marina Häcker ¹, Leon H. H. Olde Damink ², Sabrina Ehnert ^{1,†} and Andreas K. Nussler ^{1,†} 

¹ Department of Traumatology, Siegfried Weller Institute, BG-Klinik Tübingen, Eberhard Karls University, 72076 Tübingen, Germany; vanessa@kieber.de (V.K.); silasrebholz@gmail.com (S.R.); caren.linnemann@student.uni-tuebingen.de (C.L.); helen.rinderknecht@student.uni-tuebingen.de (H.R.); victor.haessling@student.uni-tuebingen.de (V.H.); marina.haecker@web.de (M.H.); sabrina.ehnert@gmail.com (S.E.); andreas.nuessler@gmail.com (A.K.N.)

² Matricel GmbH, 52134 Herzogenrath, Germany; olde_damink@matricel.de

* Correspondence: m.ruoss@hotmail.de; Tel.: +49-7071-606-1065

† These authors contributed equally to this work.

Received: 13 June 2019; Accepted: 18 December 2019; Published: 23 December 2019



Abstract: In order to increase the metabolic activity of human hepatocytes and liver cancer cell lines, many approaches have been reported in recent years. The metabolic activity could be increased mainly by cultivating the cells in 3D systems or co-cultures (with other cell lines). However, if the system becomes more complex, it gets more difficult to quantify the number of cells (e.g., on a 3D matrix). Until now, it has been impossible to quantify different cell types individually in 3D co-culture systems. Therefore, we developed a PCR-based method that allows the quantification of HepG2 cells and 3T3-J2 cells separately in a 3D scaffold culture. Moreover, our results show that this method allows better comparability between 2D and 3D cultures in comparison to the often-used approaches based on metabolic activity measurements, such as the conversion of resazurin.

Keywords: quantification; 3D culture; co-culture; cell number; PCR-based method

1. Introduction

In recent years, both the cultivation of liver cells in 3D cultures and their cultivation in co-culture with other cell types have been described in various studies [1,2]. These approaches aim to maintain the metabolic activity of primary hepatocytes or to increase the metabolic activity of liver model hepatoblastoma cell lines, such as HepG2 cells [3–6]. However, as the cultivation systems become more complex, difficulties arise. In conventional 2D culture, the quantification of cells can be done relatively quick in various ways. In addition to counting the cells by the classical trypan blue exclusion method, quantification of cells can be done by measuring the activity of mitochondrial dehydrogenases using substrates (e.g., resazurin, MTT, or XTT), ATP levels, total protein content (e.g., by sulforhodamine B (SRB) staining or Lowry measurement), or the DNA content (e.g., by using DNA staining dyes like CyQuant or Hoechst 33342) [7–14].

All these methods cited have their advantages and disadvantages (described in Table 1) [15]. The main disadvantage of most methods is that their use in 3D culture is limited or not possible at all. Furthermore, cell lysis is needed in all methods, except for the measurement of resazurin turnover. Additionally, interactions of the test reagent with scaffold ingredients could affect the results of the quantification between 2D and 3D and such an interference cannot easily be identified.

Table 1. Comparison of different cell quantification techniques.

	Mitochondrial Activity (Resazurin, MTT, or XTT)	ATP Measurement	LDH Measurement	DNA Staining (CyQuant)	Protein Staining (SRB)	Protein Quantification (Lowry)
Assay principle	Measurement of mitochondrial dehydrogenase activity	Measurement of total ATP levels	Measurement of released LDH	Staining of total DNA	Staining of total protein	Measurement of soluble protein
Advantages	Wide range of applications, distinction of dead and living cells is possible	Very sensitive assay, distinction of dead and living cells possible, not affected by stress level of the cells	Very sensitive assay, not affected by stress level of the cells	Very sensitive assay, not affected by stress level of the cells	Favorable and stable assay for quantification of adherent cells, not affected by stress level of the cells	Used for adherent and suspension cells
Disadvantages	Affected by stress level of the cells	Lysis of cells necessary	Lysis of cells necessary for normalization, assay is susceptible to interference (e.g., by FCS)	Lysis of cells necessary, assay is susceptible to interference (e.g., by phenol red of the medium)	Cannot be used for quantification in 3D culture	Lysis of cells necessary, assay is susceptible to interference (e.g., by FCS or scaffold ingredients)
No distinction between the different cell types in co-culture possible						
References	[4,6,16,17]	[8]	[18]	[7]	[12,13,19]	[11]

Measurement of the mitochondrial activity (e.g., by measurement of resazurin conversion) is often used for quantification of 3D approaches, but it has its limitations since the results of 2D and 3D approaches are often not comparable [20]. The activity of mitochondrial dehydrogenase in these assays (resazurin, MTT, or XTT) gives only an estimation of the combination of metabolic activity and redox potential of the cultured cells [21]. In order to use resazurin conversion for quantification, the stress level and redox potential of the cells between different conditions have to be constant. When comparing 2D to 3D culture, surface properties are one factor that can modify the stress level of the cells [22]. Therefore, constant conditions cannot be assumed. The same is true for matrix stiffness. Scaffolds often mimic natural organ stiffness (e.g., in the liver ≤ 6 kPa [23]), while standard tissue culture plastic with ~ 100 MPa is much stiffer [24].

Thus, it is necessary to develop a normalization method that is mostly independent of external factors, such as cell stress, pH, or stiffness. Only then a realistic comparison between 2D and 3D culture is possible. Since the DNA content in all cells is the same independent of the cultivation condition, we decided to use DNA to quantify and compare our 2D and 3D results. In this study, we tested different approaches of DNA quantification of 2D and 3D cultures and compared the results to the commonly used measurement of resazurin conversion. Additionally, we developed a PCR-based measurement of the DNA content as a normalization method of our 2D and 3D co-culture assays. We used murine 3T3-J2 cells in co-culture with HepG2 cells to increase the liver cell metabolic activity. The 3T3-J2 cells are an established model to increase not only the metabolic capacity of HepG2 cells but also of hepatocytes [25–27]. By using species-specific primers, we succeeded to quantify the individual numbers of the different cell types. This approach can be useful to study possible cell–cell and cell–matrix interactions of different cell types in 3D co-cultures. The aim of the study and the quantification approaches tested are summarized in Figure 1.

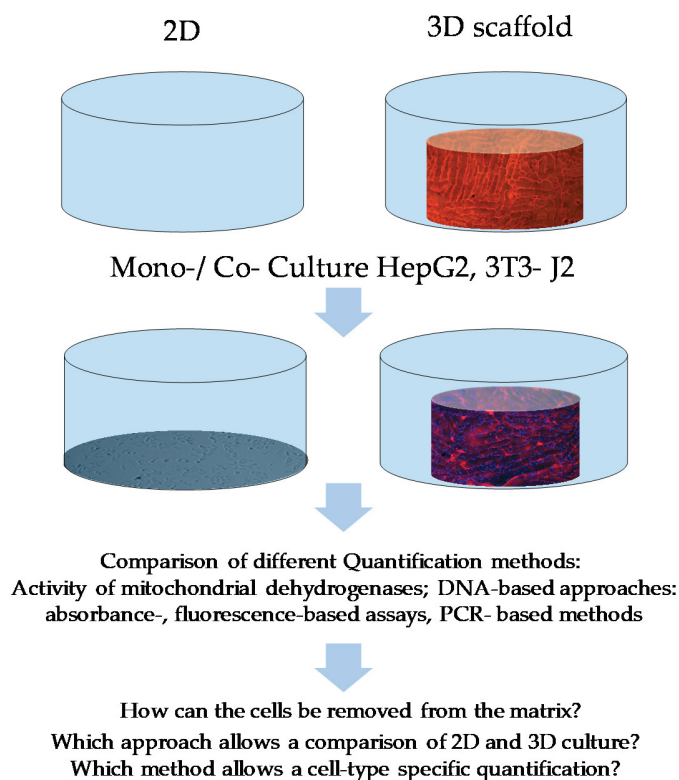


Figure 1. Comparison of different methods for the quantification of HepG2 and/or 3T3-J2 in mono- or co-culture. Three-dimensional culture environment Optimaix-3D scaffolds are used. The Optimaix-3D scaffolds (height 1.5 mm, \varnothing 5 mm) have a mean pore size of $88.9 \pm 21.1 \mu\text{m}$ and a porosity of $96.3 \pm 0.3\%$ as described before [4]. Representative pictures of HepG2/3T3-J2 cells plated on scaffolds are shown in Supplementary Figure S1.

2. Materials and Methods

2.1. Cell Culture and Cell Seeding

The cultivation of both cell types used was carried out in an incubator at 37°C and $5\% \text{CO}_2$ in a humidified atmosphere. For the cultivation of HepG2 cells, DMEM with high glucose (4.5 g/L) medium (Sigma-Aldrich, Munich, Germany) containing 10% fetal calf serum (FCS) (Thermo Fisher Scientific, Waltham, MA, USA) and 1% penicillin-streptomycin (P/S) (10,000 units penicillin and 10 mg streptomycin/mL) (Sigma-Aldrich) was used [28]. For the culture of 3T3-J2 cells, DMEM medium containing 10% bovine calf serum (BCS) (Sigma-Aldrich) and 1% P/S was used [26]. For the experiments, cells cultivated in cell culture flasks were washed once with PBS followed by incubation for 10 min at 37°C with trypsin/EDTA solution (0.5 g/L trypsin and 0.2 g/L EDTA). The detachment of the cells was checked microscopically. When cell detachment was complete, DMEM medium containing 10% FCS was added to stop the reaction. The cells were transferred in a reaction tube and were centrifuged at $600 \times g$ for 10 min. The supernatant was removed, and the cells were resuspended in a defined amount of DMEM medium containing 10% FCS and 1% penicillin-streptomycin. The cell number was determined using a Neubauer chamber. For the comparison of different quantification techniques, we used HepG2 and 3T3-J2 cells in mono-culture. HepG2/3T3-J2 cells ($1, 0.5, 0.25, \text{ and } 0.125 \times 10^5$) were plated in 24-well plates for the comparison of the different quantification techniques. For testing our newly developed co-culture quantification approach, we used constant cell numbers of 0.5×10^5 cells for mono-culture. In the co-cultures, 0.5×10^5 cells for each cell type were used. All experiments in 2D and 3D culture were carried out in 24-well plates using high glucose DMEM medium (containing 10% FCS and 1% P/S).

For 3D culture, Optimaix-3D scaffolds (Matricel, Herzogenrath, Germany) and self-made cryogels were used. For optimal cell attachment on the Optimaix-3D scaffold, the so-called “drop-on” seeding method was used [4]. Therefore, the cell suspension was concentrated by centrifugation to obtain a cell density of 3.33×10^6 cells/mL. For both cell types, serial dilutions were prepared. For mono-culture, 30 μ L of the respective cell solution was added on top of each scaffold (prepared in a well of a 24-well plate). For co-culture, 30 μ L of a cell solution containing both cell types were added on top of the scaffolds. After an attachment period of 4 h, additional medium was added to obtain a total volume of 500 μ L in all conditions. For our self-made cryogels, we increased the volume (but not the cell number) of the cell solution, since this scaffold was larger (10 mm in diameter). The volume of the cell solution was increased to 40 μ L to achieve a uniform distribution. Furthermore, the total volume of the medium was adapted to 700 μ L.

2.2. Cell Quantification by Optical Methods

The quantification of cell numbers under the different conditions was carried out 18 h after seeding. For our self-made scaffold, we reduced this period in the course of the study to 12 h to avoid possible influence due to different doubling times of the cells caused by the culture conditions. For cell quantification, resazurin conversion and DNA content (absorption- and fluorescence-based with Hoechst 33342 and CyQuant) were measured. In addition, quantification of the species-specific DNA content was tested by PCR-based methods.

2.2.1. Resazurin Conversion

As previously described, measurement of mitochondrial dehydrogenase activity is often used to quantify cells. Resazurin is particularly suitable for the 3D culture since the water-soluble product is released into the supernatant. To measure resazurin conversion, the scaffolds were transferred into a new 24-well plate to avoid the influence of cells attached to the plate surface. The medium of the 2D cultures was also removed. A 0.0025% resazurin solution in medium was added and, after incubation for 1 h at 37 °C, the formed resorufin was quantified (fluorescence) at a wavelength of 544 nm/590–10 nm using the OMEGA Plate Reader (BMG Labtech, Ortenberg, Germany) [4].

2.2.2. DNA Isolation in 2D and 3D Scaffold Cultures

Previous experiments have proven that it is impossible to collect all living cells from the scaffold. Treatment with trypsin is unsuccessful because FCS from remaining medium (even after washing) inactivates the enzyme. Therefore, we decided to isolate the DNA directly from the scaffolds, using a modified protocol developed initially for DNA extraction from tissue [29]. For extraction of DNA from cells plated on scaffolds, the scaffolds were first washed with PBS. Two scaffolds of each group were pooled for further DNA isolation. To remove disturbing fluid from the scaffolds, they were transferred to a cell strainer and centrifuged at $600 \times g$ for 10 min before being transferred to a 2 mL reaction tube. Supernatants were discarded. Detached cells, which can be found after centrifugation as a pellet in the reaction tube, were resuspended in 250 μ L 50 mM NaOH solution, which was then added to the scaffolds in a new reaction tube. The cells in 2D culture were also washed with PBS and then detached from the plate by using the same amount of heated (98 °C) 50 mM NaOH solution for 5 min. Cell detachment was verified by microscopy. For DNA extraction, the cells/scaffolds were incubated at 98 °C for 30 min. Subsequently, the reaction tubes were vortexed thoroughly and briefly frozen at -80 °C. Vortexing and freezing improved cell lysis. To all thawed samples, 250 μ L ddH₂O and 25 μ L Tris/HCl (1 M, pH = 8) were added. These DNA lysates were used for all tested DNA-based quantification methods. Since our self-made scaffold had a higher water uptake, we doubled the volumes of NaOH solution, ddH₂O, and Tris/HCl that were used.

2.2.3. Absorption Measurement by Using LVIS Micro Drop Plate

For the absorption-based quantification, all samples were measured on the LVIS Plate (BMG Labtech). One run consists of two steps. For the first part, a blank was measured. In our case, it was 2 μ L of DNA isolation buffer (1 mL demineralized water, 1 mL NaOH (50 mM), and 100 μ L Tris/HCl (1 M, pH = 8)). In the second step, 2 μ L of each sample was measured in duplicate. The DNA concentrations were calculated by the BMG Labtech OMEGA (Ortenberg, Germany) analyzation software MARS.

2.2.4. Fluorescence-Based CyQuant Measurement

For the fluorescence-based CyQuant measurement, we adapted the manufacturer's protocol. Briefly, the CyQUANT™ Cell Proliferation Assay Dye (Thermo Fisher Scientific, Waltham, USA) was diluted 1:400 in our DNA isolation buffer, which consisted of 250 μ L demineralized water, 250 μ L NaOH (50 mM), and 25 μ L Tris/HCl (1 M, pH = 8). The detection range was verified with the DNA standard from the CyQuant kit. A total of 10 μ L of each sample was pipetted into a 96-well plate in duplicate. Afterwards, 100 μ L of staining solution (CyQuant in DNA isolation buffer) was added to each well. The fluorescence measurements were carried out at an excitation wavelength of 485–12 nm and an emission wavelength of 520 nm.

2.2.5. Fluorescence-Based Hoechst 33342 Measurement

For the Hoechst 33342 measurement, we used a modified protocol following Richards et al. [30]. Therefore, Hoechst 33342 was diluted in a stock concentration of 2 mg/mL in PBS. This stock solution was diluted 1:100 in the earlier described DNA isolation buffer. A total of 90 μ L of each sample was pipetted into a 96-well plate in duplicate before 10 μ L staining solution was added per well. The samples were measured (fluorescence) at an excitation wavelength of 355 nm and an emission wavelength of 460 nm.

2.3. Cell-Type-Specific DNA Quantification

2.3.1. Test of Different Primers for the Usability in a Species-Specific DNA Quantification Method

For species-specific DNA quantification, it is necessary that the used primers are completely species-specific. An amplicon length of 150 to 250 bp is beneficial because it enables use in both conventional PCR and qPCR. Additionally, the used primers are not allowed to be exon spanning. Our criteria-fulfilling primers can be found in Table 2. By using primer blast (National Center for Biotechnology Information, U.S. National Library of Medicine USA), the species-specificity of the sequences was ensured. To avoid products on potentially unintended templates in the other species, we verified the species-specificity experimentally (Supplementary Figure S2). Additionally, we used the highest cell number of the mono-culture of the respective other cell line as a negative control for the quantification of our co-culture experiments.

Table 2. Primers used in species-specific DNA amplification.

Gene	<i>mIL-11</i>	<i>hUGT1A6</i>
Forward-Sequence 5'-3'	TGCTGACAAGGCTTCGAGTAG	TGGTGCCTGAAGTTAATTTGCT
Reverse-Sequence 5'-3'	ACATCAAGAGCTGTAAACGGC	GCTCTGGCAGTTGATGAAGTA
Amplicon in bp	156	209
Annealing Temperature in °C	62	62
Cycle Number	30	30
Reference Sequence	NC_000073.6	NC_000002.12

2.3.2. Conventional Semi-Quantitative PCR

PCR reactions were carried out by using the Red HS Taq Master Mix from Biozym (Vienna, Austria) according to the manufacturer's instruction. Briefly, a master mix was prepared that contained 10 μ L

Biozym Red HS Taq Master Mix, 1 μL each of forward primer and reverse primer (final concentration 400 nM), and 4 μL DEPC water for a single 20 μL PCR reaction. After distribution of the master mix to PCR tubes (16 μL each), 4 μL template DNA was added. The PCR was performed with the following program: initial denaturation 2 min at 95 °C; for the amplification, 30 cycles of the following steps: 15 s denaturation at 95 °C, 15 s annealing (temperature is primer-dependent (see Table 2)), and 45 s extensions at 72 °C, final denaturation 10 min at 72 °C. For analysis of the results, 8 μL of each sample was loaded onto a 2% agarose gel, which contained ethidium bromide for DNA staining. For separation of the samples, gel electrophoresis was carried out (80 V for 45 min). As referenced for DNA molecular weights, the DNA-Marker pUC19/Msp I (Carl Roth, Karlsruhe, Germany) or the Bionline Hyperladder II (Bionline, Memphis, TN, USA) were used. Intensity of the bands was measured with ImageJ software version 1.5 (National Institutes of Health, Bethesda, MD, USA). To analyze the PCR products in the logarithmic phase of the amplification, the cycle number and amount of template were optimized (Supplementary Figure S2).

2.3.3. Quantitative Real-Time PCR

In addition to conventional PCR, quantitative real-time PCR was performed. Therefore, Step One Plus® Real-Time PCR System (Life Technologies, Carlsbad, CA, USA) and GreenMasterMix, High ROX (Genaxxon Bioscience, Ulm, Germany) were used [19]. The same primer and DNA concentrations used for conventional PCR were used here. qPCR was carried out with the following parameters: 15 min at 95 °C for initial denaturation; 40 cycles of amplification with the following steps: denaturation for 15 s at 95 °C, annealing for 30 s at 62 °C, and extension for 30 s at 72 °C. Evaluation of the results was performed using StepOne Software version 2.3 (Life Technologies).

2.4. Cell-Type-Specific Cell Labeling

In addition to resazurin conversion measurement and the isolation of DNA, we took light microscopy pictures of the cells using the cell concentrations previously described. For better visualization of the cells in 3D culture and distinction between the two cell types in co-culture, the 3T3-J2 cells were stained using red fluorescent Cytoplasmic Membrane Staining Kit (PromoCell, Heidelberg, Germany), according to the manufacturer's instructions. Briefly, 3T3-J2 cells were detached by treatment with trypsin/EDTA and diluted to a concentration of 1×10^6 3T3-J2 cells. A total of 10 μL of cell labeling solution was added per mL of cell suspension. Cells were then incubated for 10 min at 37 °C and afterwards centrifuged at $600 \times g$ for 10 min. The supernatant was removed, the cells were washed once with PBS, and then resuspended in pre-warmed medium. Stained 3T3-J2 cells (0.5×10^5) and 1×10^5 unstained HepG2 cells were seeded in 2D and on the Optimaix-3D scaffold as described before. After approximately 18 h, the nuclei were stained with Hoechst 33342 (1:1000 dilution, 2 $\mu\text{g}/\text{mL}$ final concentration). Pictures were taken by fluorescence microscopy (EVOS FL, Life Technologies, Darmstadt, Germany).

Statistics

Statistical significance between two different groups was evaluated by the non-parametric Mann–Whitney U test. Statistical significance of more than two groups was evaluated by the non-parametric Kruskal–Wallis H test followed by Dunn's multiple comparison test (GraphPad Prism 8.00 Software, San Diego, CA, USA). All data are presented as mean \pm SEM of at least three independent experiments ($n \geq 3$). All statistical comparisons were performed two-sided using $p < 0.05$ (*), $p < 0.01$ (**), and $p < 0.001$ (***) as levels of significance.

3. Results

This study aimed to develop a simple and precise method for the quantification of a scaffold-based co-culture system. For improving the metabolic activity of human hepatic cells (e.g., HepG2 but also primary hepatocytes), a co-culture with fibroblasts (e.g., murine 3T3-J2 cells) was carried out.

Planning to continue the work with a combination of these cells, we selected a combination of HepG2 cells and 3T3-J2 cells as a test model. The design of the study will allow a rapid transfer into other co-culture systems.

3.1. Morphological Differences of HepG2 and 3T3-J2 Cells Can Be Used with Restrictions for Quantification in 2D Co-Culture but Not in 3D Co-Culture

As shown in Figure 2, in principle, the morphological differences of the two cell types in 2D culture can be used for a cell-type-specific quantification. While the fibroblasts have a spindle-shaped morphology, HepG2 cells are more hexagonal. The limitation of this eye-based quantification is quickly reached when cells grow dense or in 3D culture. Furthermore, the microscopic counting of the cells is very time-consuming. When adding fluorescent dyes into this quantification method, visualization and distinction of both cell types become easier, and quantification can be automated using software tools [31–33]. But this method is still not applicable to 3D scaffold cultures since cells inside the scaffold cannot be counted. Figure 2 shows the microscopic pictures and fluorescent staining of mono- and co-cultures in 2D and 3D.

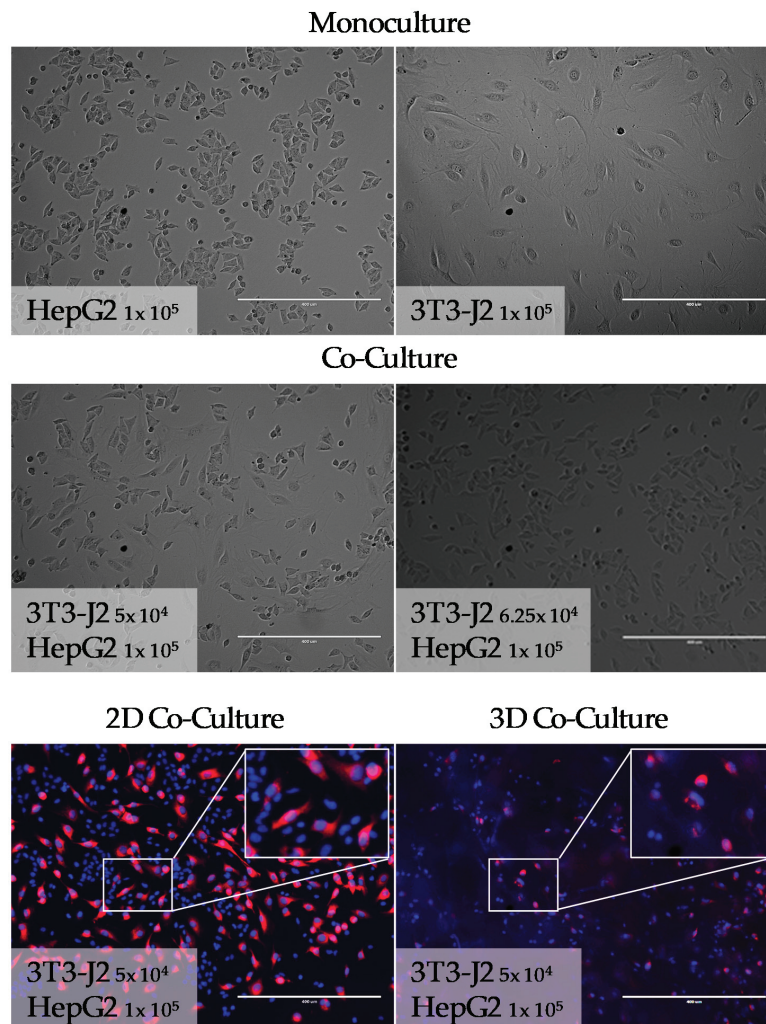


Figure 2. Light microscopy images of HepG2 cells and 3T3-J2 cells in mono- and co-cultures. HepG2 cells and 3T3-J2 cells were plated out using the cell numbers indicated in the pictures. Images were taken 18 h after plating the cells. For the fluorescence images, a carbocyanine dye was used to stain the cell membranes of the 3T3-J2 cells (red). All cell nuclei were stained with Hoechst 33342 (blue) and 100-fold magnification was used for all images. Scale bar is 400 μm .

3.2. Quantification of Conventional 2D Culture and 3D Scaffold Culture by Measuring the Mitochondrial Activity

Measurement of resazurin conversion, or similar methods such as MTT or XTT, has been widely used in the past to quantify cells in 3D scaffold culture [4,6]. As shown in Figure 3 (in detail in Supplementary Figure S3a, for each cell type separately including error bars), a correlation between increasing resazurin turnover and increasing cell counts was found in both systems. Therefore, the conversion of resazurin could be applied to our 2D system as well as in the 3D system. Regardless of the cell type, a significant difference in the resazurin conversion can be observed between the 2D culture and the corresponding 3D culture. To compare the different quantification methods, we calculated the area under the curve (AUC) of the 2D and 3D cultures, which allowed a method-independent comparison of the different quantification techniques.

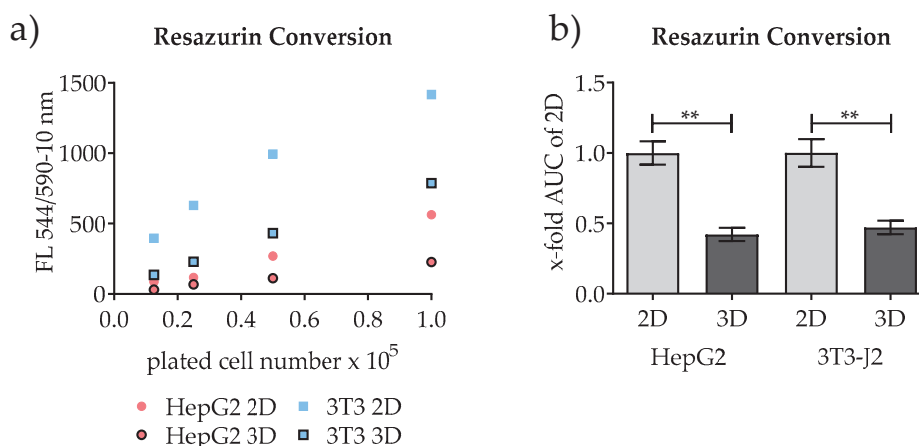


Figure 3. Shown here are 2D culture and 3D culture quantification by measurement of resazurin conversion. (a) Resazurin conversion of mono-cultures of HepG2 cells and 3T3-J2 cells in correlation to the plated number of cells. (b) Calculated area under the curve (AUC) of the resazurin conversion in HepG2 cells and 3T3-J2 cells (3D culture compared to the conventional 2D culture). $n = 3$, $n = 4$ (three independent runs, four technical replicates for each run); mean \pm SEM; ** $p < 0.01$.

3.3. Comparison of Alternatives to Resazurin Conversion for the Quantification of Conventional 2D Culture and 3D Scaffold Culture

In order to investigate whether the observed differences in resazurin conversion are due to different metabolic activities or different adherence of the cells in 2D and 3D cultures, we looked for a quantification approach that is mostly independent of external factors (e.g., cell stress). Since each cell contains the same amount of DNA and DNA is physically stable, we decided to test the quantification of cell numbers via quantification of the DNA.

3.3.1. Comparison of Different Approaches for Cell Detachment in 2D and from the Optimaix-3D Scaffold

In order to quantify the amount of DNA, the cells or the DNA have to be effectively retrieved from the scaffold. To determine the best approach for cell detachment in 3D, 1×10^5 HepG2 cells were plated in 2D and 3D. On the next day, the scaffolds were washed with PBS once. In the following, the cells or their DNA were removed from the scaffolds using one of three different approaches: centrifugation for 10 min at $600 \times g$, and incubated with trypsin/EDTA for 10 min or treatment with NaOH as described in 2.2.2. As shown in Figure 4, effective removal of DNA is only possible by using NaOH. Only there an amount of DNA comparable to 2D can be obtained. Therefore, this method was used for further experiments.

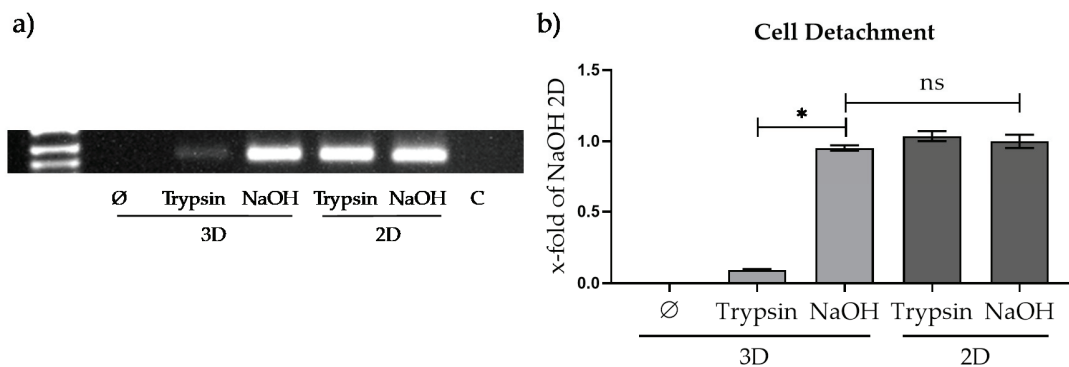


Figure 4. Cell detachment experiment, HepG2 cells were seeded onto Optimaix-3D scaffolds and in 2D culture plates. On the next day by PCR, it was tested whether the cells can be detached from the scaffold by centrifugation only or via incubation with trypsin. Additionally, cells seeded on scaffolds were lysed using pre-heated NaOH. As controls, 2D cultured cells treated with trypsin or NaOH were used. The number of cells (DNA) was determined by performing a conventional PCR targeting *hUGT1A6* gene (using the respective primer). (a) Representative gel picture of the *hUGT1A6* PCR using pooled samples of $n = 3$, $n = 3$. (b) $n = 3$: three scaffolds from each run were pooled and measured together within two technical replicates; mean \pm SEM; * $p < 0.05$.

3.3.2. Comparison of Methods for the Quantification of Conventional 2D Culture and 3D Scaffold Culture

Different DNA quantification methods were tested including an absorption-based measurement of DNA concentrations and two fluorescence-based methods (Hoechst 33342 and CyQuant). The tested fluorescent dyes showed a strong increase in fluorescence when binding to DNA. Figure 5 (in detail in Supplementary Figure S3b–e, separated for each cell type with error bars) shows that the results of all tested DNA-based methods differ significantly from the results of the resazurin measurements. While the conversion of resazurin in 3D cultures was less than half that of 2D cultures, the measured amount of DNA in 3D cultures was comparable or higher than that of 2D cultures, regardless of the method.

Comparing the single methods, we observed for the absorption-based measurement that the 3D cultures showed higher absorption values than the 2D cultures (Figure 5a). The measurement using CyQuant showed a contrary result (Figure 5c). Measurement with Hoechst showed nearly the same amount of DNA in both 2D and 3D cultures (Figure 5b). Except for the absorption-based measurements in 3D cultures, all tested methods showed a correlation between the increase in cell number and the increase in the measured signal. These results proved that isolation of DNA from 3D scaffold cultures and 2D cultures were feasible with the DNA isolation method used.

However, all these methods do not allow cell-type-specific quantification, since only the total DNA content is measured. Therefore, a PCR-based method for quantification was tested. By using human and mouse cell lines in the test system, a species-specific signal can be generated by using species-specific DNA primers. The complete specificity of the used primers (*hUGT1A6* and *mIL-11*) used was checked with primer blast and by preliminary experiments (Supplementary Figure S2). Figure 5d clearly shows a correlation between cell number and the measured cycle threshold (Ct) value when using the qPCR-based quantification method. Independent of the cell type, no difference between 2D and 3D cultured cells could be detected. Since this method can also be used for cell-type quantification, we selected it for the evaluation of the following co-culture experiments.

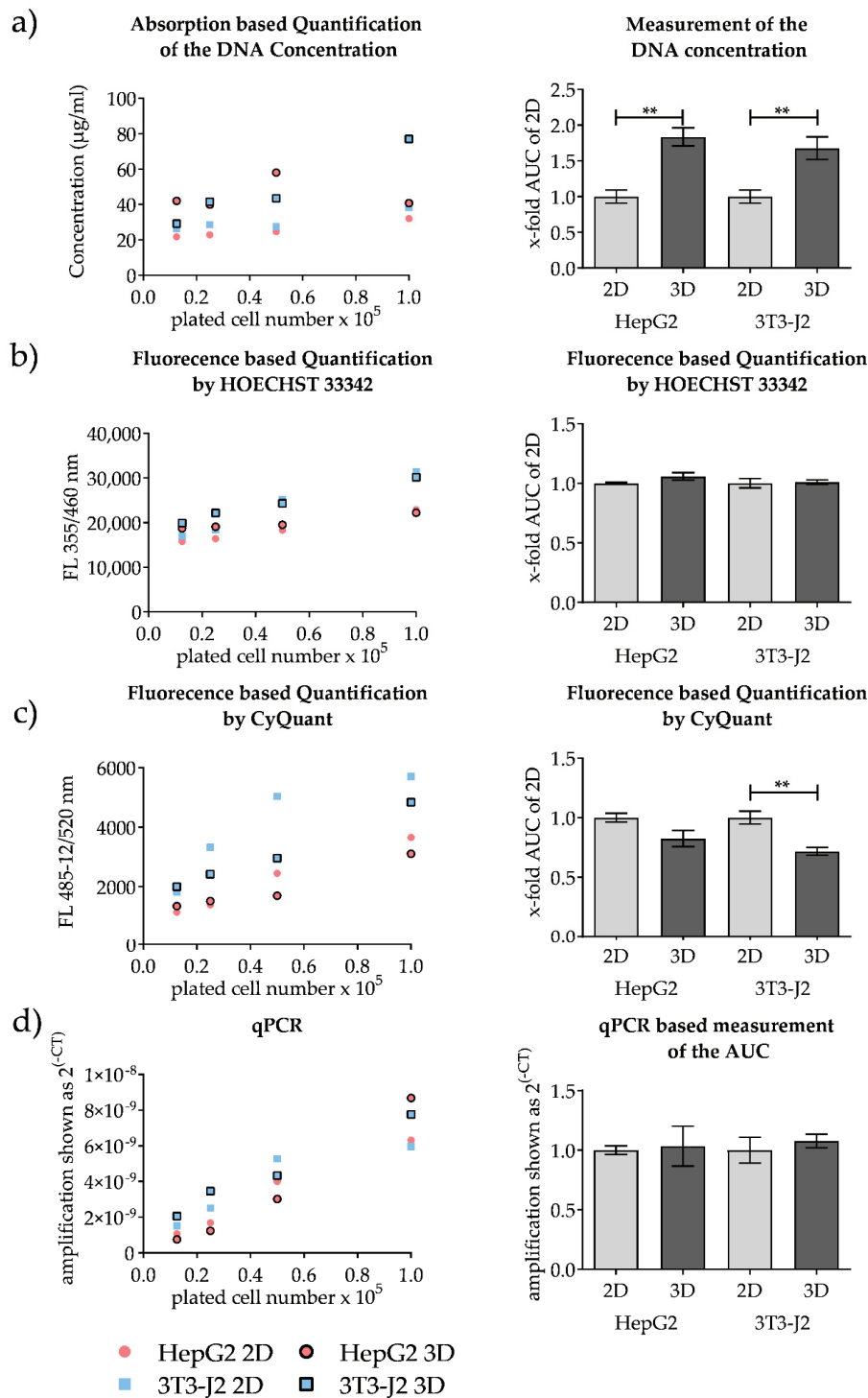


Figure 5. Comparison of different DNA-based approaches for 2D and 3D scaffold cell culture quantification. HepG2 cells and 3T3-J2 cells were plated in 2D and 3D as mono-cultures using different cell numbers. After an incubation time of 18 h, cells were lysed and the DNA was isolated. Four different quantification techniques were tested. The measured values of each quantification technique and the calculated area under the curve (AUC) are shown. (a) Absorption-based DNA quantification, (b,c) fluorescence-based DNA measurement using Hoechst 33342 and CyQuant, and (d) quantification of absolute cell numbers by qPCR with cell-type specific primers. $n = 3$, $n = 2$ (three independent runs with four replicates, pooled to two technical replicates prior DNA isolation); mean \pm SEM; ** $p \leq 0.01$.

For better comparison of the used methods, three independent standards of both cell lines (HepG2 and 3T3-J2) (Supplementary Figure S4) in the range of 1, 0.5, 0.25, 0.125, and 0.0625×10^5 cells were prepared. The following standards were used to create standard curves for each method separately (three independent standard curves at least in duplicates). The standard error of the y-intercept and the slope of the linear regression were used to calculate the analytical figures of merit. As shown in Table 3, all methods showed a Limit of Quantitation (LOQ) $> 2 \times 10^3$ cells regardless of the cell type. The fluorescence-based CyQuant measurement and the qPCR-based method show the lowest Limits of Detection (LOD) and LOQ values. Since only the qPCR-based approach allowed the discrimination between the two tested cell lines, this method was used in the further course of the study.

Table 3. Limits of Detection (LOD), Limits of Quantitation (LOQ), and sensitivity of the tested DNA-based quantification methods.

Method	Number of Cells			
	Cell Line	LOD	LOQ	Sensitivity (%)
Absorption-based quantification	HepG2	2183	7277	95
	3T3-J2	2557	8523	98
Fluorescence-based quantification (HOECHST 33342)	HepG2	5291	17,635	88
	3T3-J2	3400	11,334	98
Fluorescence-based quantification (CyQuant)	HepG2	1506	5018	104
	3T3-J2	471	1571	101
qPCR-based quantification	HepG2	1742	5808	99
	3T3-J2	1447	4824	99

The standard curves shown in Supplementary Figure S4 were used to calculate the analytical figures of merit. The Limit of Detection (LOD) and Limit of Quantitation (LOQ) were calculated as three-/ten-times of the standard error of the y-intercept. The slope of the standard curve showed the sensitivity of the respective method.

3.4. PCR-Based Co-Culture Quantification

For co-culture experiments, we used the same number of cells for all conditions (co-culture and mono-culture of both cell types, each in 2D and 3D). To avoid saturation of the scaffold or the plate with cells, we used 5×10^4 3T3-J2 cells and 5×10^4 HepG2 cells at each culture condition. We measured the conversion of resazurin as an established method for co-culture quantification. In addition, we also carried out qPCR and conventional semi-quantitative PCR of DNA samples (for quantification of each cell type independently). As shown in Figure 6a, resazurin conversion of cells in co-culture exceeds that of the combination of the respective mono-cultures, regardless of whether the cells were plated in 2D or 3D. This result was initially surprising. Due to the limited space for each cell available in co-culture, we assumed that herein total fewer cells would adhere to the scaffold/plate. However, we found the opposite in the measured resazurin conversion (Figure 6a). This result is also accompanied by a higher amount of measured DNA, which could be observed especially in the 3T3-J2 cells in the co-culture approach (Figure 6c,d, right). As Figure 6b clearly shows, a cell-type-specific quantification was possible with the selected primers, since the corresponding signal in the controls (5×10^5 cells of the other cell type, lane C) is missing. Overall, the qPCR and semi-quantitative PCR showed nearly the same results. The qPCR displayed a higher scattering, which resulted in a higher standard deviation.

Next, we verified whether or not this quantification method could be translated to other scaffolds. Therefore, we tested the quantification method on our recently developed HEMA-based cryogel scaffold. Since this scaffold has a larger diameter and a higher volume (see Material and Methods), an adaptation of the volumes for the DNA isolation was necessary. To reduce differences between the culture conditions, which are possibly caused by different proliferation rates under the varying conditions, we reduced the cultivation time for this experiment from 18 h to 12 h.

As the results in Figure 7 show, the conversion of resazurin in the HEMA-based 3D cryogel was independent of the cell line significantly lower than in the 2D cultures. Regardless of the cell type, no significant differences were found in the PCR-based method between the 2D and 3D cultures. The amount of cell-type-specific PCR products in the 2D co-cultures was also higher than in the respective mono-cultures (Figure 7b,c, right), but this effect was significantly lower compared to the results shown in Figure 6. In general, a clear correlation between the number of cells and the measured PCR signals could be demonstrated. Species-specificity of the primers could also be confirmed, which proved the cell-type-specificity of this method (Figure 7b,c). Overall, the quantification method could be transferred to the self-made scaffolds by modification of the amounts of DNA isolation buffer.

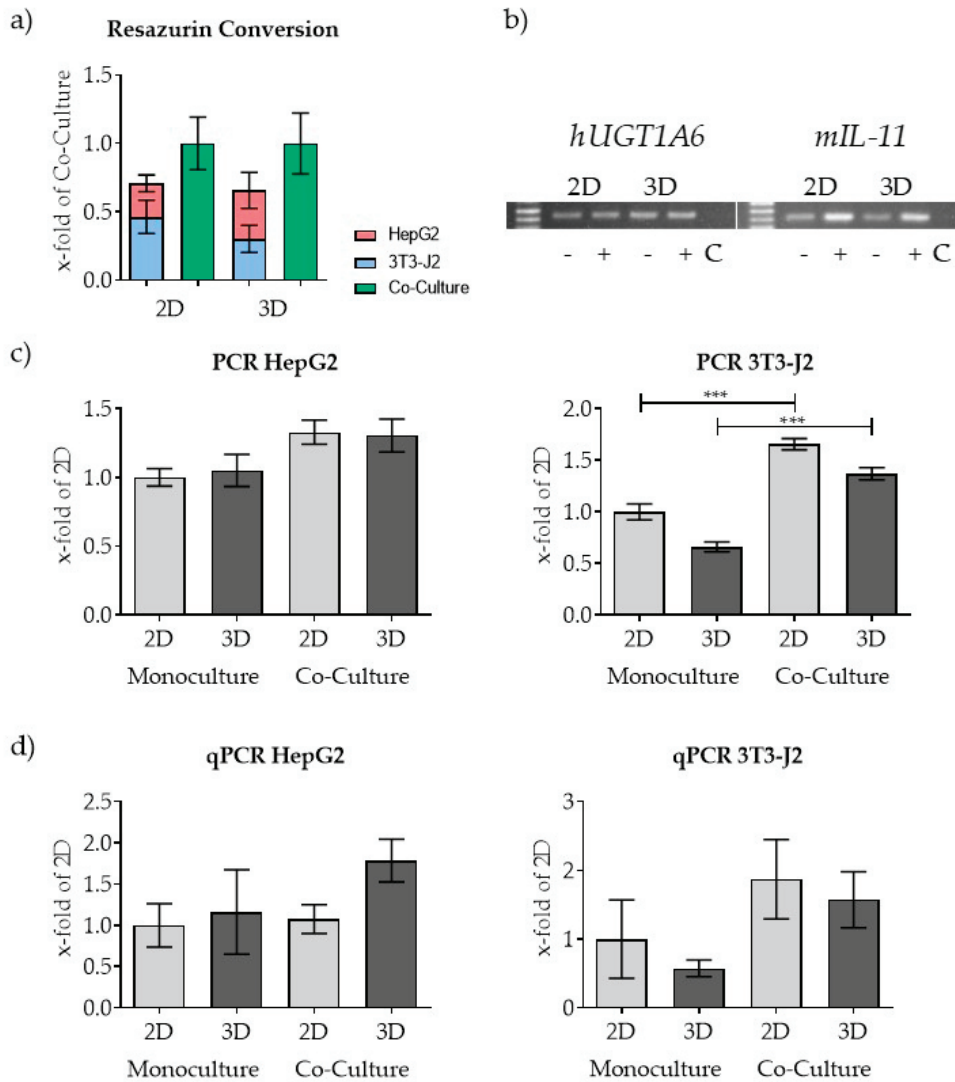


Figure 6. Application of the newly developed PCR-based quantification method on a co-culture consisting of 5×10^4 HepG2 and 5×10^4 3T3-J2 cells. Both cell lines were plated in co-cultures and in mono-cultures. (a) Measurement of the resazurin conversion of the mono- and co-cultures after 1 h incubation. (b) Representative figure of the pooled samples analyzed by conventional PCR (co-cultures (+) and the mono-cultures (-)) also showing the negative signal of the control (c), which consists of DNA of the 2D mono-culture from the other respective cell line. Images of gels used for analysis can be found in Supplementary Figure S5. The amount of DNA for each cell type was measured by conventional PCR (b,c) and by qPCR (d) using cell-type-specific primers. $n = 4$, $n = 2$; mean \pm SEM; *** $p < 0.001$.

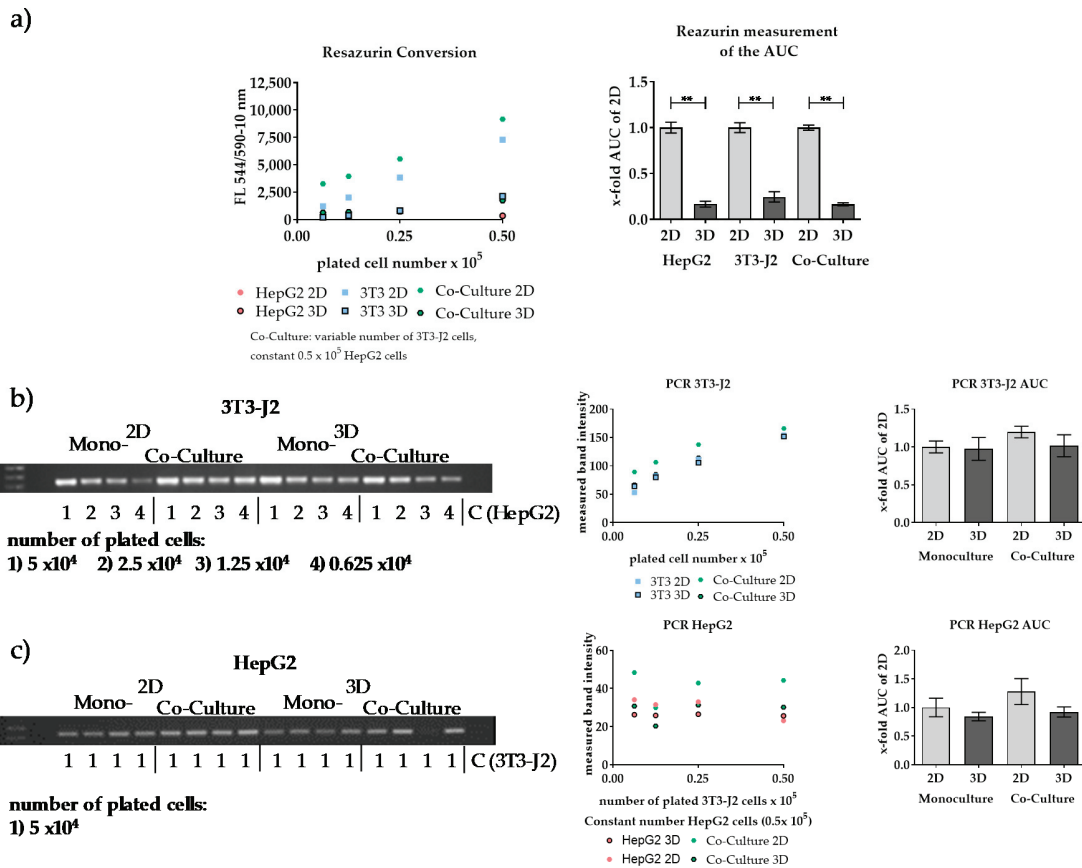


Figure 7. Transfer of the newly developed cell-type-specific quantification method to a self-made cryogel scaffold. Both cell lines were plated in co-cultures and in mono-cultures. Therefore, a constant number of HepG2 cells (5×10^4 cells) and a variable number of 3T3-J2 cells (5×10^4 – 6.25×10^3 cells) were plated on scaffolds as well as in 2D. (a) Resazurin conversion of the mono- and co-cultures was measured. (b,c) The DNA amount of each cell type was measured by conventional PCR using species-specific primers. (b) 3T3-J2 cells with *mIL-11* primers. (c) HepG2 cells with *hUGT1A6* primers. $n = 3, n = 2$; mean \pm SEM; ** $p < 0.01$.

4. Discussions

The cultivation of cells in 3D systems or of different cell types in co-culture systems are two approaches that often better mimic the in vivo environment [1,2]. Both approaches can also be combined [34], resulting in a system where both cell–cell and cell–matrix interactions can be modeled [35,36]. However, especially 3D systems are associated with limitations in the analysis methods [37]. In terms of normalization, many quantification methods that are successfully used in conventional 2D cultures cannot be used or are of limited use in 3D cultures [7,12,18]. A detachment of the cells from a 3D matrix, which would simplify the analysis, is often not possible without destroying the cells [2]. Therefore, normalization of mitochondrial dehydrogenase activity (resazurin, MTT, or XTT) or measurements of intracellular ATP levels are currently commonly used to quantify 3D culture experiments [4,6,8]. But these quantification methods do not allow direct comparison between 2D and 3D cultures, which is important for a comparison of the results of both cultivation techniques [38]. Metabolic activity assays, such as resazurin conversion, are highly susceptible to cell stress, which can easily be affected by culture conditions, such as oxygenation, temperature, 3D scaffolds, etc. [39]. The present work shows, when applying the fluorescent dye Hoechst 33342, it is easily possible to quantify various cell numbers in 2D and 3D mono-cultures. The measurement of the DNA amount with an absorption measurement or the alternative fluorescence-based CyQuant measurement differs

from the results determined by Hoechst 33342, PCR, and qPCR. Absorption-based DNA measurement is sensitive to scaffold components released during culture or washing steps. This might explain the differences seen between the DNA content in our 2D and 3D cultures when quantified photometrically. In the case of the CyQuant measurement, it is known that FCS and phenol red from residual medium can lower the measured values, giving an explanation for the decreased DNA amounts measured in 3D cultures. Optimization of the CyQuant protocol could improve its suitability for use with 3D cultures. However, the major drawback of this method is the absence of cell-type-specific quantification in a co-culture system. A quantification just based on the plated cell number is not possible since it is not predictable whether the cells behave differently in 2D and 3D mono- or co-cultures [40,41]. Therefore, prior to establishing a scaffold-based co-culture model, it seems essential to develop a method that allows cell-specific quantification and thus allows an interpretation of functional results. To our surprise, no suitable method was available in the literature, except using flow cytometry with cell-type-specific surface markers and FISH analysis with specific gene sequences [42–46]. But both of these techniques require living/intact cells in suspension, which is impossible in scaffold cultures [2].

Another method that can be used for quantification of a co-culture is the (computer-based) analysis of microscopic images, which has been successfully established for 2D cultures [31–33] but cannot be used in 3D scaffold cultures since the scaffold-penetrating cells cannot be detected.

Thus, we searched in the literature for an alternative approach. Several studies using pellet cultures for the differentiation of Mesenchymal stem cells (MSCs) into cartilage cells determined the ratio of MSCs from different species by qPCR [41,47]. Another work has shown that it is possible to determine the ratio of different bacteria strains in a biofilm by species-specific primers [48]. Based on the latter, we adapted this technology to our needs. As shown in our results, the species-specific quantification with the adapted PCR-based method is possible. The method is very sensitive and can detect signals for less than 10,000 cells. For cell-specific quantification of a co-culture of human HepG2 cells with murine 3T3-J2 cells, PCR-based methods were the best choice. Semi-quantitative PCR and qPCR allowed for species-specific quantification. The transfer to another scaffold was also possible, underlining the universality of this approach.

Interestingly, when using 3T3-J2 cells in co-culture over 18 h, a higher amount of DNA compared to the respective mono-culture could be measured. Based on our data, we cannot state whether this was due to a promotion of cell division by the co-culture or due to improved adherence in the co-culture. The effect is less strong after 12 h, suggesting a proliferative effect by the co-culture system alone. Paracrine or autocrine actions that stimulate cell proliferation could be responsible for this effect [49]. A positive effect of 3D culture and co-culture on cell attachment or proliferation was also described by Fasolino et al. [50]. These results clearly underline the importance of cell-type-specific quantification of different cell types in a co-culture system in order to validate the effects of the same cell type generated in conventional mono-culture.

One limitation of this system is the dependency on different gene sequences. For example, it is not yet possible to quantify a co-culture model with primary human hepatocytes and non-parenchymal cells from the same donor. However, Callaghan et al. suggested to overcome this problem by determining the telomere length of different somatic cell types [51,52]. DNA barcoding is another interesting technique that enables tracking of cells from different origins in co-cultures. Therefore, the cells are transduced with a library of viral vectors. This theoretically allows the tracking of clones from each individual cell in the co-culture approach [53–55]. For data evaluation, DNA sequencing of cells is necessary, which makes this interesting approach quite expensive and not feasible for many laboratories. Another alternative might be the stable integration of foreign genes into cells of interest, for which specific primers could then be used. One example of this approach is immortalized hepatocytes [56]. For immortalization, primary human hepatocytes are transduced with virus particles containing the DNA sequence of human papillomavirus (HPV16) E6/E7 [56]. Alternatively, cells can be transfected with fluorescence proteins like GFP or mCherry. This approach does not only result in the implementation of foreign genes but also gives the possibility to differentiate between cell types

via fluorescence microscopy [57]. Independent of the kind of foreign gene sequence, it is possible with the help of specific primers to quantify this non-human gene sequence to quantify the cells in the co-culture approach. A pitfall of this approach is the necessary efficiency of nearly 100% for both primers, which can only be reached using qPCR with perfectly optimized primers.

Nevertheless, our newly developed PCR-based co-culture quantification method has limitations. For example, it cannot be used in spheroid cultures. In the spheroid interior, there is a necrotic core that contains DNA and would lead to false-positive results [58]. Dead cells therefore should always be removed prior to DNA isolation.

Despite the limitations mentioned above, this quantification method can find, as summarized in Table 4, broad application in recently published co-culture approaches of different organ systems.

Table 4. Possible applications for the PCR-based co-culture quantification method. Shown is a selection of publications in which cells from different species were used in a co-culture approach. For a combination other than human/mouse cells, another species-specific primer needs to be used.

Organ System	Cell Type I	Cell Type II	Ref
Liver (HEPATOPAC®)	Primary human hepatocytes	m3T3-J2	[25]
Liver	HepG2	m3T3-J2	[26]
Liver	primary rat hepatocytes	m3T3-J2	[27]
Liver	human cord blood stem cells	hepatic alpha mouse liver 12 cells	[59]
Nervous system	human oral mucosal stem cells	mouse neural stem cells	[60]
Bone	SaOS2	RAW 264.7 cells	[61]
Cartilage	bovine primary chondrocytes	Three different cell lines from mouse/human	[62]

5. Conclusions

As our data demonstrate, we developed a PCR-based 3D co-culture quantification method that allows the quantification of two different cell types (of human and mouse origin) accurately. In comparison to conventional quantification methods (such as resazurin conversion), this method not only enables the separate quantification of the individual cell types but also improves the comparability of 2D to 3D culture results by excluding culture-related differences in metabolism.

Supplementary Materials: The following are available online at <http://www.mdpi.com/2409-9279/3/1/1/s1>, Figure S1: Representative pictures of the Optimaix-3D scaffold; Figure S2, Optimization of the hUGT1A6 and the mIL-11 primer; Figure S3, Comparison of different approaches for 2D and 3D scaffold cell culture quantification; Figure S4, Standard curves of the different DNA based approaches used for calculation of the limit of detection, limit of quantitation and the sensitivity of each method; Figure S5, Gel pictures of all four runs of the co-culture experiment analyzed via conventional PCR showing co-cultures [+], monocultures [-], and additionally a negative control (c) consisting of DNA from the 2D monoculture of the other cell line.

Author Contributions: M.R. conceived and designed the experiments. M.R., V.K. and S.R. performed the experiments. M.R., V.K. and S.R. analyzed the data. M.R., S.R., M.H. and S.E. developed and optimized the quantification method, which was used for the experiments. L.H.H.O.D. developed the Optimaix-3D scaffold and provided them for the experiments. M.R. wrote the manuscript. S.E., C.L., H.R., V.H. and A.K.N. reviewed and edited the manuscript. All authors have read and agreed to the published version of the manuscript.

Funding: This study was partially funded by the Federal Ministry for Economic Affairs and Energy within the framework of the ZIM program (ZF 4301401CS6, ZF4301001CS6).

Acknowledgments: We want to thank Andrew McCaffrey for proofreading the article.

Conflicts of Interest: The authors declare no conflict of interest.

Abbreviations

AUC	Area under the curve
BCS	Bovine calf serum
Ct	Cycle threshold
FCS	Fetal calf serum
HPV	Human papillomavirus
LOD	Limits of Detection
LOQ	Limits of Quantitation
MSCs	Mesenchymal stem cells
P/S	Penicillin-streptomycin
SRB	Sulforhodamine B

References

- Godoy, P.; Hewitt, N.J.; Albrecht, U.; Andersen, M.E.; Ansari, N.; Bhattacharya, S.; Bode, J.G.; Bolleyn, J.; Borner, C.; Bottger, J.; et al. Recent advances in 2d and 3d in vitro systems using primary hepatocytes, alternative hepatocyte sources and non-parenchymal liver cells and their use in investigating mechanisms of hepatotoxicity, cell signaling and adme. *Arch. Toxicol.* **2013**, *87*, 1315–1530.
- Bachmann, A.; Moll, M.; Gottwald, E.; Nies, C.; Zantl, R.; Wagner, H.; Burkhardt, B.; Sánchez, J.; Ladurner, R.; Thasler, W.; et al. 3d cultivation techniques for primary human hepatocytes. *Microarrays* **2015**, *4*, 64–83. [[CrossRef](#)]
- Luckert, C.; Schulz, C.; Lehmann, N.; Thomas, M.; Hofmann, U.; Hammad, S.; Hengstler, J.G.; Braeuning, A.; Lampen, A.; Hessel, S. Comparative analysis of 3d culture methods on human hepg2 cells. *Arch. Toxicol.* **2017**, *91*, 393–406. [[CrossRef](#)]
- Ruoss, M.; Haussling, V.; Schugner, F.; Olde Damink, L.H.H.; Lee, S.M.L.; Ge, L.; Ehnert, S.; Nussler, A.K. A standardized collagen-based scaffold improves human hepatocyte shipment and allows metabolic studies over 10 days. *Bioengineering* **2018**, *5*, 86. [[CrossRef](#)]
- Schyschka, L.; Sanchez, J.J.; Wang, Z.; Burkhardt, B.; Muller-Vieira, U.; Zeilinger, K.; Bachmann, A.; Nadalin, S.; Damm, G.; Nussler, A.K. Hepatic 3d cultures but not 2d cultures preserve specific transporter activity for acetaminophen-induced hepatotoxicity. *Arch. Toxicol.* **2013**, *87*, 1581–1593. [[CrossRef](#)]
- Kumari, J.; Karande, A.A.; Kumar, A. Combined effect of cryogel matrix and temperature-reversible soluble–insoluble polymer for the development of in vitro human liver tissue. *ACS Appl. Mater. Interfaces* **2015**, *8*, 264–277. [[CrossRef](#)] [[PubMed](#)]
- Jones, L.J.; Gray, M.; Yue, S.T.; Haugland, R.P.; Singer, V.L. Sensitive determination of cell number using the cyquant[®] cell proliferation assay. *J. Immunol. Methods* **2001**, *254*, 85–98. [[CrossRef](#)]
- Bell, C.C.; Hendriks, D.F.G.; Moro, S.M.L.; Ellis, E.; Walsh, J.; Renblom, A.; Puigvert, L.F.; Dankers, A.C.A.; Jacobs, F.; Snoeys, J.; et al. Characterization of primary human hepatocyte spheroids as a model system for drug-induced liver injury, liver function and disease. *Sci. Rep.* **2016**, *6*, 25187. [[CrossRef](#)] [[PubMed](#)]
- Aspera-Werz, R.H.; Ehnert, S.; Heid, D.; Zhu, S.; Chen, T.; Braun, B.; Sreekumar, V.; Arnscheidt, C.; Nussler, A.K. Nicotine and cotinine inhibit catalase and glutathione reductase activity contributing to the impaired osteogenesis of scp-1 cells exposed to cigarette smoke. *Oxidative Med. Cell. Longev.* **2018**, *2018*, 13. [[CrossRef](#)] [[PubMed](#)]
- Gomes, C.J.; Harman, M.W.; Centuori, S.M.; Wolgemuth, C.W.; Martinez, J.D. Measuring DNA content in live cells by fluorescence microscopy. *Cell Div.* **2018**, *13*, 6. [[CrossRef](#)]
- Lowry, O.H.; Rosebrough, N.J.; Farr, A.L.; Randall, R.J. Protein measurement with the folin phenol reagent. *J. Biol. Chem.* **1951**, *193*, 265–275. [[PubMed](#)]
- Skehan, P.; Storeng, R.; Scudiero, D.; Monks, A.; McMahon, J.; Vistica, D.; Warren, J.T.; Bokesch, H.; Kenney, S.; Boyd, M.R. New colorimetric cytotoxicity assay for anticancer-drug screening. *J. Natl. Cancer Inst.* **1990**, *82*, 1107–1112. [[CrossRef](#)] [[PubMed](#)]
- Van Tonder, A.; Joubert, A.M.; Cromarty, A.D. Limitations of the 3-(4,5-dimethylthiazol-2-yl)-2,5-diphenyl-2h-tetrazolium bromide (mtt) assay when compared to three commonly used cell enumeration assays. *BMC Res. Notes* **2015**, *8*, 47. [[CrossRef](#)] [[PubMed](#)]

14. Sreekumar, V.; Aspera-Werz, R.; Ehnert, S.; Strobel, J.; Tendulkar, G.; Heid, D.; Schreiner, A.; Arnscheidt, C.; Nussler, A.K. Resveratrol protects primary cilia integrity of human mesenchymal stem cells from cigarette smoke to improve osteogenic differentiation in vitro. *Arch. Toxicol.* **2018**, *92*, 1525–1538. [[CrossRef](#)] [[PubMed](#)]
15. Aslantürk, Ö.S. In vitro cytotoxicity and cell viability assays: Principles, advantages, and disadvantages. In *Genotoxicity-A Predictable Risk to Our Actual World*; IntechOpen: Rijeka, Croatia, 2017.
16. Huyck, L.; Ampe, C.; Van Troys, M. The xtt cell proliferation assay applied to cell layers embedded in three-dimensional matrix. *Assay Drug Dev. Technol.* **2012**, *10*, 382–392. [[CrossRef](#)] [[PubMed](#)]
17. Rampersad, S.N. Multiple applications of alamar blue as an indicator of metabolic function and cellular health in cell viability bioassays. *Sensors* **2012**, *12*, 12347–12360. [[CrossRef](#)]
18. Allen, M.; Millett, P.; Dawes, E.; Rushton, N. Lactate dehydrogenase activity as a rapid and sensitive test for the quantification of cell numbers in vitro. *Clin. Mater.* **1994**, *16*, 189–194. [[CrossRef](#)]
19. Ruoff, M.; Damm, G.; Vosough, M.; Ehret, L.; Grom-Baumgarten, C.; Petkov, M.; Naddalin, S.; Ladurner, R.; Seehofer, D.; Nussler, A.; et al. Epigenetic modifications of the liver tumor cell line hepg2 increase their drug metabolic capacity. *Int. J. Mol. Sci.* **2019**, *20*, 347. [[CrossRef](#)]
20. Uzarski, J.S.; DiVito, M.D.; Wertheim, J.A.; Miller, W.M. Essential design considerations for the resazurin reduction assay to noninvasively quantify cell expansion within perfused extracellular matrix scaffolds. *Biomaterials* **2017**, *129*, 163–175. [[CrossRef](#)]
21. Rai, Y.; Pathak, R.; Kumari, N.; Sah, D.K.; Pandey, S.; Kalra, N.; Soni, R.; Dwarakanath, B.S.; Bhatt, A.N. Mitochondrial biogenesis and metabolic hyperactivation limits the application of mtt assay in the estimation of radiation induced growth inhibition. *Sci. Rep.* **2018**, *8*, 1531. [[CrossRef](#)]
22. Surmaitis, R.L.; Arias, C.J.; Schlenoff, J.B. Stressful surfaces: Cell metabolism on a poorly adhesive substrate. *Langmuir* **2018**, *34*, 3119–3125. [[CrossRef](#)] [[PubMed](#)]
23. Mueller, S.; Sandrin, L. Liver stiffness: A novel parameter for the diagnosis of liver disease. *Hepatic Med.* **2010**, *2*, 49–67. [[CrossRef](#)] [[PubMed](#)]
24. Skardal, A.; Mack, D.; Atala, A.; Soker, S. Substrate elasticity controls cell proliferation, surface marker expression and motile phenotype in amniotic fluid-derived stem cells. *J. Mech. Behav. Biomed. Mater.* **2013**, *17*, 307–316. [[CrossRef](#)] [[PubMed](#)]
25. Chan, T.S.; Yu, H.; Moore, A.; Khetani, S.R.; Tweedie, D. Meeting the challenge of predicting hepatic clearance of compounds slowly metabolized by cytochrome p450 using a novel hepatocyte model, hepatopac. *Drug Metab. Dispos.* **2013**, *41*, 2024–2032. [[CrossRef](#)] [[PubMed](#)]
26. Rajendran, D.; Hussain, A.; Yip, D.; Parekh, A.; Shrirao, A.; Cho, C.H. Long-term liver-specific functions of hepatocytes in electrospun chitosan nanofiber scaffolds coated with fibronectin. *J. Biomed. Mater. Res. Part A* **2017**, *105*, 2119–2128. [[CrossRef](#)]
27. Cho, C.H.; Berthiaume, F.; Tilles, A.W.; Yarmush, M.L. A new technique for primary hepatocyte expansion in vitro. *Biotechnol. Bioeng.* **2008**, *101*, 345–356. [[CrossRef](#)]
28. Lin, J.; Schyschka, L.; Muhl-Benninghaus, R.; Neumann, J.; Hao, L.; Nussler, N.; Dooley, S.; Liu, L.; Stockle, U.; Nussler, A.K.; et al. Comparative analysis of phase i and ii enzyme activities in 5 hepatic cell lines identifies huh-7 and hcc-t cells with the highest potential to study drug metabolism. *Arch. Toxicol.* **2012**, *86*, 87–95. [[CrossRef](#)]
29. Meeker, N.D.; Hutchinson, S.A.; Ho, L.; Trede, N.S. Method for isolation of pcr-ready genomic DNA from zebrafish tissues. *Biotechniques* **2007**, *43*, 610–614. [[CrossRef](#)]
30. Richards, W.L.; Song, M.K.; Krutzsch, H.; Everts, R.P.; Marsden, E.; Thorgeirsson, S.S. Measurement of cell-proliferation in microculture using hoechst-33342 for the rapid semiautomated microfluorimetric determination of chromatin DNA. *Exp. Cell Res.* **1985**, *159*, 235–246. [[CrossRef](#)]
31. Logan, D.J.; Shan, J.; Bhatia, S.N.; Carpenter, A.E. Quantifying co-cultured cell phenotypes in high-throughput using pixel-based classification. *Methods* **2016**, *96*, 6–11. [[CrossRef](#)]
32. Krtolica, A.; Ortiz de Solorzano, C.; Lockett, S.; Campisi, J. Quantification of epithelial cells in coculture with fibroblasts by fluorescence image analysis. *Cytometry* **2002**, *49*, 73–82. [[CrossRef](#)] [[PubMed](#)]
33. Asthana, V.; Tang, Y.; Ferguson, A.; Bugga, P.; Asthana, A.; Evans, E.R.; Chen, A.L.; Stern, B.S.; Drezek, R.A. An inexpensive, customizable microscopy system for the automated quantification and characterization of multiple adherent cell types. *PeerJ* **2018**, *6*, e4937. [[CrossRef](#)] [[PubMed](#)]

34. Wei, G.; Wang, J.; Lv, Q.; Liu, M.; Xu, H.; Zhang, H.; Jin, L.; Yu, J.; Wang, X. Three-dimensional coculture of primary hepatocytes and stellate cells in silk scaffold improves hepatic morphology and functionality in vitro. *J. Biomed. Mater. Res. Part A* **2018**, *106*, 2171–2180. [[CrossRef](#)] [[PubMed](#)]
35. Lu, H.F.; Chua, K.N.; Zhang, P.C.; Lim, W.S.; Ramakrishna, S.; Leong, K.W.; Mao, H.Q. Three-dimensional co-culture of rat hepatocyte spheroids and nih/3t3 fibroblasts enhances hepatocyte functional maintenance. *Acta Biomater.* **2005**, *1*, 399–410. [[CrossRef](#)] [[PubMed](#)]
36. Glicklis, R.; Shapiro, L.; Agbaria, R.; Merchuk, J.C.; Cohen, S. Hepatocyte behavior within three-dimensional porous alginate scaffolds. *Biotechnol. Bioeng.* **2000**, *67*, 344–353. [[CrossRef](#)]
37. Antoni, D.; Burckel, H.; Josset, E.; Noel, G. Three-dimensional cell culture: A breakthrough in vivo. *Int. J. Mol. Sci.* **2015**, *16*, 5517–5527. [[CrossRef](#)]
38. Bonnier, F.; Keating, M.E.; Wrobel, T.P.; Majzner, K.; Baranska, M.; Garcia-Munoz, A.; Blanco, A.; Byrne, H.J. Cell viability assessment using the alamar blue assay: A comparison of 2d and 3d cell culture models. *Toxicol. In Vitro* **2015**, *29*, 124–131. [[CrossRef](#)]
39. Kepp, O.; Galluzzi, L.; Lipinski, M.; Yuan, J.Y.; Kroemer, G. Cell death assays for drug discovery. *Nat. Rev. Drug Discov.* **2011**, *10*, 221–237. [[CrossRef](#)]
40. Koh, B.; Jeon, H.; Kim, D.; Kang, D.; Kim, K.R. Effect of fibroblast co-culture on the proliferation, viability and drug response of colon cancer cells. *Oncol. Lett.* **2019**, *17*, 2409–2417. [[CrossRef](#)]
41. Breslin, S.; O'Driscoll, L. The relevance of using 3d cell cultures, in addition to 2d monolayer cultures, when evaluating breast cancer drug sensitivity and resistance. *Oncotarget* **2016**, *7*, 45745–45756. [[CrossRef](#)]
42. Zhang, H.X.; Xiao, G.Y.; Wang, X.; Dong, Z.G.; Ma, Z.Y.; Li, L.; Li, Y.H.; Pan, X.; Nie, L. Biocompatibility and osteogenesis of calcium phosphate composite scaffolds containing simvastatin-loaded plga microspheres for bone tissue engineering. *J. Biomed. Mater. Res. Part A* **2015**, *103*, 3250–3258. [[CrossRef](#)] [[PubMed](#)]
43. Fang, Y.X.; Wang, B.; Zhao, Y.N.; Xiao, Z.F.; Li, J.; Cui, Y.; Han, S.F.; Wei, J.S.; Chen, B.; Han, J.; et al. Collagen scaffold microenvironments modulate cell lineage commitment for differentiation of bone marrow cells into regulatory dendritic cells. *Sci. Rep.* **2017**, *7*, 42049. [[CrossRef](#)] [[PubMed](#)]
44. Lv, D.; Yu, S.C.; Ping, Y.F.; Wu, H.; Zhao, X.; Zhang, H.; Cui, Y.; Chen, B.; Zhang, X.; Dai, J.; et al. A three-dimensional collagen scaffold cell culture system for screening anti-glioma therapeutics. *Oncotarget* **2016**, *7*, 56904–56914. [[CrossRef](#)] [[PubMed](#)]
45. Flaibani, M.; Luni, C.; Sbalchiero, E.; Elvassore, N. Flow cytometric cell cycle analysis of muscle precursor cells cultured within 3d scaffolds in a perfusion bioreactor. *Biotechnol. Prog.* **2009**, *25*, 286–295. [[CrossRef](#)] [[PubMed](#)]
46. Bigdeli, N.; Karlsson, C.; Strehl, R.; Concaro, S.; Hyllner, J.; Lindahl, A. Coculture of human embryonic stem cells and human articular chondrocytes results in significantly altered phenotype and improved chondrogenic differentiation. *Stem Cells* **2009**, *27*, 1812–1821. [[CrossRef](#)] [[PubMed](#)]
47. Wu, L.; Prins, H.J.; Helder, M.N.; van Blitterswijk, C.A.; Karperien, M. Trophic effects of mesenchymal stem cells in chondrocyte co-cultures are independent of culture conditions and cell sources. *Tissue Eng. Part A* **2012**, *18*, 1542–1551. [[CrossRef](#)]
48. Ren, D.; Madsen, J.S.; de la Cruz-Perera, C.I.; Bergmark, L.; Sorensen, S.J.; Burmolle, M. High-throughput screening of multispecies biofilm formation and quantitative pcr-based assessment of individual species proportions, useful for exploring interspecific bacterial interactions. *Microb. Ecol.* **2014**, *68*, 146–154. [[CrossRef](#)]
49. Simmons, J.G.; Pucilowska, J.B.; Lund, P.K. Autocrine and paracrine actions of intestinal fibroblast-derived insulin-like growth factors. *Am. J. Physiol.* **1999**, *276*, G817–G827. [[CrossRef](#)]
50. Fasolino, I.; Guarino, V.; Marrese, M.; Cirillo, V.; Vallifuoco, M.; Tamma, M.L.; Vassallo, V.; Bracco, A.; Calise, F.; Ambrosio, L. Hepg2 and human healthy hepatocyte in vitro culture and co-culture in pcl electrospun platforms. *Biomed. Mater.* **2017**, *13*, 015017. [[CrossRef](#)]
51. O'Callaghan, N.J.; Fenech, M. A quantitative pcr method for measuring absolute telomere length. *Biol. Proced. Online* **2011**, *13*, 3. [[CrossRef](#)]
52. Wang, F.; Pan, X.; Kalmbach, K.; Seth-Smith, M.L.; Ye, X.; Antunes, D.M.; Yin, Y.; Liu, L.; Keefe, D.L.; Weissman, S.M. Robust measurement of telomere length in single cells. *Proc. Natl. Acad. Sci. USA* **2013**, *110*, E1906–E1912. [[CrossRef](#)] [[PubMed](#)]

53. Nguyen, L.V.; Cox, C.L.; Eirew, P.; Knapp, D.J.; Pellacani, D.; Kannan, N.; Carles, A.; Moksa, M.; Balani, S.; Shah, S.; et al. DNA barcoding reveals diverse growth kinetics of human breast tumour subclones in serially passaged xenografts. *Nat. Commun.* **2014**, *5*, 5871. [[CrossRef](#)]
54. Nolan-Stevaux, O.; Tedesco, D.; Ragan, S.; Makhanov, M.; Chenchik, A.; Ruefli-Brasse, A.; Quon, K.; Kassner, P.D. Measurement of cancer cell growth heterogeneity through lentiviral barcoding identifies clonal dominance as a characteristic of in vivo tumor engraftment. *PLoS ONE* **2013**, *8*, e67316. [[CrossRef](#)] [[PubMed](#)]
55. Nguyen, L.V.; Makarem, M.; Carles, A.; Moksa, M.; Kannan, N.; Pandoh, P.; Eirew, P.; Osako, T.; Kardel, M.; Cheung, A.M.; et al. Clonal analysis via barcoding reveals diverse growth and differentiation of transplanted mouse and human mammary stem cells. *Cell Stem Cell* **2014**, *14*, 253–263. [[CrossRef](#)] [[PubMed](#)]
56. Tsuruga, Y.; Kiyono, T.; Matsushita, M.; Takahashi, T.; Kasai, H.; Matsumoto, S.; Todo, S. Establishment of immortalized human hepatocytes by introduction of hpv16 e6/e7 and htert as cell sources for liver cell-based therapy. *Cell Transplant.* **2008**, *17*, 1083–1094. [[CrossRef](#)]
57. Truong, A.S.; Lochbaum, C.A.; Boyce, M.W.; Lockett, M.R. Tracking the invasion of small numbers of cells in paper-based assays with quantitative pcr. *Anal. Chem.* **2015**, *87*, 11263–11270. [[CrossRef](#)]
58. Gaskell, H.; Sharma, P.; Colley, H.E.; Murdoch, C.; Williams, D.P.; Webb, S.D. Characterization of a functional c3a liver spheroid model. *Toxicol. Res.* **2016**, *5*, 1053–1065. [[CrossRef](#)] [[PubMed](#)]
59. Stecklum, M.; Wulf-Goldenberg, A.; Purfürst, B.; Siegert, A.; Keil, M.; Eckert, K.; Fichtner, I. Cell differentiation mediated by co-culture of human umbilical cord blood stem cells with murine hepatic cells. *In Vitro Cell. Dev. Biol. Anim.* **2015**, *51*, 183–191. [[CrossRef](#)]
60. Alajbeg, I.; Alic, I.; Andabak-Rogulj, A.; Brailo, V.; Mitrecic, D. Human- and mouse-derived neurons can be simultaneously obtained by co-cultures of human oral mucosal stem cells and mouse neural stem cells. *Oral Dis.* **2018**, *24*, 5–10. [[CrossRef](#)]
61. Schröder, H.C.; Wang, X.H.; Wiens, M.; Diehl-Seifert, B.; Kropf, K.; Schloßmacher, U.; Müller, W.E.G. Silicate modulates the cross-talk between osteoblasts (saos-2) and osteoclasts (raw 264.7 cells): Inhibition of osteoclast growth and differentiation. *J. Cell. Biochem.* **2012**, *113*, 3197–3206. [[CrossRef](#)]
62. Hendriks, J.A.A.; Miclea, R.L.; Schotel, R.; de Bruijn, E.; Moroni, L.; Karperien, M.; Riesle, J.; van Blitterswijk, C.A. Primary chondrocytes enhance cartilage tissue formation upon co-culture with a range of cell types. *Soft Matter* **2010**, *6*, 5080–5088. [[CrossRef](#)]



© 2019 by the authors. Licensee MDPI, Basel, Switzerland. This article is an open access article distributed under the terms and conditions of the Creative Commons Attribution (CC BY) license (<http://creativecommons.org/licenses/by/4.0/>).

Chapter 7: Discussion

The prediction of hepatotoxic effects is one of the major challenges in the development of new drugs (Kaplowitz, 2005, Olson et al., 2000). Despite intensive research over the last 40 years, it is still not possible to satisfactorily predict hepatotoxic effects in preclinical studies (Babai et al., 2018). Due to the high variability in the human population, in several cases it is also not possible to detect such effects in the subsequent clinical phase (Raschi and De Ponti, 2019). One example is the antidiabetic drug troglitazone. After approval, the use of this medication caused severe acute liver failure in some patients (0.2-1.2 cases per 1000 patients) (Lee, 2003, Knowler et al., 2005). Due to the relatively small number of cases, it took some years before the observed hepatotoxic effects could be attributed to the side effects of troglitazone. The severity of the effects and the fact that they could not be predicted in advance despite intensive monitoring of the patients meant that this substance had to be withdrawn from the market three years after its approval (Cluxton et al., 2005). Despite intensive research on the hepatotoxic mechanism of this substance, the cause of its hepatotoxicity is still not fully understood, an outcome that demonstrates how difficult it is to predict such effects (Babai et al., 2018). The example of troglitazone illustrates that the development of predictive models is of enormous importance. Such a model could enable the early detection of such side effects, at best already in the preclinical substance screening. This would prevent negative effects on the health of the affected patients as well as significantly reduce the number of animals used and the costs of developing new drugs.

A suitable *in vitro* test model for the successful pre-clinical testing of new drugs must therefore meet the following parameters:

- Unrestricted availability;
- Possibility of long term cultivation to be able to detect even delayed effects;
- Mimic biological processes that lead to the toxicity of drugs in healthy individuals, as well as patients suffering from liver disease;
- Generation of valid results even with complex approaches.

Various studies, including the published articles which are the basis of this thesis, have developed approaches to address these requirements, in order to generate a test system that can be successfully used for pre-clinical testing of drugs. The possibilities and limitations of these approaches are discussed below.

7.1 Availability of hepatic cells for *in vitro* models for pre-clinical drug testing

Due to their metabolic capacity, human hepatocytes are considered to be the most suitable model for *in vitro* testing of new drugs (Bachmann et al., 2015). However, the limited availability of these cells significantly limits their usage in this area. The reasons for the limited availability are, in addition to the limited number of donors, the fact that the cells cannot be kept in culture permanently and that it is not yet possible to cryopreserve the cells in such a way that they do not lose the majority of their metabolic activity (Godoy et al., 2013). In addition, the number of donors is not being increased; rather, the number of tumor surgeries in which residual tissue accrues, as well as the amount of residual tissue that is generated by these surgeries, is expected to decrease in the future as a result of improved treatment strategies (Ruoss et al., 2020b). Thus, it is necessary to use the available cells as effectively as possible. This use includes a loss-free transport of the cells from point A to point B, improvement in the cultivation conditions, or the possibility of freezing the cells without loss of viability and metabolic activity. Although progress has been made in all the above-mentioned fields in recent years, in particular, the shipment of the cells is still associated with a massive loss of living cells and damage to the

remaining cells (Stephene et al., 2010, Pless-Petig et al., 2012, Rauen et al., 1999, Hengstler et al., 2000). As our data showed, shipping the cells in suspension on ice, which is the most common method of cell shipment, results in a loss of almost 50% of the living cells. By purifying the cells by Percoll density centrifugation, the initial viability can be approximately regained. However, this purification step is also associated with a further loss of living cells so that after purification, frequently less than 50% of the cells are available for experiments. As our data further demonstrated, the viability of the cells can be significantly improved by direct plating and shipping at 37°C. It can be assumed that most shipped cells survive the transport. One day after shipment, the viability of plated cells in 2D and 3D cultures was significantly higher than that of cells sent in suspension and subsequently plated. Notably, more than 50% of the cells shipped in suspension were lost during shipping and purification and could, therefore, not be plated at all. When comparing the shipping of cells plated out in 2D with the shipping of cells on the 3D scaffold, it becomes clear that the scaffold-based method has several advantages. For example, a high cell concentration per area can be shipped here. In addition, a large portion of the medium is absorbed by the scaffold, which prevents the medium from leaking during transport, thus minimizing the risk of the cells drying out and possible contamination risks during transport. In summary, we concluded that plating the cells onto scaffolds before shipment is a suitable method to reduce the loss of cells during shipment. Together with the improved metabolic activity in the 3D scaffold culture, we established a model that allows the transport and culture of metabolically active hepatocytes over a 10-day period. However, the established method also has limitations that curb its possible applications. The decisive limitation is that despite improved transport; no model allows unlimited availability of the cells. Additionally, in comparison to transport in suspension on ice, but also in comparison to cryopreservation, it is not possible to take the cells off the scaffold and plate them again. Furthermore, it should be noted that the use of some standard assays and the isolation of RNA and protein in hepatocytes plated on scaffolds is only possible to a limited extent, a factor which further restricts the possible applications of this

model. The key problem that only a few cells can be isolated and that these cells do not proliferate in culture also remains (Ruoss et al., 2020b).

For this reason, various approaches have been developed to enable the proliferation of hepatocytes *in vitro* (Katsura et al., 2002, Sadri and Amini-Nik, 2017, Levy et al., 2015). This phenomenon is possible, for example, through the transduction of PHH with the human papillomavirus genes E6 and E7. In addition, the de-differentiation of hepatocytes was prevented by the MEK1/2 inhibitor U0126, which reduces the EMT. The expression of E6 and E7 leads to the upregulation of the Oncostatin M (OSM) receptor. By administering OSM, the transduced hepatocytes can be stimulated to proliferate. From one hepatocyte, more than 1000 hepatocytes can be generated for experiments. OSM removal stops proliferation and allows the differentiation of the cells into functional hepatocytes (Levy et al., 2015). The extent to which the metabolic function of freshly isolated hepatocytes can be restored in these cells, which are commercially distributed as so-called upcyte hepatocytes, have been evaluated differently in different studies (Tolosa et al., 2016, Sison-Young et al., 2015). However, it must be assumed that these cells do not have the same metabolic activity as freshly isolated hepatocytes; instead, they are comparable to HepaRG cells (Kammerer and Küpper, 2018). In another study, upcyte hepatocytes even showed a 90% reduction of cytochrome P450 expression compared to PHH, which would mean that they are more comparable to HepG2 cells regarding their metabolic activity (Sison-Young et al., 2015). An advantage of upcyte hepatocytes in contrast to conventional cell lines such as HepaRG is the fact that they come from different donors and are therefore better suited to represent variances within the human population (Tolosa et al., 2016).

Another approach to generate an *in vitro* model with unrestricted availability is the use of hepatic cell lines (Lin et al., 2012). These cells are available in sufficient quantities due to their unlimited ability to proliferate. A further advantage compared to other possible alternatives (*e.g.*; the use of iPSCs) is the fact that these cells can be cultivated in standard medium; time and cost-intensive differentiation, which are required for iPSCs, are not necessary. Nevertheless, the metabolic activity of hepatic

cell lines such as HepG2 is comparable to the activity found in differentiated iPSCs (Kratochwil et al., 2017). However, compared to freshly isolated PHH, most hepatic cell lines have a much lower metabolic activity compared to PHH (Donato et al., 2008a). This fact is the major limitation to the use of these cells as *in vitro* models. Despite this limitation, these cells are already used for substance screening in the early phase of drug development (Donato et al., 2013). As shown in one study, HepG2 cells correctly identified 6 out of 9 hepatotoxic substances—despite their low metabolic activity. This finding makes them a more predictive test system than the above-mentioned upcyte cells, which only detected 3 out of the 9 hepatotoxic drugs (Sison-Young et al., 2017). On the other hand, due to their low metabolic activity, hepatic cell lines are a less suitable model in the case of drugs in which the formed metabolite and not the parent drug is responsible for the toxic potential (Schyschka et al., 2013). This phenomenon may be one reason why the toxicity of acetaminophen was not detected using HepG2 cells in the above mentioned study. Furthermore, these cells are less suitable for CYP induction studies because they do not express the corresponding CYP enzymes, or they express them only at a low level (Westerink and Schoonen, 2007). In order to extend the range of application of these cells, various studies have been conducted to test whether it is possible to increase the metabolic activity of the cells in order to generate a favorable but predictive *in vitro* test system. The tested approaches include transfection of the cells, e.g.; with the hepatocyte nuclear factor-1 alpha as well as different approaches for epigenetic reactivation of the cells (Chiang et al., 2014, Snykers et al., 2009). In addition, various small molecules have been used to intervene in the metabolism of the cells in such a way that proliferation can be stopped and the functionality of the cells increased (Snykers et al., 2009, Sajadian and Nussler, 2015, Sajadian et al., 2016). In many of these approaches, there is a slight increase in metabolic activity or expression of epithelial genes such as E-cadherin or HNF4 α . However, none of these studies have revealed biologically relevant changes or even the level of fresh isolated PHH (Dannenbergh and Edenberg, 2006, Snykers et al., 2009). In the study we conducted (Ruoß et al., 2019), the treatment of HepG2 cells with 5-AZA and vitamin C resulted in a positive change in the expression of various genes that are

essential for the epithelial phenotype and hepatocyte function. Nevertheless, our study revealed the limitations of such approaches. For example, we found that several genes that may also play essential roles in the de-differentiation of hepatocytes are deregulated more than 100-fold compared to PHH. Moreover, there is no significant effect on the expression of these genes by the tested treatment. As studies by other authors have shown, treatment with 5-AZA leads to global demethylation of the DNA (Seeliger et al., 2013). These changes are on the one hand side positive—as they may lead to a reactivation of hepatocyte-specific genes—but on the other hand, this global demethylation also leads to nonspecific upregulation of non-hepatocyte-specific genes. Thus, one study showed that treatment with 5-AZA increased the expression of spermatogenesis genes in HepG2 cells (Dannenberg and Edenberg, 2006), which is not the goal of epigenetic reactivation (Ruoss et al., 2020b). Our chromatin array demonstrated that an epigenetic reactivation of liver cells would nevertheless be useful (Ruoß et al., 2019) because many of the epigenetically active enzymes tested are, in part, significantly deregulated compared to PHH. However, specific modification of individual epigenetic modifications is necessary and not a nonspecific global epigenetic change.

An alternative to the modification of cells of existing cell lines is the establishment of new cell lines that are in their metabolic properties more similar to human hepatocytes. The most substantial model of this in the last 20 years is the HepaRG cell line, which has significantly higher metabolic activity compared to standard cell lines such as HepG2 and Huh7 (Guo et al., 2011). The HepaRG cell line was isolated from the tumor tissue of a patient suffering from HCC (Gripon et al., 2002). The treatment of the cells with dimethyl sulfoxide (DMSO), insulin, and hydrocortisone leads to the differentiation of the cells and an increase in their metabolic activity (Jang et al., 2019). Genome-wide analyses have shown that the gene expression profile of HepaRG correlates much better with that of primary hepatocytes than that of other cell lines such as cells of the HepG2 cell line or stem cell-based hepatocyte-like cells (Godoy et al., 2016). Another study revealed that the metabolic activity of HepaRG cells is comparable to that in cryopreserved hepatocytes, with the

exception of a lower CYP2D6 activity (Kratochwil et al., 2017). By culturing the HepaRG cells in a 3D spheroid culture, their metabolic activity can be further increased (Takahashi et al., 2015). The generation of HepaRG spheroids also can be applied in the 384-well format with only 2.5×10^4 cells/spheroid, which makes this model interesting for high-throughput applications (Ramaiahgari et al., 2014). On the other hand, the sensitivity to hepatotoxic substances of HepaRG is relatively low: Only 3 of 9 hepatotoxic substances were identified as such with the help of this cell line, which represents a lower predictivity compared to HepG2 but is still comparable to the level found using the upcyte hepatocytes. Hence, these cells have limited suitability as an alternative to PHH for testing new drugs (Sison-Young et al., 2017).

7.2 Establishment of cultivation techniques for long-term culture of primary hepatocytes

Acute toxicity tests play a subordinate role in the testing scheme of drugs. More important is how the organism reacts to the repeated dose administration of a substance. For this purpose, 28-day studies have been performed in rodents according to the corresponding ICH Guidelines e.g. M3/S3A (Parasuraman, 2011, Colerangle, 2017). These studies allow an assessment of the toxicity of a substance and the identification of the most sensitive target organs and provide information on the absorption, distribution, metabolism, and excretion of the substance (Denny and Stewart, 2017). Due to the complexity of an organism, these data can only be generated using *in vivo* studies. However, in order to better transfer these findings to the human population, it may be useful to mimic the observed effects *in vitro* (Ruoss et al., 2020b). For this purpose, it is necessary to reduce the complexity so that the biological processes underlying the toxicity of a substance can be measured separately. Such a strategy is used in the adverse outcome pathway concept. Here, key events—which are necessary for the development of the toxicity of the substance—are defined. *In vitro* studies may test whether the substance triggers these individual key events, which, in their entirety, might predict possible toxicity in humans (Horvat et al., 2017, Vinken, 2013). Cells suitable for such tests should correspond as closely as possible to the *in vivo* situation, which is undoubtedly the

case for drug metabolism and liver toxicity studies when PHH are used. In order to be able to reproduce even slowly occurring effects, a sufficient cultivation time of the cells is required (Soldatow et al., 2013). This phenomenon has been difficult when using PHH because they lose their metabolic activity after only a few days in culture (Godoy et al., 2013). To increase the cultivation time of these cells, different approaches have been tested. For example, mimicking the *in vivo* conditions (e.g.; a 3D culture approach) slows down the de-differentiation of the hepatocytes. This fact enables cells to be cultivated in a functionally active state over a more extended time period (Bachmann et al., 2015). For a model that provides valid results, such a 3D culture model must be based on standardizable 3D matrices, especially those that are small enough to be used in a 96-well format (for a 3D model in a high-throughput approach) (Macdonald et al., 2018, Nakayama, 1998) As our data show, the Optimaix-3D Scaffold from Matricel fulfills the above-mentioned requirements (Ruoss et al., 2018). In addition, its porous structure allows an optimal supply of cells even inside the scaffold. Another advantage of this scaffold is its low stiffness of 7.5 kPa, which corresponds approximately to the stiffness found in healthy human liver (Wong et al., 2010). Furthermore, the collagen used for this scaffold could at least partially mimic the ECM of the liver (Martinez-Hernandez and Amenta, 1993). These beneficial properties may be the reason why this scaffold enables hepatocytes to be cultivated over 10 days while largely maintaining metabolic activity. For example, on day 10 there was a five-fold higher CYP3A4 activity compared to the 2D control. The maintenance of CYP3A4 activity is important because this CYP enzyme is responsible for the metabolism of more than 30% of drugs (Zanger and Schwab, 2013). The detoxification of urea and the production of albumin, which are both important functions of hepatocytes, can be maintained much better compared to a 2D culture, data that further suggest the positive effect of scaffold culture on the maintenance of the functionality of the hepatocytes. Compared to other studies in which 3D scaffold cultures were used to maintain hepatocyte function, coating the scaffold with fibronectin or by the additional use of a co-culture with 3T3-J2 cells better maintained metabolic function compared to what we found in our study (Wei et al., 2018, Rajendran et al., 2017). Nevertheless, these approaches are much more

complex and difficult to standardize, a factor that limits their use for testing new drugs. Furthermore, the cultivation of 3T3-J2 cells is also possible on the Optimaix-3D Scaffold, as we have recently shown (Ruoß et al., 2020). A pre-incubation of the scaffolds with synthetic peptides that represent the binding sites of fibronectin or their integration into the scaffold matrix during production could also be useful to create a scaffold that is standardizable and also better represents the *in vivo* situation and thus allows longer maintenance of the metabolic activity of the PHH (Huettner et al., 2018). The Optimaix-3D Scaffold is also suitable to be integrated into a fluid-flow model due to its high permeability. It would be conceivable, for example, to cultivate the scaffolds in the Quasi Vivo® system from Lonza (Buesch et al., 2018). This system allows incubating hepatocytes in a Matrigel-coated coverslip over 21 days using a constant flow. These conditions maintain CYP1A2, CYP2B6, and CYP3A4 activities at a higher level compared to static culture over 21 days (Buesch et al., 2018). The use of the Optimaix-3D Scaffold in this system, possibly in combination with a co-culture with 3T3-J2 cells, might allow maintaining the activity of the cells over a long period of time, and thus minimize the problem of cell availability.

7.3 Development of *in vitro* models capable of mimicking the physiological environment of the human liver, but also disease-specific changes that lead to altered drug metabolism

To detect toxic effects of a new drug *in vitro*, the potential utilized *in vitro* model must be capable of reproducing the biological processes that underline this toxicity. An example that illustrates the need for a suitable test system is paracetamol toxicity. The intake of this substance is the most common cause of acute liver damage in both Europe and the US (Yoon et al., 2016). However, in conventional 2D culture, this substance shows only a low toxic potential (Prot et al., 2011). This is due to the low activity of the 2D culture transporters, which are responsible for the uptake of the substance in the cells. The low uptake of paracetamol in hepatocytes results in the formation of lower concentrations of the toxic NAPQI metabolite, which logically results in the low toxicity. In contrast, by cultivating the hepatocytes in a 3D sandwich

culture, it is possible to maintain the activity of the transporters, a phenomenon that leads to better uptake of the substance and, consequently, higher toxicity (Schyschka et al., 2013). These results better represent the *in vivo* situation. In other cases, the hepatotoxicity observed *in vivo* is due to systemic or local inflammation induced by the substance. This inflammatory process is accompanied by the migration of macrophages and neutrophils into the hepatic vascular system and the release of inflammatory mediators (Jaeschke et al., 2002). The prediction of such an effect *in vitro* requires that the cells responsible for the inflammation and/or the release of inflammation mediators are also part of the *in vitro* model. Only then it is possible to detect the effects that occur in humans also in an *in vitro* study (Ruoss et al., 2020b, Godoy et al., 2013). A further limitation of current test systems for evaluating new drugs is the fact that usually young and healthy animals are used for *in vivo* studies, whereas for *in vitro* studies, the available hepatocytes are usually from older patients who often have prominent liver diseases. Therefore, only limited information on the metabolism and toxicity of a substance can be derived from the above-mentioned models for the entire population (Ruoss et al., 2020b, Rodighiero, 1999). In order to make such predictions for healthy individuals as well as for patients with previous diseases, models must imitate the situation in healthy individuals as well as disease-specific alterations. For this purpose, in animal research, there are several models that mimic certain diseases (Liu et al., 2013). However, such models are not available for *in vitro* research. The need for such *in vitro* models also results from observations made in clinical studies. In one of them, the expression of different phase I/II enzymes in patient population changes depending on liver stiffness (Theile et al., 2013). Such changes can lead to altered drug metabolism, which can either stop the medication from working or lead to an overdose of the substance and toxic effects (Elbekai et al., 2004, Baillie and Rettie, 2011).

Changes in liver stiffness are one characteristic of liver fibrosis pathology (Mueller and Sandrin, 2010). The altered stiffness results from a restructuring of the ECM and an increased deposition of collagen (Bataller and Brenner, 2005). In order to predict such disease-specific changes in drug metabolism *in vitro*, we have developed a model that represents the stiffness of both healthy and fibrotic livers (Ruoss et al.,

2020a). To provide cells with ideal cultivation conditions, we used HEMA-BAA-based cryogels. The porous structure and optimal pore size for hepatocyte environment offer an ideal environment for the cultivation of cells (Heydari et al., 2020, Ye et al., 2019). Besides, we modified the surface of the scaffolds to allow optimal cell adherence. As our data showed, the cultivation of the HepG2 on the healthy liver scaffold generally leads to a higher activity of the measured phase I/III enzymes. A similar effect has already been shown by Natarajan *et al.* in hepatocytes (Natarajan et al., 2015). The data from that study and our results confirm the clinical observations of the effect of stiffness on the metabolic activity of the hepatocytes (Theile et al., 2013).

Our model also mimicked the accumulation of ECM, which is *in vivo* the major reason for the increased stiffness (Klaas et al., 2016, Mueller and Sandrin, 2010). This was possible given by the fact that the healthy and fibrotic liver scaffolds differ mainly in their gelatin concentration. Gelatin is hydrolyzed collagen; it has the same binding sites as collagen, and therefore the accumulation of collagen can be imitated by increasing the gelatin concentration (Wissemann and Jacobson, 1985, Zhang et al., 2006).

In summary, we have developed a model that could mimic some of the changes that occur in fibrotic livers (Ruoss et al., 2020a). However, liver fibrosis is also associated with other pathological changes that we did not address in the current study, including changes in the ECM that go beyond the accumulation of collagen type I. Such alterations comprise the accumulation of collagen type III and elastin as well as the de-regulation of various matrix metalloproteases, that also play an important role in ECM remodeling (Bonnans et al., 2014, Iredale et al., 2013). It is also noteworthy, that the development of liver fibrosis is a multifactorial process in which, in addition to hepatocytes, stellar cells and Kupffer cells play a decisive role in the pathogenesis (Bale et al., 2016, Sacchi et al., 2020). A model that can actually mimic a fibrotic liver should therefore also include these non-parenchymal cells. How such a model based on our scaffolds could look like and which parameters could be mimicked are summarized in Figure 3

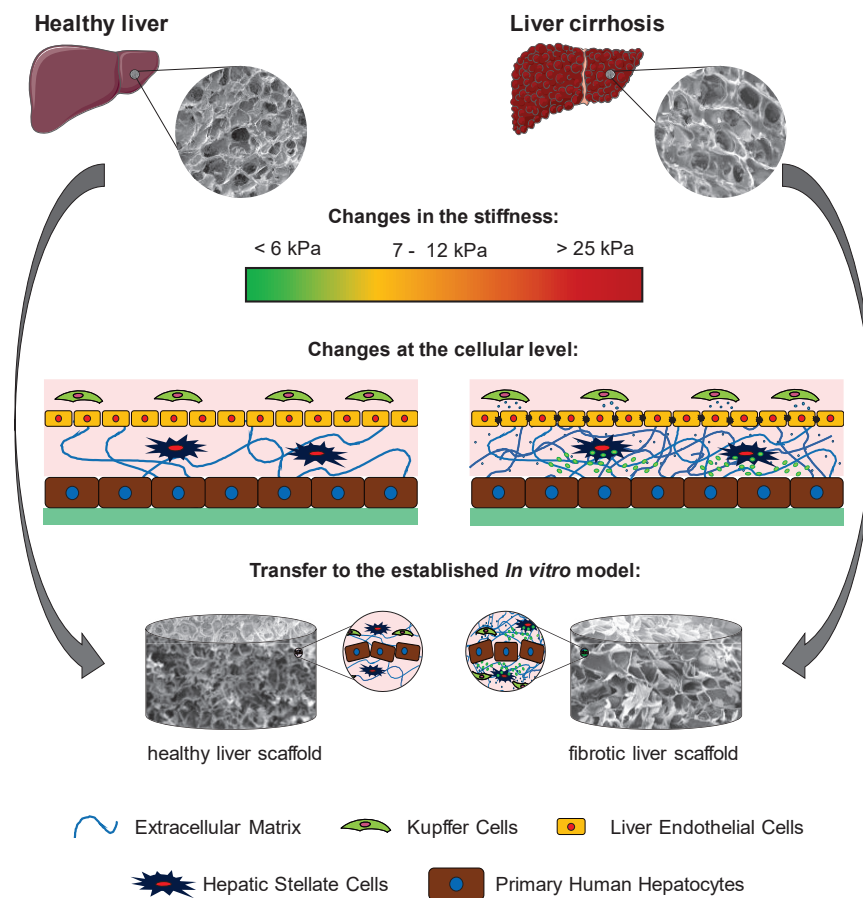


Figure 3 Development of a 3D scaffold Co-Culture model, which represents some parameters of the healthy and the fibrotic altered liver. The image is modified our recent publication, where it was partly used as the cover image of the published issue (Ruoss et al., 2020a). This figure was produced using Servier Medical Art (<http://smart.servier.com/>).

In such a model, it may also be useful to replace the FCS used in many cell culture media with serum from healthy individuals and patients suffering from liver fibrosis. Preliminary data in our laboratory revealed a positive effect of human serum from healthy donors on the metabolic activity of the cells, which had previously been observed in other studies (Katsura et al., 2002, Steenbergen et al., 2018). The use of this serum from healthy donors as well as the use of patient serum would lead to an even more realistic modelling of the *in vivo* situation. Additionally, the collagen used for the production of scaffolds could also be replaced by decellularized ECM from healthy and fibrotic livers, a design that would allow the ECM changes to be imitated even more realistically (Damania et al., 2018, Sellaro et al., 2010). Such a complex model could be used in the *in vitro* testing of new drugs and would make it

possible to predict possible negative effects in different individuals within the human population (Figure 4).

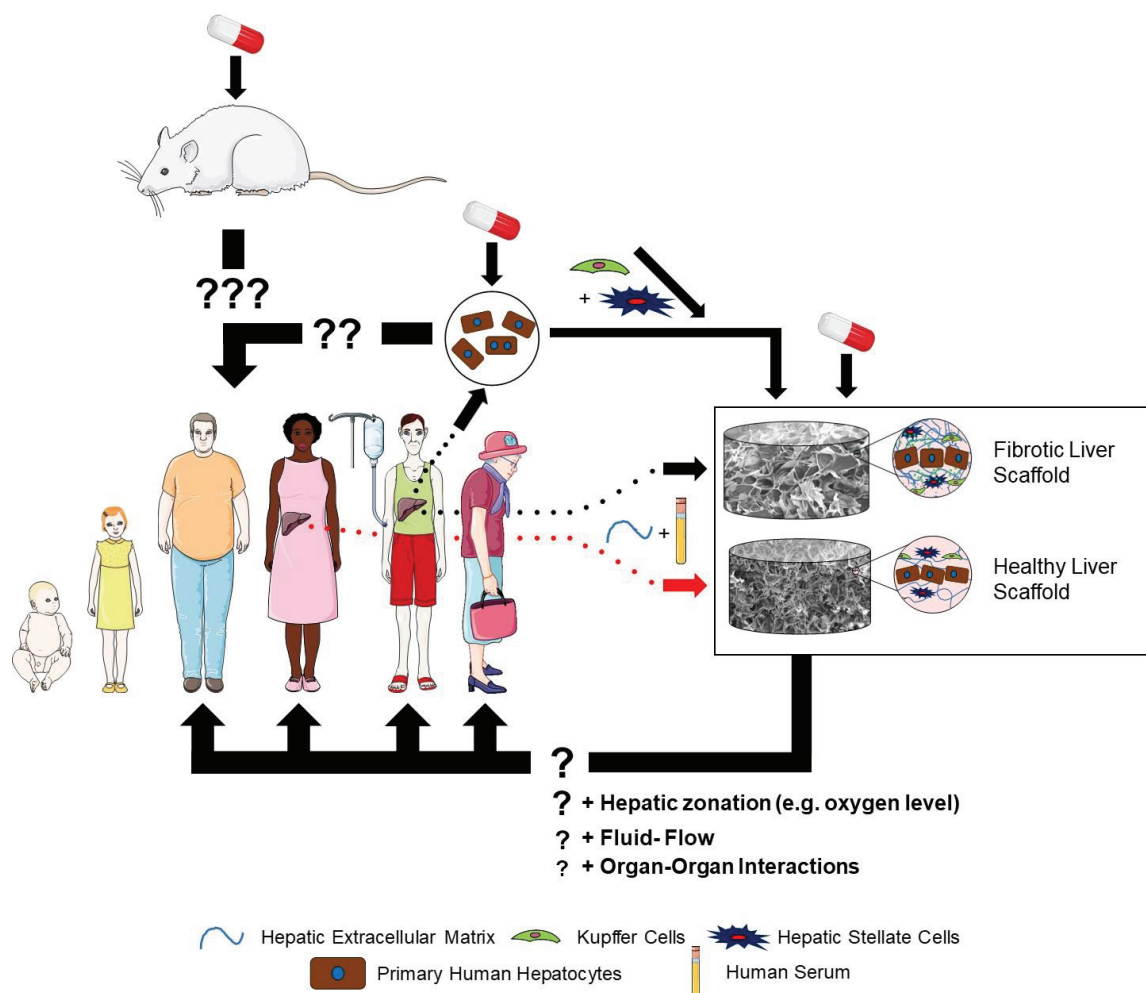


Figure 4 Schematic illustration of the application of a scaffold-based 3D co-culture model, which also takes into account disease-specific differences. Additionally, possible approaches for further improvement of this model are described. This is a modified image from, where it was partly used as the cover image of the published issue (Ruoss et al., 2020a). This figure was produced using Servier Medical Art (<http://smart.servier.com/>).

However, one must consider that, especially for a co-culture or triple culture approach, using stellate and/or Kupffer cells would significantly increase the complexity of the model. For this purpose, the culture medium must be suitable for all cells, and there must be a technique developed to quantify the used cell types separately from each other, since this is the only way to obtain information on how the individual cells behave in co-culture.

7.4 Development of quantification methods to normalize the results even with complex cultivation approaches

As described in the previous section, the development of advanced strategies for the cultivation of hepatocytes is necessary for mapping *in vitro* all relevant biological processes that are related to the development of hepatotoxicity. However, as the complexity of the test system increases, the generation of reliable results also becomes more difficult. In traditional 2D culture, numerous methods are available to quantify the cells used in the experiment. However, most of the methods are not transferable to a 3D culture (Ruoß et al., 2020). Moreover, some methods that work in 3D cultures can only be used to a limited extent, since the results obtained here cannot be compared with those from 2D cultures for various reasons: Some reasons include interferences of the test reagent with the scaffold matrix or changes in the metabolic activity of the cells due to different stress levels caused by the different rigidities of the surface between the stiff cell culture plastic and the soft scaffold matrix, among others. Furthermore, the isolation of cells, their RNA, or proteins from the scaffold—an approach which would simplify the analysis considerably—is often not possible (Ruoss et al., 2018). Similar limitations regarding the quantifiability of the results can be observed when using co-cultures (Ruoß et al., 2020). With current methods, it is not possible to quantify independently the individual cell types in a co-culture. However, such independent quantification is absolutely necessary to be able to evaluate the results. Indeed, separate quantification is the only way to investigate the influence of the co-culture on the individual cell types (Ruoß et al., 2020).

In recent years, 3D culture and co-culture approaches have been combined in various studies, and different 3D-based co-culture models have been established (Chan et al., 2013, Wei et al., 2018). However, only few of these studies have addressed the problem of cell-type-specific quantification of the results (Ruoß et al., 2020). This fact limits the significance of the results obtained in such 3D co-culture studies. It should also be noted that some of the available approaches dealing with the problem of cell type-specific quantification are very complex, but they allow the tracing of each individual cell in a tumor model using DNA barcoding technique

(Nguyen et al., 2014a, Nolan-Stevaux et al., 2013). This method requires the sequencing of the individual cells; thus, these approach are rather unsuitable for broad application for the quantification.

The lack of a suitable quantification technique that can be carried out quickly and easily and yet provides reliable results was the reason why, as a first step toward establishing a 3D co-culture liver fibrosis model, we developed a precise and straightforward way for the separate quantification of each cell type. Our data revealed that the qPCR-based quantification method can achieve this objective by quantifying different cell types on a 3D matrix independent of each other. Further, the sensitivity of the developed method is sufficient for most applications. By incubating the scaffold for 30 min in 98°C NaOH, we succeeded in generating a technique that allows isolating the DNA completely from the scaffold. Besides, we showed that the quantification method works on our pHEMA-BAA based scaffolds as well as on the Optimaix-3D Scaffold from Matricel. This finding suggests a broad application of this method for different test systems (Ruoß et al., 2020).

The only limitation of this method is the fact that the utilized cells must differ at least at one point in their sequence. In the model we tested, this requirement was achieved by using human HepG2 cells and murine 3T3-J2 cells. However, this method is also conceivable for use in the mentioned liver fibrosis co-culture model. In addition to human hepatocytes, murine stellate cells and rat Kupffer cells may be used. A purely human-cell-based approach is also conceivable. In order to distinguish between the different cell types, sequences such as E6/E7 from the human papillomavirus, which were introduced into the genome during immortalization, could be used to quantify the individual cell types (Levy et al., 2015). Also, the use of male and female cells and the quantification on the Y-chromosome gene *SRY* can allow a cell-type-specific quantification of the co-culture model (Drobnič, 2006). Due to the described adaptations, a broad application of the method developed by our laboratory is conceivable for many co-culture models.

7.5 Conclusion and possible future research directions

When testing new drugs, animal experiments are considered to be the gold standard due to the lack of eligible alternative methods (Ferreira et al., 2019). Indeed, the great complexity of a whole organism cannot yet be represented using *in vitro* models (Bhanu Prasad, 2016). The data obtained from animal models can only be transferred to humans to a limited extent; hence, the development of suitable models that can supplement animal experiments is urgently needed (Akhtar, 2015, Balls et al., 2019). It is also conceivable to use such *in vitro* models to pre-screen new substances. In doing so, substances with a hepatotoxic potential can be excluded at an early stage of drug development, an outcome that saves money and reduces the number of tested animals (O'Brien et al., 2006). Overall, assessing possible hepatotoxicity during the early phases of drug development is still of central importance because the prediction of such effects in animal experiments is insufficient due to pronounced species differences (Martignoni et al., 2006).

Over the past 40 years, numerous approaches have been developed to establish suitable *in vitro* models. Despite intensive research, no model can be considered successful, as central problems have not yet been sufficiently solved. These include the inadequate availability of human hepatocytes, which are considered to be the most suitable cell type for such a model, and the fact that these cells lose their metabolic activity after only a few days in culture (Godoy et al., 2013). The use of alternative cell types, such as differentiated stem cells or hepatic stem cells, is also generally possible; however, they are still unable to adequately represent the functionality of PHH, which sets significant limits to their usage as an alternative to PHH (Ruoss et al., 2020b, Godoy et al., 2015). This thesis evaluated different approaches in solving the problems described above by using primary hepatocytes and hepatic cell lines. Epigenetic reactivation of tumor cells in the HepG2 hepatoma cell line was possible to a limited extent because treatment with AZA and vitamin C had only a slight positive effect on the metabolic activity of the cells (Ruoss et al., 2019). Still, we identified epigenetic changes in all tested HCC cell lines as well as—but to a lesser extent—in the de-differentiation of primary hepatocytes. These

changes are probably associated with the loss of metabolic activity in hepatic cell lines, but they have not yet been associated with it. In the future, modification of these targets by a specific treatment could enable the epigenetic reactivation, to a certain extent, of liver cell lines or stop the de-differentiation of PHH. A delay in PHH de-differentiation might be achievable by cultivating the cells on the Optimaix scaffold from Matricel (Ruoss et al., 2018). Thus, we showed that the Optimaix Scaffold from Matricel enables the maintenance of the metabolic activity of the PHH cultivated on it over a period of 10 days. In addition, we demonstrated that the use of this scaffold as a transport carrier allows almost loss-free transport of PHH. Thus, the number of available PHH at the destination point can be increased by more than 50% in comparison to the shipment as a suspension culture on ice. This outcome allows more efficient use of the limited number of available cells. Compared to shipping as a 2D culture, significantly more cells per area can be shipped on the scaffold. In addition, the cells are better protected against contamination and dehydration because a large part of the medium is absorbed by the scaffold.

The development of pHEMA/BAA-based scaffolds that mimic different characteristics of a healthy and fibrotically altered liver is an innovative approach. This tactic would allow modeling disease-related changes in the liver, something that is currently only possible using *in vivo* disease models. However, the model we have established can only be considered a first step in this direction. For a more comprehensive representation of the *in vivo* situation, a combination of different approaches is necessary, e.g., the application of our pHEMA/BAA-based scaffold model on which PHH are cultivated in a co-culture together with Kupffer cells and/or hepatic stellate cells. An appropriate quantification method, which enables the evaluation of the data generated in such a complex model, has been developed through the work presented in this thesis. This approach can be used for the cell type specific evaluation of the results.

To more closely reflect the *in vivo* situation, it would also be useful to adjust other parameters that are important for hepatocyte function or in the development of hepatotoxicity. Possible parameters that should be considered in this context are

summarized in Figure 5 and described in more detail in our recently published review (Ruoss et al., 2020b).

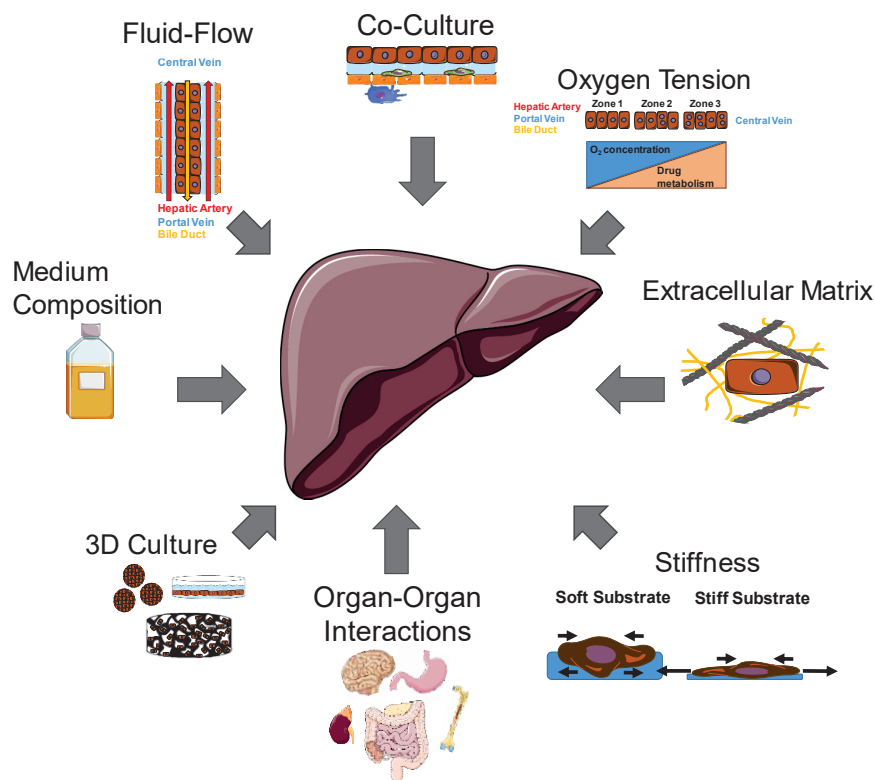


Figure 5 Techniques and approaches for improved culture of freshly isolated human hepatocytes (PHH) and liver cell lines by adapting the culture conditions and mimicking the *in vitro* situation (Ruoss et al., 2020b). This figure was produced using Servier Medical Art (<http://smart.servier.com/>).

Some of the approaches described in Figure 5 are already part of our pHEMA/BAA-based scaffold model. An important point that has not been addressed in this thesis—and has not been considered in our model—is mimicking the functional zoning of hepatocytes within the liver lobe (Birchmeier, 2016, Probst et al., 1982, Camp and Capitano, 2007). This functional zonation within a liver lobe occurs, for example, by the gradual availability of oxygen and gradual expression of *WNT*. Hence, catabolic metabolic processes such as the formation of albumin mainly occur in the periportal area, while anabolic processes such as the metabolism of drugs are primarily performed in the perivenous area (Birchmeier, 2016). Given that functional zoning significantly influences the functionality of the individual hepatocytes, it makes sense to map it in an *in vitro* model, an endeavor that, surprisingly, has only

been implemented in a few studies (Ahn et al., 2019, Guo et al., 2011). One of these studies achieved functional zoning by the gradual induction of *WNT* expression within a hydrogel gel. As the results of the study show, this functional zoning leads to zonal toxicity caused by hepatotoxic substances such as paracetamol (Ahn et al., 2019). This result underlines the importance of hepatic zoning in the development of new *in vitro* models, in which the detection of possible hepatotoxicity seems to be crucial.

The development of an “optimal” model that includes all the above parameters would make it possible to better predict the hepatotoxic properties of new substances. This eventuality can be assumed because all the biological processes required for hepatotoxicity could also occur in the *in vitro* model. Ideally, this kind of a model would also allow nearly unlimited cultivation of hepatocytes; however, such a model would not be able to completely replace animal experiments. To achieve that goal, the employed *in vitro* model must be able to imitate all the processes that take place in the whole organism, from the uptake of the substance to its excretion. While existing models with so-called “body on a chip” approaches target this potential, they only rudimentarily reflect the *in vivo* situation. This fact is not surprising given the high complexity of the human organism (Ruoss et al., 2020b, Reif, 2014). For example, it is hardly possible to map complex functional units such as the individual liver lobules or the individual nephrons of the kidney *in vitro*, not to mention the complexity of the human brain (Bang et al., 2019, Nishinakamura, 2019). Another challenge is to find a medium suitable for all the different cell types used in a possible model. One potential solution would be to separate the different cell types into distinct compartments, but this approach has the negative side effect of hindering the necessary exchange between the different cell types (Kimura et al., 2018). For this reason, it makes sense to reduce the complexity of the employed models and focus on the interaction of two or three different cell types. Several *in vitro* studies have demonstrated that this approach might also reflect interactions between different organs (Oleaga et al., 2018, Chong et al., 2018). One of these studies tested whether it is possible to visualize *in vitro* the skin sensitization caused by

reactive drug metabolites using a Liver-Immune-Co-Culture Array. The developed array comprises two compartments—one for liver cells (HepaRG) and one for immune cells (U937) which are connected by thin nanotubes to provide an exchange of different factors, such as drug metabolites produced by HepaRG cells, between them. This model mimics the formation of reactive metabolites as well as the activation of immune cells responsible for skin sensitization as a reaction to carbamazepine (Chong et al., 2018). If models like the Liver-Immune-Co-Culture Array, as well as our novel 3D model, can correctly predict the effects of a large number of substances, they could be used for *in vitro* testing of new substances in the future. Even if animal experiments cannot be completely replaced by such approaches, because they cannot represent the complexity of a whole organism, they could be considerably reduced. This potential is illustrated with the following example. For the approval of one new substance, about 100 candidate substances are currently tested in animal models. For a 28-day toxicity study in rodents, which is frequently used, 40 animals are required, which costs about €120,000 per candidate substance. If it is possible to identify negative substance effects in advance using predictive *in vitro* models, these candidate substances could be excluded before the first *in vivo* studies are carried out. In the end, it might be possible to reduce the costs for the development of new substances through the data from predictive *in vitro* models as well as increase the safety of new drugs.

Chapter 8: Abstract

In order to detect the hepatotoxic effects of new drugs at an early stage of drug development, the establishment of predictive *in vitro* models is necessary. PHH are particularly suitable for this purpose because these cells have metabolic properties comparable to the *in vivo* situation. However, due to various reasons, such as insufficient availability and rapid loss of function in culture, PHH can only be used to a limited extent for testing new drugs. Among others, hepatic cell lines are considered to be a possible alternative with unlimited availability. However, hepatic cell lines such as HepG2 are only partially suitable as an alternative for PHH, as our results have shown. The reason for this outcome is that they differ significantly from PHH in their epigenetic profile as well as metabolic properties. Although the tested epigenetic reactivation with AZA and vitamin C partially led to positive changes in gene expression of the tested cell lines, comparable gene expression and activity of drug-metabolizing enzymes to PHH could not be achieved. As already described, the use of PHH is also only possible to a limited extent. In order to increase the availability of metabolically competent PHH, we have developed a method that allows the transport of PHH at high concentrations per area from A to B with almost no loss of viability. As our data further showed, the scaffold used for this purpose is suitable as a transport carrier and enables the cultivation of metabolically active PHH over a period of 10 days. The extension of the possible cultivation time also allows the investigation of delayed toxic effects. This potential is important because hepatotoxicity, for example, as in the case of acetaminophen, is a process that often occurs after a delay (Tolosa et al., 2019, Soldatow et al., 2013). In the course of this thesis, we also developed pHEMA-BAA based scaffolds, whose properties make them ideal for the cultivation of liver cells and additionally represent the stiffness of healthy or the fibrotically altered liver. With these scaffolds, it is possible, at least partially, to imitate disease-specific changes in the liver. Besides, a method has been developed that allows cell type-specific quantification for such a model. This method is also suitable for the quantification of more complex models, such as a scaffold-based 3D co-culture with Kupffer and/or hepatic stellate cells, which can better represent the *in vitro* situation. In the future, a combination of our scaffold model with

such a co-culture approach may contribute to better transfer of observations from animal experiments to humans, thus reducing the number of animal experiments while increasing safety for patients.

Chapter 9: Zusammenfassung

Um hepatotoxische Effekte neuer Medikamente bereits in einer frühen Phase der Arzneimittelentwicklung detektieren zu können ist die Etablierung von prädiktiven *in vitro* Modellen erforderlich. Hierzu eignen sich vor allem isolierte PHHs, da diese Zellen mit der *in vitro* Situation vergleichbare metabolische Eigenschaften aufweisen. Aufgrund unterschiedlicher Ursachen wie beispielsweise einer zu geringen Verfügbarkeit sowie einem raschen Funktionsverlust in Kultur können diese Zellen jedoch bisher für die Testung neuer Medikamente nur begrenzt eingesetzt werden. Als mögliche unbegrenzt verfügbare Alternative kommen unter anderem hepatische Zelllinien in Betracht. Wie unsere Ergebnisse zeigen, eignen sich hepatische Zelllinien wie HepG2 jedoch nur bedingt als Alternative für PHHs. Gründe hierfür sind, dass sie sich nicht nur in ihrem epigenetischen Profil, sondern auch insbesondere in ihren metabolischen Eigenschaften deutlich von den PHH unterscheiden. Durch die getestete epigenetische Reaktivierung mithilfe von AZA und Vitamin C konnten zwar teilweise positive Veränderung der Genexpression erreicht werden, eine mit PHH vergleichbare Genexpression und Aktivität der Fremdstoff-metabolisierenden Enzyme konnten jedoch bei weitem nicht erreicht werden. Auch die Verwendung von PHHs ist wie bereits beschrieben nur eingeschränkt möglich. Um die Verfügbarkeit metabolisch kompetenter PHH zu steigern haben wir daher eine Methode entwickelt, welche es ermöglicht PHHs in einer hohen Konzentration auf engem Raum nahezu verlustfrei von A nach B zu transportieren. Wie unsere Daten weiter zeigen eignet sich das hierfür verwendete Optimaix Scaffold von Matricel jedoch nicht nur als Transport Carrier, sondern ermöglicht auch die Kultivierung metabolisch aktiver PHH über einen Zeitraum von 10 Tagen. Dies bietet die Möglichkeit auch langsame oder verzögerte hepatotoxische Effekte *in vitro* zu untersuchen. Im Rahmen dieser Arbeit konnten wir zudem pHEMA-BAA basierte Scaffolds entwickeln, welche die Steifigkeiten der gesunden sowie der fibrotisch veränderten Leber repräsentieren. Mithilfe dieser Scaffolds war es möglich krankheitsspezifische Veränderungen der Leber zumindest teilweise zu imitieren. Für solch ein Modell aber insbesondere für noch komplexere Modelle, wie beispielsweise einer Scaffold-basierten 3D Co-Kultur mit

Kupffer und/ oder Stellarzellen welche die *in vitro* Situation noch besser abbilden könnten, konnte eine Methode entwickelt werden, welche die Zelltyp-spezifische Quantifizierung innerhalb solcher Ansätze ermöglicht. Die Verfügbarkeit einer solchen Quantifizierungsmethode ist die Voraussetzung für die Bewertung der in solch komplexen Modellen gewonnen Daten, weil nur so eine Zelltyp-spezifische Evaluation der Effekte möglich ist. Solche Modelle können in Zukunft dazu beitragen in Tierversuchen gewonnen Erkenntnisse besser auf den Menschen übertragen zu können, was es möglich macht die Zahl der Tierversuche zu senken und gleichzeitig die Sicherheit für die Patienten erhöhen.

References

- ADAMS, D. H., JU, C., RAMAIAH, S. K., UETRECHT, J. & JAESCHKE, H. 2010. Mechanisms of immune-mediated liver injury. *Toxicol Sci*, 115, 307-21.
- AGGER, K., CLOOS, P. A., RUDKJAER, L., WILLIAMS, K., ANDERSEN, G., CHRISTENSEN, J. & HELIN, K. 2009. The H3K27me3 demethylase JMJD3 contributes to the activation of the INK4A-ARF locus in response to oncogene- and stress-induced senescence. *Genes Dev*, 23, 1171-6.
- AHN, J., AHN, J. H., YOON, S., NAM, Y. S., SON, M. Y. & OH, J. H. 2019. Human three-dimensional in vitro model of hepatic zonation to predict zonal hepatotoxicity. *J Biol Eng*, 13, 22.
- AKHTAR, A. 2015. The flaws and human harms of animal experimentation. *Camb Q Healthc Ethics*, 24, 407-19.
- ALAJBEG, I., ALIC, I., ANDABAK-ROGULJ, A., BRAILO, V. & MITRECIC, D. 2018. Human- and mouse-derived neurons can be simultaneously obtained by co-cultures of human oral mucosal stem cells and mouse neural stem cells. *Oral Dis*, 24, 5-10.
- ALLEN, M., MILLETT, P., DAWES, E. & RUSHTON, N. 1994. Lactate dehydrogenase activity as a rapid and sensitive test for the quantification of cell numbers in vitro. *Clinical Materials*, 16, 189-194.
- AMIRIKIA, M., SHARIATZADEH, S. M. A., JORSARAEI, S. G. A. & SOLEIMANI MEHRANJANI, M. 2017. Impact of pre-incubation time of silk fibroin scaffolds in culture medium on cell proliferation and attachment. *Tissue Cell*, 49, 657-663.
- ANTONI, D., BURCKEL, H., JOSSET, E. & NOEL, G. 2015. Three-dimensional cell culture: a breakthrough in vivo. *Int J Mol Sci*, 16, 5517-27.
- ARIAS, I. M., ALTER, H. J., BOYER, J. L., COHEN, D. E., SHAFRITZ, D. A., THORGEIRSSON, S. S. & WOLKOFF, A. W. 2020. *The liver: biology and pathobiology*, John Wiley & Sons.
- ASLANTÜRK, Ö. S. 2017. In Vitro Cytotoxicity and Cell Viability Assays: Principles, Advantages, and Disadvantages. *Genotoxicity-A Predictable Risk to Our Actual World*. Rijeka - Croatia: IntechOpen.
- ASPERA-WERZ, R. H., EHNERT, S., HEID, D., ZHU, S., CHEN, T., BRAUN, B., SREEKUMAR, V., ARNSCHEIDT, C. & NUSSLER, A. K. 2018. Nicotine and Cotinine Inhibit Catalase and Glutathione Reductase Activity Contributing to the Impaired Osteogenesis of SCP-1 Cells Exposed to Cigarette Smoke. *Oxid Med Cell Longev*, 2018, 3172480.
- ASTHANA, V., TANG, Y., FERGUSON, A., BUGGA, P., ASTHANA, A., EVANS, E. R., CHEN, A. L., STERN, B. S. & DREZEK, R. A. 2018. An inexpensive, customizable microscopy system for the automated quantification and characterization of multiple adherent cell types. *PeerJ*, 6, e4937.
- BABAI, S., AUCLERT, L. & LE-LOUET, H. 2018. Safety data and withdrawal of hepatotoxic drugs. *Therapie*.
- BACHMANN, A., MOLL, M., GOTTWALD, E., NIES, C., ZANTL, R., WAGNER, H., BURKHARDT, B., SANCHEZ, J. J., LADURNER, R., THASLER, W., DAMM,

- G. & NUSSLER, A. K. 2015. 3D Cultivation Techniques for Primary Human Hepatocytes. *Microarrays (Basel)*, 4, 64-83.
- BACHTIAR, M. & LEE, C. G. L. 2013. Genetics of Population Differences in Drug Response. *Current Genetic Medicine Reports*, 1, 162-170.
- BAILLIE, T. A. & RETTIE, A. E. 2011. Role of biotransformation in drug-induced toxicity: influence of intra- and inter-species differences in drug metabolism. *Drug Metab Pharmacokinet*, 26, 15-29.
- BAIOCCHINI, A., MONTALDO, C., CONIGLIARO, A., GRIMALDI, A., CORREANI, V., MURA, F., CICCOSANTI, F., ROTIROTI, N., BRENNAN, A., MONTALBANO, M., D'OFFIZI, G., CAPOBIANCHI, M. R., ALESSANDRO, R., PIACENTINI, M., SCHININA, M. E., MARAS, B., DEL NONNO, F., TRIPODI, M. & MANCONE, C. 2016. Extracellular Matrix Molecular Remodeling in Human Liver Fibrosis Evolution. *PLoS One*, 11, e0151736.
- BALE, S. S., GEERTS, S., JINDAL, R. & YARMUSH, M. L. 2016. Isolation and co-culture of rat parenchymal and non-parenchymal liver cells to evaluate cellular interactions and response. *Sci Rep*, 6, 25329.
- BALE, S. S., GOLBERG, I., JINDAL, R., MCCARTY, W. J., LUITJE, M., HEGDE, M., BHUSHAN, A., USTA, O. B. & YARMUSH, M. L. 2015. Long-term coculture strategies for primary hepatocytes and liver sinusoidal endothelial cells. *Tissue Eng Part C Methods*, 21, 413-22.
- BALLET, F. 1997. Hepatotoxicity in drug development: detection, significance and solutions. *J Hepatol*, 26 Suppl 2, 26-36.
- BALLS, M., BAILEY, J. & COMBES, R. D. 2019. How viable are alternatives to animal testing in determining the toxicities of therapeutic drugs? *Expert Opin Drug Metab Toxicol*, 15, 985-987.
- BALTRUSKEVICIENE, E., KAZBARIENE, B., BADARAS, R., BAGDONAITE, L., KRIKSTAPONIENE, A., ZDANAVICIUS, L., ALEKNAVICIUS, E. & DIDZIAPETRIENE, J. 2016. Glutathione and glutathione S-transferase levels in patients with liver metastases of colorectal cancer and other hepatic disorders. *Turk J Gastroenterol*, 27, 336-41.
- BANG, S., JEONG, S., CHOI, N. & KIM, H. N. 2019. Brain-on-a-chip: A history of development and future perspective. *Biomicrofluidics*, 13, 051301.
- BATALLER, R. & BRENNER, D. A. 2005. Liver fibrosis. *J Clin Invest*, 115, 209-18.
- BELL, C. C., DANKERS, A. C. A., LAUSCHKE, V. M., SISON-YOUNG, R., JENKINS, R., ROWE, C., GOLDRING, C. E., PARK, K., REGAN, S. L., WALKER, T., SCHOFIELD, C., BAZE, A., FOSTER, A. J., WILLIAMS, D. P., VAN DE VEN, A. W. M., JACOBS, F., HOUDT, J. V., LAHTENMAKI, T., SNOEYS, J., JUHILA, S., RICHERT, L. & INGELMAN-SUNDBERG, M. 2018. Comparison of Hepatic 2D Sandwich Cultures and 3D Spheroids for Long-term Toxicity Applications: A Multicenter Study. *Toxicol Sci*, 162, 655-666.
- BELL, C. C., HENDRIKS, D. F. G., MORO, S. M. L., ELLIS, E., WALSH, J., RENBLUM, A., FREDRIKSSON PUIGVERT, L., DANKERS, A. C. A., JACOBS, F., SNOEYS, J., SISON-YOUNG, R. L., JENKINS, R. E., NORDLING, Å., MKRTCHIAN, S., PARK, B. K., KITTERINGHAM, N. R., GOLDRING, C. E. P., LAUSCHKE, V. M. & INGELMAN-SUNDBERG, M. 2016. Characterization of primary human hepatocyte spheroids as a model

- system for drug-induced liver injury, liver function and disease. *Scientific Reports*, 6, 25187.
- BERENDSEN, T. A., IZAMIS, M. L., XU, H., LIU, Q., HERTL, M., BERTHIAUME, F., YARMUSH, M. L. & UYGUN, K. 2011. Hepatocyte viability and adenosine triphosphate content decrease linearly over time during conventional cold storage of rat liver grafts. *Transplant Proc*, 43, 1484-8.
- BHANU PRASAD, C. 2016. A review on drug testing in animals. *Transl Biomedicine*, 7, 4.
- BHARDWAJ, N. & KUNDU, S. C. 2010. Electrospinning: a fascinating fiber fabrication technique. *Biotechnol Adv*, 28, 325-47.
- BHATIA, S. N., BALIS, U. J., YARMUSH, M. L. & TONER, M. 1999. Effect of cell-cell interactions in preservation of cellular phenotype: cocultivation of hepatocytes and nonparenchymal cells. *FASEB J*, 13, 1883-900.
- BHOGAL, R. H., HODSON, J., BARTLETT, D. C., WESTON, C. J., CURBISHLEY, S. M., HAUGHTON, E., WILLIAMS, K. T., REYNOLDS, G. M., NEWSOME, P. N., ADAMS, D. H. & AFFORD, S. C. 2011. Isolation of primary human hepatocytes from normal and diseased liver tissue: a one hundred liver experience. *PLoS One*, 6, e18222.
- BIGDELI, N., KARLSSON, C., STREHL, R., CONCARO, S., HYLLNER, J. & LINDAHL, A. 2009. Coculture of human embryonic stem cells and human articular chondrocytes results in significantly altered phenotype and improved chondrogenic differentiation. *Stem Cells*, 27, 1812-21.
- BIRCHMEIER, W. 2016. Orchestrating Wnt signalling for metabolic liver zonation. *Nat Cell Biol*, 18, 463-5.
- BONNANS, C., CHOU, J. & WERB, Z. 2014. Remodelling the extracellular matrix in development and disease. *Nat Rev Mol Cell Biol*, 15, 786-801.
- BONNIER, F., KEATING, M. E., WROBEL, T. P., MAJZNER, K., BARANSKA, M., GARCIA-MUNOZ, A., BLANCO, A. & BYRNE, H. J. 2015. Cell viability assessment using the Alamar blue assay: a comparison of 2D and 3D cell culture models. *Toxicol In Vitro*, 29, 124-31.
- BORLAK, J., SINGH, P. K. & RITTELMAYER, I. 2015. Regulation of Liver Enriched Transcription Factors in Rat Hepatocytes Cultures on Collagen and EHS Sarcoma Matrices. *PLoS One*, 10, e0124867.
- BRESLIN, S. & O'DRISCOLL, L. 2016. The relevance of using 3D cell cultures, in addition to 2D monolayer cultures, when evaluating breast cancer drug sensitivity and resistance. *Oncotarget*, 7, 45745-45756.
- BREWE, M. 2006. *Embryonenschutz und Stammzellgesetz: rechtliche Aspekte der Forschung mit embryonalen Stammzellen*, Springer-Verlag.
- BROWN, J. H., DAS, P., DIVITO, M. D., IVANCIC, D., TAN, L. P. & WERTHEIM, J. A. 2018. Nanofibrous PLGA electrospun scaffolds modified with type I collagen influence hepatocyte function and support viability in vitro. *Acta Biomater*, 73, 217-227.
- BUAL, R. P. & IJIMA, H. 2019. Intact extracellular matrix component promotes maintenance of liver-specific functions and larger aggregates formation of primary rat hepatocytes. *Regen Ther*, 11, 258-268.

- BUESCH, S., SCHROEDER, J., BUNGER, M., D'SOUZA, T. & STOSIK, M. 2018. A Novel In Vitro Liver Cell Culture Flow System Allowing Long-Term Metabolism and Hepatotoxicity Studies. *Applied In Vitro Toxicology*, 4, 232-237.
- BURKHARDT, B., MARTINEZ-SANCHEZ, J. J., BACHMANN, A., LADURNER, R. & NUSSLER, A. K. 2014. Long-term culture of primary hepatocytes: new matrices and microfluidic devices. *Hepatol Int*, 8, 14-22.
- BURLEY, M. R. & ROTH, C. M. 2007. Effects of Retinoic Acid on Proliferation and Differentiation of HepG2 Cells. *The Open Biotechnology Journal*, 1.
- CAMP, J. P. & CAPITANO, A. T. 2007. Induction of zone-like liver function gradients in HepG2 cells by varying culture medium height. *Biotechnol Prog*, 23, 1485-91.
- CASSIM, S., RAYMOND, V. A., LAPIERRE, P. & BILODEAU, M. 2017. From in vivo to in vitro: Major metabolic alterations take place in hepatocytes during and following isolation. *PLoS One*, 12, e0190366.
- CASTELL, J. V., JOVER, R., MARTINEZ-JIMENEZ, C. P. & GOMEZ-LECHON, M. J. 2006. Hepatocyte cell lines: their use, scope and limitations in drug metabolism studies. *Expert Opin Drug Metab Toxicol*, 2, 183-212.
- CHAN, T. S., YU, H., MOORE, A., KHETANI, S. R. & TWEEDIE, D. 2013. Meeting the challenge of predicting hepatic clearance of compounds slowly metabolized by cytochrome P450 using a novel hepatocyte model, HepatoPac. *Drug Metab Dispos*, 41, 2024-32.
- CHENG, P. Y. & MORGAN, E. T. 2001. Hepatic cytochrome P450 regulation in disease states. *Curr Drug Metab*, 2, 165-83.
- CHIANG, T. S., YANG, K. C., CHIOU, L. L., HUANG, G. T. & LEE, H. S. 2014. Enhancement of CYP3A4 activity in Hep G2 cells by lentiviral transfection of hepatocyte nuclear factor-1 alpha. *PLoS One*, 9, e94885.
- CHO, C. H., BERTHIAUME, F., TILLES, A. W. & YARMUSH, M. L. 2008. A new technique for primary hepatocyte expansion in vitro. *Biotechnol Bioeng*, 101, 345-56.
- CHOI, S., SAINZ, B., JR., CORCORAN, P., UPRICHARD, S. & JEONG, H. 2009. Characterization of increased drug metabolism activity in dimethyl sulfoxide (DMSO)-treated Huh7 hepatoma cells. *Xenobiotica*, 39, 205-17.
- CHONG, L. H., LI, H., WETZEL, I., CHO, H. & TOH, Y. C. 2018. A liver-immune coculture array for predicting systemic drug-induced skin sensitization. *Lab Chip*, 18, 3239-3250.
- CHUNG, E. J., JU, H. W., PARK, H. J. & PARK, C. H. 2015. Three-layered scaffolds for artificial esophagus using poly(varepsilon-caprolactone) nanofibers and silk fibroin: An experimental study in a rat model. *J Biomed Mater Res A*, 103, 2057-65.
- CICCHINI, C., FILIPPINI, D., COEN, S., MARCHETTI, A., CAVALLARI, C., LAUDADIO, I., SPAGNOLI, F. M., ALONZI, T. & TRIPODI, M. 2006. Snail controls differentiation of hepatocytes by repressing HNF4alpha expression. *J Cell Physiol*, 209, 230-8.
- CIESLAR-POBUDA, A., KNOFLACH, V., RINGH, M. V., STARK, J., LIKUS, W., SIEMIANOWICZ, K., GHAVAMI, S., HUDECKI, A., GREEN, J. L. & LOS, M. J. 2017. Transdifferentiation and reprogramming: Overview of the processes,

- their similarities and differences. *Biochim Biophys Acta Mol Cell Res*, 1864, 1359-1369.
- CLEVERS, H. 2016. Modeling Development and Disease with Organoids. *Cell*, 165, 1586-1597.
- CLUXTON, R. J., JR., LI, Z., HEATON, P. C., WEISS, S. R., ZUCKERMAN, I. H., MOOMAW, C. J., HSU, V. D. & RODRIGUEZ, E. M. 2005. Impact of regulatory labeling for troglitazone and rosiglitazone on hepatic enzyme monitoring compliance: findings from the state of Ohio medicaid program. *Pharmacoepidemiol Drug Saf*, 14, 1-9.
- COLERANGLE, J. B. 2017. Preclinical Development of Nononcogenic Drugs (Small and Large Molecules). In: FAQI, A. S. (ed.) *A Comprehensive Guide to Toxicology in Nonclinical Drug Development*. Boston: Academic Press.
- COZZOLINO, A. M., NOCE, V., BATTISTELLI, C., MARCHETTI, A., GRASSI, G., CICCINI, C., TRIPODI, M. & AMICONE, L. 2016. Modulating the Substrate Stiffness to Manipulate Differentiation of Resident Liver Stem Cells and to Improve the Differentiation State of Hepatocytes. *Stem Cells Int*, 2016, 5481493.
- CUI, J., WANG, H., SHI, Q., SUN, T., HUANG, Q. & FUKUDA, T. 2019. Multicellular Co-Culture in Three-Dimensional Gelatin Methacryloyl Hydrogels for Liver Tissue Engineering. *Molecules*, 24, 1762.
- CUI, J., WANG, H., ZHENG, Z., SHI, Q., SUN, T., HUANG, Q. & FUKUDA, T. 2018. Fabrication of perfusable 3D hepatic lobule-like constructs through assembly of multiple cell type laden hydrogel microstructures. *Biofabrication*, 11, 015016.
- DAMANIA, A., KUMAR, A., TEOTIA, A. K., KIMURA, H., KAMIHIRA, M., IJIMA, H., SARIN, S. K. & KUMAR, A. 2018. Decellularized Liver Matrix-Modified Cryogel Scaffolds as Potential Hepatocyte Carriers in Bioartificial Liver Support Systems and Implantable Liver Constructs. *ACS Appl Mater Interfaces*, 10, 114-126.
- DAMBACH, D. M., ANDREWS, B. A. & MOULIN, F. 2005. New technologies and screening strategies for hepatotoxicity: use of in vitro models. *Toxicol Pathol*, 33, 17-26.
- DANNENBERG, L. O. & EDENBERG, H. J. 2006. Epigenetics of gene expression in human hepatoma cells: expression profiling the response to inhibition of DNA methylation and histone deacetylation. *BMC Genomics*, 7, 181.
- DAVIDSON, M. D., BALLINGER, K. R. & KHETANI, S. R. 2016. Long-term exposure to abnormal glucose levels alters drug metabolism pathways and insulin sensitivity in primary human hepatocytes. *Sci Rep*, 6, 28178.
- DE BRUYN, T., CHATTERJEE, S., FATTAH, S., KEEMINK, J., NICOLAI, J., AUGUSTIJNS, P. & ANNAERT, P. 2013. Sandwich-cultured hepatocytes: utility for in vitro exploration of hepatobiliary drug disposition and drug-induced hepatotoxicity. *Expert Opin Drug Metab Toxicol*, 9, 589-616.
- DENNY, K. H. & STEWART, C. W. 2017. Acute, Subacute, Subchronic, and Chronic General Toxicity Testing for Preclinical Drug Development. In: FAQI, A. S. (ed.) *A Comprehensive Guide to Toxicology in Nonclinical Drug Development*. Boston: Academic Press.

- DESAI, S. S., TUNG, J. C., ZHOU, V. X., GRENER, J. P., MALATO, Y., REZVANI, M., ESPANOL-SUNER, R., WILLENBRING, H., WEAVER, V. M. & CHANG, T. T. 2016. Physiological ranges of matrix rigidity modulate primary mouse hepatocyte function in part through hepatocyte nuclear factor 4 alpha. *Hepatology*, 64, 261-75.
- DIETRICH, C. G., GÖTZE, O. & GEIER, A. 2016. Molecular changes in hepatic metabolism and transport in cirrhosis and their functional importance. *World journal of gastroenterology*, 22, 72.
- DOI, I., NAMBA, M. & SATO, J. 1975. Establishment and Some Biological Characteristics of Human Hepatoma Cell Lines. *Gann*, 66, 385-392.
- DONATO, M. T., GOMEZ-LECHON, M. J. & CASTELL, J. V. 1991. Rat hepatocytes cultured on a monkey kidney cell line: Expression of biotransformation and hepatic metabolic activities. *Toxicol In Vitro*, 5, 435-8.
- DONATO, M. T., JOVER, R. & GOMEZ-LECHON, M. J. 2013. Hepatic cell lines for drug hepatotoxicity testing: limitations and strategies to upgrade their metabolic competence by gene engineering. *Curr Drug Metab*, 14, 946-68.
- DONATO, M. T., LAHOZ, A., CASTELL, J. V. & GOMEZ-LECHON, M. J. 2008a. Cell lines: a tool for in vitro drug metabolism studies. *Curr Drug Metab*, 9, 1-11.
- DONATO, M. T., TOLOSA, L. & GOMEZ-LECHON, M. J. 2015. Culture and Functional Characterization of Human Hepatoma HepG2 Cells. *Methods Mol Biol*, 1250, 77-93.
- DONATO, T., LAHOZ, A., MONTERO, S., BONORA, A., PAREJA, E., MIR, J., CASTELL, J. & GÓMEZ-LECHÓN, M. J. 2008b. *Functional Assessment of the Quality of Human Hepatocyte Preparations for Cell Transplantation*.
- DONG, C., WU, Y., YAO, J., WANG, Y., YU, Y., RYCHAHOU, P. G., EVERS, B. M. & ZHOU, B. P. 2012. G9a interacts with Snail and is critical for Snail-mediated E-cadherin repression in human breast cancer. *J Clin Invest*, 122, 1469-86.
- DROBNIČ, K. A new primer set in a SRY gene for sex identification. International Congress Series, 2006. Elsevier, 268-270.
- DURET, C., MORENO, D., BALASIDDAIAH, A., ROUX, S., BRILOTTI, P., RAULET, E., HERRERO, A., RAMET, H., BIRON-ANDREANI, C., GERBAL-CHALOIN, S., RAMOS, J., NAVARRO, F., HARDWIGSEN, J., MAUREL, P., ALDABE, R. & DAUJAT-CHAVANIEU, M. 2015. Cold Preservation of Human Adult Hepatocytes for Liver Cell Therapy. *Cell Transplant*, 24, 2541-55.
- EGGER, G., LIANG, G., APARICIO, A. & JONES, P. A. 2004. Epigenetics in human disease and prospects for epigenetic therapy. *Nature*, 429, 457-63.
- EHNERT, S., FALLDORF, K., FENTZ, A. K., ZIEGLER, P., SCHROTER, S., FREUDE, T., OCHS, B. G., STACKE, C., RONNIGER, M., SACHTLEBEN, J. & NUSSLER, A. K. 2015. Primary human osteoblasts with reduced alkaline phosphatase and matrix mineralization baseline capacity are responsive to extremely low frequency pulsed electromagnetic field exposure - Clinical implication possible. *Bone Rep*, 3, 48-56.
- EHNERT, S., KNOBELOCH, D., BLANKENSTEIN, A., MULLER, A., BOCKER, U., GILLEN, S., FRIESS, H., THASLER, W. E., DOOLEY, S. & NUSSLER, A. K. 2010. Neohepatocytes from alcoholics and controls express hepatocyte

- markers and display reduced fibrogenic TGF- β /Smad3 signaling: advantage for cell transplantation? *Alcohol Clin Exp Res*, 34, 708-18.
- ELBEKAI, R. H., KORASHY, H. M. & EL-KADI, A. O. 2004. The effect of liver cirrhosis on the regulation and expression of drug metabolizing enzymes. *Curr Drug Metab*, 5, 157-67.
- ENGLER, A. J., SEN, S., SWEENEY, H. L. & DISCHER, D. E. 2006. Matrix elasticity directs stem cell lineage specification. *Cell*, 126, 677-89.
- ESREFOGLU, M. 2013. Role of stem cells in repair of liver injury: experimental and clinical benefit of transferred stem cells on liver failure. *World J Gastroenterol*, 19, 6757-73.
- ESTELLER, M. 2006. Epigenetics provides a new generation of oncogenes and tumour-suppressor genes. *Br J Cancer*, 94, 179-83.
- FAN, J., JIA, X., HUANG, Y., FU, B. M. & FAN, Y. 2015. Greater scaffold permeability promotes growth of osteoblastic cells in a perfused bioreactor. *J Tissue Eng Regen Med*, 9, E210-8.
- FANG, Y., WANG, B., ZHAO, Y., XIAO, Z., LI, J., CUI, Y., HAN, S., WEI, J., CHEN, B., HAN, J., MENG, Q., HOU, X., LUO, J., DAI, J. & JING, Z. 2017. Collagen scaffold microenvironments modulate cell lineage commitment for differentiation of bone marrow cells into regulatory dendritic cells. *Sci Rep*, 7, 42049.
- FASOLINO, I., GUARINO, V., MARRESE, M., CIRILLO, V., VALLIFUOCO, M., TAMMA, M. L., VASSALLO, V., BRACCO, A., CALISE, F. & AMBROSIO, L. 2017. HepG2 and human healthy hepatocyte in vitro culture and co-culture in PCL electrospun platforms. *Biomed Mater*, 13, 015017.
- FAUSTO, N. & CAMPBELL, J. S. 2003. The role of hepatocytes and oval cells in liver regeneration and repopulation. *Mech Dev*, 120, 117-30.
- FERREIRA, G. S., VEENING-GRIFFIOEN, D. H., BOON, W. P. C., MOORS, E. H. M., GISPEN-DE WIED, C. C., SCHELLEKENS, H. & VAN MEER, P. J. K. 2019. A standardised framework to identify optimal animal models for efficacy assessment in drug development. *PLoS One*, 14, e0218014.
- FERRETTI, A. C., HIDALGO, F., TONUCCI, F. M., ALMADA, E., PARIANI, A., LAROCCA, M. C. & FAVRE, C. 2019. Metformin and glucose starvation decrease the migratory ability of hepatocellular carcinoma cells: targeting AMPK activation to control migration. *Sci Rep*, 9, 2815.
- FEY, S. J. & WRZESINSKI, K. 2012. Determination of drug toxicity using 3D spheroids constructed from an immortal human hepatocyte cell line. *Toxicol Sci*, 127, 403-11.
- FILIPP, F. V. 2017. Crosstalk between epigenetics and metabolism-Yin and Yang of histone demethylases and methyltransferases in cancer. *Brief Funct Genomics*, 16, 320-325.
- FLAIBANI, M., LUNI, C., SBALCHIERO, E. & ELVASSORE, N. 2009. Flow cytometric cell cycle analysis of muscle precursor cells cultured within 3D scaffolds in a perfusion bioreactor. *Biotechnol Prog*, 25, 286-95.
- FREESE, K., SEITZ, T., DIETRICH, P., LEE, S. M. L., THASLER, W. E., BOSSERHOFF, A. & HELLERBRAND, C. 2019. Histone Deacetylase Expressions in Hepatocellular Carcinoma and Functional Effects of Histone

- Deacetylase Inhibitors on Liver Cancer Cells In Vitro. *Cancers (Basel)*, 11, 1587.
- FUNG, J., LEE, C. K., CHAN, M., SETO, W. K., WONG, D. K., LAI, C. L. & YUEN, M. F. 2013. Defining normal liver stiffness range in a normal healthy Chinese population without liver disease. *PLoS One*, 8, e85067.
- FUNG, M., THORNTON, A., MYBECK, K., WU, J. H.-H., HORNBUCKLE, K. & MUNIZ, E. 2016. Evaluation of the Characteristics of Safety Withdrawal of Prescription Drugs from Worldwide Pharmaceutical Markets-1960 to 1999. *Drug Information Journal*, 35, 293-317.
- GAILHOUSTE, L., LIEW, L. C., YASUKAWA, K., HAGIWARA, K., IWAZAKI, N., YAMADA, Y., HATADA, I. & OCHIYA, T. 2018. Epigenetic Reprogramming of Human Hepatoma Cells: A Low-Cost Option for Drug Metabolism Assessment. *Cell Mol Gastroenterol Hepatol*, 5, 454-457 e1.
- GALPERIN, A., LONG, T. J. & RATNER, B. D. 2010. Degradable, thermo-sensitive poly(N-isopropyl acrylamide)-based scaffolds with controlled porosity for tissue engineering applications. *Biomacromolecules*, 11, 2583-92.
- GARNIER, D., LI, R., DELBOS, F., FOURRIER, A., COLLET, C., GUGUEN-GUILLOUZO, C., CHESNE, C. & NGUYEN, T. H. 2018. Expansion of human primary hepatocytes in vitro through their amplification as liver progenitors in a 3D organoid system. *Sci Rep*, 8, 8222.
- GASKELL, H., SHARMA, P., COLLEY, H. E., MURDOCH, C., WILLIAMS, D. P. & WEBB, S. D. 2016. Characterization of a functional C3A liver spheroid model. *Toxicol Res (Camb)*, 5, 1053-1065.
- GERETS, H. H., TILMANT, K., GERIN, B., CHANTEUX, H., DEPELCHIN, B. O., DHALLUIN, S. & ATIENZAR, F. A. 2012. Characterization of primary human hepatocytes, HepG2 cells, and HepaRG cells at the mRNA level and CYP activity in response to inducers and their predictivity for the detection of human hepatotoxins. *Cell Biol Toxicol*, 28, 69-87.
- GISSEN, P. & ARIAS, I. M. 2015. Structural and functional hepatocyte polarity and liver disease. *J Hepatol*, 63, 1023-37.
- GLICKLIS, R., SHAPIRO, L., AGBARIA, R., MERCHUK, J. C. & COHEN, S. 2000. Hepatocyte behavior within three-dimensional porous alginate scaffolds. *Biotechnology and Bioengineering*, 67, 344-353.
- GODOY, P., HENGSTLER, J. G., ILKAVETS, I., MEYER, C., BACHMANN, A., MULLER, A., TUSCHL, G., MUELLER, S. O. & DOOLEY, S. 2009. Extracellular matrix modulates sensitivity of hepatocytes to fibroblastoid dedifferentiation and transforming growth factor beta-induced apoptosis. *Hepatology*, 49, 2031-43.
- GODOY, P., HEWITT, N. J., ALBRECHT, U., ANDERSEN, M. E., ANSARI, N., BHATTACHARYA, S., BODE, J. G., BOLLEYN, J., BORNER, C., BOTTGER, J., BRAEUNING, A., BUDINSKY, R. A., BURKHARDT, B., CAMERON, N. R., CAMUSSI, G., CHO, C. S., CHOI, Y. J., CRAIG ROWLANDS, J., DAHMEN, U., DAMM, G., DIRSCH, O., DONATO, M. T., DONG, J., DOOLEY, S., DRASDO, D., EAKINS, R., FERREIRA, K. S., FONSA TO, V., FRACZEK, J., GEBHARDT, R., GIBSON, A., GLANEMANN, M., GOLDRING, C. E., GOMEZ-LECHON, M. J., GROOTHUIS, G. M., GUSTAVSSON, L., GUYOT,

- C., HALLIFAX, D., HAMMAD, S., HAYWARD, A., HAUSSINGER, D., HELLERBRAND, C., HEWITT, P., HOEHME, S., HOLZHUTTER, H. G., HOUSTON, J. B., HRACH, J., ITO, K., JAESCHKE, H., KEITEL, V., KELM, J. M., KEVIN PARK, B., KORDES, C., KULLAK-UBLICK, G. A., LECLUYSE, E. L., LU, P., LUEBKE-WHEELER, J., LUTZ, A., MALTMAN, D. J., MATZ-SOJA, M., MCMULLEN, P., MERFORT, I., MESSNER, S., MEYER, C., MWINYI, J., NAISBITT, D. J., NUSSLER, A. K., OLINGA, P., PAMPALONI, F., PI, J., PLUTA, L., PRZYBORSKI, S. A., RAMACHANDRAN, A., ROGIERS, V., ROWE, C., SCHELCHER, C., SCHMICH, K., SCHWARZ, M., SINGH, B., STELZER, E. H., STIEGER, B., STOBER, R., SUGIYAMA, Y., TETTA, C., THASLER, W. E., VANHAECKE, T., VINKEN, M., WEISS, T. S., WIDERA, A., WOODS, C. G., XU, J. J., YARBOROUGH, K. M. & HENGSTLER, J. G. 2013. Recent advances in 2D and 3D in vitro systems using primary hepatocytes, alternative hepatocyte sources and non-parenchymal liver cells and their use in investigating mechanisms of hepatotoxicity, cell signaling and ADME. *Arch Toxicol*, 87, 1315-530.
- GODOY, P., SCHMIDT-HECK, W., HELLWIG, B., NELL, P., FEUERBORN, D., RAHNENFUHRER, J., KATTLER, K., WALTER, J., BLUTHGEN, N. & HENGSTLER, J. G. 2018. Assessment of stem cell differentiation based on genome-wide expression profiles. *Philos Trans R Soc Lond B Biol Sci*, 373, 20170221.
- GODOY, P., SCHMIDT-HECK, W., NATARAJAN, K., LUCENDO-VILLARIN, B., SZKOLNICKA, D., ASPLUND, A., BJORQUIST, P., WIDERA, A., STOBER, R., CAMPOS, G., HAMMAD, S., SACHINIDIS, A., CHAUDHARI, U., DAMM, G., WEISS, T. S., NUSSLER, A., SYNNERGREN, J., EDLUND, K., KUPPERS-MUNTHNER, B., HAY, D. C. & HENGSTLER, J. G. 2015. Gene networks and transcription factor motifs defining the differentiation of stem cells into hepatocyte-like cells. *J Hepatol*, 63, 934-42.
- GODOY, P., WIDERA, A., SCHMIDT-HECK, W., CAMPOS, G., MEYER, C., CADENAS, C., REIF, R., STOBER, R., HAMMAD, S., PUTTER, L., GIANMOENA, K., MARCHAN, R., GHALLAB, A., EDLUND, K., NUSSLER, A., THASLER, W. E., DAMM, G., SEEHOFER, D., WEISS, T. S., DIRSCH, O., DAHMEN, U., GEBHARDT, R., CHAUDHARI, U., MEGANATHAN, K., SACHINIDIS, A., KELM, J., HOFMANN, U., ZAHEDI, R. P., GUTHKE, R., BLUTHGEN, N., DOOLEY, S. & HENGSTLER, J. G. 2016. Gene network activity in cultivated primary hepatocytes is highly similar to diseased mammalian liver tissue. *Arch Toxicol*, 90, 2513-29.
- GOMES, C. J., HARMAN, M. W., CENTUORI, S. M., WOLGEMUTH, C. W. & MARTINEZ, J. D. 2018. Measuring DNA content in live cells by fluorescence microscopy. *Cell Div*, 13, 6.
- GOMEZ-LECHON, M. J., TOLOSA, L., CONDE, I. & DONATO, M. T. 2014. Competency of different cell models to predict human hepatotoxic drugs. *Expert Opin Drug Metab Toxicol*, 10, 1553-68.
- GOU, Q., HE, S. & ZHOU, Z. 2017. Protein arginine N-methyltransferase 1 promotes the proliferation and metastasis of hepatocellular carcinoma cells. *Tumour Biol*, 39, 1010428317691419.

- GRANITZNY, A., KNEBEL, J., MULLER, M., BRAUN, A., STEINBERG, P., DASENBROCK, C. & HANSEN, T. 2017. Evaluation of a human in vitro hepatocyte-NPC co-culture model for the prediction of idiosyncratic drug-induced liver injury: A pilot study. *Toxicol Rep*, 4, 89-103.
- GRIPON, P., RUMIN, S., URBAN, S., LE SEYEC, J., GLAISE, D., CANNIE, I., GUYOMARD, C., LUCAS, J., TREPO, C. & GUGUEN-GUILLOUZO, C. 2002. Infection of a human hepatoma cell line by hepatitis B virus. *Proc Natl Acad Sci U S A*, 99, 15655-60.
- GUILLOUZO, A., CORLU, A., ANINAT, C., GLAISE, D., MOREL, F. & GUGUEN-GUILLOUZO, C. 2007. The human hepatoma HepaRG cells: a highly differentiated model for studies of liver metabolism and toxicity of xenobiotics. *Chem Biol Interact*, 168, 66-73.
- GUO, L., DIAL, S., SHI, L., BRANHAM, W., LIU, J., FANG, J. L., GREEN, B., DENG, H., KAPUT, J. & NING, B. 2011. Similarities and differences in the expression of drug-metabolizing enzymes between human hepatic cell lines and primary human hepatocytes. *Drug Metab Dispos*, 39, 528-38.
- HANAHAN, D. & WEINBERG, R. A. 2011. Hallmarks of cancer: the next generation. *Cell*, 144, 646-74.
- HENDRIKS, J. A. A., MICLEA, R. L., SCHOTEL, R., DE BRUIJN, E., MORONI, L., KARPERIEN, M., RIESLE, J. & VAN BLITTERSWIJK, C. A. 2010. Primary chondrocytes enhance cartilage tissue formation upon co-culture with a range of cell types. *Soft Matter*, 6, 5080-5088.
- HENGSTLER, J. G., UTESCH, D., STEINBERG, P., PLATT, K. L., DIENER, B., RINGEL, M., SWALES, N., FISCHER, T., BIEFANG, K., GERL, M., BOTTGER, T. & OESCH, F. 2000. Cryopreserved primary hepatocytes as a constantly available in vitro model for the evaluation of human and animal drug metabolism and enzyme induction. *Drug Metab Rev*, 32, 81-118.
- HESCHEL, I. & RAU, G. 2002. Method for producing porous structures. Google Patents.
- HEYDARI, Z., NAJIMI, M., MIRZAEI, H., SHPICHKA, A., RUOSS, M., FARZANEH, Z., MONTAZERI, L., PIRYAEI, A., TIMASHEV, P. & GRAMIGNOLI, R. 2020. Tissue Engineering in Liver Regenerative Medicine: Insights into Novel Translational Technologies. *Cells*, 9, 304.
- HIXON, K. R., LU, T. & SELL, S. A. 2017. A comprehensive review of cryogels and their roles in tissue engineering applications. *Acta Biomater*, 62, 29-41.
- HOFFMANN, S. A., MULLER-VIEIRA, U., BIEMEL, K., KNOBELOCH, D., HEYDEL, S., LUBBERSTEDT, M., NUSSLER, A. K., ANDERSSON, T. B., GERLACH, J. C. & ZEILINGER, K. 2012. Analysis of drug metabolism activities in a miniaturized liver cell bioreactor for use in pharmacological studies. *Biotechnol Bioeng*, 109, 3172-81.
- HORVAT, T., LANDESMANN, B., LOSTIA, A., VINKEN, M., MUNN, S. & WHELAN, M. 2017. Adverse outcome pathway development from protein alkylation to liver fibrosis. *Arch Toxicol*, 91, 1523-1543.
- HU, C. & LI, L. 2015. In vitro culture of isolated primary hepatocytes and stem cell-derived hepatocyte-like cells for liver regeneration. *Protein Cell*, 6, 562-74.

- HU, H., GEHART, H., ARTEGIANI, B., C, L. O.-I., DEKKERS, F., BASAK, O., VAN ES, J., CHUVA DE SOUSA LOPES, S. M., BEGTHEL, H., KORVING, J., VAN DEN BORN, M., ZOU, C., QUIRK, C., CHIRIBOGA, L., RICE, C. M., MA, S., RIOS, A., PETERS, P. J., DE JONG, Y. P. & CLEVERS, H. 2018. Long-Term Expansion of Functional Mouse and Human Hepatocytes as 3D Organoids. *Cell*, 175, 1591-1606 e19.
- HUCH, M., DORRELL, C., BOJ, S. F., VAN ES, J. H., LI, V. S., VAN DE WETERING, M., SATO, T., HAMER, K., SASAKI, N., FINEGOLD, M. J., HAFT, A., VRIES, R. G., GROMPE, M. & CLEVERS, H. 2013. In vitro expansion of single Lgr5+ liver stem cells induced by Wnt-driven regeneration. *Nature*, 494, 247-50.
- HUCH, M., GEHART, H., VAN BOXTEL, R., HAMER, K., BLOKZIJL, F., VERSTEGEN, M. M., ELLIS, E., VAN WENUM, M., FUCHS, S. A., DE LIGT, J., VAN DE WETERING, M., SASAKI, N., BOERS, S. J., KEMPERMAN, H., DE JONGE, J., IJZERMANS, J. N., NIEUWENHUIS, E. E., HOEKSTRA, R., STROM, S., VRIES, R. R., VAN DER LAAN, L. J., CUPPEN, E. & CLEVERS, H. 2015. Long-term culture of genome-stable bipotent stem cells from adult human liver. *Cell*, 160, 299-312.
- HUETTNER, N., DARGAVILLE, T. R. & FORGET, A. 2018. Discovering Cell-Adhesion Peptides in Tissue Engineering: Beyond RGD. *Trends Biotechnol*, 36, 372-383.
- HUGHES, C. S., POSTOVIT, L. M. & LAJOIE, G. A. 2010. Matrigel: a complex protein mixture required for optimal growth of cell culture. *Proteomics*, 10, 1886-90.
- HURRELL, T., SEGERITZ, C. P., VALLIER, L., LILLEY, K. S. & CROMARTY, A. D. 2018. Proteomic Comparison of Various Hepatic Cell Cultures for Preclinical Safety Pharmacology. *Toxicol Sci*, 164, 229-239.
- HUYCK, L., AMPE, C. & VAN TROYS, M. 2012. The XTT cell proliferation assay applied to cell layers embedded in three-dimensional matrix. *Assay Drug Dev Technol*, 10, 382-92.
- INGELMAN-SUNDBERG, M., ZHONG, X. B., HANKINSON, O., BEEDANAGARI, S., YU, A. M., PENG, L. & OSAWA, Y. 2013. Potential role of epigenetic mechanisms in the regulation of drug metabolism and transport. *Drug Metab Dispos*, 41, 1725-31.
- IREDALE, J. P., THOMPSON, A. & HENDERSON, N. C. 2013. Extracellular matrix degradation in liver fibrosis: Biochemistry and regulation. *Biochim Biophys Acta*, 1832, 876-83.
- JAESCHKE, H., GORES, G. J., CEDERBAUM, A. I., HINSON, J. A., PESSAYRE, D. & LEMASTERS, J. J. 2002. Mechanisms of hepatotoxicity. *Toxicol Sci*, 65, 166-76.
- JAIN, E., DAMANIA, A. & KUMAR, A. 2014. Biomaterials for liver tissue engineering. *Hepatol Int*, 8, 185-97.
- JANCOVA, P., ANZENBACHER, P. & ANZENBACHEROVA, E. 2010. Phase II drug metabolizing enzymes. *Biomed Pap Med Fac Univ Palacky Olomouc Czech Repub*, 154, 103-16.

- JANG, M., KLEBER, A., RUCKELSHAUSEN, T., BETZHOLZ, R. & MANZ, A. 2019. Differentiation of the human liver progenitor cell line (HepaRG) on a microfluidic-based biochip. *J Tissue Eng Regen Med*, 13, 482-494.
- JOHANSSON, L., KLINTH, J., HOLMQVIST, O. & OHLSON, S. 2003. Platelet lysate: a replacement for fetal bovine serum in animal cell culture? *Cytotechnology*, 42, 67-74.
- JONES, L. J., GRAY, M., YUE, S. T., HAUGLAND, R. P. & SINGER, V. L. 2001. Sensitive determination of cell number using the CyQUANT® cell proliferation assay. *Journal of Immunological Methods*, 254, 85-98.
- JURGENS, W. J., KROEZE, R. J., BANK, R. A., RITT, M. J. & HELDER, M. N. 2011. Rapid attachment of adipose stromal cells on resorbable polymeric scaffolds facilitates the one-step surgical procedure for cartilage and bone tissue engineering purposes. *J Orthop Res*, 29, 853-60.
- KAFERT-KASTING, S., ALEXANDROVA, K., BARTHOLD, M., LAUBE, B., FRIEDRICH, G., ARSENIJEV, L. & HENGSTLER, J. G. 2006. Enzyme induction in cryopreserved human hepatocyte cultures. *Toxicology*, 220, 117-25.
- KAMIYAMA, Y., MATSUBARA, T., YOSHINARI, K., NAGATA, K., KAMIMURA, H. & YAMAZOE, Y. 2007. Role of human hepatocyte nuclear factor 4 α in the expression of drug-metabolizing enzymes and transporters in human hepatocytes assessed by use of small interfering RNA. *Drug metabolism and pharmacokinetics*, 22, 287-298.
- KAMMERER, S. & KÜPPER, J.-H. 2018. Human hepatocyte systems for in vitro toxicology analysis. *Journal of Cellular Biotechnology*, 3, 85-93.
- KANTA, J. 2016. Elastin in the Liver. *Front Physiol*, 7, 491.
- KAPLOWITZ, N. 2005. Idiosyncratic drug hepatotoxicity. *Nat Rev Drug Discov*, 4, 489-99.
- KATSURA, N., IKAI, I., MITAKA, T., SHIOTANI, T., YAMANOKUCHI, S., SUGIMOTO, S., KANAZAWA, A., TERAJIMA, H., MOCHIZUKI, Y. & YAMAOKA, Y. 2002. Long-term culture of primary human hepatocytes with preservation of proliferative capacity and differentiated functions. *J Surg Res*, 106, 115-23.
- KEGEL, V., DEHARDE, D., PFEIFFER, E., ZEILINGER, K., SEEHOFER, D. & DAMM, G. 2016. Protocol for Isolation of Primary Human Hepatocytes and Corresponding Major Populations of Non-parenchymal Liver Cells. *J Vis Exp*, e53069.
- KEPP, O., GALLUZZI, L., LIPINSKI, M., YUAN, J. & KROEMER, G. 2011. Cell death assays for drug discovery. *Nat Rev Drug Discov*, 10, 221-37.
- KHAN, R. & KHAN, M. H. 2013. Use of collagen as a biomaterial: An update. *J Indian Soc Periodontol*, 17, 539-42.
- KHETANI, S. R. & BHATIA, S. N. 2008. Microscale culture of human liver cells for drug development. *Nat Biotechnol*, 26, 120-6.
- KIM, H., JANG, M. J., KANG, M. J. & HAN, Y. M. 2011. Epigenetic signatures and temporal expression of lineage-specific genes in hESCs during differentiation to hepatocytes in vitro. *Hum Mol Genet*, 20, 401-12.

- KIM, H. J. & PARK, J. S. 2017. Usage of Human Mesenchymal Stem Cells in Cell-based Therapy: Advantages and Disadvantages. *Dev Reprod*, 21, 1-10.
- KIM, J. A., CHOI, J. H., KIM, M., RHEE, W. J., SON, B., JUNG, H. K. & PARK, T. H. 2013. High-throughput generation of spheroids using magnetic nanoparticles for three-dimensional cell culture. *Biomaterials*, 34, 8555-63.
- KIM, U. J., PARK, J., KIM, H. J., WADA, M. & KAPLAN, D. L. 2005. Three-dimensional aqueous-derived biomaterial scaffolds from silk fibroin. *Biomaterials*, 26, 2775-85.
- KIM, Y. B. & KIM, G. 2012. Rapid-prototyped collagen scaffolds reinforced with PCL/ β -TCP nanofibres to obtain high cell seeding efficiency and enhanced mechanical properties for bone tissue regeneration. *Journal of Materials Chemistry*, 22, 16880-16889.
- KIMURA, H., SAKAI, Y. & FUJII, T. 2018. Organ/body-on-a-chip based on microfluidic technology for drug discovery. *Drug Metab Pharmacokinet*, 33, 43-48.
- KINOSHITA, T. & MIYAJIMA, A. 2002. Cytokine regulation of liver development. *Biochim Biophys Acta*, 1592, 303-12.
- KLAAS, M., KANGUR, T., VIIL, J., MAEMETS-ALLAS, K., MINAJEVA, A., VADI, K., ANTISOV, M., LAPIDUS, N., JARVEKULG, M. & JAKS, V. 2016. The alterations in the extracellular matrix composition guide the repair of damaged liver tissue. *Sci Rep*, 6, 27398.
- KLEINMAN, H. K., MCGARVEY, M. L., LIOTTA, L. A., ROBEY, P. G., TRYGGVASON, K. & MARTIN, G. R. 1982. Isolation and characterization of type IV procollagen, laminin, and heparan sulfate proteoglycan from the EHS sarcoma. *Biochemistry*, 21, 6188-93.
- KMIEC, Z. 2001. Cooperation of liver cells in health and disease. *Adv Anat Embryol Cell Biol*, 161, III-XIII, 1-151.
- KNOBELOCH, D., EHNERT, S., SCHYSCHKA, L., BÜCHLER, P., SCHOENBERG, M., KLEEFF, J., THASLER, W. E., NUSSLER, N. C., GODOY, P., HENGSTLER, J. & NUSSLER, A. K. 2012. Human Hepatocytes: Isolation, Culture, and Quality Procedures. In: MITRY, R. R. & HUGHES, R. D. (eds.) *Human Cell Culture Protocols*. Totowa, NJ: Humana Press.
- KNOWLER, W. C., HAMMAN, R. F., EDELSTEIN, S. L., BARRETT-CONNOR, E., EHRMANN, D. A., WALKER, E. A., FOWLER, S. E., NATHAN, D. M., KAHN, S. E. & DIABETES PREVENTION PROGRAM RESEARCH, G. 2005. Prevention of type 2 diabetes with troglitazone in the Diabetes Prevention Program. *Diabetes*, 54, 1150-6.
- KOCHAT, V., EQUBAL, Z., BALIGAR, P., KUMAR, V., SRIVASTAVA, M. & MUKHOPADHYAY, A. 2017. JMJD3 aids in reprogramming of bone marrow progenitor cells to hepatic phenotype through epigenetic activation of hepatic transcription factors. *PLoS One*, 12, e0173977.
- KOH, B., JEON, H., KIM, D., KANG, D. & KIM, K. R. 2019. Effect of fibroblast co-culture on the proliferation, viability and drug response of colon cancer cells. *Oncol Lett*, 17, 2409-2417.
- KOLA, I. & LANDIS, J. 2004. Can the pharmaceutical industry reduce attrition rates? *Nat Rev Drug Discov*, 3, 711-5.

- KOYAMA, Y. & BRENNER, D. A. 2017. Liver inflammation and fibrosis. *J Clin Invest*, 127, 55-64.
- KRATOCHWIL, N. A., MEILLE, C., FOWLER, S., KLAMMERS, F., EKICILER, A., MOLITOR, B., SIMON, S., WALTER, I., MCGINNIS, C., WALTHER, J., LEONARD, B., TRIYATNI, M., JAVANBAKHT, H., FUNK, C., SCHULER, F., LAVE, T. & PARROTT, N. J. 2017. Metabolic Profiling of Human Long-Term Liver Models and Hepatic Clearance Predictions from In Vitro Data Using Nonlinear Mixed-Effects Modeling. *AAPS J*, 19, 534-550.
- KRTOLICA, A., ORTIZ DE SOLORZANO, C., LOCKETT, S. & CAMPISI, J. 2002. Quantification of epithelial cells in coculture with fibroblasts by fluorescence image analysis. *Cytometry*, 49, 73-82.
- KUMARI, J., KARANDE, A. A. & KUMAR, A. 2016. Combined Effect of Cryogel Matrix and Temperature-Reversible Soluble-Insoluble Polymer for the Development of in Vitro Human Liver Tissue. *ACS Appl Mater Interfaces*, 8, 264-77.
- KUMARI, J. & KUMAR, A. 2017. Development of polymer based cryogel matrix for transportation and storage of mammalian cells. *Sci Rep*, 7, 41551.
- LANCASTER, M. A. & KNOBLICH, J. A. 2014. Organogenesis in a dish: modeling development and disease using organoid technologies. *Science*, 345, 1247125.
- LAUSCHKE, V. M., VORRINK, S. U., MORO, S. M., REZAYEE, F., NORDLING, A., HENDRIKS, D. F., BELL, C. C., SISON-YOUNG, R., PARK, B. K., GOLDRING, C. E., ELLIS, E., JOHANSSON, I., MKRTCHIAN, S., ANDERSSON, T. B. & INGELMAN-SUNDBERG, M. 2016. Massive rearrangements of cellular MicroRNA signatures are key drivers of hepatocyte dedifferentiation. *Hepatology*, 64, 1743-1756.
- LEE, C. H., SINGLA, A. & LEE, Y. 2001. Biomedical applications of collagen. *Int J Pharm*, 221, 1-22.
- LEE, D.-H. & LEE, K.-W. 2014. Hepatocyte Isolation, culture, and its clinical applications. *Hanyang Medical Reviews*, 34, 165-172.
- LEE, J. S., SHIN, J., PARK, H. M., KIM, Y. G., KIM, B. G., OH, J. W. & CHO, S. W. 2014a. Liver extracellular matrix providing dual functions of two-dimensional substrate coating and three-dimensional injectable hydrogel platform for liver tissue engineering. *Biomacromolecules*, 15, 206-18.
- LEE, S. M., SCHELCHER, C., DEMMEL, M., HAUNER, M. & THASLER, W. E. 2013. Isolation of human hepatocytes by a two-step collagenase perfusion procedure. *J Vis Exp*, 50615.
- LEE, S. M., SCHELCHER, C., LAUBENDER, R. P., FROSE, N., THASLER, R. M., SCHIERGENS, T. S., MANSMANN, U. & THASLER, W. E. 2014b. An algorithm that predicts the viability and the yield of human hepatocytes isolated from remnant liver pieces obtained from liver resections. *PLoS One*, 9, e107567.
- LEE, W. M. 2003. Drug-induced hepatotoxicity. *N Engl J Med*, 349, 474-85.
- LEVY, G., BOMZE, D., HEINZ, S., RAMACHANDRAN, S. D., NOERENBERG, A., COHEN, M., SHIBOLET, O., SKLAN, E., BRASPENNING, J. & NAHMIAS, Y.

2015. Long-term culture and expansion of primary human hepatocytes. *Nat Biotechnol*, 33, 1264-1271.
- LEWIS, D. F., IOANNIDES, C. & PARKE, D. V. 1998. Cytochromes P450 and species differences in xenobiotic metabolism and activation of carcinogen. *Environ Health Perspect*, 106, 633-41.
- LEWIS, P. L., GREEN, R. M. & SHAH, R. N. 2018. 3D-printed gelatin scaffolds of differing pore geometry modulate hepatocyte function and gene expression. *Acta Biomater*, 69, 63-70.
- LIANG, G. & ZHANG, Y. 2013. Genetic and epigenetic variations in iPSCs: potential causes and implications for application. *Cell Stem Cell*, 13, 149-59.
- LIN, J., SCHYSCHKA, L., MUHL-BENNINGHAUS, R., NEUMANN, J., HAO, L., NUSSLER, N., DOOLEY, S., LIU, L., STOCKLE, U., NUSSLER, A. K. & EHNERT, S. 2012. Comparative analysis of phase I and II enzyme activities in 5 hepatic cell lines identifies Huh-7 and HCC-T cells with the highest potential to study drug metabolism. *Arch Toxicol*, 86, 87-95.
- LIU, H., YU, Y., GLORIOSO, J., MAO, S., RODYSIL, B., AMIOT, B. P., RINALDO, P. & NYBERG, S. L. 2014. Cold storage of rat hepatocyte spheroids. *Cell Transplant*, 23, 819-30.
- LIU, Y., MEYER, C., XU, C., WENG, H., HELLERBRAND, C., TEN DIJKE, P. & DOOLEY, S. 2013. Animal models of chronic liver diseases. *Am J Physiol Gastrointest Liver Physiol*, 304, G449-68.
- LO, B. & PARHAM, L. 2009. Ethical issues in stem cell research. *Endocr Rev*, 30, 204-13.
- LOGAN, D. J., SHAN, J., BHATIA, S. N. & CARPENTER, A. E. 2016. Quantifying co-cultured cell phenotypes in high-throughput using pixel-based classification. *Methods*, 96, 6-11.
- LOH, Q. L. & CHOONG, C. 2013. Three-dimensional scaffolds for tissue engineering applications: role of porosity and pore size. *Tissue Eng Part B Rev*, 19, 485-502.
- LOPEZ-TERRADA, D., CHEUNG, S. W., FINEGOLD, M. J. & KNOWLES, B. B. 2009. Hep G2 is a hepatoblastoma-derived cell line. *Hum Pathol*, 40, 1512-5.
- LOWRY, O. H., ROSEBROUGH, N. J., FARR, A. L. & RANDALL, R. J. 1951. Protein measurement with the Folin phenol reagent. *J Biol Chem*, 193, 265-75.
- LU, H. F., CHUA, K. N., ZHANG, P. C., LIM, W. S., RAMAKRISHNA, S., LEONG, K. W. & MAO, H. Q. 2005. Three-dimensional co-culture of rat hepatocyte spheroids and NIH/3T3 fibroblasts enhances hepatocyte functional maintenance. *Acta Biomater*, 1, 399-410.
- LUCKERT, C., SCHULZ, C., LEHMANN, N., THOMAS, M., HOFMANN, U., HAMMAD, S., HENGSTLER, J. G., BRAEUNING, A., LAMPEN, A. & HESSEL, S. 2017. Comparative analysis of 3D culture methods on human HepG2 cells. *Arch Toxicol*, 91, 393-406.
- LV, D., YU, S. C., PING, Y. F., WU, H., ZHAO, X., ZHANG, H., CUI, Y., CHEN, B., ZHANG, X., DAI, J., BIAN, X. W. & YAO, X. H. 2016. A three-dimensional collagen scaffold cell culture system for screening anti-glioma therapeutics. *Oncotarget*, 7, 56904-56914.

- MACDONALD, N., MENACHERY, A., REBOUD, J. & COOPER, J. 2018. Creating tissue on chip constructs in microtitre plates for drug discovery. *RSC advances*, 8, 9603-9610.
- MANGONI, A. A. & JACKSON, S. H. 2004. Age-related changes in pharmacokinetics and pharmacodynamics: basic principles and practical applications. *Br J Clin Pharmacol*, 57, 6-14.
- MARTIGNONI, M., GROOTHUIS, G. M. & DE KANTER, R. 2006. Species differences between mouse, rat, dog, monkey and human CYP-mediated drug metabolism, inhibition and induction. *Expert Opin Drug Metab Toxicol*, 2, 875-94.
- MARTINEZ-HERNANDEZ, A. & AMENTA, P. S. 1993. The hepatic extracellular matrix. II. Ontogenesis, regeneration and cirrhosis. *Virchows Arch A Pathol Anat Histopathol*, 423, 77-84.
- MARTINEZ-JIMENEZ, C. P., JOVER, R., DONATO, M. T., CASTELL, J. V. & GOMEZ-LECHON, M. J. 2007. Transcriptional regulation and expression of CYP3A4 in hepatocytes. *Curr Drug Metab*, 8, 185-94.
- MASUGI, Y., ABE, T., TSUJIKAWA, H., EFFENDI, K., HASHIGUCHI, A., ABE, M., IMAI, Y., HINO, K., HIGE, S., KAWANAKA, M., YAMADA, G., KAGE, M., KORENAGA, M., HIASA, Y., MIZOKAMI, M. & SAKAMOTO, M. 2018. Quantitative assessment of liver fibrosis reveals a nonlinear association with fibrosis stage in nonalcoholic fatty liver disease. *Hepatol Commun*, 2, 58-68.
- MAZZA, G., AL-AKKAD, W., TELESE, A., LONGATO, L., URBANI, L., ROBINSON, B., HALL, A., KONG, K., FRENGUELLI, L., MARRONE, G., WILLACY, O., SHAERI, M., BURNS, A., MALAGO, M., GILBERTSON, J., RENDELL, N., MOORE, K., HUGHES, D., NOTINGHER, I., JELL, G., DEL RIO HERNANDEZ, A., DE COPPI, P., ROMBOUITS, K. & PINZANI, M. 2017. Rapid production of human liver scaffolds for functional tissue engineering by high shear stress oscillation-decellularization. *Sci Rep*, 7, 5534.
- MEEKER, N. D., HUTCHINSON, S. A., HO, L. & TREDE, N. S. 2007. Method for isolation of PCR-ready genomic DNA from zebrafish tissues. *Biotechniques*, 43, 610, 612, 614.
- MERRELL, M. D. & CHERRINGTON, N. J. 2011. Drug metabolism alterations in nonalcoholic fatty liver disease. *Drug Metab Rev*, 43, 317-34.
- MICHALOPOULOS, G. & PITOT, H. C. 1975. Primary culture of parenchymal liver cells on collagen membranes. Morphological and biochemical observations. *Exp Cell Res*, 94, 70-8.
- MOGHE, P. V., COGER, R. N., TONER, M. & YARMUSH, M. L. 1997. Cell-cell interactions are essential for maintenance of hepatocyte function in collagen gel but not on matrigel. *Biotechnology and Bioengineering*, 56, 706-711.
- MORGAN, E. T. 2009. Impact of infectious and inflammatory disease on cytochrome P450-mediated drug metabolism and pharmacokinetics. *Clin Pharmacol Ther*, 85, 434-8.
- MUELLER, S. & SANDRIN, L. 2010. Liver stiffness: a novel parameter for the diagnosis of liver disease. *Hepat Med*, 2, 49-67.
- MUELLER, S., SEITZ, H. K. & RAUSCH, V. 2014. Non-invasive diagnosis of alcoholic liver disease. *World J Gastroenterol*, 20, 14626-41.

- NAGASE, K., YAMATO, M., KANAZAWA, H. & OKANO, T. 2018. Poly(N-isopropylacrylamide)-based thermoresponsive surfaces provide new types of biomedical applications. *Biomaterials*, 153, 27-48.
- NAKABAYASHI, H., TAKETA, K., MIYANO, K., YAMANE, T. & SATO, J. 1982. Growth of human hepatoma cells lines with differentiated functions in chemically defined medium. *Cancer Res*, 42, 3858-63.
- NAKAMURA, S. & IJIMA, H. 2013. Solubilized matrix derived from decellularized liver as a growth factor-immobilizable scaffold for hepatocyte culture. *J Biosci Bioeng*, 116, 746-53.
- NAKAYAMA, G. R. 1998. Microplate assays for high-throughput screening. *Curr Opin Drug Discov Devel*, 1, 85-91.
- NATARAJAN, V., BERGLUND, E. J., CHEN, D. X. & KIDAMBI, S. 2015. Substrate stiffness regulates primary hepatocyte functions. *RSC Advances*, 5, 80956-80966.
- NATH, S. & DEVI, G. R. 2016. Three-dimensional culture systems in cancer research: Focus on tumor spheroid model. *Pharmacol Ther*, 163, 94-108.
- NGUYEN, L. V., COX, C. L., EIREW, P., KNAPP, D. J., PELLACANI, D., KANNAN, N., CARLES, A., MOKSA, M., BALANI, S., SHAH, S., HIRST, M., APARICIO, S. & EAVES, C. J. 2014a. DNA barcoding reveals diverse growth kinetics of human breast tumour subclones in serially passaged xenografts. *Nat Commun*, 5, 5871.
- NGUYEN, L. V., MAKAREM, M., CARLES, A., MOKSA, M., KANNAN, N., PANDOH, P., EIREW, P., OSAKO, T., KARDEL, M., CHEUNG, A. M., KENNEDY, W., TSE, K., ZENG, T., ZHAO, Y., HUMPHRIES, R. K., APARICIO, S., EAVES, C. J. & HIRST, M. 2014b. Clonal analysis via barcoding reveals diverse growth and differentiation of transplanted mouse and human mammary stem cells. *Cell Stem Cell*, 14, 253-63.
- NISHIKAWA, T., TANAKA, Y., NISHIKAWA, M., OGINO, Y., KUSAMORI, K., MIZUNO, N., MIZUKAMI, Y., SHIMIZU, K., KONISHI, S., TAKAHASHI, Y. & TAKAKURA, Y. 2017. Optimization of Albumin Secretion and Metabolic Activity of Cytochrome P450 1A1 of Human Hepatoblastoma HepG2 Cells in Multicellular Spheroids by Controlling Spheroid Size. *Biol Pharm Bull*, 40, 334-338.
- NISHINAKAMURA, R. 2019. Human kidney organoids: progress and remaining challenges. *Nat Rev Nephrol*, 15, 613-624.
- NOLAN-STEVAUX, O., TEDESCO, D., RAGAN, S., MAKHANOV, M., CHENCHIK, A., RUEFLI-BRASSE, A., QUON, K. & KASSNER, P. D. 2013. Measurement of Cancer Cell Growth Heterogeneity through Lentiviral Barcoding Identifies Clonal Dominance as a Characteristic of In Vivo Tumor Engraftment. *PLoS One*, 8, e67316.
- NUSSLER, A. K., VERGANI, G., GOLLIN, S. M., DORKO, K., MORRIS, S. M., JR., DEMETRIS, A. J., NOMOTO, M., BEGER, H. G. & STROM, S. C. 1999. Isolation and characterization of a human hepatic epithelial-like cell line (AKN-1) from a normal liver. *In Vitro Cell Dev Biol Anim*, 35, 190-7.
- O'BRIEN, F. J. 2011. Biomaterials & scaffolds for tissue engineering. *Materials Today*, 14, 88-95.

- O'BRIEN, P. J., IRWIN, W., DIAZ, D., HOWARD-COFIELD, E., KREJSA, C. M., SLAUGHTER, M. R., GAO, B., KALUDERCIC, N., ANGELINE, A., BERNARDI, P., BRAIN, P. & HOUGHAM, C. 2006. High concordance of drug-induced human hepatotoxicity with in vitro cytotoxicity measured in a novel cell-based model using high content screening. *Arch Toxicol*, 80, 580-604.
- O'CALLAGHAN, N. J. & FENECH, M. 2011. A quantitative PCR method for measuring absolute telomere length. *Biol Proced Online*, 13, 3.
- OHNO, M., MOTOJIMA, K., OKANO, T. & TANIGUCHI, A. 2008. Up-regulation of drug-metabolizing enzyme genes in layered co-culture of a human liver cell line and endothelial cells. *Tissue Eng Part A*, 14, 1861-9.
- OKA, M., MEACHAM, A. M., HAMAZAKI, T., RODIC, N., CHANG, L. J. & TERADA, N. 2005. De novo DNA methyltransferases Dnmt3a and Dnmt3b primarily mediate the cytotoxic effect of 5-aza-2'-deoxycytidine. *Oncogene*, 24, 3091-9.
- OLEAGA, C., RIU, A., ROTHEMUND, S., LAVADO, A., MCALEER, C. W., LONG, C. J., PERSAUD, K., NARASIMHAN, N. S., TRAN, M., ROLES, J., CARMONA-MORAN, C. A., SASSERATH, T., ELBRECHT, D. H., KUMANCHIK, L., BRIDGES, L. R., MARTIN, C., SCHNEPPER, M. T., EKMAN, G., JACKSON, M., WANG, Y. I., NOTE, R., LANGER, J., TEISSIER, S. & HICKMAN, J. J. 2018. Investigation of the effect of hepatic metabolism on off-target cardiotoxicity in a multi-organ human-on-a-chip system. *Biomaterials*, 182, 176-190.
- OLSON, H., BETTON, G., ROBINSON, D., THOMAS, K., MONRO, A., KOLAJA, G., LILLY, P., SANDERS, J., SIPES, G., BRACKEN, W., DORATO, M., VAN DEUN, K., SMITH, P., BERGER, B. & HELLER, A. 2000. Concordance of the toxicity of pharmaceuticals in humans and in animals. *Regul Toxicol Pharmacol*, 32, 56-67.
- OSTROWSKA, A., GU, K., BODE, D. C. & VAN BUSKIRK, R. G. 2009. Hypothermic storage of isolated human hepatocytes: a comparison between University of Wisconsin solution and a hypothermosol platform. *Arch Toxicol*, 83, 493-502.
- PALAKKAN, A. A., NANDA, J. & ROSS, J. A. 2017. Pluripotent stem cells to hepatocytes, the journey so far. *Biomed Rep*, 6, 367-373.
- PAMPALONI, F., REYNAUD, E. G. & STELZER, E. H. 2007. The third dimension bridges the gap between cell culture and live tissue. *Nat Rev Mol Cell Biol*, 8, 839-45.
- PARASURAMAN, S. 2011. Toxicological screening. *J Pharmacol Pharmacother*, 2, 74-9.
- PARK, H. J., CHOI, Y. J., KIM, J. W., CHUN, H. S., IM, I., YOON, S., HAN, Y. M., SONG, C. W. & KIM, H. 2015. Differences in the Epigenetic Regulation of Cytochrome P450 Genes between Human Embryonic Stem Cell-Derived Hepatocytes and Primary Hepatocytes. *PLoS One*, 10, e0132992.
- PAUL, S. M., MYTELKA, D. S., DUNWIDDIE, C. T., PERSINGER, C. C., MUNOS, B. H., LINDBORG, S. R. & SCHACHT, A. L. 2010. How to improve R&D productivity: the pharmaceutical industry's grand challenge. *Nat Rev Drug Discov*. England.

- PENG, L. & ZHONG, X. 2015. Epigenetic regulation of drug metabolism and transport. *Acta Pharm Sin B*, 5, 106-12.
- PEREZ GONZALEZ, N., TAO, J., ROCHMAN, N. D., VIG, D., CHIU, E., WIRTZ, D. & SUN, S. X. 2018. Cell tension and mechanical regulation of cell volume. *Mol Biol Cell*, 29, 0.
- PFEIFFER, E., KEGEL, V., ZEILINGER, K., HENGSTLER, J. G., NUSSLER, A. K., SEEHOFER, D. & DAMM, G. 2015. Featured Article: Isolation, characterization, and cultivation of human hepatocytes and non-parenchymal liver cells. *Exp Biol Med (Maywood)*, 240, 645-56.
- PLESS-PETIG, G., SINGER, B. B. & RAUEN, U. 2012. Cold storage of rat hepatocyte suspensions for one week in a customized cold storage solution-preservation of cell attachment and metabolism. *PLoS One*, 7, e40444.
- POLOZNIKOV, A., GAZARYAN, I., SHKURNIKOV, M., NIKULIN, S., DRAPKINA, O., BARANOVA, A. & TONEVITSKY, A. 2018. In vitro and in silico liver models: Current trends, challenges and opportunities. *ALTEX*, 35, 397-412.
- PRAMFALK, C., LARSSON, L., HARDFELDT, J., ERIKSSON, M. & PARINI, P. 2016. Culturing of HepG2 cells with human serum improve their functionality and suitability in studies of lipid metabolism. *Biochim Biophys Acta*, 1861, 51-59.
- PRIOR, N., INACIO, P. & HUCH, M. 2019. Liver organoids: from basic research to therapeutic applications. *Gut*, 68, 2228-2237.
- PROBST, I., SCHWARTZ, P. & JUNGGERMANN, K. 1982. Induction in primary culture of 'gluconeogenic' and 'glycolytic' hepatocytes resembling periportal and perivenous cells. *Eur J Biochem*, 126, 271-8.
- PROT, J. M., BRIFFAUT, A. S., LETOURNEUR, F., CHAFEY, P., MERLIER, F., GRANDVALET, Y., LEGALLAIS, C. & LECLERC, E. 2011. Integrated proteomic and transcriptomic investigation of the acetaminophen toxicity in liver microfluidic biochip. *PLoS One*, 6, e21268.
- PUGLISI, M. A., TESORI, V., LATTANZI, W., PISCAGLIA, A. C., GASBARRINI, G. B., D'UGO, D. M. & GASBARRINI, A. 2011. Therapeutic implications of mesenchymal stem cells in liver injury. *J Biomed Biotechnol*, 2011, 860578.
- QUINT, K., AGAIMY, A., DI FAZIO, P., MONTALBANO, R., STEINDORF, C., JUNG, R., HELLERBRAND, C., HARTMANN, A., SITTER, H., NEUREITER, D. & OCKER, M. 2011. Clinical significance of histone deacetylases 1, 2, 3, and 7: HDAC2 is an independent predictor of survival in HCC. *Virchows Arch*, 459, 129-39.
- RAI, Y., PATHAK, R., KUMARI, N., SAH, D. K., PANDEY, S., KALRA, N., SONI, R., DWARAKANATH, B. S. & BHATT, A. N. 2018. Mitochondrial biogenesis and metabolic hyperactivation limits the application of MTT assay in the estimation of radiation induced growth inhibition. *Sci Rep*, 8, 1531.
- RAJENDRAN, D., HUSSAIN, A., YIP, D., PAREKH, A., SHRIRAO, A. & CHO, C. H. 2017. Long-term liver-specific functions of hepatocytes in electrospun chitosan nanofiber scaffolds coated with fibronectin. *J Biomed Mater Res A*, 105, 2119-2128.
- RAMACHANDRAN, S. D., VIVARES, A., KLIEBER, S., HEWITT, N. J., MUENST, B., HEINZ, S., WALLE, H. & BRASPENNING, J. 2015. Applicability of

- second-generation upcyte(R) human hepatocytes for use in CYP inhibition and induction studies. *Pharmacol Res Perspect*, 3, e00161.
- RAMAIAHGARI, S. C., DEN BRAVER, M. W., HERPERS, B., TERPSTRA, V., COMMANDEUR, J. N., VAN DE WATER, B. & PRICE, L. S. 2014. A 3D in vitro model of differentiated HepG2 cell spheroids with improved liver-like properties for repeated dose high-throughput toxicity studies. *Arch Toxicol*, 88, 1083-95.
- RAMPERSAD, S. N. 2012. Multiple applications of Alamar Blue as an indicator of metabolic function and cellular health in cell viability bioassays. *Sensors (Basel)*, 12, 12347-60.
- RANUCCI, C. S., KUMAR, A., BATRA, S. P. & MOGHE, P. V. 2000. Control of hepatocyte function on collagen foams: sizing matrix pores toward selective induction of 2-D and 3-D cellular morphogenesis. *Biomaterials*, 21, 783-93.
- RASCHI, E. & DE PONTI, F. 2019. Strategies for Early Prediction and Timely Recognition of Drug-Induced Liver Injury: The Case of Cyclin-Dependent Kinase 4/6 Inhibitors. *Front Pharmacol*, 10, 1235.
- RAUEN, U., POLZAR, B., STEPHAN, H., MANNHERZ, H. G. & DE GROOT, H. 1999. Cold-induced apoptosis in cultured hepatocytes and liver endothelial cells: mediation by reactive oxygen species. *FASEB J*, 13, 155-68.
- REIF, R. 2014. The body-on-a-chip concept: possibilities and limitations. *EXCLI J*, 13, 1283-5.
- REN, D., MADSEN, J. S., DE LA CRUZ-PERERA, C. I., BERGMARK, L., SORENSEN, S. J. & BURMOLLE, M. 2014. High-throughput screening of multispecies biofilm formation and quantitative PCR-based assessment of individual species proportions, useful for exploring interspecific bacterial interactions. *Microb Ecol*, 68, 146-54.
- RICHARDS, W. L., SONG, M. K., KRUTZSCH, H., EVARTS, R. P., MARSDEN, E. & THORGEIRSSON, S. S. 1985. Measurement of cell proliferation in microculture using hoechst 33342 for the rapid semiautomated microfluorimetric determination of chromatin DNA. *Experimental Cell Research*, 159, 235-246.
- RICHERT, L., LIGUORI, M. J., ABADIE, C., HEYD, B., MANTION, G., HALKIC, N. & WARING, J. F. 2006. Gene expression in human hepatocytes in suspension after isolation is similar to the liver of origin, is not affected by hepatocyte cold storage and cryopreservation, but is strongly changed after hepatocyte plating. *Drug Metab Dispos*, 34, 870-9.
- ROCHE, J. 2018. The Epithelial-to-Mesenchymal Transition in Cancer. *Cancers (Basel)*, 10, 52.
- RODIGHIRO, V. 1999. Effects of liver disease on pharmacokinetics. An update. *Clin Pharmacokinet*, 37, 399-431.
- RODRIGUEZ-ANTONA, C., DONATO, M. T., BOOBIS, A., EDWARDS, R. J., WATTS, P. S., CASTELL, J. V. & GOMEZ-LECHON, M. J. 2002. Cytochrome P450 expression in human hepatocytes and hepatoma cell lines: molecular mechanisms that determine lower expression in cultured cells. *Xenobiotica*, 32, 505-20.

- ROSE, K. A., HOLMAN, N. S., GREEN, A. M., ANDERSEN, M. E. & LECLUYSE, E. L. 2016. Co-culture of Hepatocytes and Kupffer Cells as an In Vitro Model of Inflammation and Drug-Induced Hepatotoxicity. *J Pharm Sci*, 105, 950-964.
- ROTHSCHILD, D. E., SRINIVASAN, T., APONTE-SANTIAGO, L. A., SHEN, X. & ALLEN, I. C. 2016. The Ex Vivo Culture and Pattern Recognition Receptor Stimulation of Mouse Intestinal Organoids. *J Vis Exp*, 10.3791/54033.
- RUOß, M., DAMM, G., VOSOUGH, M., EHRET, L., GROM-BAUMGARTEN, C., PETKOV, M., NADDALIN, S., LADURNER, R., SEEHOFER, D., NUSSLER, A. & SAJADIAN, S. 2019. Epigenetic Modifications of the Liver Tumor Cell Line HepG2 Increase Their Drug Metabolic Capacity. *International Journal of Molecular Sciences*, 20, 347.
- RUOSS, M., HAUSSLING, V., SCHUGNER, F., OLDE DAMINK, L. H. H., LEE, S. M. L., GE, L., EHNERT, S. & NUSSLER, A. K. 2018. A Standardized Collagen-Based Scaffold Improves Human Hepatocyte Shipment and Allows Metabolic Studies over 10 Days. *Bioengineering (Basel)*, 5, 86.
- RUOß, M., KIEBER, V., REBHOLZ, S., LINNEMANN, C., RINDERKNECHT, H., HÄUSSLING, V., HÄCKER, M., OLDE DAMINK, L. H., EHNERT, S. & NUSSLER, A. K. 2020. Cell-Type-Specific Quantification of a Scaffold-Based 3D Liver Co-Culture. *Methods and Protocols*, 3, 1.
- RUOSS, M., REBHOLZ, S., WEIMER, M., GROM-BAUMGARTEN, C., ATHANASOPOULU, K., KEMKEMER, R., KASS, H., EHNERT, S. & NUSSLER, A. K. 2020a. Development of Scaffolds with Adjusted Stiffness for Mimicking Disease-Related Alterations of Liver Rigidity. *J Funct Biomater*, 11, 17.
- RUOSS, M., VOSOUGH, M., KONIGSRAINER, A., NADALIN, S., WAGNER, S., SAJADIAN, S., HUBER, D., HEYDARI, Z., EHNERT, S., HENGSTLER, J. G. & NUSSLER, A. K. 2020b. Towards improved hepatocyte cultures: Progress and limitations. *Food Chem Toxicol*, 138, 111188.
- SACCHI, M., BANSAL, R. & ROUWKEMA, J. 2020. Bioengineered 3D Models to Recapitulate Tissue Fibrosis. *Trends Biotechnol*, 38, 623-636.
- SADRI, A. R. & AMINI-NIK, S. 2017. De-liver CLiPs and revitalize hepatocytes. *Stem Cell Investig*, 4, 30.
- SAHA, S., BARDELLI, A., BUCKHAULTS, P., VELCULESCU, V. E., RAGO, C., ST CROIX, B., ROMANS, K. E., CHOTI, M. A., LENGAUER, C., KINZLER, K. W. & VOGELSTEIN, B. 2001. A phosphatase associated with metastasis of colorectal cancer. *Science*, 294, 1343-6.
- SAJADIAN, S. & NUSSLER, A. 2015. DNA Methylation: A Possible Target for Current and Future Studies on Cancer? *Epigenetic Diagnosis & Therapy*, 1, 5-13.
- SAJADIAN, S. O., EHNERT, S., VAKILIAN, H., KOUTSOURAKI, E., DAMM, G., SEEHOFER, D., THASLER, W., DOOLEY, S., BAHARVAND, H., SIPOS, B. & NUSSLER, A. K. 2015. Induction of active demethylation and 5hmC formation by 5-azacytidine is TET2 dependent and suggests new treatment strategies against hepatocellular carcinoma. *Clin Epigenetics*, 7, 98.
- SAJADIAN, S. O., TRIPURA, C., SAMANI, F. S., RUOSS, M., DOOLEY, S., BAHARVAND, H. & NUSSLER, A. K. 2016. Vitamin C enhances epigenetic

- modifications induced by 5-azacytidine and cell cycle arrest in the hepatocellular carcinoma cell lines HLE and Huh7. *Clin Epigenetics*, 8, 46.
- SCHLEICHER, J., TOKARSKI, C., MARBACH, E., MATZ-SOJA, M., ZELLMER, S., GEBHARDT, R. & SCHUSTER, S. 2015. Zonation of hepatic fatty acid metabolism - The diversity of its regulation and the benefit of modeling. *Biochim Biophys Acta*, 1851, 641-56.
- SCHOOF, H., APEL, J., HESCHEL, I. & RAU, G. 2001. Control of pore structure and size in freeze-dried collagen sponges. *J Biomed Mater Res*, 58, 352-7.
- SCHRODER, H. C., WANG, X. H., WIENS, M., DIEHL-SEIFERT, B., KROPF, K., SCHLOSSMACHER, U. & MULLER, W. E. 2012. Silicate modulates the cross-talk between osteoblasts (SaOS-2) and osteoclasts (RAW 264.7 cells): inhibition of osteoclast growth and differentiation. *J Cell Biochem*, 113, 3197-206.
- SCHYSCHKA, L., SANCHEZ, J. J., WANG, Z., BURKHARDT, B., MULLER-VIEIRA, U., ZEILINGER, K., BACHMANN, A., NADALIN, S., DAMM, G. & NUSSLER, A. K. 2013. Hepatic 3D cultures but not 2D cultures preserve specific transporter activity for acetaminophen-induced hepatotoxicity. *Arch Toxicol*, 87, 1581-93.
- SCIACOVELLI, M. & FREZZA, C. 2017. Metabolic reprogramming and epithelial-to-mesenchymal transition in cancer. *FEBS J*, 284, 3132-3144.
- SEELIGER, C., CULMES, M., SCHYSCHKA, L., YAN, X., DAMM, G., WANG, Z., KLEEFF, J., THASLER, W. E., HENGSTLER, J., STOCKLE, U., EHNERT, S. & NUSSLER, A. K. 2013. Decrease of global methylation improves significantly hepatic differentiation of Ad-MSCs: possible future application for urea detoxification. *Cell Transplant*, 22, 119-31.
- SELLARO, T. L., RANADE, A., FAULK, D. M., MCCABE, G. P., DORKO, K., BADYLAK, S. F. & STROM, S. C. 2010. Maintenance of human hepatocyte function in vitro by liver-derived extracellular matrix gels. *Tissue Eng Part A*, 16, 1075-82.
- SERRANO-GOMEZ, S. J., MAZIVEYI, M. & ALAHARI, S. K. 2016. Regulation of epithelial-mesenchymal transition through epigenetic and post-translational modifications. *Mol Cancer*, 15, 18.
- SHAO, C., LIU, Y., CHI, J., WANG, J., ZHAO, Z. & ZHAO, Y. 2019. Responsive Inverse Opal Scaffolds with Biomimetic Enrichment Capability for Cell Culture. *Research (Wash D C)*, 2019, 9783793.
- SHARMA, N. S., NAGRATH, D. & YARMUSH, M. L. 2010. Adipocyte-derived basement membrane extract with biological activity: applications in hepatocyte functional augmentation in vitro. *FASEB J*, 24, 2364-74.
- SHIMIZU, K., ITO, A. & HONDA, H. 2006. Enhanced cell-seeding into 3D porous scaffolds by use of magnetite nanoparticles. *J Biomed Mater Res B Appl Biomater*, 77, 265-72.
- SILTANEN, C., DIAKATOU, M., LOWEN, J., HAQUE, A., RAHIMIAN, A., STYBAYEVA, G. & REVZIN, A. 2017. One step fabrication of hydrogel microcapsules with hollow core for assembly and cultivation of hepatocyte spheroids. *Acta Biomater*, 50, 428-436.

- SIMMONS, J. G., PUCILOWSKA, J. B. & LUND, P. K. 1999. Autocrine and paracrine actions of intestinal fibroblast-derived insulin-like growth factors. *Am J Physiol*, 276, G817-27.
- SISON-YOUNG, R. L., LAUSCHKE, V. M., JOHANN, E., ALEXANDRE, E., ANThERIEU, S., AERTS, H., GERETS, H. H. J., LABBE, G., HOET, D., DORAU, M., SCHOFIELD, C. A., LOVATT, C. A., HOLDER, J. C., STAHL, S. H., RICHERT, L., KITTINGHAM, N. R., JONES, R. P., ELMASRY, M., WEAVER, R. J., HEWITT, P. G., INGELMAN-SUNDBERG, M., GOLDRING, C. E. & PARK, B. K. 2017. A multicenter assessment of single-cell models aligned to standard measures of cell health for prediction of acute hepatotoxicity. *Arch Toxicol*, 91, 1385-1400.
- SISON-YOUNG, R. L., MITSU, D., JENKINS, R. E., MOTTRAM, D., ALEXANDRE, E., RICHERT, L., AERTS, H., WEAVER, R. J., JONES, R. P., JOHANN, E., HEWITT, P. G., INGELMAN-SUNDBERG, M., GOLDRING, C. E., KITTINGHAM, N. R. & PARK, B. K. 2015. Comparative Proteomic Characterization of 4 Human Liver-Derived Single Cell Culture Models Reveals Significant Variation in the Capacity for Drug Disposition, Bioactivation, and Detoxication. *Toxicol Sci*, 147, 412-24.
- SKARDAL, A., MACK, D., ATALA, A. & SOKER, S. 2013. Substrate elasticity controls cell proliferation, surface marker expression and motile phenotype in amniotic fluid-derived stem cells. *J Mech Behav Biomed Mater*, 17, 307-16.
- SKEHAN, P., STORENG, R., SCUDIERO, D., MONKS, A., MCMAHON, J., VISTICA, D., WARREN, J. T., BOKESCH, H., KENNEY, S. & BOYD, M. R. 1990. New colorimetric cytotoxicity assay for anticancer-drug screening. *J Natl Cancer Inst*, 82, 1107-12.
- SNYKERS, S., HENKENS, T., DE ROP, E., VINKEN, M., FRACZEK, J., DE KOCK, J., DE PRINS, E., GEERTS, A., ROGIERS, V. & VANHAECKE, T. 2009. Role of epigenetics in liver-specific gene transcription, hepatocyte differentiation and stem cell reprogramming. *J Hepatol*, 51, 187-211.
- SOLDATOW, V. Y., LECLUYSE, E. L., GRIFFITH, L. G. & RUSYN, I. 2013. In vitro models for liver toxicity testing. *Toxicol Res (Camb)*, 2, 23-39.
- SOLDIN, O. P. & MATTISON, D. R. 2009. Sex differences in pharmacokinetics and pharmacodynamics. *Clin Pharmacokinet*, 48, 143-57.
- SREEKUMAR, V., ASPERA-WERZ, R., EHNERT, S., STROBEL, J., TENDULKAR, G., HEID, D., SCHREINER, A., ARNSCHIEDT, C. & NUSSLER, A. K. 2018. Resveratrol protects primary cilia integrity of human mesenchymal stem cells from cigarette smoke to improve osteogenic differentiation in vitro. *Arch Toxicol*, 92, 1525-1538.
- STADLER, S. C. & ALLIS, C. D. 2012. Linking epithelial-to-mesenchymal-transition and epigenetic modifications. *Semin Cancer Biol*, 22, 404-10.
- STECKLUM, M., WULF-GOLDENBERG, A., PURFURST, B., SIEGERT, A., KEIL, M., ECKERT, K. & FICHTNER, I. 2015. Cell differentiation mediated by co-culture of human umbilical cord blood stem cells with murine hepatic cells. *In Vitro Cell Dev Biol Anim*, 51, 183-91.
- STEENBERGEN, R., OTI, M., TER HORST, R., TAT, W., NEUFELDT, C., BELOVODSKIY, A., CHUA, T. T., CHO, W. J., JOYCE, M., DUTILH, B. E. &

- TYRRELL, D. L. 2018. Establishing normal metabolism and differentiation in hepatocellular carcinoma cells by culturing in adult human serum. *Sci Rep*, 8, 11685.
- STEENBERGEN, R. H., JOYCE, M. A., THOMAS, B. S., JONES, D., LAW, J., RUSSELL, R., HOUGHTON, M. & TYRRELL, D. L. 2013. Human serum leads to differentiation of human hepatoma cells, restoration of very-low-density lipoprotein secretion, and a 1000-fold increase in HCV Japanese fulminant hepatitis type 1 titers. *Hepatology*, 58, 1907-17.
- STEPHENNE, X., NAJIMI, M. & SOKAL, E. M. 2010. Hepatocyte cryopreservation: is it time to change the strategy? *World J Gastroenterol*, 16, 1-14.
- SUDHAKARAN, P. R. 1999. Hepatocyte-matrix interaction. *Proceedings of the Indian Academy of Sciences-Chemical Sciences*, 111, 331-342.
- SUGIMACHI, K., TANAKA, S., KAMEYAMA, T., TAGUCHI, K., AISHIMA, S., SHIMADA, M., SUGIMACHI, K. & TSUNEYOSHI, M. 2003. Transcriptional repressor snail and progression of human hepatocellular carcinoma. *Clin Cancer Res*, 9, 2657-64.
- SUN, P., ZHANG, G., SU, X., JIN, C., YU, B., YU, X., LV, Z., MA, H., ZHANG, M., WEI, W. & LI, W. 2019. Maintenance of Primary Hepatocyte Functions In Vitro by Inhibiting Mechanical Tension-Induced YAP Activation. *Cell Rep*, 29, 3212-3222 e4.
- SURMAITIS, R. L., ARIAS, C. J. & SCHLENOFF, J. B. 2018. Stressful Surfaces: Cell Metabolism on a Poorly Adhesive Substrate. *Langmuir*, 34, 3119-3125.
- TAKAHASHI, Y., HORI, Y., YAMAMOTO, T., URASHIMA, T., OHARA, Y. & TANAKA, H. 2015. 3D spheroid cultures improve the metabolic gene expression profiles of HepaRG cells. *Biosci Rep*, 35.
- TAMJID, E., SIMCHI, A., DUNLOP, J. W., FRATZL, P., BAGHERI, R. & VOSSOUGH, M. 2013. Tissue growth into three-dimensional composite scaffolds with controlled micro-features and nanotopographical surfaces. *J Biomed Mater Res A*, 101, 2796-807.
- THASLER, W. E., WEISS, T. S., SCHILLHORN, K., STOLL, P. T., IRRGANG, B. & JAUCH, K. W. 2003. Charitable State-Controlled Foundation Human Tissue and Cell Research: Ethic and Legal Aspects in the Supply of Surgically Removed Human Tissue For Research in the Academic and Commercial Sector in Germany. *Cell Tissue Bank*, 4, 49-56.
- THEILE, D., HAEFELI, W. E., SEITZ, H. K., MILLONIG, G., WEISS, J. & MUELLER, S. 2013. Association of liver stiffness with hepatic expression of pharmacokinetically important genes in alcoholic liver disease. *Alcohol Clin Exp Res*, 37 Suppl 1, E17-22.
- THEVENOT, P., NAIR, A., DEY, J., YANG, J. & TANG, L. 2008. Method to analyze three-dimensional cell distribution and infiltration in degradable scaffolds. *Tissue Eng Part C Methods*, 14, 319-31.
- THIERY, J. P., ACLOQUE, H., HUANG, R. Y. & NIETO, M. A. 2009. Epithelial-mesenchymal transitions in development and disease. *Cell*, 139, 871-90.
- TOLOSA, L., GOMEZ-LECHON, M. J., LOPEZ, S., GUZMAN, C., CASTELL, J. V., DONATO, M. T. & JOVER, R. 2016. Human Upcyte Hepatocytes:

- Characterization of the Hepatic Phenotype and Evaluation for Acute and Long-Term Hepatotoxicity Routine Testing. *Toxicol Sci*, 152, 214-29.
- TOLOSA, L., JIMENEZ, N., PELECHA, M., CASTELL, J. V., GOMEZ-LECHON, M. J. & DONATO, M. T. 2019. Long-term and mechanistic evaluation of drug-induced liver injury in Upcyte human hepatocytes. *Arch Toxicol*, 93, 519-532.
- TREYER, A. & MUSCH, A. 2013. Hepatocyte polarity. *Compr Physiol*, 3, 243-87.
- TRUONG, A. S., LOCHBAUM, C. A., BOYCE, M. W. & LOCKETT, M. R. 2015. Tracking the Invasion of Small Numbers of Cells in Paper-Based Assays with Quantitative PCR. *Anal Chem*, 87, 11263-70.
- TSURUGA, Y., KIYONO, T., MATSUSHITA, M., TAKAHASHI, T., KASAI, H., MATSUMOTO, S. & TODO, S. 2008. Establishment of immortalized human hepatocytes by introduction of HPV16 E6/E7 and hTERT as cell sources for liver cell-based therapy. *Cell Transplant*, 17, 1083-94.
- TUNG, Y. C., HSIAO, A. Y., ALLEN, S. G., TORISAWA, Y. S., HO, M. & TAKAYAMA, S. 2011. High-throughput 3D spheroid culture and drug testing using a 384 hanging drop array. *Analyst*, 136, 473-8.
- ULLAH, I., KIM, Y., LIM, M., OH, K. B., HWANG, S., SHIN, Y., KIM, Y., IM, G.-S., HUR, T.-Y. & OCK, S. A. 2017. In vitro 3-D culture demonstrates incompetence in improving maintenance ability of primary hepatocytes. *Animal Cells and Systems*, 21, 332-340.
- UZARSKI, J. S., DIVITO, M. D., WERTHEIM, J. A. & MILLER, W. M. 2017. Essential design considerations for the resazurin reduction assay to noninvasively quantify cell expansion within perfused extracellular matrix scaffolds. *Biomaterials*, 129, 163-175.
- VAN DER VALK, J. & GSTRAUNTHALER, G. 2017. Fetal Bovine Serum (FBS) - A pain in the dish? *Altern Lab Anim*, 45, 329-332.
- VAN NORMAN, G. A. 2016. Drugs, Devices, and the FDA: Part 1: An Overview of Approval Processes for Drugs. *JACC Basic Transl Sci*, 1, 170-179.
- VAN TONDER, A., JOUBERT, A. M. & CROMARTY, A. D. 2015. Limitations of the 3-(4,5-dimethylthiazol-2-yl)-2,5-diphenyl-2H-tetrazolium bromide (MTT) assay when compared to three commonly used cell enumeration assays. *BMC Res Notes*, 8, 47.
- VILDHEDE, A., WISNIEWSKI, J. R., NOREN, A., KARLGREN, M. & ARTURSSON, P. 2015. Comparative Proteomic Analysis of Human Liver Tissue and Isolated Hepatocytes with a Focus on Proteins Determining Drug Exposure. *J Proteome Res*, 14, 3305-14.
- VINKEN, M. 2013. The adverse outcome pathway concept: a pragmatic tool in toxicology. *Toxicology*, 312, 158-65.
- VINKEN, M. & HENGSTLER, J. G. 2018. Characterization of hepatocyte-based in vitro systems for reliable toxicity testing. *Arch Toxicol*, 92, 2981-2986.
- VINKEN, M., PAPELEU, P., SNYKERS, S., DE ROP, E., HENKENS, T., CHIPMAN, J. K., ROGIERS, V. & VANHAECKE, T. 2006. Involvement of cell junctions in hepatocyte culture functionality. *Crit Rev Toxicol*, 36, 299-318.
- VOSOUGH, M., OMIDINIA, E., KADIVAR, M., SHOKRGOZAR, M. A., POURNASR, B., AGHDAMI, N. & BAHARVAND, H. 2013. Generation of functional

- hepatocyte-like cells from human pluripotent stem cells in a scalable suspension culture. *Stem Cells Dev*, 22, 2693-705.
- WAHID, B., ALI, A., RAFIQUE, S. & IDREES, M. 2017. New Insights into the Epigenetics of Hepatocellular Carcinoma. *Biomed Res Int*, 2017, 1609575.
- WANG, F., PAN, X., KALMBACH, K., SETH-SMITH, M. L., YE, X., ANTUMES, D. M., YIN, Y., LIU, L., KEEFE, D. L. & WEISSMAN, S. M. 2013a. Robust measurement of telomere length in single cells. *Proc Natl Acad Sci U S A*, 110, E1906-12.
- WANG, Y., KIM, M. H., SHIRAHAMA, H., LEE, J. H., NG, S. S., GLENN, J. S. & CHO, N. J. 2016. ECM proteins in a microporous scaffold influence hepatocyte morphology, function, and gene expression. *Sci Rep*, 6, 37427.
- WANG, Y., SHI, J., CHAI, K., YING, X. & ZHOU, B. P. 2013b. The Role of Snail in EMT and Tumorigenesis. *Curr Cancer Drug Targets*, 13, 963-972.
- WARE, B. R., DURHAM, M. J., MONCKTON, C. P. & KHETANI, S. R. 2018. A Cell Culture Platform to Maintain Long-term Phenotype of Primary Human Hepatocytes and Endothelial Cells. *Cell Mol Gastroenterol Hepatol*, 5, 187-207.
- WARE, B. R. & KHETANI, S. R. 2017. Engineered Liver Platforms for Different Phases of Drug Development. *Trends Biotechnol*, 35, 172-183.
- WEI, G., WANG, J., LV, Q., LIU, M., XU, H., ZHANG, H., JIN, L., YU, J. & WANG, X. 2018. Three-dimensional coculture of primary hepatocytes and stellate cells in silk scaffold improves hepatic morphology and functionality in vitro. *J Biomed Mater Res A*, 106, 2171-2180.
- WELLS, R. G. 2008a. Cellular sources of extracellular matrix in hepatic fibrosis. *Clin Liver Dis*, 12, 759-68, viii.
- WELLS, R. G. 2008b. The role of matrix stiffness in regulating cell behavior. *Hepatology*, 47, 1394-400.
- WENG, M. K., NATARAJAN, K., SCHOLZ, D., IVANOVA, V. N., SACHINIDIS, A., HENGSTLER, J. G., WALDMANN, T. & LEIST, M. 2014. Lineage-specific regulation of epigenetic modifier genes in human liver and brain. *PLoS One*, 9, e102035.
- WENG, Y. R., CUI, Y. & FANG, J. Y. 2012. Biological functions of cytokeratin 18 in cancer. *Mol Cancer Res*, 10, 485-93.
- WESTERINK, W. M. & SCHOONEN, W. G. 2007. Cytochrome P450 enzyme levels in HepG2 cells and cryopreserved primary human hepatocytes and their induction in HepG2 cells. *Toxicol In Vitro*, 21, 1581-91.
- WEWERING, F., JOUY, F., WISSENBACH, D. K., GEBAUER, S., BLUHER, M., GEBHARDT, R., PIROW, R., VON BERGEN, M., KALKHOF, S., LUCH, A. & ZELLMER, S. 2017. Characterization of chemical-induced sterile inflammation in vitro: application of the model compound ketoconazole in a human hepatic co-culture system. *Arch Toxicol*, 91, 799-810.
- WISSEMANN, K. W. & JACOBSON, B. S. 1985. Pure gelatin microcarriers: synthesis and use in cell attachment and growth of fibroblast and endothelial cells. *In Vitro Cell Dev Biol*, 21, 391-401.
- WONG, V. W., VERGNIOL, J., WONG, G. L., FOUCHER, J., CHAN, H. L., LE BAIL, B., CHOI, P. C., KOWO, M., CHAN, A. W., MERROUCHE, W., SUNG, J. J.

- & DE LEDINGHEN, V. 2010. Diagnosis of fibrosis and cirrhosis using liver stiffness measurement in nonalcoholic fatty liver disease. *Hepatology*, 51, 454-62.
- WU, J., DU, C., LV, Z., DING, C., CHENG, J., XIE, H., ZHOU, L. & ZHENG, S. 2013. The up-regulation of histone deacetylase 8 promotes proliferation and inhibits apoptosis in hepatocellular carcinoma. *Dig Dis Sci*, 58, 3545-53.
- WU, L., PRINS, H. J., HELDER, M. N., VAN BLITTERSWIJK, C. A. & KAPERIEN, M. 2012. Trophic effects of mesenchymal stem cells in chondrocyte co-cultures are independent of culture conditions and cell sources. *Tissue Eng Part A*, 18, 1542-51.
- XING, Q., YATES, K., VOGT, C., QIAN, Z., FROST, M. C. & ZHAO, F. 2014. Increasing mechanical strength of gelatin hydrogels by divalent metal ion removal. *Sci Rep*, 4, 4706.
- YAMADA, M., SUGAYA, S., NAGANUMA, Y. & SEKI, M. 2012. Microfluidic synthesis of chemically and physically anisotropic hydrogel microfibers for guided cell growth and networking. *Soft Matter*, 8, 3122-3130.
- YAMASHITA, Y., SHIMADA, M., HARIMOTO, N., RIKIMARU, T., SHIRABE, K., TANAKA, S. & SUGIMACHI, K. 2003. Histone deacetylase inhibitor trichostatin A induces cell-cycle arrest/apoptosis and hepatocyte differentiation in human hepatoma cells. *Int J Cancer*, 103, 572-6.
- YAN, S., WEI, J., LIU, Y., ZHANG, H., CHEN, J. & LI, X. 2015. Hepatocyte spheroid culture on fibrous scaffolds with grafted functional ligands as an in vitro model for predicting drug metabolism and hepatotoxicity. *Acta Biomater*, 28, 138-148.
- YE, S., BOETER, J. W. B., PENNING, L. C., SPEE, B. & SCHNEEBERGER, K. 2019. Hydrogels for Liver Tissue Engineering. *Bioengineering (Basel)*, 6, 59.
- YIN, M., TALWALKAR, J. A., GLASER, K. J., MANDUCA, A., GRIMM, R. C., ROSSMAN, P. J., FIDLER, J. L. & EHMAN, R. L. 2007. Assessment of hepatic fibrosis with magnetic resonance elastography. *Clin Gastroenterol Hepatol*, 5, 1207-1213 e2.
- YOON, E., BABAR, A., CHOUDHARY, M., KUTNER, M. & PYRSOPOULOS, N. 2016. Acetaminophen-Induced Hepatotoxicity: a Comprehensive Update. *J Clin Transl Hepatol*, 4, 131-42.
- ZACHARIAS, D. G., NELSON, T. J., MUELLER, P. S. & HOOK, C. C. 2011. The science and ethics of induced pluripotency: what will become of embryonic stem cells? *Mayo Clin Proc*, 86, 634-40.
- ZANGER, U. M. & SCHWAB, M. 2013. Cytochrome P450 enzymes in drug metabolism: regulation of gene expression, enzyme activities, and impact of genetic variation. *Pharmacol Ther*, 138, 103-41.
- ZEILINGER, K., FREYER, N., DAMM, G., SEEHOFER, D. & KNOSPEL, F. 2016. Cell sources for in vitro human liver cell culture models. *Exp Biol Med (Maywood)*, 241, 1684-98.
- ZHAEENTAN, S., AMJADI, F. S., ZANDIE, Z., JOGHATAEI, M. T., BAKHTIYARI, M. & AFLATOONIAN, R. 2018. The effects of hydrocortisone on tight junction genes in an in vitro model of the human fallopian epithelial cells. *Eur J Obstet Gynecol Reprod Biol*, 229, 127-131.

- ZHANG, H., GAO, N., TIAN, X., LIU, T., FANG, Y., ZHOU, J., WEN, Q., XU, B., QI, B., GAO, J., LI, H., JIA, L. & QIAO, H. 2015a. Content and activity of human liver microsomal protein and prediction of individual hepatic clearance in vivo. *Sci Rep*, 5, 17671.
- ZHANG, H. X., XIAO, G. Y., WANG, X., DONG, Z. G., MA, Z. Y., LI, L., LI, Y. H., PAN, X. & NIE, L. 2015b. Biocompatibility and osteogenesis of calcium phosphate composite scaffolds containing simvastatin-loaded PLGA microspheres for bone tissue engineering. *J Biomed Mater Res A*, 103, 3250-8.
- ZHANG, J., MUIRHEAD, B., DODD, M., LIU, L., XU, F., MANGIACOTTE, N., HOARE, T. & SHEARDOWN, H. 2016. An Injectable Hydrogel Prepared Using a PEG/Vitamin E Copolymer Facilitating Aqueous-Driven Gelation. *Biomacromolecules*, 17, 3648-3658.
- ZHANG, P. P., WANG, X. L., ZHAO, W., QI, B., YANG, Q., WAN, H. Y., SHUANG, Z. Y., LIU, M., LI, X., LI, S. & TANG, H. 2014a. DNA methylation-mediated repression of miR-941 enhances lysine (K)-specific demethylase 6B expression in hepatoma cells. *J Biol Chem*, 289, 24724-35.
- ZHANG, Q., LEI, X. & LU, H. 2014b. Alterations of epigenetic signatures in hepatocyte nuclear factor 4alpha deficient mouse liver determined by improved ChIP-qPCR and (h)MeDIP-qPCR assays. *PLoS One*, 9, e84925.
- ZHANG, Z., LI, G. & SHI, B. 2006. Physicochemical properties of collagen, gelatin and collagen hydrolysate derived from bovine lamed split wastes. *Journal-society of leather technologists and chemists*, 90, 23.
- ZHONG, X. Y., YUAN, X. M., XU, Y. Y., YIN, M., YAN, W. W., ZOU, S. W., WEI, L. M., LU, H. J., WANG, Y. P. & LEI, Q. Y. 2018. CARM1 Methylates GAPDH to Regulate Glucose Metabolism and Is Suppressed in Liver Cancer. *Cell Rep*, 24, 3207-3223.
- ZHU, J. & MARCHANT, R. E. 2011. Design properties of hydrogel tissue-engineering scaffolds. *Expert Rev Med Devices*, 8, 607-26.

Declaration

The dissertation was carried out at the Siegfried Weller Institute under the supervision of Prof. Dr. Andreas K. Nüssler.

Only manuscripts for which I was significantly involved in the planning, execution, and evaluation of the experiments, as well as in the writing of the manuscripts and visualization of the results, were included in this dissertation. The manuscripts included in this dissertation are collaborative projects; the participation of the individual authors is explained in more detail below.

The dissertation was corrected by Prof. Nüssler and linguistically by a commercial proofreading service (Proof-Reading-Service.com).

I assure that I wrote this manuscript independently and that I did not use any other sources than those I indicated.

Tübingen, 8/20/2020

Marc Ruoff

Author Contributions

A Standardized Collagen-Based Scaffold Improves Human Hepatocyte Shipment and Allows Metabolic Studies over 10 Days, Bioengineering, 2018

The conceptualization of the study was performed by Marc Ruoß and Prof. Andreas K. Nüssler

The formal analysis was done by Marc Ruoß

The investigation was carried out by Marc Ruoß

Resources were provided by Frank Schügner, Dr. Leon H. H. Olde Damink, Dr. Serene M. L. Lee, Dr. Liming Ge and Victor Häussling

The manuscript was written and prepared by Marc Ruoß, PD Dr. Sabrina Ehnert and Prof. Andreas K. Nüssler

Additional writing, review and editing of the manuscript was performed by Victor Häussling, Frank Schügner, Dr. Leon H. H. Olde Damink, Dr. Serene M. L. Lee and Dr. Liming Ge

Visualization was carried out by Marc Ruoß

The supervision was achieved by Prof. Andreas K. Nüssler

Prof. Andreas K. Nüssler, Dr. Liming Ge and Dr. Leon H. H. Olde Damink were involved in the funding acquisition.

Epigenetic Modifications of the Liver Tumor Cell Line HepG2 Increase Their Drug Metabolic Capacity, International Journal of Molecular Sciences, 2019

The conceptualization of the study was performed by Marc Ruoß, Dr. Sahar Sajadian and Prof. Andreas K. Nüssler

The formal analysis was done by Marc Ruoß and Dr. Sahar Sajadian

The investigation was carried out by Marc Ruoß, Dr. Lisa Ehret and Dr. Sahar Sajadian

Resources were provided by Dr. Georg Damm, Prof. Daniel Seehofer, Prof. Silvio Nadalin and PD Dr. Ruth Ladurner

The manuscript was written and prepared by Marc Ruoß, Dr. Georg Damm, Dr. Sahar Sajadian and Prof. Andreas K. Nüssler

Prof. Massoud Vosough contributed to data interpretation

Additional writing, review and editing of the manuscript was performed by Prof. Massoud Vosough, Dr. Lisa Ehret, Carl Grom-Baumgarten, Martin Petkov, Prof. Daniel Seehofer, Prof. Silvio Nadalin and PD Dr. Ruth Ladurner

Visualization was carried out by Marc Ruoß

The supervision was achieved by Prof. Andreas K. Nüssler

Prof. Andreas K. Nüssler were involved in the funding acquisition.

Development of Scaffolds with Adjusted Stiffness for Mimicking Disease-Related Alterations of Liver Rigidity, Journal of Functional Biomaterials, 2020

The conceptualization of the study was performed by Marc Ruoß and Prof. Andreas K. Nüssler

The formal analysis was done by Marc Ruoß, Marina Weimer and Silas Rebholz

The investigation was carried out by Marc Ruoß, Marina Weimer and Silas Rebholz

Marc Ruoß, Marina Weimer, Silas Rebholz, Carl Grom-Baumgarten and PD Dr. Sabrina Ehnert were involved in the development of the cryogels used in this study

Resources were provided by Kiriaki Athanasopulu, Prof. Ralf Kemkemer and Prof. Hanno Käß

The manuscript was written and prepared by Marc Ruoß

Additional writing, review and editing of the manuscript was performed by Marina Weimer, Silas Rebholz, Carl Grom-Baumgarten, Kiriaki Athanasopulu, Prof. Ralf Kemkemer, Prof. Hanno Käß, PD Dr. Sabrina Ehnert and Prof. Andreas K. Nüssler

Visualization was carried out by Marc Ruoß

The supervision was achieved by Prof. Andreas K. Nüssler

Cell-Type-Specific Quantification of a Scaffold-Based 3D Liver Co-Culture, Methods and Protocols, 2020

The conceptualization of the study was performed by Marc Ruoß

The formal analysis was done by Marc Ruoß, Vanessa Kieber and Silas Rebholz

The investigation was carried out by Marc Ruoß, Vanessa Kieber and Silas Rebholz

Marc Ruoß, Silas Rebholz, Marina Häcker and PD Dr. Sabrina Ehnert developed and optimized the quantification method, which was used for the experiments.

Resources were provided by Dr. Leon H. H. Olde Damink

The manuscript was written and prepared by Marc Ruoß

Additional writing, review and editing of the manuscript was performed by Caren Linnemann, Helen Rinderknecht, Victor Häussling, PD Dr. Sabrina Ehnert and Prof. Andreas K. Nüssler

Visualization was carried out by Marc Ruoß

Prof. Andreas K. Nüssler was responsible for the project administration

Prof. Andreas K. Nüssler and Dr. Leon H. H. Olde Damink were involved in the funding acquisition.

Acknowledgements

First of all, I would like to thank Prof. Dr. Andreas Nüssler who, as head of the Siegfried Weller Institute (SWI), made it possible for me to write my doctoral thesis at his institute and supported me as a supervisor during my entire doctoral phase with his constructive criticism. I would also like to thank him for giving me a lot of freedom to work on my project while simultaneously providing me more support in writing my publications.

Many thanks also go to Anja Tschida, Dr. Sahar Sajadian, and Bianca Braun, who introduced me to the liver project at the beginning of my time at SWI.

I would also like to thank PD Dr. Sabrina Ehnert, who has been an important contact person for me in a wide variety of problems.

Special thanks go to Romina Aspera-Werz, who worked with me at SWI during my entire doctoral phase and with whom I was able to discuss small and large problems around my doctoral thesis and beyond over countless cups of coffee.

Thank you to the other doctoral students at SWI, in particular Dr. Gauri Tendulkar, Helen Rinderknecht, and Caren Linnemann, who were also able to help me with a wide variety of questions.

I would also like to thank Silas Rebholz, Marina Weimer, Vanessa Kieber, Noah Adamtey, Diana Huber, Dr. Lisa Ehret, Carl Grom-Baumgarten, and Martin Petkov, who work together with me on the liver project.

I would also like to thank all other former and current employees of the SWI for the time spent together at the SWI.

Thank you to Prof. Kemkemer and Kiriaki Athanasopulu from Reutlingen University and Dr. Kraut and Prof. Käß from Esslingen University for their technical support in the characterization of our scaffolds

I would also like to thank Prof. Königsrainer and his colleagues for providing liver tissue. In this context, special thanks are due to Dr. Wagner's team from the Surgical Study Centre for the acquisition of suitable donors of liver tissue and the coordination between our laboratory and the OP

I would also like to thank the employees of Matricel and Hepacult, who participated in the joint research project and provided us with scaffolds and primary hepatocytes respectively.

I would also like to thank Dr. Georg Damm and his team at the University of Leipzig for providing primary human hepatocytes

I would also like to thank Prof. Massoud Vosough for his interest in the projects of my doctoral thesis and his helpful suggestions and ideas.

Finally, I would like to thank my wife Christine and my parents, who supported me throughout my studies and also during my doctoral thesis.